Nonlinear Phenomena in Plasma Physics and Hydrodynamics

Edited by R.Z. SAGDEEV

Advances
in
Science
and
Technology
in
the USSR

Physics Series

MIR Publishers
Moscow

Mir Publishers Moscow

Advances
in
Science
and
Technology
in
the USSR

Physics Series

Nonlinear Phenomena in Plasma Physics and Hydrodynamics

Edited by R. Z. SAGDEEV,
Mem. USSR Acad. Sc.

Translated from the Russian by
Valerii Ilyushchenko, Cand. Sc. (Phys.-Math.)

Mir Publishers
Moscow

Нелинейные явления
в физике плазмы и гидродинамике

Под редакцией акад. *Р. З. Сагдеева*

Издательство «Мир» Москва

First published 1986

На английском языке

© Издательство «Мир», 1986
© English translation, Mir Publishers, 1986

CONTENTS

Preface 7

1. **Vortices in Plasma and Hydrodynamics** *by A. B. Mikhailovskii* 8
1.1. Introduction 8
1.2. Nonlinear Equations for Rossby Waves 12
1.3. The Simplest Nonlinear Equations for Drift Waves 14
1.4. Vector Vortical Structures 16
1.5. Scalar Vortical Structures 18
1.6. Further Development of Concepts Concerning Electrostatic Vortices in Plasma 19
1.7. Electromagnetic Vortices 22
1.8. Conclusion 24
References 28

2. **Oscillations and Bifurcations in Reversible Systems** *by V. I. Arnol'd and M. B. Sevryuk* 31
2.1. Introduction 31
2.2. Reversible Mappings 32
2.3. Reversible Flows 33
2.4. Integrable Reversible Mappings and Vector Fields 34
2.5. Kolmogorov's Tori 35
2.6. Weak Reversibility 37
2.7. The Local Theory 37
2.8. Weak Reversibility in a Local Situation 42
2.9. Periodic Solutions 42
2.10. Kolmogorov's Tori for Additional "Even" Coordinates 44
2.11. The Local Theory for Additional "Even" Coordinates 45
2.12. Application to Reversible Equations 48
2.13. Non-Autonomous Reversible Systems 49
2.14. The Lyapunov-Devaney Theorem 51
2.15. The Resonance 1:1 52
2.16. Further Resonances $1:N$ $(N \geqslant 2)$ 54
References 63

3. **Regular and Chaotic Dynamics of Particles in a Magnetic Field** *by R. Z. Sagdeev and G. M. Zaslavskii* 65
3.1. Introduction 65
3.2. Equations of Motion 67
3.3. The Resonances of Longitudinal Motion 69
3.4. The Overlapping of the Resonances of Longitudinal Motion 72
3.5. A Kinetic Description 75
3.6. Equations of Transverse Motion 78
3.7. The Resonances of High-Energy Particles 83
3.8. Resonances in a Weak Magnetic Field 84
3.9. Generalization to a Wave Packet 85

3.10. A Kinetic Description of Transverse Motion 86
3.11. Quasi-Resonance Particles 88
References 92

4. The Renormalization Group Method and Kolmogorov-Arnold Moser Theory *by K. M. Khanin and Ya. G. Sinai* 93
4.1. Introduction 93
4.2. Rectification of the Nonlinear Rotation of a Circle 97
4.3. Construction of Invariant KAM Curves by the Renormalization Group Method 110
References 118

5. Nonlinear Problems of Turbulent Dynamo *by Ya. B. Zel'dovich and A. A. Ruzmaikin* 119
5.1. Introduction 119
5.2. Nonlinear Mean Field Dynamo 121
5.3. MHD Turbulence 130
References 135

6. Problems of the Theory of Strong Turbulence and Topological Solitons *by R. Z. Sagdeev, S. S. Moiseev, A. V. Tur, and V. V. Yanovskii* 137
6.1. Introduction 137
6.2. The Scaling Group and Functional Method 140
6.3. "Null-Modes" and the Self-Similar Spectrum 152
6.4. Invariant Properties of Hydrodynamic Models and Topological Solitons 163
References 180

7. Self-Oscillations and Auto-Waves in Chemical Systems *by A. M. Zhabotinskii* 183
7.1. Introduction 183
7.2. Experimental Studies 184
7.3. Theoretical Studies 195
7.4. Conclusion 207
References 208

8. Auto-Waves in Biologically Active Media *by V. I. Krinskii* 210
8.1. Introduction 210
8.2. Mathematical Description 211
8.3. Local Sources of Auto-Waves 213
8.4. Cardiac Disorders 215
8.5. Mathematical Simulation of Auto-Wave Sources 216
8.6. A Chemically Active Medium 216
8.7. New Auto-Wave Modes 217
8.8. Auto-Wave Sources in Three-Dimensional Active Media 217
8.9. The Effect of Medium Parameters on Auto-Wave Sources 218
8.10. An Anomalous Reverberator 219
8.11. Theoretical Studies of Reverberators 220
8.12. Conclusion 221
References 222

PREFACE

The modern theory of nonlinear phenomena is going through a period of explosive growth. Each "invention" in the field is disseminated rapidly, generating general interest and unexpected applications. This was for instance the case with solitons, strange attractors, and stochasticity. That scientists from each of the different branches of the theory of nonlinear phenomena should cooperate needs no proof, and the value of this cooperation could be seen at a conference held in Kiev on nonlinear and turbulent processes in physics.* The same approach has been adopted for this collection, which includes articles on regular nonlinear phenomena (vortices, solitons, auto-waves) and some on stochasticity and turbulence. In addition, the collection includes two mathematical articles that develop the Kolmogorov-Arnold-Moser theory, the importance of which for the theory of nonlinear dynamic systems is undoubted.

The articles are to some degree grouped around the nonlinear problems of plasma physics and hydrodynamics, in their broadest sense.

Hydrodynamics and plasma physics are traditional sources of exciting problems and ideas for the physics of nonlinear phenomena. We need only recall the classical examples of the discovery of solitons in shallow water, the exact integrability of the Korteweg-de Vries equation, and the discoveries of a strange attractor in the Lorentz system and stochasticity in Hamiltonian systems with small numbers of degrees of freedom.

These ideas and results, all stimulated by problems in hydrodynamics and plasma physics, quickly gained more general significance for physics as a whole. In turn, many new and efficient techniques are tested on such traditionally difficult subjects as turbulence. For instance, there is the recent application to turbulence of the renormalization group methods, which were successfully employed first in field theory and the physics of phase transitions.

Finally, all this culminates in general fund of knowledge in the physics of nonlinear phenomena. I hope that the publication of this collection will advance the progress of physics.

R.Z. Sagdeev

---

* *Nonlinear and Turbulent Processes in Physics*, Vols. 1-3, ed. R. Z Sagdeev, Harwood Academic Publishers, New York, 1984.

1 Vortices in Plasma and Hydrodynamics

A. B. Mikhailovskii, D. Sc. (Phys.-Math.)

1.1. INTRODUCTION

Problems on magnetized plasma often deal with low-frequency potential (electrostatic) waves propagating across (or almost across) an equilibrium magnetic field $\mathbf{B}_0$. Waves are said to be low-frequency (with respect to electrons or ions) if their characteristic frequency ω is low as compared with the cyclotron frequency ω_B of corresponding particles. Waves are called potential (or electrostatic) if their electric field $\mathbf{E}$ is, with an adequate accuracy, a potential one, i.e.

$$\mathbf{E} = -\nabla\phi, \tag{1.1}$$

where ϕ is the electrostatic potential.

Under the action of the fields $\mathbf{E}$, $\mathbf{B}_0$ particles (electrons or ions) acquire a transverse velocity $V_\perp$ defined by the equation of motion

$$\frac{dV_\perp}{dt} = -\frac{e}{M}\nabla_\perp\phi + \omega_B[\mathbf{V}_\perp, \mathbf{e}_z]. \tag{1.2}$$

where M, e are the mass and charge of particles, respectively, $\omega_B = eB_0/Mc$ the above mentioned cyclotron frequency, c the velocity of light, $\mathbf{e}_z$ the unit vector along the magnetic field (it is assumed that $\mathbf{B}_0 \parallel \mathbf{z}$), $d/dt = \partial/\partial t + \mathbf{V}\nabla$, $\mathbf{V} = \mathbf{V}_\perp + \mathbf{e}_z V_z$ the total velocity of a particle, and V_z its longitudinal velocity. The considered plasma component is assumed to be cold and collisionless. For low-frequency waves and $V_z = 0$, Eq. (1.2) approximately implies

$$\mathbf{V}_\perp = \mathbf{V}_E + \mathbf{V}_I, \tag{1.3}$$

where $\mathbf{V}_E$ is the velocity of an electric drift or of a cross field drift defined by the following equation:

$$\mathbf{V}_E = c[\mathbf{E}, \mathbf{e}_z]/B_0 = -c[\nabla\phi, \mathbf{e}_z]/B_0 \tag{1.4}$$

$\mathbf{V}_I$ stands for the inertial part of the transverse particle velocity

$$\mathbf{V}_I = \frac{1}{\omega_B}\left[\mathbf{e}_z, \frac{d_0\mathbf{V}_E}{dt}\right], \tag{1.5}$$

where

$$d_0/dt = \partial/\partial t + \mathbf{V}_E\nabla. \tag{1.6}$$

Equation (1.4) implies that

$$\mathrm{div}\ \mathbf{V}_E = 0. \tag{1.7}$$

$$\mathrm{curl}_z\,\mathbf{V}_E = -\frac{c}{B_0}\Delta_\perp\phi, \tag{1.8}$$

where $\Delta_\perp = \partial^2/\partial x^2 + \partial^2/\partial y^2$. The motion of the relevant plasma component is seen to be approximately vortical, hence the low-frequency potential waves are one of the versions of plasma vortices.

The class of low-frequency potential waves in magnetized plasma is fairly extensive, yet the special place among those is occupied by drift waves due to their role in an enhanced (anomalous) plasma transport across magnetic field. The drift waves have been predicted by Rudakov and Sagdeev [1.1], later they were in great detail investigated in many theoretical papers (see [1.2], Ch. 6 and [1.3]). The theory of drift waves was experimentally corroborated by Buchel'nikova [1.4], D'Angelo [1.5] and many other authors. The simplest dispersion relation for drift waves has the form

$$\omega = \frac{k_y V_{*e}}{1 + k_\perp^2\rho_0^2}. \tag{1.9}$$

where $\mathbf{k}$ is the wave vector, V_{*e} the electron drift velocity due to density gradient, ρ_0 the ion Larmor radius due to electron temperature, $k_\perp^2 = k_x^2 + k_y^2$, x the direction of plasma inhomogeneity, and y the "drift" direction. Theoretical studies on the anomalous plasma transport across magnetic field due to drift waves are reviewed in [1.6].

In many respects the above motion of charged particles is similar to a two-dimensional motion of a shallow incompressible rotating fluid placed in gravitational field. The hydrodynamic analogue of the equation of motion (1.2) is the following one [1.7]:

$$d\mathbf{V}/dt = -g\nabla H + f\,[\mathbf{V}, \mathbf{e}_z], \tag{1.10}$$

where g is the gravitational force, H the fluid depth, and f the Coriolis parameter. Similar to (1.3), when $d/dt \ll f$, Eq. (1.10) implies

$$\mathbf{V} = \mathbf{V}_D + \mathbf{V}_I \tag{1.11}$$

where $\mathbf{V}_D$, $\mathbf{V}_I$ are the drift and inertial velocity components defined by the relations

$$\mathbf{V}_D = \frac{g}{f}\,[\nabla H, \mathbf{e}_z], \tag{1.12}$$

$$\mathbf{V}_I = \frac{1}{f}\left[\mathbf{e}_z, \frac{d_0\mathbf{V}_D}{dt}\right] \tag{1.13}$$

while d_0/dt is defined by an equation like (1.6), with the substitution $\mathbf{V}_E \to \mathbf{V}_D$. In an approximation both of $g = \mathrm{const}$ and of waves having a characteristic scale small as compared with the characteristic size of a change in the Coriolis parameter we have

$$|\nabla \ln H| \gg |\nabla \ln f| \tag{1.14}$$

and it follows from (1.12), similar to (1.7) and (1.8), that

$$\operatorname{div} \mathbf{V}_{\mathrm{D}} = -\frac{g}{f}[\nabla \ln f, \nabla H]_z, \tag{1.15}$$

$$\operatorname{curl}_z \mathbf{V}_{\mathrm{D}} = -\frac{g}{f}\Delta_\perp H \tag{1.16}$$

It is seen that in this approximation we have

$$|\operatorname{curl}_z \mathbf{V}_{\mathrm{D}}| \gg |\operatorname{div} \mathbf{V}_{\mathrm{D}}|, \tag{1.17}$$

i.e. the two-dimensional fluid motion, just as the above plasma motion, is vortical too.

The indicated analogy in the character of motion of magnetized plasma and rotating fluids is also supported by an analogy in their wave properties. In this connection of importance is the existence of a hydrodynamic analogue of drift waves, this being Rossby waves [1.8]. To derive the dispersion relation for the latter, let us supplement the above Eqs. (1.11)-(1.13) by the continuity equation that in this case takes the form [1.7]

$$\partial H/\partial t + \operatorname{div}(H\mathbf{V}) = 0. \tag{1.18}$$

Substituting (1.11)-(1.13) and linearizing the resultant equation, we arrive at a dispersion relation, similar to (1.9), with the substitutions

$$\rho_0 \to r_{\mathrm{R}}, \quad V_{*e} \to V_{\mathrm{R}}, \tag{1.19}$$

where r_{R} is the Rossby-Obukhov radius, and V_{R} is the Rossby velocity defined respectively by the relationships

$$r_{\mathrm{R}} = \frac{(gH_0)^{1/2}}{f}, \quad V_{\mathrm{R}} = -\frac{gH_0}{f}\frac{d\ln f}{dx}, \tag{1.20}$$

where H_0 is the equilibrium fluid depth.

The establishment of the analogy between drift and Rossby waves has a curious history. According to Nezlin, this analogy was first indicated by Leontovich at the beginning of the 1960s. However, this remark by Leontovich was made in private and played its role only in the early 1980s (!), when Nezlin and coworkers started laboratory studies on Rossby waves (the essence of these experiments will be discussed later). The first published paper, where the above analogy was revealed, was the paper by Hasegawa *et al.* [1.9], from which, however, followed that this analogy had been identified not by the authors themselves, but by Taniuti whom they thanked for the relevant information!

The analogy between drift and Rossby waves serves as a prerequisite for an interchange by conceptual and methodical achievements between the theories of hydrodynamic vortices and magnetized plasma. Also, it is clear that the hydrodynamic vortices observed in nature and in the laboratory can be considered as models of wave processes in magnetized plasma and that, vice versa, there exists a possibility of the plasma simulation of hydrodynamic vortices. The real picture of this interchange, however, is not so symmetric as the above stated one in the sense that until now plasma physics has borrowed from hydrodynamics much more than it has returned. Therefore, within our presentation, at the interface between the theories of plasma and hydrodynamic vortices, our main aim is to explain what impetus hydrodynamics has given to plasma theory.

The interplay of plasma physics and hydrodynamics has settled the issue on the possible existence of regular (ordered) drift structures as well as assisted in affirming the soliton trend in the theory of drift waves and thus undermined the conventional approach to this theory, which is based on the concepts of turbulence theory [1.10, 1.11].

The issue of regular drift structures has a long history. Such structures in the form of high-amplitude sawtooth oscillations were in due time observed by Buchel'nikova [1.4]. An important stage in the theory of regular drift structures was also the shaping of ideas about convective cells in magnetized plasma [1.12] (see also [1.13, 1.14]). It is important for our subsequent presentation to indicate that the nonlinear terms taken into account in the papers on convective cells have a structure of type $[\nabla a, \nabla b]_z$, where a and b are certain functions characterizing wave field. Such a nonlinearity can be called a vector one as opposed to the nonlinearity of type ϕ^2, which we will call a scalar (or ordinary) one.

The vector nonlinearity enters also into the equations for Rossby waves. Larichev and Reznik [1.15] were engaged in studying Rossby waves, with the vector nonlinearity included. They have demonstrated that the vector nonlinearity, like the scalar one, can play a localizing role, i.e. can result in the formation of solitons. The transfer of the concepts concerning "vector" solitons [1.15] to the physics of drift and driftlike waves in magnetized plasma is indeed one of the main outcomes of the interaction between the theories of plasma and hydrodynamic vortices.

The soliton trend in the theory of drift waves was also tangibly supported by laboratory experiments on Rossby waves conducted by Nezlin *et al.* [1.16, 1.17]. Their activity was fostered by the problem of Jupiter's Great Red Spot, on the one hand, and by the above analogy between Rossby and drift waves, on the other. The duo account of both these facts and the role of Rossby waves in the physics of atmosphere, oceanology, as well as the problem of heliomagnetic dynamo have led the authors of [1.16, 1.17] to the general physical understanding of the problem of the laboratory simulation of Rossby waves. In other words, the main aim of these papers was to get information on the most fundamental properties of Rossby waves. These properties include the possibility of the formation of regular Rossby structures and, above all, solitons of Rossby waves. The experiments [1.16, 1.17] afforded conclusive evidence of the existence of these solitons and affirmed the idea that analogous structures in magnetized plasma do exist. As to the purposeful experimentation with the solitons of drift waves, until now this has not been done.

The ensuing presentation can be treated as an introduction into the theory of the Rossby wave solitons and of corresponding types of magnetized plasma solitons. Section 1.2 discusses the structure of nonlinear equations for Rossby waves, Sec. 1.3, nonlinear equations for drift waves. The magnetized plasma vortical structures, due to vector nonlinearity, are considered in Sec. 1.4, while those due to scalar nonlinearity, in Sec. 1.5. This treatment is performed for the simplest instances of electrostatic vortices. An advanced picture of these vortices is presented in Sec. 1.6, while Sec. 1.7 shows that the properties similar to those of Rossby vortices are inherent not only in electrostatic vortices but also in some versions of electromagnetic vortices.

Our exposition concerns, mainly, stationary vortices. A part of modern research is dedicated to the problems of the stability and relaxation of vortices. The results of these and some other studies will be exposed in Sec. 1.8.

1.2. NONLINEAR EQUATIONS FOR ROSSBY WAVES

Assuming the fluid depth perturbation $\widetilde{H}$ to be small as compared with the equilibrium depth H_0, i.e. $\widetilde{H} \ll H_0$, by (1.11)-(1.13), (1.18) we get

$$\frac{\partial h}{\partial t} + V_{\mathrm{R}}(1+h)\frac{\partial h}{\partial y} - r_{\mathrm{R}}^2\left(\frac{\partial}{\partial t} + \mathbf{V}_{\mathbf{D}}\nabla\right)\Delta_\perp h = 0, \qquad (1.21)$$

where $h \equiv \widetilde{H}/H_0$ and the role of $\mathbf{V}_{\mathrm{D}}$ is played by (cf. (1.12))

$$\mathbf{V}_{\mathbf{D}} = \frac{gH_0}{f}[\nabla h,\ \mathbf{e}_z]. \qquad (1.22)$$

Equation (1.21) contains two types of nonlinearity: the vector one related to $\mathbf{V}_{\mathrm{D}}$ and the scalar one (ordinary), i.e. the term with $h\,\partial h/\partial y$. Equation (1.21) without the latter term, i.e. the equation like

$$\left(\frac{\partial}{\partial t} + V_{\mathrm{R}}\frac{\partial}{\partial y}\right)h - r_{\mathrm{R}}^2\left(\frac{\partial}{\partial t} + \mathbf{V}_{\mathbf{D}}\nabla\right)\Delta_\perp h = 0, \qquad (1.23)$$

has been derived in [1.18] and is often called the Charney equation. The scalar nonlinearity in the Rossby wave equation became to be accounted for starting from the works [1.19, 1.20]. Clearly, it is important if only $k_\perp^2 r_R^2 \ll 1$ and $\omega \approx k_y V_R$.

For stationary travelling waves, i.e. at $h = h\,(x,\, y - Ut)$, where U is the wave velocity, Eq (1.21) yields

$$\hat{D}\Delta_\perp h - \Lambda\,\partial h/\partial y + S\,\partial h^2/\partial y = 0, \tag{1.24}$$

where

$$\hat{D} = \frac{\partial}{\partial y} + \frac{gH_0}{fU}[\nabla h,\ \nabla]_z, \tag{1.25}$$

$$\Lambda = \frac{1}{r_R^2}\left(1 - \frac{V_R}{U}\right), \tag{1.26}$$

$$S = \frac{1}{2}\frac{V_R}{r_R^2 U}. \tag{1.27}$$

Introducing the notation

$$F \equiv \Delta_\perp h - \Lambda h + Sh^2, \tag{1.28}$$

we notice that (1.24) can be represented as

$$[\nabla F,\ \nabla\,(h + x/x_0)]_z = 0, \tag{1.29}$$

where

$$x_0 \equiv gH_0/fU. \tag{1.30}$$

Whence it follows that

$$\Delta_\perp h - \Lambda h + Sh^2 = C\,(h + x/x_0), \tag{1.31}$$

where C is a constant that can have different values in different space regions. Thus, if integrated, Eq. (1.24) can be reduced to a combination of simpler equations similar to (1.31). Such an integration at $S = 0$ was performed, in particular, in [1.15] and at $S \neq 0$, in [1.20, 1.21] and in a number of other papers.

Let us distinguish between the situations with $C \neq 0$ in a certain space region and those with $C \equiv 0$ for all x, y. In the first case, the scalar nonlinearity in (1.31) often proves to be of little significance. By neglecting it, Eq. (1.31) gives

$$\Delta_\perp h - \Lambda h = C(h + x/x_0). \tag{1.32}$$

Here the problem of stationary structures is reduced to finding solutions of the linear Eq. (1.32) in the relevant space regions and to their matching at the interregional boundaries. The equations similar to (1.32) are due to a vector nonlinearity. In this context the stationary structures described by such equations will be termed vortical structures or, simply, vector vortices.

For $C \equiv 0$ Eq. (1.31) yields the following relation:

$$\Delta_\perp h - \Lambda h + Sh^2 = 0, \tag{1.33}$$

which, unlike (1.32), is the same for all x, y. Here the term with vector nonlinearity in (1.24) vanishes identically. In this connection the stationary structures described by Eq. (1.33) will be termed scalar vortical structures or, simply, scalar vortices.

1.3. THE SIMPLEST NONLINEAR EQUATIONS FOR DRIFT WAVES

Let us consider the simplest plasma problems leading to the equations of the type (1.23), (1.32) and (1.33).

Above we have derived formulas (1.3)-(1.5) for the transverse velocity of charged particles in the field of a low-frequency electrostatic wave having a potential ϕ. To derive a closed equation for ϕ, let us supplement these formulas with the continuity equation for the appropriate plasma component (cf. (1.18)):

$$\partial n/\partial t + \operatorname{div} n\mathbf{V}_{\perp} = 0, \tag{1.34}$$

where n is the density of this plasma component. Putting $\mathbf{V}_{\perp}$ from (1.3)-(1.5) we arrive at the following equation:

$$\operatorname{div} \mathbf{V}_{\mathrm{I}} + d_0 n/dt = 0, \tag{1.35}$$

where the operator d_0/dt is defined by Eq. (1.6). Using (1.5) and (1.1), (1.4) we find (cf. (1.7))

$$\operatorname{div} \mathbf{V}_{\mathrm{I}} = \frac{1}{\omega_{\mathrm{B}}} \frac{d_0}{dt} \operatorname{curl}_z \mathbf{V}_{\mathrm{E}} = -\frac{c}{B_0\omega_{\mathrm{B}}} \frac{d_0}{dt} \Delta_{\perp}\phi. \tag{1.36}$$

Accounting for $n = n_0 + \tilde{n}$, where n_0, $\tilde{n}$ are the equilibrium and wave density parts, respectively, and assuming $|\tilde{n}| \ll n_0$, we get from (1.35) the following:

$$\frac{d_0}{dt} \operatorname{curl}_z \mathbf{V}_{\mathrm{E}} + \omega_{\mathrm{B}} \mathbf{V}_{\mathrm{E}} \nabla \ln n_0 + \frac{\omega_{\mathrm{B}}}{n_0} \frac{d_0 \tilde{n}}{dt} = 0. \tag{1.37}$$

Thus we have approached our aim, i.e. the derivation of the closed equation for ϕ. The regular procedure of the next stage requires Poisson's equation (and at a sufficiently large equilibrium plasma density—the quasi-neutrality condition) and the calculation of the wave part of the second plasma component density. The procedure will be explained somewhat later. As to now, for simplicity of the exposition we will assume that only one plasma component is involved in the wave motion and, besides, we will restrict ourselves to the case of quasi-neutral waves. Then

$$\tilde{n} = 0, \tag{1.38}$$

while Eq. (1.37) reduces to a closed equation for ϕ which is written as

$$\left(\frac{\partial}{\partial t} + \frac{c}{B_0} [\nabla\phi, \nabla]_z\right) \Delta_{\perp}\phi + \varkappa_n \omega_{\mathrm{B}} \frac{\partial \phi}{\partial y} = 0. \tag{1.39}$$

For stationary waves, i.e. when $\phi = \phi(x, \eta)$, $\eta \equiv y - Ut$, Eq. (1.39) yields

$$\hat{D}\Delta_\perp \phi = \Lambda\, \partial\phi/\partial\eta, \tag{1.40}$$

where

$$\hat{D} = \frac{\partial}{\partial\eta} - \frac{c}{UB_0} [\nabla\phi,\ \nabla]_z, \tag{1.41}$$

$$\Lambda = \omega_B \varkappa_n / U. \tag{1.42}$$

The comparison of (1.42) with (1.9) clearly shows that formulas (1.40)-(1.42) describe the drift waves with a characteristic size being smaller as compared with ρ_0, with $k_\perp \rho_0 \gg 1$.

Now let us clarify what effects are associated with $\tilde{n} \neq 0$. Till now it has been insignificant for us, what kind of particles is described by Eq. (1.37), electrons or ions. Now we will specify our problem by assuming that this equation is associated with ions and will mentally put into (1.37) ion indices at ω_B and $\tilde{n}$. In this case Eq. (1.37) must be supplemented with an equation for electron density. The electrons are assumed to be distributed in the field of the potential ϕ according to the Boltzmann law, i.e.

$$n_e = n_0 \exp(-e_e\phi/T_e). \tag{1.43}$$

We take $\nabla T_e = 0$. On calculating $\tilde{n}_e$ by means of (1.43) and allowing for the quasi-neutrality condition we substitute the final result in (1.37). Then in place of (1.39) we obtain

$$\left(\frac{\partial}{\partial t} + \frac{c}{B_0} [\nabla\phi,\ \nabla]_z\right) \Delta_\perp \phi - \frac{1}{\rho_0^2} \left(\frac{\partial\phi}{\partial t} + V_{*e} \frac{\partial\phi}{\partial y}\right) = 0. \tag{1.44}$$

This equation was obtained in [1.22, 1.23] and it is often called the Hasegawa-Mima equation. It describes the electron drift waves (or, simply, drift waves) which in the linear approximation are characterized by the dispersion relation (1.9). The Hasegawa-Mima equation is analogous in structure to the Charney equation (1.23) for Rossby waves. This analogy was stressed in [1.9]. When $\phi = \phi(x, \eta)$, Eq. (1.44) can be reduced to the (1.40) form with

$$\Lambda = \frac{1}{\rho_0^2}\left(1 - \frac{V_{*e}}{U}\right) \tag{1.45}$$

At $\omega \ll k_y V_{*e}$, i.e. at $k_\perp^2 \rho_0^2 \gg 1$, Eq. (1.45) can be reduced to (1.42).

In the inverse limiting case of long waves, i.e. at $k_\perp^2 \rho_0^2 \ll 1$, of importance can be scalar nonlinearity, i.e. the terms analogous to $h\, \partial h/\partial y$ in Eq. (1.21).

For stationary waves $\phi = \phi\,(x, \eta)$ and one can find the equation (cf. (1.24))

$$\hat{D}\Delta_\perp\phi - \Lambda\,\partial\phi/\partial\eta + S\,\partial\phi^2/\partial\eta = 0, \tag{1.46}$$

where $\hat{D}$ and Λ are given by (1.41) and (1.45), while the expression for S has the form (cf. (1.27))

$$S = \frac{e_0}{2\rho_s^2 T_e \varkappa_n^2}\,\frac{\partial\varkappa_n}{\partial x}. \tag{1.47}$$

Similar to (1.32) and (1.33), Eq. (1.46) yields the equations

$$\Delta_\perp\phi - \Lambda\phi = C\left(\phi - \frac{UB_0}{c}\,x\right), \tag{1.48}$$

$$\Delta_\perp\phi - \Lambda\phi + S\phi^2 = 0 \tag{1.49}$$

describing vector and scalar structures in magnetized plasma, respectively.

1.4. VECTOR VORTICAL STRUCTURES

Now we turn to the analysis of vortical structures described by equations like (1.32) and (1.48). Along with the Cartesian coordinates x, η there will be also used the polar coordinates $r = (x^2 + \eta^2)^{1/2}$, $\theta = \tan^{-1}\,(\eta/x)$. Following [1.15], for simplicity we will confine ourselves to the case of "two-layer" structures, i.e. two regions corresponding to different values of the constant C. The vortices of a more involved structure ("three-layer" vortices) see, e.g. in [1.24] and [1.25], Sec. 2.3.

For spatially localized (solitary) vortices, let us introduce the notion of external and internal regions of a vortex assuming that these regions are separated by a certain spatial curve $r = r\,(\theta)$ and that $C = 0$ in the external region. (In this statement of the problem our analysis omits the localized vortices in a flow with a nonuniform velocity profile like those found in [1.21, 1.26].) Then for corresponding regions Eqs. (1.48) combined will take the following form:

$$\Delta_\perp\phi = \begin{cases} \Lambda\phi, & r > r\,(\theta), \\ \Lambda\phi + C\,(\phi - UB_0x/c), & r < r\,(\theta). \end{cases} \tag{1.50}$$

At $r = r\,(\theta)$ the potential ϕ, its derivative with respect to the normal n to the interregional boundary, $\mathrm{n}\nabla\phi$, and $\Delta_\perp\phi$ are all assumed to be continuous, i.e.

$$\{\phi,\ \mathrm{n}\nabla\phi,\ \Delta_\perp\phi\}|_i^e = 0. \tag{1.51}$$

The continuity conditions for ϕ and $\Delta_\perp\phi$ as well as Eq. (1.50) imply that the function $r\,(\theta)$ should satisfy the relation

$$\phi\,[r\,(\theta),\ \theta] = (UB_0/c)\,r\cos\theta. \tag{1.52}$$

An important vortex type is the dipole one, i.e. that with

$$\phi\ (r,\ \theta) = \Phi \cos\theta, \tag{1.53}$$

where $\Phi = \Phi\ (r)$ is a function of radius r. Here the condition (1.52) is satisfied at $r\ (\theta) = a$, where a is a constant termed vortex radius. According to (1.52), this constant is determined by the equation

$$\Phi\ (a) = UB_0 a/c. \tag{1.54}$$

For a dipole vortex Eq. (1.50) means

$$\Delta_\perp \phi = \begin{cases} (\beta/a)^2 \phi, & r > a, \\ -(\gamma/a)^2 \phi + \dfrac{\gamma^2+\beta^2}{a^2}\, \dfrac{UB_0}{c}\, x, & r < a, \end{cases} \tag{1.55}$$

where β and γ are related to Λ and C as follows:

$$\beta^2 = a^2 \Lambda, \tag{1.56}$$

$$\gamma^2 = -\, a^2\ (\Lambda + C). \tag{1.57}$$

It is clear that ϕ is vanishing at infinity only if $\beta^2 > 0$, i.e.

$$\Lambda > 0. \tag{1.58}$$

It follows from (1.55) that

$$\Phi(r) = \Phi(a) \begin{cases} K_1(r\beta/a)/K_1(\beta), & r > a, \\ \left(1 + \dfrac{\beta^2}{\gamma^2}\right) \dfrac{r}{a} - \dfrac{\beta^2}{\gamma^2}\, \dfrac{J_1(r\gamma/a)}{J_1(\gamma)}, & r < a, \end{cases} \tag{1.59}$$

where J_1 and K_1 are the Bessel function and modified Bessel function of the second kind (McDonald function), respectively. At $\Phi\ (r)$ like that in (1.54) the first and third conditions from (1.51) are satisfied for arbitrary γ (i.e. for arbitrary C). To satisfy the second condition of (1.51) needs the following relationship between γ and β to be valid:

$$K_2\ (\beta)/\beta K_1\ (\beta) = -\ J_2\ (\gamma)/\gamma J_1\ (\gamma). \tag{1.60}$$

A remarkable property of the dipole vortex is that Eq. (1.46) reduces to the one-dimensional one [1.27]. To see that it is so we substitute (1.53) into (1.46). In terms of

$$X \equiv c\Phi/UB_0 r, \quad \xi = r\Lambda^{1/2} \tag{1.61}$$

the resultant one-dimensional equation can be written as

$$(1-X)\, X'' + X'X'' - X' + \frac{3}{\xi}\left[X'^2 + (1-X)\left(X'' - \frac{X'}{\xi}\right)\right] = 0, \tag{1.62}$$

where the prime means the derivative with respect to ξ. The point $\xi = \xi_0$, where $X\ (\xi_0) = 1$, is seen to be a singular point of Eq. (1.62). Referring now to (1.61) we see that this singular point is nothing else but the boundary between external and internal regions of a vortex, i.e. the point $r = a$.

Equation (1.62) can be also represented as

$$(1-X)^2\left(\frac{X''-X+3X'/\xi}{1-X}\right)'=0. \tag{1.63}$$

At $\xi \neq \xi_0$ Eq. (1.63) is trivially integrable to agree with (1.48). It is clear from (1.63) that mathematically the discontinuity of solution (1.59) is due to the above singular point. It is also clear that to construct a smooth (analytical) solution needs to supplement Eq. (1.63) by terms with higher derivatives with respect to X having coefficients not vanishing at $\xi = \xi_0$.

The solution similar to (1.53), (1.59) has been obtained by Larichev and Reznik [1.15] in the case of Rossby waves having a specific scale small as compared with the Rossby radius. The notions of dipole vortices have been carried over from hydrodynamics to plasma physics by Makino *et al.* [1.28] who considered the case of drift waves with Λ of the form (1.45).

1.5. SCALAR VORTICAL STRUCTURES

Now let us consider some consequences from the equation of the scalar vortical structures (1.49). We assume the waves described by this equation to be spatially localized in the x, η-plane. In a sufficiently remote peripheral region Eq. (1.49) transforms into a linear equation similar to the first equation of (1.50). Therefore for scalar structures, as for vector ones, the condition of ϕ being bounded at infinity means $\Lambda > 0$ (cf. (1.58)).

Multiplying Eq. (1.49) by ϕ and integrating over space we arrive at the integral form

$$\int [(\nabla_\perp \phi)^2+\Lambda\phi^2-S\phi^3]\, d\mathbf{r}=0. \tag{1.64}$$

Whence, taking into account $\Lambda > 0$, for the solitons with a sign-constant ϕ we will obtain

$$\operatorname{sgn} \phi = \operatorname{sgn} S. \tag{1.65}$$

The problem of scalar vortical structures can be analytically examined at $\partial^2/\partial x^2 \ll \partial^2/\partial\eta^2$, when in place of (1.49) we have

$$\partial^2\phi/\partial\eta^2 - \Lambda\phi + S\phi^2 = 0. \tag{1.66}$$

In this case it is feasible to discuss one-dimensional η-structures.

Equation (1.66) has the soliton solution

$$\phi = \phi_0/\cosh^2 (\varkappa\eta/2), \tag{1.67}$$

where $\varkappa = \Lambda^{1/2}$ and the maximum potential amplitude ϕ_0 is defined by

$$\phi_0 = 3\Lambda/2S. \tag{1.68}$$

An interesting consequence of the equation of scalar vortical structures (1.49) is that it permits of the cylindrically symmetric solutions like $\phi = \phi(r)$ corresponding to solitons known as "round". Then Eq. (1.49) takes the form

$$\frac{1}{r}\frac{\partial}{\partial r}\left(r\frac{\partial\phi}{\partial r}\right) = \Lambda\phi - S\phi^2. \tag{1.69}$$

The possibility of the round solitons of Rossby waves in a rotating fluid was investigated in [1.19, 1.20] (see also [1.29]).

In addition to a single round soliton, Eq. (1.49) also describes more involved two-dimensional structures and, in particular, two-dimensional chains of solitons. This was indicated in [1.30], where the approximate solution of Eq. (1.49) was found in the form

$$\phi = \frac{\phi_0}{\cosh^2(\varkappa\eta/2)}\left[1 + \frac{\varepsilon\cos(\sqrt{5}\,\varkappa x/2)}{\cosh(\varkappa\eta/2)}\right], \tag{1.70}$$

where ε is an arbitrary small parameter, while ϕ_0 and $\varkappa$ are the same as in Eq. (1.67). The solution (1.70) corresponds to a chain of solitons localized in η.

1.6. FURTHER DEVELOPMENT OF CONCEPTS CONCERNING ELECTROSTATIC VORTICES IN PLASMA

The above mentioned papers by Larichev and Reznik [1.15] on the solitary vortices of Rossby waves and by Hasegawa *et al.* [1.9], referring to the analogy between nonlinear equations for drift and Rossby waves, substantially influenced the development of the notions concerning vector vortical structures in the physics of magnetized plasma. As has been stated above, the first step in this direction was made by Makino *et al.* [1.28]. The notions were corroborated in plasma physics by the works of Meiss and Horton [1.31], Pavlenko and Petviashvili [1.32]. The paper [1.31] continued the analysis of the problem of drift vortices [1.28]. The authors of [1.31] assumed that the drift wave potential is dependent on the variables x, η, where

$$\eta = y - Ut + \alpha z \tag{1.71}$$

(α is a certain constant). Thereby they generalized the results of [1.28] to the case of $\alpha \neq 0$ corresponding to drift waves intermixed with ion-acoustic waves. Here, unlike (1.45), we have

$$\Lambda = \frac{1}{\rho_s^2}\left(1 - \frac{V_{*e}}{U} - \frac{\alpha^2 C_s^2}{U^2}\right), \tag{1.72}$$

where C_s is the ion sound velocity. In [1.32] drift-flute modes ($\alpha = 0$) were studied in an inhomogeneous plasma placed in crossed magnetic and gravitational fields (usually, the gravitational field is introduced into the plasma waves problem to simulate the effects of magnetic field curvature [1.2]). The authors of [1.32] have demonstrated that the drift-flute modes can also have the form of solitary vortices of the type considered in [1.15]. (The concrete results of [1.32] are inaccurate, see criticism in [1.30].)

According to (1.55), in an external region of the vortex potential ϕ is specified by the equation

$$\Delta_\perp \phi = \varkappa^2 \phi, \tag{1.73}$$

where $\varkappa$ is a certain real constant ($\varkappa^2 = \beta^2/a^2$, see (1.56)). Therefore for the indicated vortex region Eq. (1.50) yields

$$\Lambda = \varkappa^2, \tag{1.74}$$

where, generally, $\Lambda = \Lambda\,(U,\, \alpha)$ (see (1.72)). The relationship like (1.74) formally coincides with the dispersion relation of a linear approximation for the waves of frequency ω and wave vector $\mathbf{k}$ accurate to the substitution

$$\varkappa^2 \to -k_\perp^2, \quad U \to \omega/k_y, \quad \alpha \to k_z/k_y. \tag{1.75}$$

This is why (1.74) can be called a modified dispersion relation (MDR). It is clear from (1.74) that for the problem of solitary vortices of interest are only such waves in plasma for which (cf. (1.58))

$$\Lambda\,(U,\, \alpha) > 0. \tag{1.76}$$

For example, for a Λ like that in (1.45) the condition (1.76) corresponds to waves both propagating in the same direction as V_{*e} and at a velocity exceeding V_{*e}, i.e.

$$U/V_{*e} > 1, \tag{1.77}$$

and propagating in the opposite direction to V_{*e}, i.e.

$$U/V_{*e} < 0. \tag{1.78}$$

Also of importance is the question on what other wave modes in magnetized plasma the vortical structures can be realized. It follows from Secs. 1.1 and 1.3 that such waves should possess the following properties:

(1) They should be low-frequency and long-wavelength ones, at least with respect to one of the plasma components (ions or electrons).

(2) Generally speaking, in such waves the transverse inertia of a relevant plasma component should be quite essential (an exception to this rule see in [1.33]).

(3) The electric wave field perpendicular to the equilibrium magnetic field should be, if only approximately, a potential one.

Let us illustrate these properties and the condition (1.78) with reference to searching for solitary vortices of purely electron waves. It is well known [1.34] that a homogeneous plasma with a fairly high density ($\omega_{pe}^2 \gg \omega_{Be}^2$) has a mode of electrostatic low-frequency waves that propagate almost perpendicularly to the magnetic field and are described by the dispersion relation

$$\omega^2 = \omega_{Be}^2 k_z^2/k_\perp^2, \tag{1.79}$$

where ω_{Be}, ω_{pe} are the cyclotron and plasma frequencies of electrons, respectively. Such waves possess the above properties (1)-(3), yet for them, according to (1.74), (1.75), and (1.79), we have

$$\Lambda = -\alpha^2\omega_{Be}^2/U^2 < 0. \tag{1.80}$$

Therefore on this mode the solitary vortex like (1.53), (1.59) is not realized. Given the equilibrium plasma density gradient, $\partial n_0/\partial x \neq 0$, we have, in place of (1.79), the following dispersion relation [1.2]:

$$\omega^2 + \omega k_y \varkappa_n \omega_{Be}/k_\perp^2 = \omega_{Be}^2 k_z^2/k_\perp^2. \tag{1.81}$$

Thereby

$$\Lambda = (\alpha\omega_{Be}/U)^2 (U\varkappa_n/\alpha^2\omega_{Be} - 1). \tag{1.82}$$

It is seen that for a fairly small α (or for a fairly large $\varkappa_n$) and for an appropriate sign of U the condition $\Lambda > 0$ can be realized that is necessary for a solitary vortex to exist. Note also that as $\alpha \to 0$ Eq. (1.82) transforms into (1.42) (with the change $\omega_{Be} \to \omega_B$), therefore the purely electron vortices are an exact analogue of the above mentioned short-wavelength Rossby vortices.

Thus the situation concerning the drift-flute vortices mentioned above in connection with [1.32] is as follows. The drift-flute waves possess the properties (1)-(3). The dispersion relation for the simplest case of such waves is [1.2]

$$\omega^2 = -\Gamma^2 k_y^2/k_\perp^2, \tag{1.83}$$

where $\Gamma^2 = -g\varkappa_n$ is the squared growth rate of the flute instability and g the gravitational force. It follows both from (1.83) and the correspondence rules (1.75) that

$$\Lambda = \Gamma^2/U^2 \tag{1.84}$$

so that for $\Gamma^2 > 0$ (i.e. with the flute instability present) condition (1.76) is satisfied.

Equation (1.83) refers to the waves with $\omega > k_y V_{*i}$, where V_{*i} is the ion drift velocity. At $\omega \simeq k_y V_{*i}$ we have instead of Eq. (1.83)

$$\omega^2 - \omega k_y V_{*i} = -\Gamma^2 k_y^2/k_\perp^2. \tag{1.85}$$

Thereby

$$\Lambda = \Gamma^2/U\,(U - V_{*i}). \tag{1.86}$$

It can be seen that at $U < V_{*i}$ a drift-flute vortex is also realizable at $\Gamma^2 < 0$, i.e. with the flute instability absent.

The examples considered are indicative of the substantial role played by a plasma inhomogeneity in the problem of solitary vortices. The inhomogeneity either modifies "nonsoliton" wave types into the "soliton" ones or leads to novel wave types possessing soliton properties. In physical terms, these penomena are due to the gradient or drift effects, the same effects that result in gradient or drift instabilities [1.2].

This, however, does not imply that solitary vortices are feasible only in an inhomogeneous plasma. Consider, e.g. the ion-acoustic waves with a finite $k_\perp \rho_0$. Such waves obey the following dispersion relation:

$$\omega^2 = k_z^2 C_s^2 (1 - k_\perp^2 \rho_0^2), \tag{1.87}$$

under the assumption that $k_\perp^2 \rho_0^2 \ll 1$. Here

$$\Lambda = \frac{1}{\rho_0^2} \left(1 - \frac{\alpha^2 C_s^2}{U^2} \right), \tag{1.88}$$

the latter being a special case of Eq. (1.72) as $V_{*e} \to 0$. Equation (1.88) shows that ion-acoustic solitary vortices with a finite $k_\perp \rho_0$ can exist. This is also supported by the analysis made by Meiss and Horton [1.31].

The above general approach to the theoretical search for concrete types of solitary vortices in magnetized plasma has been formulated in [1.27], where the initial equations for a wide family of vector vortices have been derived, both of electrostatic vortices discussed here and of electromagnetic vortices considered in Sec. 1.7.

The paper [1.27] was preceded by brief communications [1.33, 1.35, 1.36]. In [1.35] emphasis is placed on short-wavelength drift vortices of vector type. Such vortices are characterized by Λ's like those of (1.45), yet with the substitution of ion subscripts for electron ones and vice versa. These have specific dimensions being much smaller than the ion Larmor radius. In [1.33] purely electron electrostatic vortices with Λ's like those in (1.42) are considered. The work [1.36] deals with electromagnetic vortices, therefore we will comment its results in Sec. 1.7.

1.7. ELECTROMAGNETIC VORTICES

Let us return to formulas (1.7) and (1.8) favouring the vortical nature of the motion of charged particles in the field of low-frequency electrostatic waves and let us consider the sensitivity of these formulas to the assumption on the potentiality of the waves expressed mathematically by the equality (1.1). Notice that the first formula from (1.4) for $\mathbf{V}_E$ only involves the components of $\mathbf{E}$

transversal to $\mathbf{B}_0$. Therefore Eqs. (1.7) and (1.8) are also valid for nonpotential waves with an electric field like

$$\mathbf{E}_\perp = -\nabla_\perp \phi, \quad E_z = -\partial\psi/\partial z, \tag{1.89}$$

where $\psi \neq \phi$. (The subscript $\perp$ indicates the components perpendicular to the equilibrium magnetic field.) Here we also have the wave magnetic field $\widetilde{\mathbf{B}}_\perp$ perpendicular to $\mathbf{B}_0$, this corresponding to the bending of the lines of the total magnetic field $\mathbf{B} = \mathbf{B}_0 + \widetilde{\mathbf{B}}$. According to the Maxwell equations, the field $\mathbf{B}_\perp$ is related to ϕ and ψ by the following equations:

$$\frac{\partial \mathbf{B}_\perp}{\partial t} = -c \frac{\partial}{\partial z} [\nabla(\phi - \psi), \ \mathbf{e}_z]. \tag{1.90}$$

Vortices with $\mathbf{B}_\perp \neq 0$ are one of the types of electromagnetic vortices in magnetized plasma. For such vortices, as noted above, the drift particle motion is strictly incompressible, i.e. div $\mathbf{V}_\mathbf{E} = 0$ (see (1.7)). Another type of electromagnetic vortices is discovered at

$$\operatorname{div} \mathbf{V}_\mathbf{E} \neq 0, \tag{1.91}$$

i.e. in the class of compressible perturbations. The relevant vortices can be termed compressible. However, when speaking of compressible vortices, we, similar to Rossby vortices, assume that the compressibility is weak, i.e. (cf. (1.17))

$$|\operatorname{curl}_z \mathbf{V}_\mathbf{E}| \gg |\operatorname{div} \mathbf{V}_\mathbf{E}|. \tag{1.92}$$

Generally speaking, the problem of compressible vortices should include the z-component of the wave magnetic field $\widetilde{B}_z$

$$\widetilde{B}_z \neq 0. \tag{1.93}$$

In this case, for $\mathbf{V}_\mathbf{E}$ one should use the expression (cf. (1.4))

$$\mathbf{V}_\mathbf{E} = c\,[\mathbf{E}, \ \mathbf{B}]/B^2, \tag{1.94}$$

where $\mathbf{B}$ is the total magnetic field. Equation (1.94) implies that

$$\operatorname{div} \mathbf{V}_\mathbf{E} = -\frac{\mathbf{B}}{B^2}\frac{\partial \mathbf{B}}{\partial t} - c\mathbf{E} \operatorname{curl} \frac{\mathbf{B}}{B^2}. \tag{1.95}$$

In the simplest case of a uniform equilibrium magnetic field, with nonlinear terms neglected, Eq. (1.95) means

$$\operatorname{div} \mathbf{V}_\mathbf{E} = -\frac{1}{B_0}\frac{\partial \widetilde{B}_z}{\partial t}, \tag{1.96}$$

this favouring the above relation between the compressibility conditions for plasma, (1.91), and those for magnetic field, (1.93).

One instance of electromagnetic vortices with $\widetilde{\mathbf{B}}_{\perp} \neq 0$ is the ballooning vortex [1.36]. The latter is specified by the relation

$$\Lambda = \Gamma^2/(U^2 - \alpha^2 C_A^2), \tag{1.97}$$

where C_A is the Alfvén velocity and Γ is defined in Sec. 1.6. The comparison of (1.97) with (1.84) demonstrates that the ballooning vortex is a generalization of the flute vortex to the case of $\alpha \neq 0$.

Another instance of electromagnetic compressible vortices is purely electron gradient vortices (vector and scalar ones) in strongly inhomogeneous plasma treated in [1.37]. The linear dispersion relation for such waves is

$$\omega = \frac{k_y u_n}{1 + c^2 k_{\perp}^2/\omega_{pe}^2}, \tag{1.98}$$

where $u_n = -\varkappa_n c^2 \omega_{Be}/\omega_{pe}^2$ and ω_{pe} is the electron plasma frequency. The vortices of waves like those in (1.98) are described by Eq. (1.24), where the role of function h is played by the quantity $h = \widetilde{B}_z/B_0$, while the operator $\hat{D}$ and the coefficients Λ and S are given by the relations

$$\hat{D} = \frac{\partial}{\partial y} + \frac{c^2 \omega_{Be}}{U \omega_{pe}^2} [\nabla h, \nabla]_z, \tag{1.99}$$

$$\Lambda = \frac{\omega_{pe}^2}{c^2} \left(1 - \frac{u_n}{U}\right), \tag{1.100}$$

$$S = \frac{\omega_{pe}^2 u_n}{2c^2 U}. \tag{1.101}$$

The problem of electromagnetic vortices was also considered in [1.38-1.40]. In [1.38], based on equations derived in [1.27], two-potential vortices with $(\phi, \psi) \neq 0$, $\phi \neq \psi$ (see (1.89)) were studied. The works [1.39, 1.40] continued the studies of ballooning vortices initiated in [1.36]. In [1.39], in place of gravitational force, a real curvilinear magnetic field of the tokamak type was used. In [1.40], a longitudinal perturbed magnetic field, $\widetilde{B}_z \neq 0$, was included, as well as drift and magnetodrift effects due to a finite ion temperature, this being important for plasma with a finite value of β (β is the ratio between plasma and magnetic field pressures).

1.8. CONCLUSION

Thus, as a result of many-years' hydrodynamic studies on Rossby waves and of the plasma physics research on drift waves, common fund of knowledge has emerged that is used and developed by researchers in both fields, hydrodynamics and plasma physics. Above we have traced the history of initiating this fund and have exposed the notions of basic research objects, i.e. vector and scalar vortical structures whose simplest versions are dipole and round solitary vortices.

The notions of the solitary vortices of Rossby and drift waves were formed when the theory of the simpler types of solitary waves described by integrable models, i.e. solitons, was constructed. Therefore, researchers studying solitary vortices wanted to clarify (and still do) to what extent the properties of these vortices are similar to those of ordinary solitons and, in particular, whether collisions between vortices are elastic as is the case with ordinary solitons. The issue has been settled for dipole vortices in the framework of Eq. (1.23) in the papers by Makino *et al.* [1.28] and by Larichev and Reznik [1.41], where the elastic nature of collisions between such vortices has been established by numerical simulation. The collisions between round vortices were studied experimentally [1.17, 1.42] and by numerical simulation within the framework of Eq. (1.21) [1.43, 1.44]. All these investigations have resulted in a conclusion that under rather low relative velocities vortices collide elastically, while at rather high velocities vortices fuse. However, the papers [1.17, 1.42] stress the inelastic nature of vortex interaction. These papers also indicate that the convergence of vortices can result not only in their fusion, but in their destruction and reorganization into a zonal flow as well.

The above-mentioned studies on the interaction between vortices are the outcome of analyzing the problem of vortices within the conventional theory of solitons. However, at the interface of the theory of solitons and the theory of vortices we consider the ordinary solitons within the theory of vortices and can clarify whether some of those soliton types possess vortical properties or not and, in a more narrow context, whether the vector nonlinearity dealt with in Secs. 1.1 and 1.2 is of importance in the problems of ordinary solitons or not. The studies of the vortical properties of ordinary soliton types in magnetized plasma were started in [1.45] where ion-acoustic solitons in magnetized plasma were analyzed (see [1.46]). It was noted in [1.45] that within the theory of vortices such solitons are essentially a version of scalar vortices. The fruitfulness of the "vortical" approach to ion-acoustic solitons has been demonstrated in [1.45] by analyzing the effect of vector nonlinearity on the stability of one-dimensional (plane) ion-acoustic solitons. The stability of such solitons relative to bending perturbations [1.47], with vector nonlinearity neglected, was considered in [1.48]. In this approximation the ion-acoustic solitons proved to be unstable. On allowing for vector nonlinearity, substantial for not too low soliton amplitudes, the bending perturbations become stable. Such a conclusion agrees with the experimental evidence [1.49] about the plane ion-acoustic solitons of sufficiently high amplitude being stable in magnetized plasma.

It was noted in [1.50] that vortical properties are also inherent in magnetoacoustic solitons having characteristic frequencies higher than the ion cyclotron frequency, $\omega > \omega_{Bi}$ (high-frequency magnetoacoustic (HFMA) solitons). In such waves the role of a magnetized plasma component is played by electrons. HFMA vortices are a version of compressible vortices discussed in Sec. 1.7, and the condition of weak compressibility of such vortices, (1.92), coincides with the high-frequency condition $\omega > \omega_{Bi}$. The condition $\omega < \omega_{LH}$ puts an upper bound on the characteristic frequencies of HFMA solitons, ω_{LH} being the lower-hybrid frequency. Following the concepts of the vortical nature of HFMA waves the authors of [1.50] have constructed a three-dimensional nonlinear equation for such waves, with the vector nonlinear effects included. Such an approach is conceptually close to that developed in [1.51-1.53] which investigates the role of vector nonlinearity in the problem of lower-hybrid waves that are a short-wavelength continuation of the HFMA mode. The paper [1.50] elucidates the effect of vector nonlinearity on the stability of one-dimensional HFMA solitons. Such a nonlinearity proved to affect both the growth rate and the excitation condition of instability, yet such an effect is mainly of quantitative rather than qualitative nature.

If vector nonlinearity can be of some importance in the soliton stability problem, then why could not it manifest itself in the stability problem of another type of scalar structures such as cnoidal waves? This question was analyzed in [1.54] for drift waves. It has been shown that for a sufficiently strong vector nonlinearity cnoidal drift waves as well as one-dimensional drift solitons [1.45] are stable. This result can be used in experiments on the laboratory simulation of the spiral branches of galaxies [1.55]. Such an approach can quite naturally explain why rather long spirals do not decay into individual "beads", as it would be within a simplified approach to the stability of scalar vortices [1.56], this explicitly or implicitly ignoring the role of vector nonlinearity.

Standard equations like (1.23) do not allow for some very important factors. One such factor is dissipation. The role of the latter in the problem of Rossby waves can be played by viscosity. In the absence of linear instabilities viscosity, along with dispersion, limits the lifetime of Rossby waves in laboratory experiments [1.16, 1.57]. In the presence of instabilities a mutual compensation of wave buildup and damping can occur and, as a consequence, dissipative nonlinear structures will be formed. Such dissipative stationary structures under the conditions of the Kelvin-Helmholtz instability due to an inhomogeneity in the zonal flow velocity profile were observed in [1.58, 1.59]. A chain of dissipative Rossby solitons [1.58] and a solitary dissipative Rossby vortex [1.59] were observed. According to an assumption made in [1.59], such a dissipative vortex models Jupiter's Great Red Spot (GRS). This approach to the nature of Jupiter's GRS has something in common with an analogous approach from [1.26], which stresses the important role played in the GRS problem by both the velocity profile inhomogeneity and viscosity.

The authors of [1.59] called the dissipative soliton observed by them a Rossby auto-soliton, thus underlining the relation between the physics of Rossby waves in a dissipative-unstable fluid and the physics of auto-waves in other nonlinear dissipative-unstable systems [1.60, 1.61]. Such an approach [1.59] facilitates further understanding of the role of auto-wave processes in the problem of Rossby waves. It is only natural that a certain role must be played by the auto-wave processes in plasma vortices either, since plasma is characterized both by the abundance of instabilities and by the diversity of dissipative factors. However, when speaking not of plasma in general but of a high-temperature plasma specific for magnetic thermonuclear confinement systems (e.g. tokamaks), we can state that, in the present state-of-the-art, the analysis of instabilities and dissipative factors in the problem of waves in such a plasma has revealed no wave modes interesting for the theory of auto-waves. In the high-temperature plasma, waves that are aperiodically unstable in the linear approximation (e.g. flute ones) are feasible, yet the role of dissipation in such waves is of little significance. There are a few types of waves responsible for resistive magnetohydrodynamic (MHD) instabilities [1.62, 1.63], but it is not clear whether auto-waves can be associated with the latter.

As to drift waves, there the role of dissipation is similar to that of viscosity in stable Rossby waves with the only distinction that the dissipation sign can be both positive (conventional dissipation) and negative (the analogue of negative viscosity in hydrodynamics [1.64]). Negative dissipation in a plasma is due to its thermodynamic nonequilibrium state (i.e. plasma inhomogeneity across magnetic field), the presence of beams, an anisotropy in particle velocity distribution and some other factors [1.2, 1.34]. The simplest manifestation of dissipation in drift waves is the interaction of the latter with resonant electrons. Such an interaction, as has been established in [1.1], results in drift instabilities. An important issue in the problem of drift vortices is whether the resonance interaction of electrons or some other dissipative factors can cause the buildup of vortices, i.e. it is the issue of the drift instability of vortices. The first steps in this direction have been made in [1.65, 1.66].

It is vital for the concept of solitary vortices in magnetized plasma, i.e. that of gradient solitons, that the existence of such solitons be experimentally verified. As to experiments on gradient solitons we should turn many years back to pay tribute to observations made by Buchel'nikova *et al.* [1.67]. The aim of these experiments was to study a turbulence that arises during the development of a drift instability. However, the authors of [1.67] conclude that under their experimental conditions the drift instability results not in the turbulence but rather in the regular sawtooth oscillations, i.e. in the language of the modern nonlinear theory, the drift instability results in a chain (or a lattice) of solitons. The regular behaviour of the gradient waves was also noted in experiments on the high-frequency centrifugal drift instability [1.68] and on the beam-drift instability [1.69] (see also [1.70]). However, the relation between these waves and gradient solitons was not discussed in the above papers, because in those times the concepts of such solitons had not been formed. (As to the corresponding types of gradient solitons, see [1.33, 1.71].) Of the modern experimental papers, the studies of convective cells [1.72] are the most relevant to the issue of solitary plasma vortices. In [1.72], a nonlinear interaction between two convective cells of the same or opposite polarities is considered. In the problem of solitary vortices, as is evident from the preceding exposition, of major importance is the localizing role of nonlinearity. However, this issue has not been discussed in [1.72]. The experimental verification of the existence of solitary plasma vortices similar to hydrodynamic Rossby solitons would be one of the most fundamental achievements in plasma physics.

References

1.1. L. I. Rudakov and R. Z. Sagdeev, *Dokl. Akad. Nauk SSSR*, 138, 581 (1961).

1.2. A. B. Mikhailovskii, *The Theory of Plasma Instabilities*, Vol. 2, Consultants Bureau, New York, 1974.

1.3. A. B. Mikhailovskii, in: *Basic Plasma Physics*, Vol. 1, ed. A. A. Galeev and R. N. Sudan, North-Holland, Amsterdam, 1983, p. 587.

1.4. N. S. Buchel'nikova, *The Studies of Plasma Turbulence under Some Instabilities*, Izd. IYaF SO AN SSSR, Novosibirsk, 1970 (in Russian).

1.5. N. D'Angelo, in: *Advances in Plasma Physics*, Vol. 2, ed. A. Simon and W. B. Thompson, Intersc. Publ., New York, 1969.

1.6. W. Horton, in: *Basic Plasma Physics*, Vol. 2, ed. A. A. Galeev and R. N. Sudan, North-Holland, Amsterdam, 1984.

1.7. G. K. Morikawa, *J. Meteorol.*, 17, 148 (1960).

1.8. S. G. Rossby, *J. Marine Res.*, 2, 38 (1939).

1.9. A. Hasegawa, C. G. Maclennan, and Y. Kodama, *Phys. Fluids*, 22, 2122 (1979).

1.10. B. B. Kadomtsev, *Zh. Eksp. Teor. Fiziki*, 45, 1230 (1963).

1.11. B. B. Kadomtsev, *Plasma Turbulence*, Academic Press, London, 1965.

1.12. H. Okuda and J. M. Dawson, *Phys. Fluids*, 16, 408 (1973).

1.13. R. Z. Sagdeev, V. D. Shapiro, and V. I. Shevchenko, *Fizika Plazmy*, 4, 551 (1978).

1.14. P. K. Shukla, M. Y. Yu, H. U. Rahman, and K. H. Spatschek, *Phys. Reports*, 105, 227 (1984).

1.15. V. D. Larichev and G. M. Reznik, *Dokl. Akad. Nauk SSSR*, 231 1077 (1976).

1.16. S. V. Antipov, M. V. Nezlin, E. N. Snezhkin, and A. S. Trubnikov, *Zh. Eksp. Teor. Fiziki*, 82, 145 (1982).

1.17. S. V. Antipov, M. V. Nezlin, V. K. Rodionov, E. N. Snezhkin, and A. S. Trubnikov, *Zh. Eksp. Teor. Fiziki*, 84, 1357 (1983).
1.18. J. G. Charney, *Geophys. Publ. Kosjones Nors. Videnshap. Acad. Oslo*, 17, 3 (1948).
1.19. E. N. Mikhailova and N. B. Shapiro, *Izv. Akad. Nauk SSSR, Ser. Fiz. Atm. i Okeana*, 16, 823 (1980).
1.20. V. I. Petviashvili, *Pis'ma Zh. Eksp. Teor. Fiziki*, 32, 632 (1980).
1.21. A. S. Volokitin and V. V. Krasnosel'skikh, *Dokl. Akad. Nauk SSSR*, 260, 588 (1981).
1.22. A. Hasegawa and K. Mima, *Phys. Rev. Lett.*, 39, 205 (1977).
1.23. A. Hasegawa and K. Mima, *Phys. Fluids*, 21, 87 (1978).
1.24. A. L. Berestov, *Izv. Akad. Nauk SSSR, Ser. Fiz. Atm. i Okeana*, 15, 648 (1979).
1.25. V. M. Kamenkovich, M. N. Koshlyakov, and A. S. Monin, *The Synoptical Vortices in Ocean*, Gidrometeoizdat, Moscow, 1982, p. 63 (in Russian).
1.26. R. Z. Sagdeev, V. D. Shapiro, and V. I. Shevchenko, *Pis'ma Astron. Zhurn.*, 7, 505 (1981).
1.27. A. B. Mikhailovskii, V. P. Lakhin, L. A. Mikhailovskaya, and O. G. Onishchenko, *Zh. Eksp. Teor. Fiziki*, 86, 2061 (1984).
1.28. M. Makino, T. Kamimura, and T. Taniuti, *J. Phys. Soc. Japan*, 50, 980 (1981).
1.29. Yu. A. Danilov and V. I. Petviashvili, in: *Itogi Nauki i Tekhniki, Ser. Fiz. Plazmy*, Vol. 4, VINITI, Moscow, 1983, p. 5.
1.30. A. B. Mikhailovskii, V. R. Kudashev, V. P. Lakhin, L. A. Mikhailovskaya, A. I. Smolyakov, and S. Yu. Shishkov, *Pis'ma Zh. Eksp. Teor. Fiziki*, 40, 273 (1984).
1.31. J. D. Meiss and W. Horton, *Phys. Fluids*, 26, 990 (1983).
1.32. V. P. Pavlenko and V. I. Petviashvili, *Fizika Plazmy*, 9, 1034 (1983).
1.33. G. D. Aburdzhaniya, F. F. Kamenets, V. P. Lakhin, A. B. Mikhailovskii, and O. G. Onishchenko, *Phys. Lett.*, 105A, 48 (1984).
1.34. A. B. Mikhailovskii, *Theory of Plasma Instabilities*, Vol. 1, Consultants Bureau, New York, 1974.
1.35. A. B. Mikhailovskii, G. D. Aburdzhaniya, O. G. Onishchenko, and S. E. Sharapov, *Phys. Lett.*, 104A, 94 (1984).
1.36. A. B. Mikhailovskii, G. D. Aburdzhaniya, O. G. Onishchenko, and S. E. Sharapov, *Phys. Lett.*, 100A, 503 (1984).
1.37. A. B. Mikhailovskii, V. P. Lakhin, and L. A. Mikhailovskaya, *Zh. Eksp. Teor. Fiziki*, 87, 1221 (1984).
1.38. A. B. Mikhailovskii, V. P. Lakhin, and L. A. Mikhailovskaya, *Fizika Plazmy*, 11, 836 (1985).
1.39. A. B. Mikhailovskii, V. P. Lakhin, and V. A. Marchenko, *Fizika Plazmy*, 11, 633 (1985).
1.40. V. N. Ivanov and A. B. Mikhailovskii, *Fizika Plazmy*, 11, 477 (1985).
1.41. V. D. Larichev and G. M. Reznik, *Dokl. Akad. Nauk SSSR*, 264, 229 (1982).
1.42. S. V. Antipov, M. V. Nezlin, V. K. Rodionov, E. N. Snezhkin, and A. S. Trubnikov, *Pis'ma Astron. Zhurn.*, 9, 58 (1983).
1.43. V. I. Petviashvili and A. P. Smirnov, *Dokl. Akad. Nauk SSSR*, 277, 88 (1984).
1.44. V. P. Pavlenko and V. B. Taranov, *Fizika Plazmy*, 10, 1303 (1984).
1.45. A. B. Mikhailovskii, V. P. Lakhin, O. G. Onishchenko, and A.I. Smolyakov, *Zh. Eksp. Teor. Fiziki*, 88, 798 (1985).
1.46. V. E. Zakharov and E. A. Kuznetsov, *Zh. Eksp. Teor. Fiziki*, 66, 594 (1974).

1.47. B. B. Kadomtsev and V. I. Petviashvili, *Dokl. Akad. Nauk SSSR*, 192, 753 (1970).
1.48. K. H. Spatschek, P. K. Shukla, and M.Y. Yu, *Phys. Lett.*, 54A, 419 (1975).
1.49. L. Schott, *Phys. Fluids*, 23, 147 (1980).
1.50. A. B. Mikhailovskii, G. D. Aburdzhaniya, O. G. Onishchenko, and A. I. Smolyakov, *Zh. Eksp. Teor. Fiziki*, 89, 482 (1985).
1.51. S. L. Musher and B. I. Sturman, *Pis'ma Zh. Eksp. Teor. Fiziki*, 22, 537 (1975).
1.52. V. I. Sotnikov, V. D. Shapiro, and V. I. Shevchenko, *Fizika Plazmy*, 4, 450 (1978).
1.53. A. Sen, C. F. F. Karney, G. L. Johnson, and A. Bers, *Nucl. Fusion*, 18, 171 (1978).
1.54. A. B. Mikhailovskii, S.V. Makurin, and A.I. Smolyakov, *Zh. Eksp. Teor. Fiziki*, 89, 1603 (1985).
1.55. A. G. Morozov, M. V. Nezlin, E. N. Snezhkin, and A. M. Fridman, *Pis'ma Zh. Eksp. Teor. Fiziki*, 39, 504 (1984).
1.56. V. I. Petviashvili and V. V. Yan'kov, *Dokl. Akad. Nauk SSSR*, 267, 825 (1982).
1.57. R. A. Antonova, G. P. Zhvaniya, D. G. Lominadze, D. I. Nanobashvili, and V. I. Petviashvili, *Pis'ma Zh. Eksp. Teor. Fiziki*, 37, 545 (1983).
1.58. M. V. Nezlin, E. M. Snezhkin, and A. S. Trubnikov, *Pis'ma Zh. Eksp. Teor. Fiziki*, 36, 190 (1982).
1.59. S. V. Antipov, M. V. Nezlin, and A. S. Trubnikov, *Pis'ma Zh. Eksp. Teor. Fiziki*, 41, 25 (1985).
1.60. B. S. Kerner and V. V. Osipov, *Zh. Eksp. Teor. Fiziki*, 83, 2201 (1982).
1.61. A. V. Gaponov-Grekhov and M. I. Rabinovich, in: *Physics of the 20th Century* (Development and Prospects), Nauka, Moscow, 1984, p. 219 (in Russian).
1.62. A. B. Mikhailovskii, *Plasma Instabilities in Magnetic Confinement Systems*, Atomizdat, Moscow, 1978 (in Russian).
1.63. R. B. White, in: *Basic Plasma Physics*, Vol. 1, ed. A. A. Galeev and R. N. Sudan, North-Holland, Amsterdam, 1983, p. 611.
1.64. V. P. Starr, *Physics of Negative Viscosity Phenomena*, McGraw-Hill, New York, 1968.
1.65. G. D. Aburdzhaniya, A. B. Mikhailovskii, and S. E. Sharapov, *Phys. Lett.*, 100A, 134 (1984).
1.66. G. D. Aburdzhaniya, A. B. Mikhailovskii, and S. E. Sharapov, *Plasma Phys. Contr. Fusion*, 26, 603 (1984).
1.67. N. S. Buchel'nikova, R. A. Salimov, and Yu. I. Eidel'man, *Zh. Eksp. Teor. Fiziki*, 52, 837 (1967).
1.68. V. G. Marinin, *Ukr. Fiz. Zh.*, 13, 1872 (1968).
1.69. M.V. Nezlin, M. I. Taktakishvili, and A. S. Trubnikov, *Zh. Eksp. Teor. Fiziki*, 55, 397 (1968).
1.70. M. V. Nezlin, *The Dynamics of Beams in Plasma*, Energoizdat, Moscow, 1982 (in Russian).
1.71. G. D. Aburdzhaniya, V. P. Lakhin, and A. B. Mikhailovskii, *Fizika Plazmy*, 11, 1262 (1985).
1.72. H. L. Pecseli, J. J. Rasmussen, and K. Thomsen, *Phys. Rev. Lett.*, 52, 2148 (1984).

2

Oscillations and Bifurcations in Reversible Systems

V. I. Arnol'd, Corr. Mem. USSR Acad. Sc. and
M. B. Sevryuk

2.1. INTRODUCTION

A typical example of a reversible system is the equation

$$\ddddot{x} + A\ddot{x} + Bx + C\dot{x}^2 = 0 \tag{2.1}$$

invariant under the sign change of the independent variable. This equation describes various physical phenomena (see, e.g. the papers by Demekhin [2.19] on a viscous fluid draining off along an inclined plane or by Malomed and Tribel'skii [2.20, 2.28] on the evolution of the fronts of some non-equilibrium first-kind phase transitions, e.g. of the gas combustion or the laser evaporation of a condensed substance). Equation (2.1) with the fixed coefficients A, B, and C has a one-parameter family of cycles. Such families are typical of Hamiltonian systems, while the cycles in the phase space of general non-Hamiltonian systems are, as a rule, isolated.

The similarity between Hamiltonian and reversible systems is not confined to uniting the cycles into families but extends much farther. For example, the evolution of a reversible system near an equilibrium position or a periodic motion is described by the same Birkhoff series as in the case of Hamiltonian systems. For reversible systems an analogue of the Lyapunov theorem is valid that concerns strictly periodic oscillations of a multidimensional nonlinear Hamiltonian system around the equilibrium position in the nonresonant elliptic case. Also coincident are the equations of phase oscillations near resonances and the normal forms of bifurcations. Finally, in the phase space of a reversible system the same invariant Kolmogorov tori can be found as in the case of Hamiltonian systems.

The present paper begins with the definition of reversible systems with discrete and continuous times (Secs. 2.2 and 2.3). Then integrable reversible systems (Sec. 2.4) and their small perturbations (Sec. 2.5) are considered. The results obtained are carried over to a more general class of "weakly reversible" systems (Sec. 2.6). Then we investigate the equilibrium position neighbourhood of reversible (Sec. 2.7) and weakly reversible (Sec. 2.8) systems and study the symmetric, strictly periodic oscillations in reversible systems (Sec. 2.9). A neighbourhood of a closed symmetric trajectory of a reversible system is treated in Sec. 2.12 and appropriate preliminary remarks are exposed in Secs. 2.10 and 2.11. At the beginning we study all phenomena in the simplest situation of a minimum number of degrees of freedom and then turn to a general multidimensional case as well as to a non-autonomous one (Sec. 2.13).

The paper concludes in a study of the bifurcations of the families of low-amplitude periodic motions of reversible systems oscillating near equilibrium when passing through resonances between small oscillation frequencies. This study reveals unexpected relations of the object at hand with the theory of singularities of differentiable mappings (e.g. in analyzing the resonance 1:1 there emerges the Whitney umbrella) and leads to new results in this general theory (e.g. a rearrangement of the umbrella's cross sections).

The first coauthor is responsible for the statement of the problem, the study of the solutions of reversible systems in the case of small dimensions [2.1] and the formulations of hypotheses on a multidimensional case as well as on the bifurcation normal forms for the families of the low-amplitude periodic motions of reversible systems around the equilibrium position when passing through the resonance 1:1 (Sec. 2.15). The expedience of generalizing the concept of reversibility to that of weak reversibility was also noted in [2.1]. The transfer of the results from [2.1] to the multidimensional case (as well as to the case of an odd-dimensional phase space) and the derivation of proofs were carried out by the second coauthor. The results of Sec. 2.16 (where the passage through further resonances $1:N$, $N \geqslant 2$ is studied) and the proofs of the theorems exposed in Sec. 2.15 are also his.

2.2. REVERSIBLE MAPPINGS

Definition. A diffeomorphism $G : M \to M$ of a phase space M onto itself is called an involution if its square is an identical transformation, $G^2 = \mathrm{id}$. The most important is the following example.

Example. The reflection of an Euclidean space $\mathbb{R}^{m+k}$ with respect to a subspace $\mathbb{R}^m$,

$$G : (p, q) \mapsto (p, -q),$$

where $p \in \mathbb{R}^m$, $q \in \mathbb{R}^k$, is an involution.

Locally (i.e. in a neighbourhood of a fixed point) any involution can be written in such a form under an appropriate choice of coordinates (Bochner's theorem).

Definition. A diffeomorphism $A : M \to M$ is called reversible with respect to an involution G if G conjugates A with A^{-1}, i.e. $A^{-1} = GAG$.

Example. A plane rotation is reversible since, by a reflection with respect to a straight line passing through the rotation centre, this rotation is transformed into the inverse one. The same holds for a rotation through a variable (dependent on radius) angle: $(r, \varphi) \to (r, \varphi + \gamma(r))$.

The reversibility condition $A^{-1} = GAG$ that can be rewritten as $AGAG = \mathrm{id}$ shows that AG is an involution and, thus, any reversible diffeomorphism $A = (AG)G$ is a product of two involutions. A converse theorem is also evident:

Theorem (Birkhoff [2.3]). A product of two involutions is reversible with respect to any of them.

Proof. If $\sigma^2 = \tau^2 = \mathrm{id}$, then $\sigma(\sigma\tau)\sigma(\sigma\tau) = \tau(\sigma\tau)\tau(\sigma\tau) = \mathrm{id}$.

Pairs of involutions (and, consequently, reversible mappings) appear in different branches of mathematics (see in [2.1] the discussion of the Birkhoff billiard transformation ([2.4] and [2.5], Ch. 6, §§ 6-9) and of the Melrose billiard transformation [2.6], and pairs of involutions emerging in the studies of discontinuous differential equations[*] and in the problem of a holomorphic classification of real surfaces in a plane of two complex variables [2.7]).

A reversible mapping can be considered as an action of the symmetry group of arithmetic progression. Indeed, this group consists of translations and reflections, where a reflection acts as an involution reversing the action of a translation.

Definition. Given a certain group H, the action of this group on the phase space by diffeomorphisms is called a dynamic system whose time is H.

From this viewpoint, a reversible mapping is a dynamic system whose time is the symmetry group of arithmetic progression.

2.3. REVERSIBLE FLOWS

Definition. A reversible flow is a dynamic system whose time is the real line symmetry group.

In other words, a reversible flow is specified by a one-parameter group of phase space diffeomorphisms that transforms into the group of inverse diffeomorphisms under a certain phase space involution.

Under this involution the velocity field of a reversible flow transforms into the opposite field.

Definition. A vector field V changing its sign due to an involution G, $G_* V = -V$ (and a differential equation specified by the field), is called reversible (with respect to this involution).

Thus, the velocity field of a reversible flow is reversible too. The converse is also true.

Example 1. The differential equation

$$\dot{z} = \sum_{l,s} a_{l,s} z^l \bar{z}^s$$

---

[*] *Teixeira*, private communication (1982).

in the plane of the variable z is reversible with respect to the involution $z \mapsto \bar{z}$ of complex conjugation if and only if all the coefficients $a_{l,s}$ are pure imaginary (Fig. 2.1*a*).

Example 2. The differential equations $\dot{z} = \bar{z}$ and $\dot{z} = z^2$ (Figs. 2.1*b* and 2.1*c*) in the z-plane are also reversible (the corresponding involutions are the reflections with respect to the straight lines $\operatorname{Re} z = \operatorname{Im} z$ and $\operatorname{Re} z = 0$).

Example 3. The system of the Newtonian equations, $\ddot{x} = F(x, \dot{x})$, is reversible if forces are independent of velocities or are even in velocities, $F(x, -y) = F(x, y)$ (a phase space involution changes the signs of all velocities).

Example 4. An even-order equation is reversible if it is autonomous and if odd derivatives enter into it only in even combinations (a phase space involution changes the signs of all odd derivatives). In particular, Eq. (2.1) is reversible.

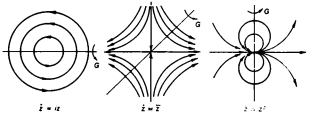

Fig. 2.1

Note that in all instances of reversible systems and mappings mentioned above the phase space dimension was even and the manifold of fixed points of the involution had a middle dimension.

2.4. INTEGRABLE REVERSIBLE MAPPINGS AND VECTOR FIELDS

As a plane rotates through a variable (dependent on radius) angle around the origin, each circle centered in the origin is invariant both under a mapping itself and an involution reversing it, the restriction of the mapping to any such circle being a conventional rotation.

Generalizing this example to higher dimensions we will give the following definition.

Definition. A reversible mapping (vector field) with the phase space D of an even dimension $2m$ is called integrable if D is foliated into m-dimensional tori invariant under both the mapping itself (the vector field itself) and the involution reversing the mapping (the vector field), the initial mapping (vector field) inducing a quasi-periodic motion on each torus.

By a suitable choice of coordinates each integrable reversible mapping can be written in the form

$$(\varphi, I) \mapsto (\varphi + \omega(I), I)$$

and each integrable reversible differential equation, in the form

$$\dot{\varphi} = \omega(I), \ \dot{I} = 0,$$

in both cases the involution is

$$(\varphi, I) \mapsto (-\varphi, I), \tag{2.2}$$

where $I = (I_1, \ldots, I_m)$ is the torus parameter (an analogue of the action variable in integrable Hamiltonian systems), $\varphi = (\varphi_1, \ldots, \varphi_m)$ is the angular variable on each torus $I = \text{const}$, and $\omega_1(I), \ldots, \omega_m(I)$ are the frequencies.

An integrable reversible mapping (vector field) is called nondegenerate if nondegenerate is the frequency mapping $I \mapsto \omega(I)$, i.e. $\partial\omega/\partial I \neq 0$. Here, after an appropriate renumbering of invariant tori, the initial mapping can be written as

$$(\varphi, I) \mapsto (\varphi + I, I) \tag{2.3}$$

and, respectively, the vector field, in the form

$$\dot{\varphi} = I, \ \dot{I} = 0, \tag{2.3'}$$

with the reversing involution here being that of (2.2). Indeed, the form (2.3), or (2.3′), is used to write the mapping (vector field) in a certain region of the variation of I.

2.5. KOLMOGOROV'S TORI

It happens that in the phase space of a reversible mapping (vector field) that is close to a nondegenerate integrable one invariant (Kolmogorov's) tori exist on which a quasi-periodic motion is again induced (this is fully analogous to the effects arising in the Hamiltonian case).

Theorem. Let be given a nondegenerate integrable and reversible mapping (2.3) or vector field (2.3′) with a reversing involution (2.2). Let us consider a small perturbation of the mapping

$$(\varphi, I) \mapsto (\varphi + I + f(\varphi, I),\ I + g(\varphi, I)), \tag{2.4}$$

and, respectively, that of the vector field

$$\dot{\varphi} = I + f(\varphi, I), \quad \dot{I} = g(\varphi, I). \tag{2.4′}$$

as well as that of the reversing involution

$$(\varphi, I) \mapsto (-\varphi + \tilde{f}(\varphi, I),\ I + \tilde{g}(\varphi, I)). \tag{2.5}$$

such that (2.4), or (2.4′), is reversible (with respect to the involution (2.5)) as before.

Then, if the perturbations f, g, $\tilde{f}$, and $\tilde{g}$ are analytical and sufficiently small, the majority of the invariant tori $I = \text{const}$ of the mapping (2.3) (vector field (2.3′)) under such a perturbation will not decay but only slightly deform. Namely, those tori do not decay which participated in the quasi-periodic motion with "strongly incommensurable" frequencies. On the deformed (Kolmogorov's) tori invariant under both the perturbed mapping (2.4), or the differential equation (2.4′), and the reversing involution (2.5) a quasi-periodic motion is again induced having the same set of frequencies.

For vector fields the theorem was enunciated by Moser in [2.8] and proved by him in [2.9], Secs. 5, 6. It is essential for Moser's proof that the perturbation of the initial integrable and reversible differential equation is not simply small but dependent on the small parameter ε ($\varepsilon = 0$ corresponds to the unperturbed equation). The applications are discussed in [2.8].

The smaller the perturbation the larger the union measure of all Kolmogorov's tori.

For reversible vector fields in a plane (i.e. for a two-dimensional phase space) all those invariant circles do not decay the frequencies of motion along which are sufficiently high and, consequently, the perturbation of a nondegenerate integrable and reversible vector field in the plane remains integrable.

The proof of the theorem is based on the standard (Kolmogorov's) method of constructing an infinite sequence of Newtonian approximations, i.e. changes of variables whose definition domains are more and more contracted to the deformed torus sought for. At each iteration step one has to solve a certain homological equation and it is the verification of its solvability for which one uses the reversibility of the objects considered. An obstruction for the solvability is due to the one-dimensional cohomology of a certain algebraic system (in particular, for discrete time, the cohomology of the group generated by the unperturbed reversible diffeomorphism and by the involution reversing the latter) which thus is trivial.

2.6. WEAK REVERSIBILITY

Many properties of reversible objects are typical of those mappings (vector fields) which transform into the inverse ones (opposite) under the action of some phase space diffeomorphism being not necessarily an involution. Such mappings (vector fields) will be called weakly reversible. Thus, a phase space diffeomorphism A is weakly reversible with respect to another phase space diffeomorphism G if $A^{-1} = GAG^{-1}$ and a vector field V (or the differential equation $\dot{x} = V(x)$) is weakly reversible with respect to some phase space diffeomorphism G, if $G_* V = -V$.

If the given mapping or vector field is reversed by a diffeomorphism G, it is reversed by the diffeomorphism G^{-1} too. If a vector field is weakly reversible with respect to a certain phase space diffeomorphism, then the mapping of the phase flow of this field at any fixed time will be also weakly reversible with respect to the same diffeomorphism (and vice versa).

Kolmogorov's tori prove to exist also in the case when the perturbation of a nondegenerate integrable and reversible mapping (vector field) is assumed to be not reversible but only weakly reversible. In other words, the requirement of the diffeomorphism (2.5) reversing the mapping (2.4) (the vector field (2.4′)) to be involutary is not a necessary one. Moreover, here the restriction of (2.5) to each invariant Kolmogorov's torus of the perturbed mapping (vector field) is an involution. Therefore, if the perturbation is sufficiently small and, consequently, the union measure of invariant tori is positive, then, with analyticity included, this suggests that (2.5) is an involution. In other words, a small, weakly reversible perturbation of a nondegenerate integrable and reversible mapping (vector field) is always a "true" reversible one.

2.7. THE LOCAL THEORY

The theorem of Kolmogorov's tori of reversible mappings (vector fields) has a local analogue, i.e. the presence of invariant tori in a neighbourhood of the equilibrium position.

Consider, e.g. a reversible mapping of a plane in a neighbourhood of a fixed point (the point is also assumed to be fixed with respect to the involution reversing the given mapping).

Depending on the eigenvalues of linearization at the fixed point a general reversible mapping can be hyperbolic (the linearization is a hyperbolic rotation) or elliptic (the linearization is a conventional rotation). The eigenvalues 1 or -1 are of a nongeneral position. Consider the elliptic case in more detail.

Depending on the linearization rotation angle at a fixed point a mapping is called nonresonant (the angle is incommensurable with 2π) or resonant of order q (the angle is $2\pi p/q$).

The formal normal form for a nonresonant mapping is a rotation through an angle varying with radius. Here the fixed point is formally stable since it is surrounded by formally invariant curves.

It appears that a general analytical reversible elliptic mapping of a plane (both in the nonresonant case and in the case of a resonance of order $q \geqslant 5$) also has, in any neighbourhood of a fixed point, "genuine" (and not only formal) invariant Kolmogorov's curves which surround the fixed point. The curves are also invariant under the involution reversing the mapping. The mapping rotation number on such a curve is irrational. As a consequence, we obtain that the fixed point of a general reversible elliptic mapping of a plane is stable.

Remark 1. Here the word "general" means that by no substitution the 3-jet (a cubic Taylor polynomial) of the mapping can be reduced to its linear part (the 1-jet). For any $q \geqslant 3$ there exist examples of reversible elliptic, resonant of order q diffeomorphisms of a plane which do not satisfy this condition and whose fixed point is unstable (analogous examples for Hamiltonian (symplectic) mappings see in [2.11], § 31).

Remark 2. It is well known (see, e.g. [2.10] or [2.11], §§ 32-34) that invariant curves in a neighbourhood of a fixed point (or in an annular domain) exist for any general mapping of the plane that possesses the intersection property, i.e. the image of any curve surrounding the fixed point intersects this curve. For Hamiltonian diffeomorphisms of a plane this property is fulfilled automatically, since the figures bounded by such a curve and its image have the same area. At the same time the examples are known of the reversible diffeomorphisms of a plane which do not have the intersection property in any neighbourhood of the point fixed with respect to the diffeomorphism itself as well as to the involution reversing the latter.

Example (M.B. Sevryuk). Let us denote as ψ a smooth function $\mathbb{R} \to \mathbb{R}$ defined as $\psi(t) = t + c\exp(-t^{-2})\sin t^{-1}$ for $t \neq 0$ and $\psi(0) = 0$, where

$$0 < c < \left(\max_{t \neq 0} \left| \frac{d}{dt} \exp(-t^{-2}) \sin t^{-1} \right| \right)^{-1}.$$

The function strictly increases on the whole real line and has an inverse smooth function ψ^{-1}.

Let us introduce in a plane a Cartesian coordinate system (x, y) and consider a mapping $(x, y) \mapsto (\psi(x), \psi^{-1}(y))$. The latter is reversible with respect to an involution $(x, y) \mapsto (y, x)$.

If a and b are positive numbers such that $\psi(a) < a$ and $\psi(b) > b$ (a and b can be chosen however small), then the mapping transforms a rectangle with the apices (a, b), $(-a, b)$, $(-a, -b)$, $(a, -b)$ into another rectangle lying strictly inside the initial one.

At the fixed point all the constructed diffeomorphisms of such a kind lose analyticity (and only remain smooth), while the eigenvalues of their linearization are 1 or -1. It is unknown whether there are elliptic (let them be even non-analytical) reversible mappings not possessing the intersection property.

Let us return to a general elliptic mapping of a plane. The fixed zero point of the mapping is surrounded by invariant curves. Be-

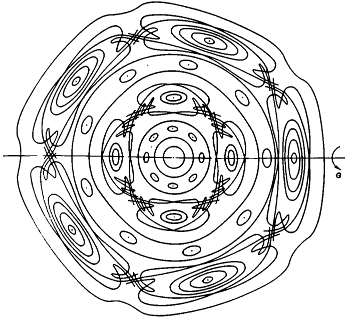

Fig. 2.2

tween the curves there are annular resonance zones which are left due to the decay of the formal invariant curves with rational rotation numbers p/q (the resonance p/q zones). A qth mapping iteration in such a zone differs but slightly from the transformation of the phase flow of a reversible vector field invariant under the rotation through the angle $2\pi/q$ and having a nonconstant first integral. As for the Hamiltonian case, these resonance zones contain cycles (fixed points of the qth iteration of the mapping).

More precisely, such zones exist in any neighbourhood of zero. In each of them two cycles (let us call them nodes) necessarily lie on the curve of fixed points of a reversing involution G on either side of zero. Any iteration A^n of the mapping A transforms a node into a point also fixed with respect to A^q, and in a neighbourhood of the latter an involution A^nGA^{-n} acts reversing A^q and leaving this point fixed.

If q is odd, the number of distinct images of the nodes, with the mapping A iterated, is $2q$ (the images of one of the nodes and of the other in going round zero alternate), and if q is even then the above number is q (since for an even q the mapping $A^{q/2}$ transforms the nodes into one another).

However, with A iterated, for an even q placed between any two adjacent (in going round zero) images of the nodes, there exists at least one additional cycle. (Note that for an odd q the resonance zone p/q can also contain the fixed points of A^q that are not the nodal images when A is iterated.) Thus, the total number of the fixed points of the qth iteration of the general mapping A in the resonance zone p/q is no less than $2q$ (for any evenness of q). Overall, the picture of the invariant curves of the iterations of A in a neighbourhood of zero is as shown in Fig. 2.2 (the same as in the Hamiltonian case).

Analogously is arranged the resonance zone p/q in a more general situation of a reversible mapping close to a nondegenerate integrable one in an annular domain.

Consider now a multidimensional case: a reversible mapping of an Euclidean space $\mathbb{R}^{2m}$ $(m \geqslant 2)$ in a neighbourhood of a fixed point lying on an m-dimensional manifold of an involution fixed points. Assume that this mapping is elliptic (i.e. its linearization at a fixed point is a direct product of m rotations) and general (linearization rotation angles have no resonance relation of low order, while the frequencies of motion on the invariant tori of a formal normal form are dependent in a nondegenerate way on the variables numbering the tori).

Then, as in the two-dimensional case, in any neighbourhood of the fixed point, m-dimensional (Kolmogorov's) tori exist that are invariant under both the mapping itself and the involution reversing the latter. The initial mapping on the tori induces a quasi-periodic motion with a discrete time (the proximity to a fixed point plays here, i.e. in the local situation, the role of the smallness of the integrable diffeomorphism perturbation). Resonance zones lie between Kolmogorov's tori.

Let us turn to the case of continuous time, i.e. to reversible flows in a neighbourhood of a singular point fixed under a reversing involution. The isolated singular points of a linear reversible vector field in a plane can only be centres (an example: $\dot{z} = iz$) and saddles (an example: $\dot{z} = \bar{z}$), besides the saddles must be "equilateral" (their eigenvalues are $\pm\lambda$). Moreover, the centre is conserved (transforming neither into a focus nor into a centrefocus) on accounting for the nonlinear terms of the reversible vector field too, since the attractors in a reversible system that intersect the manifold of involution fixed points are impossible (because under time inversion attraction transforms into repulsion). The closed phase curves of such a centre (into which a punctured neighbourhood of a fixed point is foliated) are invariant under involution.

Remark 1. The example $\dot{z} = z^2$ shows that in degenerate cases a reversible system can have no first integral nonconstant in a neighbourhood of a singular point and can conserve no integral invariant with positive density.

Remark 2. An example of an irreversible degenerate Hamiltonian system can be also readily constructed. Let a Hamiltonian H in a plane with the coordinates (x, y) be the product of five linear homogeneous functions, i.e. $H(x, y) = \prod_{i=1}^{5} (a_ix + b_iy)$. If a system with such a Hamiltonian is reversible then the union of the straight lines $a_ix + b_iy = 0$, $i = 1, \ldots, 5$, is invariant under a reversing involution, this being possible only for the exclusive fives $(l_1, \ldots, l_5)$ of straight lines (cross ratios of the fours of the straight lines l_1, l_2, l_3, l_4 and l_1, l_2, l_3, l_5 are independent invariants of the five with respect to the group of linear transformations of a plane and for the "symmetric" fives, invariant with respect to some involution, these two cross ratios are related by a functional dependence).

In a multidimensional case, reversible vector fields in a neighbourhood of a singular point fixed under a reversing involution behave like reversible diffeomorphisms. If the linearization of such a field at a singular point $0 \in \mathbb{R}^{2m}$ $(m \geqslant 2)$ is a direct product of m linear fields with a singular point of the centre type (an elliptic field), then under common nondegeneracy conditions in any neighbourhood of zero there exist m-dimensional (Kolmogorov's) tori invariant under both the phase flow and the involution, and the motion on these tori is quasi-periodic.

Different local versions of the theorem on Kolmogorov's tori for reversible systems of differential equations were analyzed by Bibikov and Pliss (see, e.g. [2.12-2.14] and [2.15], Ch. III, §§ 15-20). More precisely, these papers proved the existence of invariant tori in an arbitrary neighbourhood of a singular point of the analytical system of differential equations, if the latter fulfil some conditions in fact equivalent to reversibility (in some cases these conditions are also satisfied as a result of Hamiltonianity). In [2.13] nonautonomous systems of differential equations (with the right-hand sides being periodic in time) were considered. As to the non-autonomous case, see Sec. 2.13 of the present paper.

2.8. WEAK REVERSIBILITY IN A LOCAL SITUATION

The majority of the results presented in the preceding section can be carried over to the case when in place of reversible objects one considers those being a priori only weakly reversible. Namely, consider an elliptic, weakly reversible general mapping (vector field) in $\mathbb{R}^{2m}$ $(m \geqslant 1)$ in a neighbourhood of a fixed (singular) point, and let the latter be fixed under a reversing diffeomorphism too. In the general case this diffeomorphism turns out to be always an involution so that the weakly reversible mapping (vector field) is actually reversible. Although this result is proved only under some assumptions of a nonresonant and nondegenerate behaviour, examples of elliptic, weakly reversible mappings or vector fields not being reversible are unknown. In the non-elliptic (e.g. hyperbolic) case such examples can be readily constructed even in a two-dimensional situation (moreover, the exemplified mappings and vector fields are general).

Example 1 (M. B. Sevryuk). Let $\alpha\,(t)$ be an arbitrary real-analytical function preset in a neighbourhood of zero on the real line and satisfying the condition $\alpha\,(0) \neq 0$. According to the implicit function theorem, the relation $\beta\,(t)\,\alpha\,(-t\,\alpha\,(t)\,\beta\,(t)) \equiv 1$ defines another real-analytical function $\beta\,(t)$ in a neighbourhood of zero on the real line. This relation implies that $\alpha\,(t)\,\beta\,(-t\,\alpha\,(t)\,\beta\,(t)) \equiv 1$.

Consider a mapping $(x, y) \mapsto (x\alpha\,(xy),\ y\beta\,(xy))$ in a plane with the Cartesian coordinate system (x, y). The eigenvalues of its linearization are $\alpha\,(0)$ and $\beta\,(0) = (\alpha\,(0))^{-1}$. The mapping is weakly reversible (it is reversed by the diffeomorphism $(x, y) \to (y, -x)$). If the function α is not even, then the mapping is reversed by no zero-conserving involution.

Example 2 (M.B. Sevryuk). Let $f\,(t)$ be an even and $g\,(t)$ an odd real-analytical function preset in a neighbourhood of zero on the real line with $f\,(0) \neq 0$. Consider a vector field with the components $yf\,(x^2 - y^2) + xg\,(x^2 - y^2)$ and $xf\,(x^2 - y^2) + yg\,(x^2 - y^2)$ in a plane with the Cartesian coordinate system (x, y). The eigenvalues of its linearization are $f\,(0)$ and $-f\,(0)$. The vector field is weakly reversible (it is reversed by the same, as in the preceding example, diffeomorphism $(x, y) \mapsto (y, -x)$). If the function g is not identically zero, then this field is reversed by no zero-conserving involution.

2.9. PERIODIC SOLUTIONS

Suppose that a reversible system of differential equations has a periodic solution whose phase curve L is invariant under a reversing involution (such closed phase curves are called symmetric). Then the involution maps L onto itself with an orientation reversed so that on L exactly two points are fixed under the involution.

Conversely, if a closed phase curve (cycle) of a reversible system contains at least one point fixed under a reversing involution then it contains exactly two such points and it is invariant under this involution.

In addition, if some phase curve of a reversible system contains at least two points fixed under a reversing involution, then it is closed, i.e. it is a symmetric cycle (and thus contains exactly two such points). This property is basic in the search for the symmetric closed phase curves of reversible systems: it suffices to find the phase curves intersecting the involution fixed manifold at two points.

Note that any phase curve of a reversible system intersecting the involution fixed point manifold intersects it at a nonzero angle.

Theorem. For reversible systems with a phase space $\mathfrak{R}^{2m}$ and a reflection involution with respect to an m-dimensional subspace $\mathfrak{R}^m$ the following holds:

(1) Closed symmetric phase curves form a one-parameter family in a neighbourhood of a given general symmetric cycle.

(2) The family is conserved, with a slight deformation, under any small perturbation of the system leaving the latter reversible.

Proof. The given cycle intersects the fixed manifold $\mathfrak{R}^m$ at two points, a and b, at a nonzero angle. The phase curves passing through the points of $\mathfrak{R}^m$ close to a form an $(m+1)$-dimensional "tube" Φ that generically intersects $\mathfrak{R}^m$ at the point b transversally along a curve containing b. Through each point of the latter curve a phase curve passes intersecting $\mathfrak{R}^m$ at two points. This curve is, thus, a symmetric cycle.

For adjacent systems, the transversality of the intersection of Φ and $\mathfrak{R}^m$ near b is conserved, therefore the cycles will be conserved, too.

This theorem was considered by Devaney [2.16] and for $m = 1$ it was noted by Sharkovskii [2.17, 2.18].

Example. The symmetric cycles of Eq. (2.1) (for which $m = 2$) are included into one-parameter families structurally stable under small perturbations of the equation that do not remove the latter from the reversible class.

To study the solutions of a reversible system in a neighbourhood of a one-parameter family of symmetric cycles, which includes a given cycle, we draw a secant $(2m-1)$-dimensional Poincaré surface Σ, containing a fixed manifold $\mathfrak{R}^m$ of the involution G. Let the surface be invariant under G and intersect the cycle at the point a at a nonzero angle. The surface is drawn through one of the points of intersection of the cycle with $\mathfrak{R}^m$, e.g. through the point a. The Poincaré return mapping $A: \Sigma \to \Sigma$ transforming a into itself is reversible with respect to the action of G on Σ. For a general cycle the manifolds $\mathfrak{R}^m$ and $A\mathfrak{R}^m$ of dimension m in the $(2m-1)$-dimensional space Σ intersect at the point a transversally along a curve passing through a. Each point of the curve is fixed with respect to A and thus belongs to a symmetric cycle. In particular, this again implies the inclusion of the symmetric closed phase curves of a reversible system into one-parameter families.

Here we have the following situation: first, the involution of an odd-dimensional space Σ^{2m-1} that changes the sign of $(m - 1)$ coordinates and, second, the reversible Poincaré mapping $A : \Sigma \to \Sigma$ having a whole curve of fixed points that lies in an m-dimensional space $\mathfrak{R}^m$ of involution fixed points.

The generalization of the above mentioned results to the case when the dimension of an involution fixed manifold is not necessarily equal to half a phase space dimension (the latter can be odd) is not automatic.

Example. An autonomous equation of odd order $2m + 1$ that includes even derivatives only in even combinations is reversible with respect to a phase space involution changing the sign of all even derivatives.

Here the number $(m + 1)$ of "odd", i.e. changing their sign under an involution, phase space coordinates (these are matched here by even derivatives) exceeds the number of "even" coordinates, m, by one.

The majority of the above results on Kolmogorov's tori and the local evolution of reversible objects is *mutatis mutandis* conserved only in the case when the number of the "even" coordinates exceeds that of the "odd" ones (i.e. the dimension of the involution fixed manifold equal to the number of "even" coordinates exceeds half the phase space dimension). This is indeed so on the Poincaré surface.

2.10. KOLMOGOROV'S TORI FOR ADDITIONAL "EVEN" COORDINATES

Consider a phase space of a reversible mapping (vector field) with m "even" coordinates and $k < m$ "odd" ones, this space being foliated into k-dimensional tori invariant under both the mapping (phase flow) and the reversing involution. On these tori a quasi-periodic motion proceeds. For a nondegenerate dependence of the frequencies of this motion on the parameters numbering the tori it is possible to choose a phase space coordinates ($\varphi \in T^k$, $I^{(1)} \in \mathfrak{R}^k$, $I^{(2)} \in \mathfrak{R}^{m-k}$), where the mapping has the following form:

$$(\varphi, I^{(1)}, I^{(2)}) \mapsto (\varphi + I^{(1)}, I^{(1)}, I^{(2)}),$$

and, respectively, the vector field has the form

$$\dot{\varphi} = I^{(1)}, \quad \dot{I}^{(1)} = 0, \quad \dot{I}^{(2)} = 0,$$

while the reversing involution is

$$(\varphi, I^{(1)}, I^{(2)}) \mapsto (-\varphi, I^{(1)}, I^{(2)}).$$

The quasi-periodic motion frequencies on each torus $I^{(1)} = \text{const}$, $I^{(2)} = \text{const}$ only depend on $I^{(1)}$, therefore the tori with the same frequencies are organized into $(m - k)$-parameter families.

It turns out that for a small perturbation of the initial mapping (vector field) leaving it reversible the majority of these families does not decay but is only slightly deformed. Thus, in the phase space of a perturbed mapping (vector field) m-dimensional manifolds exist that are foliated into k-dimensional tori invariant under both the mapping (flow) itself and the involution. On these tori a quasi-periodic motion proceeds with the same (for a fixed m-dimensional manifold) set of frequencies.

Remark. Generally speaking, given additional $(m - k)$ "even" coordinates, weakly reversible perturbations as yet do not ensure the conservation of invariant tori (since they allow a translation along the m-dimensional manifolds foliated into tori with the same frequencies, and given this translation, every torus transforms into another).

2.11. THE LOCAL THEORY FOR ADDITIONAL "EVEN" COORDINATES

This theory is called upon to describe the structure of the Poincaré mapping for reversible differential equations. First, consider the case when the phase space is four-dimensional and the manifold of involution fixed points is two-dimensional, as for Eq. (2.1). We obtain an involution of a three-dimensional space (of the secant Poincaré surface) with one "odd" coordinate and a reversible mapping having a curve of fixed points that lies in the involution fixed plane. The theory of normal forms (of Birkhoff's series), with the reversibility included, shows that at the level of formal series a neighbourhood of the line of fixed points is foliated into two-dimensional, transversal to this line, surfaces invariant under both the mapping and the involution. In the elliptic case (when the linearization of the mapping restriction to each two-dimensional surface is a rotation) of general position on these two-dimensional surfaces Kolmogorov's invariant curves are encountered having an irrational rotation number and surrounding the mapping fixed point that lies on the relevant two-dimensional surface.

It turns out that, although the two-dimensional invariant surfaces exist only formally, Kolmogorov's tori lying on them do exist. Moreover, the curves with the same rotation numbers produced on different formal two-dimensional surfaces are organized together into smooth cylindrical surfaces isolating the line of fixed points from the surrounding space.

At the mapping fixed point where the linearization rotation angle corresponds to the rotation number these surfaces can intersect the line of fixed points. In a neighbourhood of such a point a surface is, generally speaking, diffeomorphic to a paraboloid of revolution (foliated into parallels) since the formal series to express the dependence of the rotation number on the point x on the line of fixed points and the distance r from this point along a formal invariant two-dimensional surface begins with the terms $\alpha(x) + r^2\beta(x) + \ldots$.

It can happen that the surface composed of Kolmogorov's circles will intersect twice the line of fixed points and therefore have the topology of a sphere (Fig. 2.3). Then the sphere locks up the points

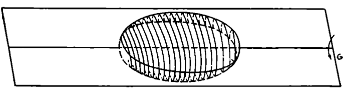

Fig. 2.3

inside it, this enabling us to establish the stability of the fixed points corresponding to either a minimum linearization rotation angle (for positive values of β) or to a maximum one (for negative values of β).

Between the considered surfaces foliated into invariant (under both the mapping and the involution) Kolmogorov's circles with irrational rotation numbers there are left resonance zones. For general mappings, these zones contain fixed points of mapping iterations. The points fixed under the qth mapping iteration are organized into several smooth curves (two of which necessarily lie on an involution fixed surface). The curves can intersect the line of fixed points (where the linearization rotation angle is $2\pi p/q$), where they are tangent to the corresponding formal invariant surface. Some of these curves themselves are surrounded by two-dimensional surfaces foliated into circles invariant under the qth mapping iteration (Fig. 2.4).

For a reversible system in a phase space of an arbitrary even dimension $2m$ (and a reflection involution with respect to an m-dimensional space) we arrive at an involution of a $(2m - 1)$-dimensional space (a secant Poincaré surface) with m "even" and $(m-1)$ "odd" coordinates and at a reversible mapping with the curve of fixed points lying in an involution fixed space $\mathfrak{R}^m$. The above results are transferred to the case of $m > 2$ as follows. A neighbourhood of the line of fixed points is formally foliated into transversal to it, $(2m - 2)$-dimensional surfaces which are invariant under both the mapping and the involution. At the pithy level, in the general elliptic case this line is surrounded by m-dimensional surfaces foliated into $(m - 1)$-

dimensional tori which are invariant under both the mapping and the involution and on which a quasi-periodic motion proceeds whose frequencies are the same for a fixed m-dimensional surface.

Now let in an $(m + k)$-dimensional space be preset an involution with m "even" and $k < m$ "odd" coordinates (in the above case $k = m - 1$) and a reversible mapping leaving fixed one of the involution fixed points, say a point a. Generically, the linearization of the mapping at the point a has r eigenvalues equal to 1 (where $0 \leqslant r \leqslant m - k$) and $(m - k - r)$ eigenvalues equal to -1 (in the above case $r = 1$). It turns out that through the point a there passes an $(m - k)$-dimensional surface invariant under the mapping and lying on the manifold of involution fixed points. The restriction of the mapping to this surface is an involution with r "even" and $(m - k - r)$ "odd" coordinates. Consider the case of $r = m - k$ in more detail. The point a is passed through by an $(m - k)$-dimensional surface of mapping fixed points lying on the manifold of involution fixed points (in the above case, when the reversible mapping was the Poincaré mapping of a reversible equation, the existence of such a line of fixed points was known a priori).

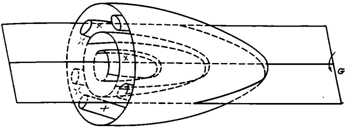

Fig. 2.4

A neighbourhood of this surface is foliated into transversal to it, formal $2k$-dimensional manifolds invariant under both the mapping and the involution. For a general elliptic mapping this surface is surrounded by k-dimensional, invariant under both the mapping and the involution tori on which a quasi-periodic motion proceeds. The tori with the same frequency set are organized into smooth $(m - k)$-parameter families.

For $k = 1$ in the resonance zones between these families one encounters the fixed points of the mapping iterations. The points fixed under the qth mapping iteration are organized into several smooth $(m - 1)$-dimensional surfaces (two of which necessarily lie on the involution fixed m-dimensional surface).

Consider now reversible vector fields. Let in an $(m + k)$-dimensional space be preset an involution with m "even" and $k < m$ "odd" coordinates and a reversible vector field having a singular point on a fixed m-dimensional involution manifold. In a general system this point is passed through by an $(m - k)$-dimensional surface lying on the involution fixed manifold and consisting of field singular points. A neighbourhood of this surface is foliated into transversal to it, formal $2k$-dimensional manifolds that are invariant under both the field and the involution. In a general elliptic system this surface is surrounded by $(m - k)$-parameter families of k-dimensional invariant tori. For $k = 1$ a certain neighbourhood of this surface in a general elliptic system is completely foliated into such families of circles.

2.12. APPLICATION TO REVERSIBLE EQUATIONS

Returning from the geometry of the Poincaré mapping near the line of fixed points to the initial reversible equation we will obtain the following results. To begin with, let the phase space be four-dimensional while the involution be a reflection with respect to a two-dimensional space (as is the case for Eq. (2.1)). We obtain a one-parameter family of symmetric cycles and a set of three-dimensional invariant manifolds numbered by the rotation numbers normally incommensurable with 1 and foliated into two-dimensional Kolmogorov's tori filled with the trajectories of quasi-periodic motions having the fixed frequency ratio on each three-dimensional manifold.

The resonance zones between the manifolds comprise other one-parameter families of symmetric cycles and other three-dimensional manifolds, also foliated into two-dimensional invariant tori. These families emerge from the fixed points of the Poincaré mapping iterations and from the phase oscillations near them.

Thus the general picture of a motion near a symmetric cycle of a reversible system with a four-dimensional phase space and with a two-dimensional manifold of involution fixed points is extremely reminiscent of the picture of the motion of a Hamiltonian system with two degrees of freedom. The only difference is that the Hamiltonian system has the first integral, therefore the existence of Kolmogorov's tori implies (under the usual conditions of nondegeneracy) the stability of the periodic motion.

At the same time, the reversible system has, generally speaking, no first integral. Therefore the existence of quasi-periodic motions (whose phase curves form three-dimensional invariant manifolds foliated into two-dimensional Kolmogorov's tori) does not prevent, in general, some trajectories of the system from escaping the initial periodic motion along a resonance zone.

It seems very likely that such an escape, although very slow, does take place in general reversible systems.

In the case of a $2m$-dimensional phase space and a reflection involution with respect to an m-dimensional subspace we obtain a one-parameter family of symmetric cycles and a set of the $(m+1)$-dimensional invariant manifolds foliated into m-dimensional Kolmogorov's tori filled with quasi-periodic motion trajectories.

Now let a system with an $(m+k)$-dimensional phase space be given that is reversible under an involution whose fixed manifold is m-dimensional (where not necessarily $k = m$). For $k > m$ the symmetric cycles of such a system of general position are isolated, for $k \leqslant m$ they are organized into the $(m-k+1)$-parameter families structurally stable under small reversible perturbations (this can be proved by the same reasoning as in the "classical" case of $k = m$). Suppose that $k \leqslant m+1$, then an $(m-k+1)$-parameter family of the symmetric cycles of an equation, under the ellipticity of the appropriate Poincaré mapping, is surrounded by the $(m+1)$-dimensional invariant manifolds foliated into the k-dimensional invariant tori, on which quasi-periodic motions proceed. For $m = 1$, $k = 2$ this implies the stability of a symmetric system's cycle (the Poincaré mapping is a reversible mapping of a plane) in the elliptic case. For two "odd" coordinates ($k = 2$) and an arbitrary m near the general "elliptic" $(m-1)$-parameter family of the symmetric cycles there exist other stemming from the fixed points of Poincaré mapping iterations, $(m-1)$-parameter families of symmetric cycles and other $(m+1)$-dimensional invariant manifolds, also foliated into two-dimensional invariant tori.

2.13. NON-AUTONOMOUS REVERSIBLE SYSTEMS

The above assertions about the invariant tori of reversible differential equations and about their behaviour in a neighbourhood of a singular point can be generalized to the non-autonomous case.

Definition. A differential equation $\dot{x} = V_t(x)$ (generally speaking, non-autonomous) is called weakly reversible if there exists a phase space diffeomorphism G that "reverses" a phase space transformation family corresponding to this equation. In other words, if $\mathcal{F}_{t_1}^{t_2}$ is a phase space transformation in a time period from t_1 to t_2, then for all t_1, t_2 we have

$$G.\mathcal{F}_{t_1}^{t_2}G^{-1} = \mathcal{F}_{-t_1}^{-t_2}.$$

This relation is equivalent to the fact that for any fixed moment of time t we will have

$$G_* V_t = -V_{-t}.$$

If the equation is autonomous then we obtain the former definition of a weakly reversible vector field.

If a diffeomorphism G "reverses" the family $\{\mathcal{F}_{t_1}^{t_2}\}$ of phase space transformations, then the diffeomorphism G^{-1} will do the same.

A weakly reversible differential equation is called reversible, if a phase space diffeomorphism, "reversing" it, is an involution.

Of special interest are weakly reversible differential equations whose right-hand sides are periodic in time.

Example. A solution $x = x(t)$ of a reversible, T-periodic in time differential equation with an initial condition $x(0)$ lying on the fixed manifold of a "reversing" involution is T-periodic if and only if $x(T/2)$ is also fixed under this involution (cf. [2.26], [2.27]).

The monodromy operator of a weakly reversible, periodic in time differential equation is also weakly reversible (with respect to the same diffeomorphism). This key remark allows all the results on (weakly) reversible mappings to be immediately carried over to (weakly) reversible, periodic in time differential equations.

In particular, in an extended phase space (whose time is factori-

Table 2.1

	Mappings and phase flows	Non-autonomous differential equations	Flows in a neighbourhood of a periodic solution	
			tori	cycles
Restrictions	$1 \leqslant k \leqslant m$	$1 \leqslant k \leqslant m$	$2 \leqslant k \leqslant m+1$	$1 \leqslant k \leqslant m$
The dimension of Kolmogorov's tori (the last column contains the number of parameters in each cycle family)	k	$k+1$	k	$m-k+1$
The dimension of the manifolds foliated into tori	m	$m+1$	$m+1$	

Remark: The first column relates to reversible mappings and phase flows close to integrable or in a neighbourhood of a fixed point, the second, to the reversible differential equations periodic in time and close to autonomous integrable or in a neighbourhood of a stationary solution, the third, to reversible phase flows in a neighbourhood of a symmetric closed trajectory. The fourth column gives what number of parameters have the families into which symmetric cycles of reversible phase flows are generically organized.

The phase space dimension is $m + k$, the dimension of the manifold of involution fixed points is m.

Kolmogorov's tori for periodic differential equations (the second column) lie in the extended phase space (the time is varying along a circle), in all other cases, in the phase space.

zed by period) of a reversible differential equation close to an autonomous integrable one there exist invariant tori. The same tori also exist near a stationary solution of a reversible differential equation in the nondegenerate elliptic case.

Table 2.1 lists the dimensions of these tori as well as those of the invariant (Kolmogorov's) tori and of the invariant manifolds, into which the tori with the same frequencies (or the same frequency ratios) are organized as dependent on the number of m "even" and k "odd" phase space coordinates in all the preceding situations. The table also shows the number of parameters of the families into which the general symmetric cycles of reversible phase flows are organized and the restrictions, imposed on both the dimension m of an involution fixed manifold and its codimension k in phase space, under which Kolmogorov's tori or non-isolated symmetric cycles exist.

2.14. THE LYAPUNOV-DEVANEY THEOREM

Lyapunov's theorem on one-parameter cycle families near a singular point of a Hamiltonian vector field can be applied to the reversible case as follows ([2.16] and [2.15], Ch. I, §§ 5-6). Consider a reversible system of differential equations in $\mathfrak{R}^{2m}$, with a singular point lying on an m-dimensional fixed manifold of the involution G that reverses this system. As in the Hamiltonian case, the number $-\lambda$, together with each eigenvalue λ of a linear reversible system, is also an eigenvalue of this system. This suggests, in particular, that for reversible systems pure imaginary eigenvalues are not an exception (as for the general systems of differential equations) but one of the typical possibilities realized in a stable manner (as for Hamiltonian systems). Let us denote by $\lambda_1, \ldots, \lambda_m, -\lambda_1, \ldots, -\lambda_m$ the eigenvalues of the linearization of vector field prescribing a reversible system at a singular point.

Let λ_1 be nonzero, pure imaginary and none of the ratios λ_j / λ_1 ($j \geqslant 2$) be integer (the nonresonance condition).

Then the singular point of our system will be passed through by a smooth two-dimensional surface being tangential to the linearization invariant plane that corresponds to the eigenvalues $\pm\lambda_1$. The surface is foliated into symmetric cycles, and as the initial conditions on this surface tend to the singular point, the cycle period tends to $2\pi/|\lambda_1|$.

The studies of resonant Hamiltonian systems are the topics of a major number of papers (see, e.g. [2.23-2.25]). Here we will consider reversible systems near resonances. For simplicity, we will limit ourselves to the case of a four-dimensional phase space (two "even" and two "odd" coordinates). Resonant reversible systems form a set of codimension 1 in the space of all reversible systems. Therefore to study the resonant systems one has to include those into families of reversible systems that depend on a small parameter ε ($\varepsilon = 0$ corresponds to the resonance). The singular point can be treated as independent of ε and placed at zero.

2.15. THE RESONANCE 1:1

Suppose that for $\varepsilon = 0$ our system has a double eigenvalue βi and a double eigenvalue $-\beta i$ ($\beta > 0$). By changing, if necessary, the time scale we can get $\beta = 1$. In the general family for one parameter sign (e.g. when $\varepsilon < 0$) the eigenvalues of the linearization of our system do not lie on the imaginary axis, while for another sign (when $\varepsilon > 0$) these are $\pm \nu_1 i$, $\pm \nu_2 i$, where ν_1 and ν_2 are real and close to 1. The resonance mismatch $| \nu_2 - \nu_1 |$ is of the order of $\sqrt{\varepsilon}$. Each symmetric cycle of our system in a neighbourhood of the origin intersects a fixed involution plane at two points. The latter form a certain curve Γ_ε that depends on ε. On the curve Γ_ε, for any ε, an involution σ permutes the points belonging to the same symmetric cycle.

Theorem. When some nondegeneracy conditions imposed on the terms of order $\leqslant 3$ of field Taylor series are fulfilled, then by a suitable choice of a smoothly ε-dependent coordinate system Oxy in a fixed plane of the involution reversing the phase flow and by a change, if necessary, of the ε sign (i.e. by multiplying ε by -1) the equation of the family of curves Γ_ε is reduced to the form

$$(\varepsilon \pm x^2)\, x^2 = y^2, \tag{2.6}$$

where the sign "+" corresponds to the hyperbolic mode and the sign "−", to the elliptic mode (the mode is controlled by the terms of order $\leqslant 3$).

(a) Elliptic mode: $\Gamma_\varepsilon = \{x,\ y : (\varepsilon - x^2)\, x^2 = y^2\}$.

For $\varepsilon \leqslant 0$, Γ_ε is just the origin, i.e. there are no symmetric cycles near the singular point at all. For $\varepsilon > 0$, Γ_ε has the form of a figure-of-eight (Fig. 2.5).

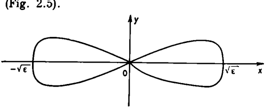

Fig. 2.5

The cycles intersect this figure-of-eight at the points symmetric about the origin.

Thus, when a four-dimensional reversible system passes through the resonance 1:1 in the elliptic mode, on one side of the resonance a foliated into symmetric cycles, two-dimensional surface is split out from the origin, this surface having the topology of a sphere with two identified points (corresponding to the origin). The size of this surface is proportional to the resonance mismatch.

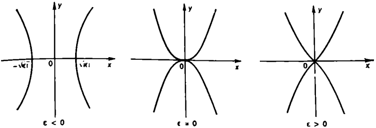

Fig. 2.6

In the paper by Malomed and Tribel'skii [2.20] (see also [2.28]) this surface was approximated for Eq. (2.1) by writing out a few first terms of the series producing the solution.

(b) Hyperbolic mode: $\Gamma_\varepsilon = \{x,\ y : (\varepsilon + x^2)\, x^2 = y^2\}$.

The bifurcation of Γ_ε has the form shown in Fig. 2.6.

In particular, at a resonance instant in the phase space of the system we obtain two tangential at zero, two-dimensional C^1-surfaces foliated into symmetric cycles.

Remark. The union of the curves Γ_ε in a three-dimensional space with coordinates x, y, ε both in the elliptic and in the hyperbolic cases is a surface called the "Whitney umbrella" (or the "Cayley umbrella").

The Whitney umbrella is a surface diffeomorphic to the image of the Whitney mapping $\mathbb{R}^2 \to \mathbb{R}^3$ preset by the following formulas (see [2.2], Ch. 1, Sec. 1.9):

$$v_1 = u_1, \quad v_2 = u_1 u_2, \quad v_3 = u_2^2,$$

where u_1, u_2 are the coordinates in $\mathbb{R}^2$ and v_1, v_2, v_3 are the coordinates in $\mathbb{R}^3$. The equation of the image of this mapping in $\mathbb{R}^3$ is $v_2^2 = v_1^2 v_3$ (the last relation, besides the points of the umbrella, is satisfied by the points of its "stick", $v_1 = v_2 = 0$, $v_3 < 0$, too). The Whitney umbrella is shown in Fig. 2.7.

All the smooth curves on the umbrella passing through its vertex are mutually tangential at this point. The direction of their common tangent (in our coordinates this is the direction of the axis v_1) is thus invariantly related to the umbrella.

In our case an umbrella's neighbourhood in $\mathbb{R}^3$ is foliated into surfaces $\varepsilon = \text{const}$. It is easy to verify that at the umbrella's vertex the derivative of the function ε along the invariant direction is zero.

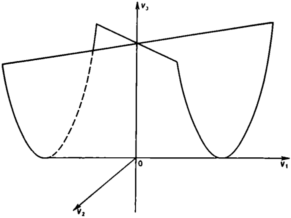

Fig. 2.7

Theorem. In a neighbourhood of the Whitney umbrella in $\mathbb{R}^3$ a function, that is of general position in the class of the functions whose values and whose derivatives along the axis v_1 at zero are both zero, by means of an $\mathbb{R}^3$ diffeomorphism conserving zero and transforming the umbrella into itself, can be reduced to the normal form

$$\pm v_3 \pm v_1^2,$$

where the functions $v_3 + v_1^2$ and $-v_3 - v_1^2$ correspond to the elliptic mode and the functions $v_3 - v_1^2$ and $-v_3 + v_1^2$, to the hyperbolic one.

Remark. Suppose that a quadratic part of the Taylor series of the initial function is $a_1 v_2 + a_2 v_3 + \sum\limits_{1 \leqslant i \leqslant j \leqslant 3} b_{ij} v_i v_j$. The words "of general position" mean that $a_2 \neq 0$, $a_1^2 \neq 4a_2 b_{11}$.

2.16. FURTHER RESONANCES 1:N ($N \geqslant 2$)

After a smooth substitution of the parameter ε and a smoothly ε-dependent change in time scale we can assume that the eigenvalues of our system's linearization at the origin are $\pm i$, $\pm (N + \varepsilon) i$. The symmetric cycles near the origin can be of two types: long-periodic (with a period close to 2π) and short-periodic (with a period close to $2\pi/N$). According to the Lyapunov-Devaney theorem applied to the eigenvalues $\pm(N+\varepsilon)\,i$, for any small value of ε the origin is passed through by a smoothly ε-dependent, two-dimensional surface tangential to the $\pm(N+\varepsilon)i$-invariant plane of the linearization and foliated into short-periodic symmetric cycles. When these cycles contract to a singular point, their periods tend to $2\pi/(N+\varepsilon)$. The surface intersects the involution fixed plane along a smoothly ε-dependent curve $\Gamma_\varepsilon(N)$.

The points of intersection of long-periodic cycles with the involution fixed plane compose a certain ε-dependent curve $\Gamma_\varepsilon(1)$ that bifurcates when ε passes through zero. Our aim is to study these bifurcations.

On the curve $\Gamma_\varepsilon(1)$ an involution σ acts permuting the points which belong to the same long-periodic symmetric cycle. For even N's, the involution is approximately a reflection with respect to the curve $\Gamma_\varepsilon(N)$, and for odd N's, a reflection with respect to the origin. Accordingly, for even N's, the curve $\Gamma_\varepsilon(1)$ is approximately symmetric about $\Gamma_\varepsilon(N)$ while for odd N's, about the origin.

Indeed, suppose that in the fixed plane of the initial involution G a coordinate system is chosen whose abscissa axis is tangential to the $(\pm i)$-eigendirection and ordinate axis is tangential to the $(\pm(N+\varepsilon)\,i)$-eigendirection. Then, if a symmetric long-periodic cycle passes through a point (u, v) in the fixed plane, this cycle will intersect, for the second time, the fixed plane at a point close to the point $(u\cos\pi,\ v\cos N\pi)$, i.e. to that of $(-u,\ (-1)^N v)$.

Analogously, on the curve $\Gamma_\varepsilon(N)$ an involution τ acts that permutes the points belonging to the same short-periodic symmetric cycle. These points are approximately symmetric about the origin.

2.16.1. The Resonance 1:2

Theorem. On fulfilling some nondegeneracy conditions imposed on the quadratic (second-order) terms of the field Taylor series, by a suitable choice of a smoothly ε-dependent coordinate system Oxy in an involution fixed plane, the curve $\Gamma_\varepsilon(N)$ acquires the form $\{x, y : x = 0\}$ (the ordinate axis in Figs. 2.8 and 2.11) and the curve $\Gamma_\varepsilon(1)$ acquires the form

$$\{x,\ \ y : y\,(\varepsilon - y) \pm x^2 = 0\}, \tag{2.7}$$

where the sign "+" corresponds to the hyperbolic mode and the sign "−", to the elliptic mode (the mode is controlled by quadratic terms).

(a) Elliptic mode: $\Gamma_\varepsilon(1) = \{x,\ y : y\,(\varepsilon - y) = x^2\}$.

The bifurcation of $\Gamma_\varepsilon(1)$ is shown in Fig. 2.8. Long-periodic symmetric cycles intersect the involution fixed plane, i.e. that of Fig. 2.8, at the points A and A_1, B and B_1, etc.

The cycle passing through the point C of the intersection between $\Gamma_\varepsilon(1)$ and $\Gamma_\varepsilon(N)$ is not long- but short-periodic. It intersects for the second time the figure plane at a point C_1 on $\Gamma_\varepsilon(N)$ and is resonant (i.e. the rotation angle of the linearization of the restriction of the Poincaré mapping of this cycle to the passing through C, formal two-dimensional invariant surface, in the three-dimensional secant Poincaré surface, is equal to $\pi/2$). Long-periodic cycles form a specific bridge between this resonant, short-periodic, closed trajectory and the singular point (cf. the description of the branching of long-periodic cycles from a resonant short-periodic one in the Hamiltonian case, as shown by Bryuno [2.21]).

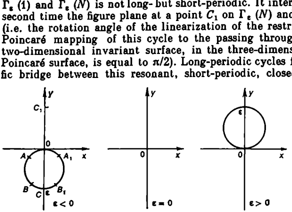

Fig. 2.8

The projection of a symmetric cycle, passing through the points A and A_1 placed near the origin, onto a two-dimensional, passing through the origin, plane of general position in the four-dimensional phase space, is nonself-intersecting. The projection of a cycle, passing through the points B and B_1 close to C, goes twice round zero and has an odd number of self-intersection points (Fig. 2.9). The transition proceeds as shown in Fig. 2.10. By Q is denoted the reverse point on the projection at the instant of its reconstruction ("beak").

(b) Hyperbolic mode: $\Gamma_\varepsilon(1) = \{x,\ y : y(y-\varepsilon) = x^2\}$.

The bifurcation of $\Gamma_\varepsilon(1)$ is shown in Fig. 2.11.

Long-periodic symmetric cycles intersect the figure plane at the points A and A_1, B and B_1, C and C_1, E and E_1, F and F_1, G and G_1, etc. The cycle passing through the point D of the intersection between $\Gamma_\varepsilon(1)$ and $\Gamma_\varepsilon(N)$ is short-periodic, it intersects for the second time the figure plane at the point D_1 on $\Gamma_\varepsilon(N)$ and is resonant.

The projection of a cycle, passing through the points B and B_1 placed near the origin, onto a zero-containing, two-dimensional plane of general position, is nonself-intersecting. The projection of a cycle, passing through the points A and A_1 placed near D, is a curve like that in Fig. 2.9. As to the projection of the cycles, passing through the points C, C_1 and E, E_1 placed far from the origin, these projections, depending on the two-dimensional direction of the projection, are either nonself-intersecting (and then the projection of a cycle, passing through some intermediate points G and G_1, has a "beak") or curves like a loop in Fig. 2.9 (then the "beak" is inherent in the projection of a cycle passing through some intermediate points F and F_1).

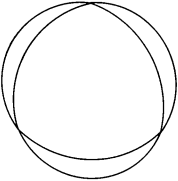

Fig. 2.9

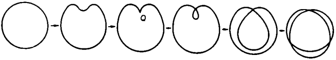

Fig. 2.10

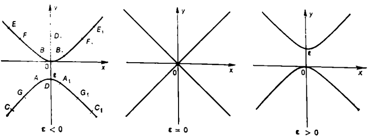

Fig. 2.11

At the resonance instant, in the hyperbolic case the origin of the four-dimensional phase space is passed through by two two-dimensional invariant surfaces having a conical singularity and foliated into long-periodic cycles.

Remark 1. In the elliptic and hyperbolic cases, when a long-periodic cycle approaches a resonant short-periodic one, its projection shown in Fig. 2.9 becomes more and more like a two-pass circle.

Remark 2. The union of the curves Γ_ε (1) in a three-dimensional space with the coordinates x, y, ε in the elliptic and hyperbolic modes is a cone. The union of the curves Γ_ε (N) is a smooth two-dimensional surface (in "normal" coordinates, the plane $x = 0$) whose tangential plane at zero is conjugated with the plane $\varepsilon = 0$ with respect to the cone (more exactly, a straight line, conjugated with each of these planes with respect to the quadratic part of the Taylor series of the equation prescribing the cone, lies in the other plane). The union of the curves Γ_ε (N) intersects the cone along two curves intersecting at the cone vertex at a nonzero angle (for both modes).

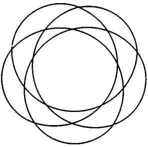

Fig. 2.12

Theorem. Suppose that in $\mathbb{R}^3$ there are given: a cone whose vertex is at zero (according to the Morse lemma we, without any loss of generality, can presume that its equation is $v_1^2 + v_2^2 - v_3^2 = 0$, where v_1, v_2, v_3 are the coordinates in $\mathbb{R}^3$), a smooth, two-dimensional, passing through zero general surface Ξ that intersects the cone along two curves; and a smooth general function ε whose zero level surface passes through zero. Tangential planes to $\varepsilon^{-1}(0)$ and to Ξ at zero are conjugated with respect to the quadratic form $v_1^2 + v_2^2 - v_3^2$. Then, by the $\mathbb{R}^3$ diffeomorphism that conserves zero and maps the cone onto itself, one can reduce the function ε to one of two normal forms: $\varepsilon = v_2$ (hyperbolic mode) or $\varepsilon = v_3$ (elliptic mode) and, simultaneously, the surface Ξ to the normal form $\{v_1, v_2, v_3 : v_1 = 0\}$.

Now let us turn to the resonances $1{:}N$, where $N \geqslant 3$. Figures 2.13-2.18 show the relevant bifurcations of Γ_ε (1). The curve Γ_ε (N) is indicated by the dashed line. A symmetric cycle, passing through the points A and A_1 of the intersection between Γ_ε (1) and Γ_ε (N), is short-periodic. It is resonant and the projections of long-periodic cycles, that branch off from it, onto a zero-containing, two-dimensional plane of general position have the form shown in Fig. 2.12 (overall N turns). The closer these cycles to a resonant short-periodic one the more their projections are similar to an N-pass circle. The "beak" phenomenon is analogous to that for the resonance 1:2.

When the resonant short-periodic cycle is connected with the origin by a "bridge" made of long-periodic symmetric closed trajectories, that branch off from it, then the part of the curve $\Gamma_\varepsilon(1)$ that is an intersection between the bridge and the involution fixed plane is shown in the subsequent figures by the heavy line.

2.16.2. The Resonance 1:3

Theorem. On fulfilling some nondegeneracy conditions imposed on the terms of order $\leqslant 3$ of the field Taylor series, by a suitable choice of a smoothly ε-dependent coordinate system Oxy in the involution fixed plane and by changing, if necessary, the sign of ε the equation of the curves $\Gamma_\varepsilon(N)$ reduces to the form

$$x = y^2 h(y, \varepsilon) + Cy, \tag{2.8}$$

where $C \in \mathbb{R}$, h is a smooth function, and the equation of the curves $\Gamma_\varepsilon(1)$ reduces to the form

$$y(\varepsilon - y^2 - \alpha xy) + x^3 = 0, \tag{2.9}$$

where $\alpha \in \mathbb{R}$, $4\alpha^3 + 27 \neq 0$.

The constant α is controlled by the terms of order $\leqslant 3$.

The inequality $4\alpha^3 + 27 > 0$ corresponds to the elliptic mode, the inequality $4\alpha^3 - 27 < 0$, to the hyperbolic one.

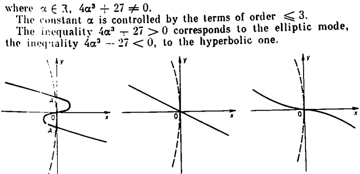

$\varepsilon < 0$ $\varepsilon = 0$ $\varepsilon > 0$

Fig. 2.13

The bifurcation of $\Gamma_\varepsilon(1)$ for the elliptic and hyperbolic modes is shown in Figs. 2.13 and 2.14, respectively. The curves $\Gamma_\varepsilon(N)$ in these figures are shown for the case of $C = 0$. The distances from the origin to A and A_1 for $\varepsilon < 0$ have the order of $\sqrt{|\varepsilon|}$. For $\varepsilon \neq 0$, Fig. 2.14 shows $\Gamma_0(1)$ by dots. For $\varepsilon > 0$ the distances ρ_1 and ρ_2 have the order of $\sqrt{\varepsilon}$.

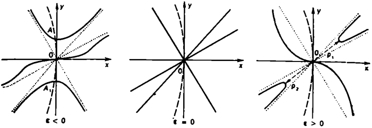

Fig. 2.14

Remark. At the resonance instant the singular point is passed through either by one (elliptic mode) or by three (hyperbolic mode) two-dimensional surfaces with a conical singularity at zero, which are foliated into long-periodic symmetric cycles. An intersection of each of these surfaces with the involution fixed plane is a smooth curve passing through zero.

2.16.3. Higher Resonances $1:N$ $(N \geqslant 4)$

Theorem. On fulfilling some nondegeneracy conditions imposed on the terms of order $\leqslant N$ of the field Taylor series, by multiplying the parameter ε by a suitable nonzero constant and by a suitable choice of a smoothly ε-dependent coordinate system Oxy in the involution fixed plane the equation of the curves $\Gamma_\varepsilon(N)$ acquires the form (2.8), where $C = 0$, and the equation of the curves $\Gamma_\varepsilon(1)$ acquires the form

$$y(\varepsilon \pm y^2 - x^2) + x^N = 0, \tag{2.10}$$

where the sign "+" corresponds to the hyperbolic mode and the sign "−", to the elliptic one (the mode is controlled by the terms of order $\leqslant 3$).

The bifurcation of $\Gamma_\varepsilon(1)$ in the elliptic mode is shown in Fig. 2.15 (even N) and in Fig. 2.16 (odd N) and in the hyperbolic mode, in Fig. 2.17 (even N) and Fig. 2.18 (odd N). In the figures corresponding to $\varepsilon > 0$, dots denote the following: in the elliptic case it is the circle $x^2 + y^2 = \varepsilon$, in the hyperbolic case it is the hyperbola $x^2 - y^2 = \varepsilon$. The distances from the origin to A and A_1 for $\varepsilon > 0$ in the elliptic case and for $\varepsilon < 0$ in the hyperbolic case have the order of $\sqrt{|\varepsilon|}$. The distances δ_1 and δ_2 for $\varepsilon > 0$ have the values of the order of $\varepsilon^{(N-1)/4}$.

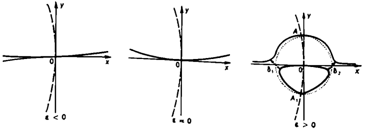

Fig. 2.15

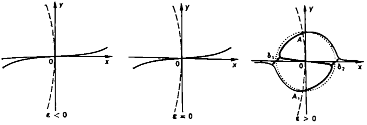

Fig. 2.16

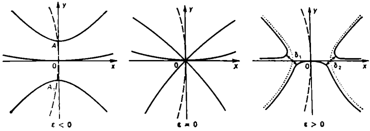

Fig. 2.17

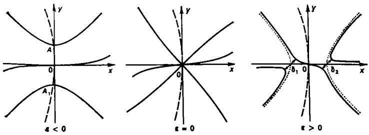

Fig. 2.18

We see that at the instant of a resonance 1:N, where $N \geqslant 4$, the singular point is passed through by a two-dimensional surface foliated into long-periodic symmetric cycles (it is possible to show that its smoothness class at zero is C^{N-3} rather than C^{N-2}), tangential to a ($\pm i$)-invariant plane of the vector field linearization at the singular point. Besides, in the hyperbolic mode the singular point is passed through by two additional two-dimensional surfaces foliated into long-periodic cycles and having a conical singularity at this point. An intersection of each of these surfaces with the involution fixed plane is a smooth curve passing through zero (for odd N) or an "angle" composed of two transversal rays with the initial point at zero (for even N).

2.16.4. Some Additional Remarks Concerning Further Resonances

In the case of the resonances 1:N, $N \geqslant 3$, the union of the curves Γ_ε (1) in a three-dimensional space with the coordinates x, y, ε is a surface having at zero the singularity A_{N-1} ([2.2], Ch. 2). Under a suitable choice of the coordinate system v_1, v_2, v_3 the equation of this surface will acquire the form $v_1v_2 + v_3^N = 0$. This surface is invariantly related to the planes $v_1 = 0$ and $v_2 = 0$ (in a tangential space to $\mathbb{R}^3$, at zero). The zero level surface of the ε-function is tangential to one of these planes.

Theorem. Suppose that in $\mathbb{R}^3$ there are preset a surface $\{v_1, v_2, v_3 : v_1v_2 + v_3^N = 0\}$ and a general function ε such that $\varepsilon(0) = 0$ and $\varepsilon^{-1}(0)$ is tangential to the plane $v_1 = 0$ at zero. Then by an $\mathbb{R}^3$ diffeomorphism conserving zero and transforming the surface into itself the function ε can be reduced to the normal form

$$\pm (v_1 + v_2^2 - \alpha v_2 v_3) \text{ for } N = 3,$$

$$\pm (v_1 + v_2^2 + \alpha v_3^2) \text{ for } N \geqslant 4,\ \alpha \in \mathbb{R}.$$

The condition of function generality (nondegeneracy) implies that $4\alpha^3 + 27 \neq 0$ for $N = 3$ and $\alpha \neq 0$ for $N \geqslant 4$.

For $N \geqslant 4$ the function considered can be reduced to the normal form

$$v_1 + v_2^2 \pm v_3^2,$$

where the sign "+" corresponds to the elliptic mode and the sign "−", to the hyperbolic one, if along with the action of the zero-conserving $\mathbb{R}^3$ diffeomorphisms transforming a surface into itself one allows a multiplication of the function by a nonzero constant.

Here the singularity of the pair (a surface of type A_{N-1}, a function) is a real analogue of the critical point of a function on a manifold with a singular boundary of type $\tilde{A}_3$ for $N = 3$ and of type $I_3(N)$, for $N \geqslant 4$, according to the classification by Lyashko [2.22].

The behaviour of reversible systems at the resonance instant is extremely similar to that of resonant Hamiltonian systems. For example, for a Hamiltonian system (with many degrees of freedom), in the case of the resonance 1:3 between two pure imaginary linearization eigenvalues, depending on Taylor series terms of order $\leqslant 4$ of the Hamiltonian, Roels [2.23] found either one two-dimensional, foliated into long-periodic cycles surface passing through a singular point or three such surfaces. For the resonance $1 : N$, $N \geqslant 4$, also in a multidimensional situation, he found [2.24] a two-dimensional surface, passing through a singular point, foliated into long-periodic cycles and being tangential to the corresponding invariant plane of the linearization. The case of a resonant Hamiltonian system with two degrees of freedom was considered in detail by Henrard [2.25] where an extended bibliography was presented too. Henrard has demonstrated that for the resonance 1:2 in a nondegenerate system near a singular point either there is no family of long-periodic cycles at all or there are two such families, while for the resonance $1:N$, $N \geqslant 3$, the number of the families of long-periodic cycles is either 1 or 3. In [2.25] the subharmonic resonances ($p:q$, where p and q are relatively prime and $q > p > 1$) have been also investigated for which Lyapunov's theorem describes both short- and long-periodic cycles, yet here the existence of the families of "very long-periodic" cycles is possible.

References

2.1. V. I. Arnol'd, in: *Nonlinear and Turbulent Processes*, Acad. Publ., New York, 1984, p. 1161.
2.2. V. I. Arnol'd, A. N. Varchenko, and S. M. Gusein-Zade, in: *Monographs in Mathematics*, Vol. 82, Birkhäuser, Basel, Stuttgart, 1985.
2.3. G. D. Birkhoff, *Rendiconti di Palermo*, 39 (1915).
2.4. G. D. Birkhoff, *Acta Math.*, 48 (1927).
2.5. G. D. Birkhoff, *Dynamical Systems*, AMS Publication, New York, 1927; revised edition, 1966.
2.6. R. B. Melrose, *Invent. Math.*, 37, 165 (1976).
2.7. J. K. Moser and S. M. Webster, *Acta Math.*, 150, 3-4, 255 (1983).
2.8. J. Moser, *SIAM Review*, 8, 2, 145 (1966).
2.9. J. Moser, *Math. Ann.*, 169, 136 (1967).
2.10. J. Moser, *Nachr. Akad. Wiss.*, Göttingen, Math.-Phys. Kl., II *a*, 1 (1962).
2.11. C. L. Siegel and J. K. Moser, *Lectures on Celestial Mechanics*, Springer-Verlag, 1971.
2.12. Yu. N. Bibikov, and V. A. Pliss, *Differ. Uravneniya*, 3, 11, 1864 (1967).
2.13. Yu. N. Bibikov, *Dokl. Akad. Nauk SSSR*, 185, 1, 9 (1969).
2.14. Yu. N. Bibikov, *Differ. Uravneniya*, 7, 8, 1347 (1971).
2.15. Yu. N. Bibikov, in: *Lect. Notes in Math.*, Springer-Verlag, 702 (1979).
2.16. R. L. Devaney, *Trans. Am. Math. Soc.*, 218, 89 (1976).
2.17. A. N. Sharkovskii, in: *The Asymptotic Behaviour of the Solutions of Differential Functional Equations*, Kiev, 1978, p. 118 (in Russian).

2.18. A. N. Sharkovskii, in: *Proc. Eighth Intern. Conf. Nonlinear Oscill.*, Prague, 1073 (1978).
2.19. E. A. Demekhin, *Izv. Akad. Nauk SSSR, Ser. Mekh. Zhidk. i Gaza*, 5, 36 (1983).
2.20. B. A. Malomed and M. I. Tribel'skii, *Dokl. Akad. Nauk SSSR*, 275, 6, 1363 (1984).
2.21. A. D. Bryuno, *Mat. Sbornik*, 83, 2, 273 (1970).
2.22. O. V. Lyashko, *Funkts. Analiz*, 17, 3, 28 (1983).
2.23. J. Roels, *J. Diff. Eqs.*, 10, 3, 431 (1971).
2.24. J. Roels, *J. Diff. Eqs.*, 9, 2, 300 (1971).
2.25. J. Henrard, *J. Diff. Eqs.*, 14, 3, 431 (1973).
2.26. V. A. Sarychev and V. V. Sazonov, Preprint No. 105, IPM (1976).
2.27. V. A. Zlatoustov and T. A. Shipovskikh, Preprint No. 124, IPM (1984).
2.28. B. A. Malomed and M. I. Tribel'skii, *Physica* D14, 1, 67 (1984).

3

Regular and Chaotic Dynamics of Particles in a Magnetic Field

R.Z. Sagdeev, Mem. USSR Acad. Sc. and
G.M. Zaslavskii, D. Sc. (Phys.-Math.)

3.1. INTRODUCTION

Advances in the analysis of the dynamics of nonlinear systems have resulted in comprehending a new range of phenomena: the initiation of a random motion under regular conditions, i.e. in the absence of random forces or random parameters in a system. In many physical situations it is now clear how, in the phase space of the system, a regular, or laminar, flow can become chaotic, or turbulent, when parameters of the system are varied. This transition is due to a specific (inherent) instability in the system that is called the local instability. The latter manifests itself as an exponential temporal growth of a separation between trajectories, D (t), in a certain region of the phase space of a finite measure Γ:

$$D\ (t) = D\ (0) \exp h_0 t, \quad D\ (0) \to 0. \tag{3.1}$$

The quantity $h(\Gamma) = \langle h_0 \rangle_\Gamma$, which is the average of the growth rate h_0 over Γ, determines the Kolmogorov entropy. Hence a transition from the regular dynamics to the chaotic one is associated with a certain specific "bifurcation" which results in the emergence of a region $\Gamma \neq 0$ with $h > 0$ while $h\ (\Gamma_0) = 0$ for arbitrary Γ_0 in a regular case.

The local instability can be attributed to some specific features of dynamic systems. The most clearcut correspondence can be established for systems of the Hamiltonian type, where stochastic dynamics appears due to the destruction of integrals of motion. Since the existence of a particular integral of motion is due to a certain symmetry of a system, it is evident that chaotic regimes could emerge when the symmetry pattern of the system is changed. Even though this conclusion seems to be both too general and too trivial, it highlights the role of a magnetic field which can substantially change the symmetry of the system's Hamiltonian.

With two (or even more) concurrent symmetries there can occur either the frustration of one of them (as exemplified e.g. by phase transitions) or the vanishing of both with the consequent appearance of a complicated dynamic picture that is most likely stochastic. The latter case corresponds to a maximally symmetric motion resulting from the "destruction" of unperturbed symmetries. Thus, the interaction between motion types with different symmetries in the system's Hamiltonian can result in the transition of the system to the state with a higher symmetry. The maximally possible symmetry of the system is realized by chaotic dynamics and, consequently, by the stochastic destruction of the integrals of motion.

These simple considerations shed new light on the specific role of magnetic field in the dynamics of charged particles. Let us illustrate the situation by an example associated with the paradox of the disappearance of the Landau damping in a magnetic field [3.1].

When an electric field is produced in plasma, e.g. in the form of a plane wave

$$E = E_0 \cos (kx - \omega t), \tag{3.2}$$

the interaction of particles with this field results in the field damping; this effect is known (in a linear approximation) as the Landau damping. The strongest interaction is due to particles being in resonance with the wave, that is those satisfying the resonance condition $kv - \omega = 0$, where v is the particle velocity. For a given particle velocity distribution $f(v)$, a certain finite velocity region Δv exists where the particles are close to a resonance with the wave. The situation changes dramatically when we introduce an arbitrary weak but finite uniform magnetic field B_0 perpendicular to the direction of wave propagation. Here we have another resonance condition

$$\omega - n\omega_H = 0, \quad \omega_H = eB_0/mc, \quad n = \pm 1, \pm 2.$$

which does not include the particle velocity. Hence the linear theory immediately leads to the conclusion that the wave damping is absent. To solve this paradox requires allowing for nonlinear effects that are associated with the overlapping of the resonances and with the resulting stochastic motions of the particles [3.1].

Particle dynamics in the wave field (3.2) or in the field of a wave packet,

$$E = \sum_k E_k \cos (kx - \omega_k t), \tag{3.3}$$

with an imposed magnetic field B_0, is a typical problem in plasma physics. There is a broad range of applications [3.2-3.4] associated with this problem, among them stochastic plasma heating and stochastic particle acceleration [3.5-3.8], bounce-resonances in the magnetosphere [3.9-3.11], etc.

Let us also indicate two kinds of closely related problems, in which the new approach of nonlinear dynamics could prove instrumental. The dynamics of an electron in a crystal is controlled, in a simplest form, by a periodic crystal lattice field with a potential $U(\mathbf{r}) = U(\mathbf{r} + \mathbf{a})$. Electronic states (wave functions and energy eigenvalues) are determined by a corresponding spatial symmetry. The presence of an external magnetic field modifies the symmetry of the system. Presently known modifications of electron dynamics are reviewed in [3.12]. The problem arising here is close, in the classical limit, to the corresponding problem of plasma physics, but with a three-dimensional wave packet (3.3) and $\omega_k = 0$.

Another interesting example of the magnetic effect and the corresponding symmetry violation is a hydrogen atom in a strong magnetic field. The latter can destruct the integral of motion and then the whole dynamics of the electron as well as spectroscopic properties of the atom will change dramatically [3.13].

Besides the above mentioned aspects of the problem of the particle motion in a regular field, e.g. as described by (3.2) or (3.3), with a uniform magnetic field included, there exists another aspect of a more formal nature. The study of stochasticity criteria for various physical situations reduces to the analysis of some typical models. A number of "standard" equations are discussed in the reviews [3.14-3.16]. The problem at hand introduces a new and poorly analyzed "standard" equation

$$\begin{aligned} &\ddot{x} + \omega_H^2 x = A \sin (kx - \omega t), \\ &A = \Omega_0^2/k, \quad \Omega_0^2 = eE_0 k/m \end{aligned} \tag{3.4}$$

that describes the motion of a linear oscillator of mass m in a travelling wave field.

The present work pursues a number of tasks. Within a unified analytical approach we shall obtain known asymptotic forms of the solution of Eq. (3.4) and some new asymptotic solutions. In particular, a special emphasis is placed on the limit $B_0 \to 0$ and on the accompanying universal stochastization of motion [3.17]. This work also considers the oblique propagation of the wave packet with respect to the magnetic field B_0, criteria for chaotic behaviour, decoupling times for phase correlations, as well as a kinetic description of the stochastic particle dynamics.

3.2. EQUATIONS OF MOTION

Let a uniform magnetic field B_0 be directed along the z-axis and all the components of a wave packet propagate in the same direction. Let us choose the x- and y-axes so that the wave vector $\mathbf{k}$ lies in the xz-plane. The Hamiltonian of a particle moving in these fields has the following standard form:

$$H_1 = \frac{1}{2m} \left(\mathbf{P} - \frac{e}{c} B_0 x \mathbf{y}^0 \right)^2 - e \sum_k \Phi_k \cos (z k_z + x k_\perp - \omega_k t), \tag{3.5}$$

where $\mathbf{P}$ is the generalized particle momentum, $\mathbf{y}^0$ the unit vector along the y-axis and Φ_k the amplitudes of the potential of the plane wave component. For simplicity, the summation over k will be understood in the following way: to each value of k_z corresponds one value of $k_\perp$ in the wave packet.

As follows from (3.5),

$$P_y = \text{const.} \tag{3.6}$$

This conservation law follows from the fact that all the wave vectors **k** are coplanar.

Let us introduce a new coordinate

$$\bar{x} = x - P_y/m\omega_H; \quad \dot{\bar{x}} = \dot{x} = v_x \tag{3.7}$$

and pass to the polar coordinates

$$\bar{x} = \rho \sin\varphi, \quad \dot{\bar{x}} = \rho\omega_H \cos\varphi, \quad \omega_H = \frac{eB_0}{mc}, \tag{3.8}$$

where ρ is the gyration radius. Let us also put

$$I = \frac{1}{2} m\omega_H \rho^2. \tag{3.9}$$

The Hamiltonian (3.5), with (3.6)-(3.9) taken into account, takes the following form:

$$H = \frac{1}{2m} P_z^2 + \omega_H I - e \sum_k \Phi_k \cos(zk_z + k_\perp \rho \sin\varphi - \omega_k t). \tag{3.10}$$

Using the expansion in terms of the Bessel functions,

$$e^{iz \sin\varphi} = \sum_{l=-\infty}^{\infty} J_l(z) e^{il\varphi}, \tag{3.11}$$

the expression (3.10) is transformed into the following one:

$$H = \frac{1}{2m} P_z^2 + \omega_H I - e \sum_k \Phi_k \sum_{l=-\infty}^{\infty} J_l(k_\perp \rho) \cos(zk_z + l\varphi - \omega_k t). \tag{3.12}$$

Below the following simpler notation will be used:

$$\begin{gathered} \mathcal{J} = (\mathcal{J}_1, \mathcal{J}_2), \quad \mathcal{J}_1 = P_z, \quad \mathcal{J}_2 = I, \\ \vartheta = (\vartheta_1, \vartheta_2), \quad \vartheta_1 = z, \quad \vartheta_2 = \varphi. \end{gathered} \tag{3.13}$$

The Hamiltonian (3.12), in terms of variables (3.13), takes the form

$$\begin{gathered} H = H(\mathcal{J}, \vartheta) = H_0(\mathcal{J}) + V(\mathcal{J}, \vartheta), \\ H_0(\mathcal{J}) = \frac{1}{2m} \mathcal{J}_1^2 + \omega_H \mathcal{J}_2, \\ V(\mathcal{J}, \vartheta) = \sum_k \sum_{l=-\infty}^{\infty} [V_{kl}(\mathcal{J}) e^{i(\vartheta_1 k_z + \vartheta_2 l - \omega_k t)} + \text{c.c.}], \end{gathered} \tag{3.14}$$

where the perturbational matrix elements V_{kl} are

$$V_{kl}(\mathcal{J}) = -\frac{1}{2} e\Phi_k J_l(k_\perp \rho), \quad \Phi_{-k} = \Phi_k^*. \tag{3.15}$$

One can easily see that the variables $(\mathcal{J}, \vartheta)$ represent a canonically conjugated pair (action-angle) and satisfy the following Hamiltonian equations of motion:

$$\dot{\mathcal{J}}_i = -\frac{\partial H}{\partial \vartheta_i}, \quad \dot{\vartheta}_i = \frac{\partial H}{\partial \mathcal{J}_i}, \quad (i = 1, 2). \tag{3.16}$$

The general analysis of the system (3.16) is a formidable task. But we will be mainly interested in the range of parameters, where the transition of the regular motion of a particle to the stochastic one takes place. It is well known (see, e.g. [3.4]) that this transition occurs as a result of the overlapping of resonances. Therefore we begin with the discussion of the types of resonances that can occur in the system (3.16) and analyze their interaction.

3.3. THE RESONANCES OF LONGITUDINAL MOTION

Consider the case when strong interaction between a longitudinal motion along the z-axis and the Larmor rotation of a particle prevails. We will start from studying particle motion in the field of a single plane wave and a single lth harmonic of a potential V rather than in the field of a wave packet. Then the expression (3.14) for $H(\mathcal{J}, \vartheta)$ reduces to

$$H_{kl} = \frac{1}{2m}\mathcal{J}_1^2 + \omega_H \mathcal{J}_2 - U_{kl}\cos\psi, \tag{3.17}$$

where

$$U_{kl} = e\Phi_k J_l(k_\perp \rho), \quad \psi = k_z\vartheta_1 + l\vartheta_2 - \omega_k t. \tag{3.18}$$

Equations (3.17), (3.18) and (3.16) yield the equations of motion

$$\begin{aligned} \dot{\mathcal{J}}_1 &= -k_z U_{kl}\sin\psi, \\ \dot{\mathcal{J}}_2 &= -lU_{kl}\sin\psi, \\ \dot{\psi} &= k_z\dot{\vartheta}_1 + l\dot{\vartheta}_2 - \omega_k = k_z\mathcal{J}_1/m + l\omega_H - \omega_k \\ &= k_z v_z + l\omega_H - \omega_k \equiv \omega_{kl}(v_z). \end{aligned} \tag{3.19}$$

The resonance condition follows from the last equation:

$$\omega_{kl}(v_z^{(r)}) = k_z v_z^{(r)} + l\omega_H - \omega_k = 0. \tag{3.20}$$

In the vicinity of a resonance, i.e. at

$$|v_z - v_z^{(r)}| \ll v_z^{(r)}, \tag{3.21}$$

there occurs a strong interaction of two degrees of freedom which are described by the variables $\mathcal{J}_i$, ϑ_i, $i = 1, 2$. This interaction is known as the cyclotron resonance for the normal Doppler effect $(l > 0)$ or the anomalous Doppler effect $(l < 0)$ (the linear theory of plasma instabilities due to the cyclotron resonance is discussed in [3.18]).

Let us consider the nonlinear theory of the resonance (3.20) [3.14]. Note first that the first two equations in (3.19) imply the following integral of motion:

$$\bar{\mathcal{J}} = l\mathcal{J}_1 - k_z\mathcal{J}_2 = \text{const}, \tag{3.22}$$

or

$$\bar{\mathcal{J}} = lP_z - k_z m\omega_H \rho^2/2. \tag{3.23}$$

Equations (3.22) and (3.23) are analogous to the Manley-Raw relations in the theory of parametric signal excitation.

The existence of the integral (3.22) makes the system (3.19) integrable. Differentiating the equation for $\dot{\psi}$ in (3.19) yields

$$\ddot{\psi} + \Omega_{kl}^2 \sin\psi = 0, \quad \Omega_{kl} = k_z (U_{kl}/m)^{1/2}. \tag{3.24}$$

Equation (3.24) is that of a nonlinear oscillator. It describes phase oscillations [3.14] with a frequency Ω_{kl} that is equal, according to (3.18), to

$$\Omega_{kl} = k_z \left| \frac{e}{m} \Phi_k J_l (k_\perp \rho) \right|^{1/2}. \tag{3.25}$$

For strong fields ($k_\perp \rho \ll 1$),

$$\Omega_{kl} = k_z [e\,|\Phi_k|\,(k_\perp \rho)^{|l|}/2m]^{1/2}. \tag{3.26}$$

If $l = 0$, then Eq. (3.26) transforms into the well-known formula

$$\Omega_{kl} = k_z\,[e\,|\Phi_k|/2m]^{1/2}$$

for the frequency of small amplitude oscillations of electrons captured by an electromagnetic wave in the absence of an external magnetic field.

The definition of the phase oscillation frequency Ω_{kl} should be refined. The resonance condition (3.20) and Eq. (3.23) for the integral of motion $\bar{\mathcal{J}}$ determine $v_z^{(r)}$ and

$$\rho^{(r)} = \rho\,(v_z^{(r)},\ \bar{\mathcal{J}}) \tag{3.27}$$

under the resonance. With an accuracy that we estimate later, in the vicinity of the resonance, one can adopt in Eqs. (3.19)

$$U_{kl} = U_{kl}\,(\rho^{(r)}),$$

where $\rho^{(r)}$ is expressed by Eq. (3.27).

Thus, in Eqs. (3.25) and (3.26) ρ's should be taken in the form (3.27). Let us put

$$\rho^{(r)} = v_\perp^{(r)}/\omega_H,$$

then Eq. (3.25) transforms into the following one:

$$\Omega_{kl} = \Omega_{kl}(v_z^{(r)}, v_\perp^{(r)}) = k_z \left| \frac{e}{m} \Phi_k J_l (k_\perp \rho^{(r)}) \right|^{1/2}. \tag{3.28}$$

Equations (3.19) and (3.20) imply that

$$\dot{\psi} = k_z \Delta v_z, \quad \Delta v_z \equiv v_z - v_z^{(r)}, \tag{3.29}$$

hence the equations of the nonlinear resonance (3.24) are determined by the effective Hamiltonian

$$H^{(r)} = \frac{1}{2} \dot{\psi}^2 - \Omega_{kl}^2 \cos \psi = \frac{1}{2} k_z^2 (\Delta v_z)^2 - \Omega_{kl}^2 \cos \psi \tag{3.30}$$

with the canonical variables $\dot{\psi}$, ψ.

A common solution of Eq. (3.24), with the definition (3.29) taken into account, is

$$k_z v_z = k_z v_z^{(r)} \pm 2\Omega_{kl} \operatorname{cn} (\Omega_{kl} t, \varkappa), \tag{3.31}$$

where cn is the elliptic cosine and $\varkappa$ its modulus:

$$\varkappa^2 = \frac{1}{2} \left(1 + \frac{\mathcal{E}^{(r)}}{\Omega_{kl}^2} \right) \leqslant 1. \tag{3.32}$$

Here $\mathcal{E}^{(r)} = H^{(r)}$ is the value of the "energy" integral in (3.30) that controls the phase oscillation amplitude.* Equation (3.31) gives the oscillations of the velocity v_z with respect to its resonant value

$$v_z^{(r)} = (\omega_k - l\omega_H)/k_z. \tag{3.33}$$

Taking into account the definition of the actions $\mathcal{J}_i$ (3.13) and the integral of motion $\bar{\mathcal{J}}$ (3.22) we find, by Eq. (3.31), that

$$\begin{aligned} I &= \frac{1}{2} m\omega_H \rho^2 = \mathcal{J}_2 = (lmv_z - \bar{\mathcal{J}})/k_z \\ &= (lmv_z^{(r)} - \bar{\mathcal{J}})/k_z + 2lm \frac{\Omega_{kl}}{k_z^2} \operatorname{cn} (\Omega_{kl} t, \varkappa). \end{aligned} \tag{3.34}$$

This expression describes the oscillations of the Larmor radius ρ (or those of the magnetic momentum) in a neighbourhood of a resonance trajectory. These oscillations depend on arbitrary values of two integrals of motion, $\bar{\mathcal{J}}$ and $\mathcal{E}^{(r)}$.

The phase oscillation amplitude (the resonance half-width in action) follows from (3.31):

$$\Delta \mathcal{J}_1 = m \times \max \Delta v_z = 2m\Omega_{kl}/k_z = 2(mU_{kl})^{1/2} \tag{3.35}$$

---

* An analogous solution can be also written for $\mathcal{E}^{(r)}/\Omega_{kl}^2 > 1$.

and, analogously, we obtain from (3.34)

$$\Delta I = 2lm\Omega_{kl}/k_z^2 = 2\frac{l}{k_z}(mU_{kl})^{1/2}. \tag{3.36}$$

Expressions (3.19) and (3.35) also yield the formula for the resonance half-width in frequency:

$$\Delta\omega_{kl}(v) = \frac{d\omega_{kl}(v)}{d\mathcal{J}_1}\Delta\mathcal{J}_1 = 2\Omega_{kl}. \tag{3.37}$$

Our analysis is valid when [3.14, 3.15]

$$\frac{\Delta\omega_{kl}(v)}{\omega_1} \ll 1, \quad \frac{\Delta\omega_{kl}(v)}{\omega_2} \ll 1, \tag{3.38}$$

where

$$\begin{gathered} \omega_l = \frac{\partial H_{kl}^0}{\partial \mathcal{J}_l} \quad (l = 1,\ 2), \\ H_{kl}^0 = \mathcal{J}_1^2/2m + \omega_H \mathcal{J}_2. \end{gathered} \tag{3.39}$$

Using Eqs. (3.37), (3.39), and (3.24), (3.25), the inequalities (3.38) can be reduced to the form

$$\begin{gathered} \frac{\Omega_{kl}}{k_z v_z} = |\, e\Phi_k J_l(k_\perp \rho)/mv_z^2\,|^{1/2} \ll 1, \\ \frac{\Omega_{kl}}{\omega_H} = \frac{k_z}{\omega_H}\,|\, e\Phi_k J_l(k_\perp \rho)/m\,|^{1/2} \ll 1. \end{gathered} \tag{3.40}$$

The first inequality from (3.40) shows that the seed longitudinal motion of a particle should be sufficiently strong, thus justifying the name of this type of resonant motion. The second inequality from (3.40) means that the uniform magnetic field should be sufficiently strong as compared with the perturbation due to a plane wave.

3.4. THE OVERLAPPING OF THE RESONANCES OF LONGITUDINAL MOTION

The preceding section has dealt with particle motion in the field of the monochromatic wave that is described by the Hamiltonian (3.17). However, even for a plane monochromatic wave with the wave number $\mathbf{k} = (k_\parallel,\ k_\perp)$ the presence of an external magnetic field results in the excitation of a great number of harmonics. This is clearly seen, if in Eqs. (3.12), (3.14) only one term in the sum over k is retained

$$\begin{gathered} H = H_0(\mathcal{J}) + V_k(\mathcal{J},\ \vartheta), \\ V_k(\mathcal{J},\ \vartheta) = \sum_{l=-\infty}^{\infty} [V_{kl}(\mathcal{J})\, e^{i(\vartheta_1 k_z + \vartheta_2 l - \omega_k t)} + \text{c.c.}]. \end{gathered} \tag{3.41}$$

Now Eq. (3.20) implies a large number of resonances corresponding to different values of l. Let $v_z^{(l)}$ and $v_z^{(l\pm 1)}$ be the values of v_z satisfying the resonance condition (3.20) for l and $l \pm 1$, respectively:

$$\omega_{kl}\,(v_z^{(l)}) = 0;\quad \omega_{k,\,l\pm 1}\,(v_z^{(l\pm 1)}) = 0. \tag{3.42}$$

Then it follows from (3.42) that the distance between the resonances in frequency is

$$\delta\omega = |\,\omega_l\,(v_z^{(l)}) - \omega_l\,(v_z^{(l\pm 1)})\,| = \omega_H. \tag{3.43}$$

Next, one has to consider the resonance overlapping parameter [3.14]

$$K = \left(\frac{\Delta\omega}{\delta\omega}\right)^2, \tag{3.44}$$

where $\Delta\omega$ is the frequency width of a nonlinear resonance. At $K \ll 1$ the motion of a resonant particle is very close to conditionally-periodic one and, vice versa, at $K \gg 1$ there occurs a stochastic wandering from one resonance to another. A criterion for the particle dynamics to be chaotic is

$$K \gtrsim 1. \tag{3.45}$$

For the Hamiltonian (3.41), the condition (3.45), according to (3.37), (3.43), and (3.44), can be reduced to

$$K = \frac{4\Omega_{kl}^2}{\omega_H^2} = 4\,\frac{k_z^2}{\omega_H^2}\,\frac{|\,U_{kl}\,|}{m} = 4\,\frac{k_z^2}{\omega_H^2}\,\frac{e}{m}\,|\,\Phi_k J_l\,(k_\perp\rho)\,| \gtrsim 1. \tag{3.46}$$

The condition (3.46) has been obtained in [3.5]. It implies that in a neighbourhood of zeros of the Bessel function $J_l\,(k_\perp\rho)$ the inequality (3.45) is violated and there arise stability "islands" with the conditionally-periodic motion of particles. The size of these islands, being of the order of 1/max K, decreases with increasing K.

Consider now the general case (3.14). Let δk be the typical distance between neighbouring wave vectors in a wave packet. Then the typical frequency difference of neighbouring harmonics is

$$\delta\omega_k = \left|\frac{d\omega_k}{dk}\right|\delta k. \tag{3.47}$$

Thus, the frequency separation between neighbouring resonances is

$$\delta\omega = \min\,(\nu_k,\ \omega_H), \tag{3.48}$$

where

$$\nu_k = \max\,(\delta\omega_k,\ v_z\delta k_z). \tag{3.49}$$

The criterion (3.45) now takes the form

$$K = 4\frac{k_z^2}{\left|\frac{d\omega_k}{dk}\right|\delta k}\frac{e}{m}\,|\,\Phi_k J_l(k_\perp \rho)\,| \gtrsim 1, \tag{3.50}$$

$$\left(\omega_H \gg \left|\frac{d\omega_k}{dk}\right|\delta k \gg v_z \delta k_z\right).$$

$$K = 4\frac{k_z^2}{v_z\delta k_z}\frac{e}{m}\,|\,\Phi_k J_l(k_\perp \rho)\,| \gtrsim 1, \tag{3.51}$$

$$\left(\omega_H \gg v_z\delta k_z \gg \left|\frac{d\omega_k}{dk}\right|\delta k\right).$$

The expression (3.46) is valid when the inverse inequalities

$$\omega_H \ll v_z\,\delta k_z, \left|\frac{d\omega_k}{dk}\right|\delta k \tag{3.52}$$

are satisfied.

The expressions admit an important physical interpretation, which should be considered in more detail. The condition (3.52) corresponds to rather weak magnetic fields and the onset of chaos is governed by the inequality (3.46). But in a strong magnetic field, one of the two conditions, (3.50) or (3.51), holds. These latter differ in following. We call the wave packet (3.3) quasi-spacelike, if the condition of a weak dispersion, $v_z \gg |\,d\omega_k/dk\,|$, is fulfilled. Evidently, it is fulfilled, e.g. for low-temperature plasma oscillations. For the inverse inequality, $v_z \ll |\,d\omega_k/dk\,|$, the wave packet is said to be quasi-timelike. The wavelength width in such a packet is small. Each of these cases is characterized by the individual condition of the motion stochastization, (3.50) or (3.51). These conditions show that for a quasi-timelike packet the inequality (3.50) contains no restrictions on v_z while for a quasi-spacelike packet the inequality (3.51) provides a certain maximum value, max v_z. As will be seen later, the stochastization of motion results in an increase, on the average, in the energy of particles. For (3.50) this increase is not limited by the condition $K > 1$ while for quasi-spacelike packets the longitudinal energy can only grow up to the value $m\,(\max v_z)^2/2$. This property of the limited longitudinal heating is also absent in the case of Eq. (3.46) and this is the main difference between the results obtained here and those considered in [3.4, 3.6].*

Notice also that the notions of quasi-spacelike and quasi-timelike wave packets are rather conventional. If primarily a packet is quasi-timelike, then an increase in longitudinal energy transforms it, within a certain time interval, into quasi-spacelike, this in turn resulting in a limitation on the increase in longitudinal energy. Thus, the mechanism of the stochastic "longitudinal" heating of particles is prone to saturation. This property is of a rather universal nature and it cannot be revealed when a single plane wave is considered instead of a wave packet. This conclusion is drastically substantiated by Eqs. (3.47)-(3.49) that determine the criterion of chaos initiation (3.45) in the general case of longitudinal resonances. Later on we will see how the substitution of the conditions (3.48) for the condition (3.43) can also substantially influence particle kinetics. The conditions (3.48) have been introduced in [3.19].

---

* In all the cases we have only assumed strong chaos. For any value of the parameter K there exist exponentially small regions of the phase space of particle diffusion.

3.5. A KINETIC DESCRIPTION

If condition (3.45) is fulfilled one can use the description of the particle dynamics by a kinetic equation. The inequalities (3.40) demonstrate that the perturbation due to a wave packet is weak as compared both with the intrinsic kinetic energy of the particle and with the energy of the Larmor rotation. Hence the kinetic equation can be constructed based on the theory of the perturbations in terms of the powers of the field Φ_k. Let us use the method proposed in [3.20].

Let

$$f = f(t, \mathcal{J}, \vartheta)$$

be the distribution function in the phase space of two degrees of freedom, (3.13), associated with longitudinal and transverse motions. This function satisfies the Liouville equation

$$\frac{\partial f}{\partial t} \pm \sum_{q=1,2} \omega_q \frac{\partial f}{\partial \vartheta_q} = \sum_{q=1,2} \left(\frac{\partial V}{\partial \vartheta_q} \frac{\partial f}{\partial \mathcal{J}_q} - \frac{\partial V}{\partial \mathcal{J}_q} \frac{\partial f}{\partial \vartheta_q} \right), \tag{3.53}$$

where the perturbation potential $V = V(\mathcal{J}, \vartheta)$ is defined in (3.14).

Let us expand f and V into series

$$\begin{aligned} f(t; \mathcal{J}, \vartheta) &= \sum_n [f^{(n)}(\mathcal{J}, t)\, e^{i(n, \vartheta - \omega t)} + \text{c.c.}], \\ V(\mathcal{J}, \vartheta) &= \sum_s [V_s e^{i(s, \vartheta) - i\omega_k t} + \text{c.c.}] \end{aligned} \tag{3.54}$$

with the following notation

$$\begin{aligned} &s = (s_1, s_2), \; s_1 = k_z, \; s_2 = l, \\ &(s, \vartheta) \equiv s_1\vartheta_1 + s_2\vartheta_2 = k_z\vartheta_1 + l\vartheta_2, \\ &(n, \vartheta - \omega t) = n_1(\vartheta_1 - \omega_1 t) + n_2(\vartheta_2 - \omega_2 t). \end{aligned} \tag{3.55}$$

Besides, the summation over k_z assumes simultaneously the summation over the relevant values of $k_\perp$.

Substituting (3.54) into (3.53) gives the following equation for $f^{(n)}(\mathcal{J}, t)$:

$$\begin{aligned}\frac{\partial f^{(n)}}{\partial t} = i \sum_s \sum_m \sum_q \Big\{ & V_s s_q \frac{\partial f^{(m)}}{\partial \mathcal{J}_q} \delta(n-s-m)\, e^{i((n-m),\,\omega t)-i\omega_k t} \\ & - V_{-s} s_q \frac{\partial f^{(m)}}{\partial \mathcal{J}_q} \delta(n+s-m)\, e^{i((n-m),\,\omega t)+i\omega_k t} \\ & - m_q \frac{\partial V_s}{\partial \mathcal{J}_q} f^{(m)} \delta(n-s-m)\, e^{i((n-m),\,\omega t)-i\omega_k t} \\ & - m_q \frac{\partial V_{-s}}{\partial \mathcal{J}_q} f^{(m)} \delta(n+s-m)\, e^{i((n-m),\,\omega t)+i\omega_k t} \Big\}. \end{aligned} \tag{3.56}$$

In particular

$$\begin{aligned}\frac{\partial f^{(0)}}{\partial t} = i \sum_s \{ & V_s (\hat{D}(s) f^{(-s)})\, e^{i(s,\,\omega t)-i\omega_k t} \\ & - V_{-s} (\hat{D}(s) f^{(s)})\, e^{-i(s,\,\omega t)+i\omega_k t} \\ & + (\hat{D}(s) V_s) f^{(-s)} e^{i(s,\,\omega t)-i\omega_k t} \\ & - (\hat{D}(s) V_{-s}) f^{(s)} e^{-i(s,\,\omega t)+i\omega_k t} \}_z \end{aligned} \tag{3.57}$$

where

$$\hat{D}(s) = \left(s, \frac{\partial}{\partial \mathcal{J}}\right) = s_1 \frac{\partial}{\partial \mathcal{J}_1} + s_2 \frac{\partial}{\partial \mathcal{J}_2}. \tag{3.58}$$

Equation (3.56) yields the formal solution

$$f^{(n)}(\mathcal{J}, t) = \int_{-\infty}^{t} dt\, [\text{right-hand side of (3.56)}]$$

and we substitute this into the right-hand side of Eq. (3.57). This yields the following:

$$\begin{aligned}\frac{\partial f^{(0)}}{\partial t} = - \int_{-\infty}^{t} dt_1 \sum_s \sum_{s_1} \Big\{ & e^{i(s,\,\omega t)} \left[V_s \left(s, \frac{\partial}{\partial \mathcal{J}}\right) + \left(s, \frac{\partial V_s}{\partial \mathcal{J}}\right) \right] \\ & \times \left[V_{s_1} e^{i(s_1,\,\omega t_1)} \left(s_1, \frac{\partial f^{(-s-s_1)}}{\partial \mathcal{J}}\right) \right. \\ & \left. - V_{-s_1} e^{-i(s_1,\,\omega t_1)} \left(s_1, \frac{\partial f^{(-s+s_1)}}{\partial \mathcal{J}}\right) \right] \\ & - e^{-i(s,\,\omega t)} \left[V_{-s} \left(s, \frac{\partial}{\partial \mathcal{J}}\right) + \left(s, \frac{\partial V_{-s}}{\partial \mathcal{J}}\right) \right] \\ & \times \left[V_{s_1} e^{i(s_1,\,\omega t_1)} \left(s_1, \frac{\partial f^{(s-s_1)}}{\partial \mathcal{J}}\right) \right. \\ & \left. - V_{-s_1} e^{-i(s_1,\,\omega t_1)} \left(s_1, \frac{\partial f^{(s+s_1)}}{\partial \mathcal{J}}\right) \right] \Big\}. \end{aligned} \tag{3.59}$$

Let us apply the "coarse grain" operator $\langle\langle\ldots\rangle\rangle$ to (3.59), this operator being an averaging over initial phases [3.20]:

$$\langle\langle\ldots\rangle\rangle=\frac{1}{(2\pi)^2}\int_0^{2\pi}d\vartheta_1(0)\int_0^{2\pi}d\vartheta_2(0)\ldots. \tag{3.60}$$

The action of this operator and the integration in terms of t_1 in (3.59) can be interchanged. Let us denote also

$$F(\mathcal{J},\ t)=\langle\langle f^{(0)}(\mathcal{J},\ t)\rangle\rangle \tag{3.61}$$

and define the correlators:

$$\mathcal{R}_s(t)=\langle\langle e^{i(s,\ \omega t)}\rangle\rangle \tag{3.62}$$

When the stochasticity criterion $K\gg 1$ is fulfilled the formulas like those of (3.62) can be approximated as [3.9, 3.10]

$$\mathcal{R}_s(t)\sim e^{i(s,\ \omega t)}e^{-t/\tau_c}, \tag{3.63}$$

where the expression for the characteristic time of correlation decoupling τ_c will be given below.

By performing the above operations, choosing the principal (nonoscillating) terms up to the second order, and taking into account (3.61)-(3.63), we obtain from Eq. (3.59) the following:

$$\frac{\partial F}{\partial t}=2\pi\sum_s\hat{D}(s)\,|\,V_s\,|^2\,\Delta\left((s,\ \omega)+\omega_k\right)\hat{D}(s)\,F, \tag{3.64}$$

where

$$\Delta(\xi)=\frac{1}{\pi}\,\frac{1/\tau_c}{(1/\tau_c)^2+\xi^2}\,. \tag{3.65}$$

As $1/\tau_c\to 0$, we have $\Delta(\xi)\to\delta(\xi)$. Now it is possible to express the kinetic Eq. (3.64) in an explicit form, with a due allowance for the notations from (3.58), (3.15), and (3.13),

$$\frac{\partial F}{\partial t}=\frac{1}{2}\pi e^2\sum_k\sum_l|\,\Phi_k\,|^2\left(k_z\frac{\partial}{\partial P_z}-2\,l\omega_H\frac{\partial}{\partial(mv_\perp^2)}\right)$$
$$\times J_l^2\left(\frac{k_\perp v_\perp}{\omega_H}\right)\Delta(k_z v_z+l\omega_H-\omega_k)\left(k_z\frac{\partial}{\partial P_z}-2l\omega_H\frac{\partial}{\partial(mv_\perp^2)}\right)F. \tag{3.66}$$

The kinetic equation for given random fields having finite correlation times for $k\rho\ll 1$ has been obtained in [3.21]. Here the characteristic time of the correlation decoupling can be found directly from particle dynamics. Consider this problem in more detail.

The papers [3.20, 3.22] have demonstrated that for $K\gg 1$

$$\tau_c\sim 2T/\ln K, \tag{3.67}$$

where T is the characteristic time interval of a mapping. However, the most important point for us is that

$$T = 2\pi/\delta\omega, \tag{3.68}$$

where $\delta\omega$ is the frequency separation between resonances. Formulas (3.67) and (3.68) have been derived for constant values of T and $\delta\omega$ and for an infinite number of resonances. These formulas are valid, if the change $\delta\omega$ is sufficiently small

$$\frac{d}{d\mathcal{J}} \ln \delta\omega \ll 1 \tag{3.69}$$

and the number of resonances is sufficiently large

$$N = \frac{\omega_{\max} - \omega_{\min}}{\delta\omega} \gg 1. \tag{3.70}$$

Here $\omega_{\max}$ and $\omega_{\min}$ are the maximum and minimum frequencies within a wave packet, respectively.

Taking into account the inequalities (3.69) and (3.70) we find, by (3.46)-(3.51), that

$$\begin{aligned}
&\frac{1}{\tau_c} \sim \frac{1}{4\pi} \left| \frac{d\omega_k}{dk} \right| \delta k \ln \frac{4k_z^2 \frac{e}{m} \mid \Phi_k J_l(k_\perp \rho) \mid}{\left| \frac{d\omega_k}{dk} \right| \delta k}, \\
&\left(\omega_H \gg \left| \frac{d\omega_k}{dk} \right| \delta k \gg v_z \delta k_z \right), \\
&\frac{1}{\tau_c} \sim \frac{1}{4\pi} v_z \delta k_z \ln \frac{4k_z^2 \frac{e}{m} \mid \Phi_k J_l(k_\perp \rho) \mid}{v_z \delta k_z}, \\
&\left(\omega_H \gg v_z \delta k_z \gg \left| \frac{d\omega_k}{dk} \right| \delta k \right), \\
&\frac{1}{\tau_c} \sim \frac{1}{4\pi} \omega_H \ln \frac{4k_z^2 \frac{e}{m} \mid \Phi_k J_l(k_\perp \rho) \mid}{\omega_H}, \\
&\left(\omega_H \ll \delta k_z v_z, \left| \frac{d\omega_k}{dk} \right| \delta k \right).
\end{aligned} \tag{3.71}$$

These expressions determine correlation times for basic possible cases of longitudinal resonances.

3.6. EQUATIONS OF TRANSVERSE MOTION

Let us study a wave packet moving perpendicular to a magnetic field. Let this direction be the x-axis, then $k_z = 0$ and one can put $P_z = \text{const} = 0$. In what follows we omit the subscript "$\perp$" at k and v to simplify notation.

The Hamiltonian (3.12) takes here the following form:

$$H = \omega_H I - e \sum_k \sum_{l=-\infty}^{\infty} \Phi_k J_l(k\rho)\cos(l\varphi - \omega_k t). \tag{3.72}$$

The problem is characterized by the fact that, in the absence of perturbation, there is no seed nonlinearity. To begin with, consider the particle motion when there is a single wave rather than a wave packet

$$\begin{aligned} H &= \omega_H I - e\Phi_k \cos(kx - \omega_k t) \\ &= \omega_H I - e\Phi_k \sum_{l=-\infty}^{\infty} J_l(k\rho)\cos(l\varphi - \omega_k t), \end{aligned} \tag{3.73}$$

where the notations (3.8) are accepted. In terms of the variables $(x, \dot{x})$, the equation of motion has the form

$$\ddot{x} + \omega_H^2 x = \frac{ek}{m}\Phi_k \cos(kx - \omega_k t). \tag{3.74}$$

In terms of the variables (I, φ), these equations acquire the following form:

$$\begin{aligned} \dot{I} &= -\frac{\partial H}{\partial \varphi} = -e\Phi_k \sum_{l=-\infty}^{\infty} lJ_l(k\rho)\sin(l\varphi - \omega_k t), \\ \dot{\varphi} &= \frac{\partial H}{\partial I} = \omega_H - e\Phi_k \sum_{l=-\infty}^{\infty} \frac{dJ_l(k\rho)}{dI}\cos(l\varphi - \omega_k t), \end{aligned} \tag{3.75}$$

where I and ρ are related by (3.9). Equations (3.74) and (3.75) demonstrate that the nonlinear character of the problem is only due to perturbation. Furthermore, the right-hand side of the system (3.75) can include a large number of harmonics that strongly affect the motion, i.e. those close to resonance.

In the lowest-order approximation,

$$\dot{\varphi} = \omega_H$$

and therefore the resonance condition takes the form

$$l_0\omega_H = \omega_k, \tag{3.76}$$

where l_0 is a certain number. Let us further presume that the condition (3.76) is approximately fulfilled for a certain $l_0 \gg 1$. We will be interested in the case of rather weak magnetic fields B_0. Hence the following condition takes place:

$$k\rho = kv/\omega_H \gg 1. \tag{3.77}$$

This inequality means that only those terms in the summations over l in (3.75) considerably affect the particle dynamics for which

$$|\, l \,| \leqslant k\rho. \tag{3.78}$$

Hence the cases are feasible when the resonance (3.76) is either within the region defined by (3.77), i.e.

$$1 \ll l_0 < k\rho, \tag{3.79}$$

or when

$$1 \ll k\rho < l_0. \tag{3.80}$$

Below we consider the situation which corresponds to (3.79), since, in the case of (3.80), the influence of the first-order resonances is exponentially small.

Qualitatively, the motion corresponding to the system (3.75) can be described in the following way. The right-hand side of Eq. (3.75) contains Δl harmonics with the numbers close to the resonant value l_0 and with action also close to the resonant one. We will determine this number below. It satisfies the evident inequality

$$1 < \Delta l < l_0$$

that will be assumed below as fulfilled in a more strong form

$$1 \ll \Delta l \ll l_0. \tag{3.81}$$

Proceeding from (3.81) one can present Eq. (3.74) as

$$\begin{aligned} \ddot{x} + \omega_H^2 x = &-\frac{ek}{m}\Phi_k \sum_{l \in \Delta l} J_l(k\rho)\sin(l\varphi - \omega_k t) \\ &-\frac{ek}{m}\Phi_k \sum_{l \notin \Delta l} J_l(k\rho)\sin(l\varphi - \omega_k t) \end{aligned} \tag{3.82}$$

and decompose the particle motion into a rapidly oscillating component ξ, that is due to all nonresonant terms, and a slowly varying component X, that is due to the action of resonances and a weak external magnetic field. Let us represent x in the form

$$x = X + \xi.$$

According to (3.82), the equation for ξ has the following form:

$$\ddot{\xi} + \omega_H^2 \xi = \frac{e}{m} k\Phi_k \sum_{l \notin \Delta l} J_l(k\rho)\sin(l\varphi - \omega_k t),$$

whence we easily find

$$\dot{\xi} = \frac{e}{m}\frac{k\Phi_k}{\omega_k} \sum_{l \notin \Delta l} J_l(k\rho)\cos(l\varphi - \omega_k t),$$

where only the terms of the order of $\Delta l/l_0$ and ω_H/ω_k are retained. The averaging over rapid oscillations enables us to derive the effective potential for a slow-term evolution:

$$\overline{\overline{V}} = \frac{1}{2} m\overline{\dot{\xi}^2} = \frac{1}{m}\left(\frac{ek\Phi_k}{2\omega_k}\right)^2 \sum_{l\in\Delta l} J_l^2(k\rho). \tag{3.83}$$

Now the effective Hamiltonian of the slow motion has the following form:

$$\begin{aligned} &\overline{H}(X) = H_0 + \overline{V} + V_r,\\ &H_0 = \omega_H I,\\ &V_r = -e\Phi_k \sum_{l\in\Delta l} J_l(k\rho)\cos(l\varphi - \omega_k t),\\ &I = \frac{1}{2} m\omega_H^2\rho^2, \quad \rho = \dot{X}^2/\omega_H^2 + X^2,\\ &X = \rho\sin\varphi, \quad \dot{X} = \rho\omega_H\cos\varphi. \end{aligned} \tag{3.84}$$

For convenience, the Hamiltonian $\overline{H}$ can be rewritten as

$$\overline{H} = \overline{H}(I, \varphi) = \overline{H}_0(I) + V_r(I, \varphi), \tag{3.85}$$

where

$$\overline{H}_0(I) = H_0(I) + \overline{V}(I).$$

Thus, the potential of a rapidly oscillating field gives rise to nonlinear particle oscillations, i.e. to the dependence of frequency on I:

$$\overline{\omega}(I) = \frac{d\overline{H}_0}{dI} = \omega_H + \frac{d\overline{V}(I)}{dI} = \omega_H + \frac{1}{m}\left(\frac{ek\Phi_k}{2\omega_k}\right)^2 \frac{d}{dI} \sum_{l\in\Delta l} J_l^2(k\rho). \tag{3.86}$$

Let us use the relation

$$\sum_{l=-\infty}^{\infty} J_l^2(k\rho) = 1$$

to reduce $\overline{\omega}(I)$ to the form

$$\overline{\omega}(I) = \omega_H - \frac{1}{m}\left(\frac{ek\Phi_k}{2\omega_k}\right)^2 \frac{d}{dI} \sum_{l\notin\Delta l} J_l^2(k\rho). \tag{3.87}$$

The emerged nonlinear correction to frequency describes a regular deviation of a particle trajectory from a circular one due to the combined action of magnetic and wave fields.

Using Eqs. (3.84)-(3.87) the equation of motion for the slow variables ($\bar{I}$, φ) can be written in the following canonical form:

$$\dot{I} = -\frac{\partial \bar{H}}{\partial \varphi} = -\frac{\partial V_r}{\partial \varphi} = e\Phi_k \sum_{l \in \Delta l} l J_l(k\rho) \sin(l\varphi - \omega_k t),$$
$$\dot{\varphi} = \frac{\partial \bar{H}}{\partial I} = \bar{\omega}(I) - e\Phi_k \frac{d}{dI} \sum_{l \in \Delta l} J_l(k\rho) \cos(l\varphi - \omega_k t). \tag{3.88}$$

In what follows, of importance is the estimate of the orders of magnitude of terms entering into the equation for $\dot{\varphi}$. Let us fix the value of l_0 that determines, via (3.76), the resonance number and let $B_0 \rightarrow 0$. The inequalities (3.79) and (3.81) then yield

$$\Delta l \ll l_0 \ll k\rho. \tag{3.89}$$

This relation enables the asymptotic form

$$J_l(k\rho) \sim (2/\pi k\rho)^{1/2} \cos(k\rho - \pi l/2 - \pi/4) \tag{3.90}$$

to be used in Eqs. (3.88). The following form of the last inequality in (3.89) is also useful

$$\frac{k\rho}{l_0} = \frac{kv}{l\omega_k} \gg 1. \tag{3.91}$$

In physical terms, this expression singles out a group of particles moving with a velocity exceeding the phase velocity of the wave.

Substituting (3.90) into (3.88) reduces the equation of motion to the form

$$\dot{I} \approx -(2/\pi k\rho)^{1/2} e\Phi_k l_0 \sum_{l \in \Delta l} \cos(k\rho - \pi l/2 - \pi/4) \sin(l\varphi - \omega_k t),$$
$$\dot{\varphi} \approx \bar{\omega}(I) - (k\rho/8\pi)^{1/2} (e\Phi_k/I) \sum_{l \in \Delta l} \sin(k\rho$$
$$- \pi l/2 - \pi/4) \cos(l\varphi - \omega_k t). \tag{3.92}$$

Let us introduce the dimensionless parameter for the perturbation of a particle by the wave field

$$\varepsilon = 2e\Phi_k/mv^2 \ll 1 \tag{3.93}$$

and estimate the orders of magnitude of various terms that are involved in Eq. (3.92) for $\dot{\varphi}$. We have

$$\delta_1 = |\bar{\omega}(I) - \omega_H'|| \sim \frac{1}{32\pi} \varepsilon^2 \frac{kv}{\omega_k^2} \omega_H^3 \Delta l. \tag{3.94}$$

Analogously, the order of magnitude of the last term in the right-hand side of Eq. (3.92) for $\dot{\varphi}$ is

$$\delta_2 \sim \frac{\varepsilon}{(8\pi)^{1/2}} (kv)^{1/2} \omega_H^{1/2}. \tag{3.95}$$

Comparing (3.94) and (3.95) yields

$$\frac{\delta_1}{\delta_2}=\frac{1}{8(2\pi)^{1/2}}\varepsilon\left(\frac{kv}{\omega_k}\right)^{1/2}\left(\frac{\omega_H}{\omega_k}\right)^{3/2}. \tag{3.96}$$

Now we can see that the ratio (3.96), combined with the inequalities (3.91), (3.93), and (3.81), describes two physically different cases. When $\delta_1 \gg \delta_2$, the main role is played by the nonlinearity due to the nonresonant, rapidly oscillating terms that induce the dependence of $\bar{\omega}$ on the action I. In the opposite case, when $\delta_2 \gg \delta_1$, one can neglect the nonlinear correction to frequency and assume $\bar{\omega}(I) \approx \omega_H$. Here the nonlinearity of the motion is due to the nonlinearity in the last term in Eq. (3.92) for $\dot{\varphi}$. Evidently, this situation is realized in the limiting case of very weak fields.

3.7. THE RESONANCES OF HIGH-ENERGY PARTICLES

Particles are said to be high-energy when they move at velocities satisfying the inequality

$$\delta_1 \gg \delta_2. \tag{3.97}$$

Under the condition (3.97) the basic dynamic features are determined, as noted above, by the system (3.92), with the last term in the equation for $\dot{\varphi}$ neglected. At an isolated resonance, the motion is governed by the system

$$\begin{aligned}\dot{I} &= -\left(\frac{2}{\pi k\rho}\right)^{1/2} e\Phi_k l_0 \cos(k\rho-\pi l/2-\pi/4)\sin(l\varphi-\omega_k t),\\ \dot{\varphi} &= \bar{\omega}(I).\end{aligned} \tag{3.98}$$

The resonance width can be found in the same manner as it has been done in Sec. 3.3. We have

$$\begin{aligned}(\Delta I)^2 &= \left(\frac{2}{\pi k\rho}\right)^{1/2} e\Phi_k \cos\Psi \Big/ \left|\frac{d\bar{\omega}}{dI}\right|\\ &= \left(\frac{2}{\pi k\rho}\right)^{1/2} e\Phi_k \cos\Psi \Big/ \left|\frac{d\delta_1}{dI}\right|,\\ \Psi &\equiv k\rho-\pi l/2-\pi/4,\end{aligned} \tag{3.99}$$

whence

$$\frac{\Delta I}{I}=\left[64(2\pi)^{1/2}\frac{1}{\varepsilon}\left(\frac{\omega_k}{kv}\right)^{3/2}\left(\frac{\omega_k}{\omega_H}\right)^{1/2}\frac{\cos\Psi}{\Delta l}\right]^{1/2}.$$

With (3.96) and (3.99) taken into account, the inequality (3.97) guarantees that the perturbation is weak, $\Delta I/I \ll 1$.

The resonance frequency width can be found from the equation

$$\Delta\omega_1 = \left|\frac{d\bar{\omega}}{dI}\right| \Delta I = \left[\left(\frac{2}{\pi k\rho}\right)^{1/2} e\Phi_k \left|\frac{d\bar{\omega}}{dI}\right| \frac{\cos\Psi}{\Delta l}\right]^{1/2}.$$

Whence

$$\frac{\Delta\omega_1}{\omega_H} = \left[\frac{1}{2(8\pi)^{3/2}} \varepsilon^3 \left(\frac{\omega_H}{\omega_k}\right)^{3/2} \left(\frac{kv}{\omega_k}\right)^{1/2} \frac{\cos\Psi}{\Delta l}\right]^{1/2}. \tag{3.100}$$

The frequency separation of resonances, $\delta\omega$, can be determined from the conditions for a pair of neighbouring resonances

$$l\bar{\omega}(I_l) = \omega_k,$$
$$(l \pm 1)\,\bar{\omega}(I_{l\pm 1}) = \omega_k.$$

Whence

$$\delta\omega = |\bar{\omega}(I_l) - \bar{\omega}(I_{l\pm 1})| = \frac{\omega_H^2}{\omega_k} + O(1/l). \tag{3.101}$$

Equations (3.100) and (3.101) yield the condition for the onset of stochasticity

$$K_1 = \left(\frac{\Delta\omega_1}{\delta\omega}\right)^2 = \frac{1}{2(8\pi)^{3/2}} \varepsilon^3 (k\rho)^{1/2} \frac{\cos\Psi}{\Delta l} \gtrsim 1. \tag{3.102}$$

As in the case of longitudinal resonances, the factor $\cos\Psi$ gives rise to narrow (of the order of $1/k$) ranges in velocity, with the stable motion. The quantity Δl characterizes the number of the nearest overlapped resonances and $\Delta l \sim 1$ in the vicinity of the stochasticity threshold.

The formulas (3.101) and (3.102) also determine the decoupling time of the phase φ correlation

$$1/\tau_c \sim \frac{\omega_H^2}{\omega_k} \ln K_1. \tag{3.103}$$

One of the most essential features of the case is the appearance of the characteristic time ω_k/ω_H^2 in phase relaxation process which replaces the Larmor period.

3.8. RESONANCES IN A WEAK MAGNETIC FIELD

The case opposite to the inequality (3.97), i.e.

$$\delta_2 \gg \delta_1, \tag{3.104}$$

is considered in [3.7]. In the system of equations of motion (3.92) one can put $\bar{\omega}(I) \approx \omega_H$ and retain the last term in the equation for $\dot{\varphi}$.

Let us demonstrate how the result of [3.7] can be derived from the same qualitative considerations as in the preceding section. By the inequality (3.104) and the notation (3.95) we have from the second equation in (3.92) the following:

$$\Delta\omega_2 = \delta_2 \sim \frac{\varepsilon}{(8\pi)^{1/2}} (k\rho)^{1/2} \omega_H . \tag{3.105}$$

Using (3.101) for the separation between resonances we have a stochasticity condition in the following form:

$$K_2 = \left(\frac{\delta_2}{\delta\omega}\right)^2 \sim \frac{1}{8\pi} \varepsilon^2 (k\rho)^3 \left(\frac{\omega_k}{kv}\right)^2 = \frac{1}{8\pi} \varepsilon^2 \frac{kv}{\omega_k} \left(\frac{\omega_k}{\omega_H}\right)^3 \gtrsim 1. \tag{3.106}$$

The factor like $\cos\Psi$ is omitted here for simplicity.

The results obtained from (3.102) and (3.106) show that, independently of the magnetic field strength, there always exist velocity ranges where particle dynamics is chaotic. This phenomenon results in an increase in the particle energy and, as a consequence, in wave damping which will be considered below.

3.9. GENERALIZATION TO A WAVE PACKET

In Sec. 3.4 it has been demonstrated how, in the presence of wave motion, one passes from the problem of a motion in the field of a single wave to that in the field of a wave packet. Let us apply this technique to the transverse motion specified by the Hamiltonian (3.72). Instead of the equations of motion (3.75) we have the following ones:

$$\begin{aligned} \dot{I} &= -e \sum_k \sum_{l=-\infty}^{\infty} \Phi_k l J_l (k\rho) \sin (l\varphi - \omega_k t), \\ \dot{\varphi} &= \omega_H - e \sum_k \sum_{l=-\infty}^{\infty} \frac{dJ_l (k\rho)}{dI} \cos (l\varphi - \omega_k t). \end{aligned} \tag{3.107}$$

Now this system admits much more diverse cases. Here we consider the simplest case, viz. when it is assumed that the characteristic frequency separation ω_k within a wave packet satisfies the inequality

$$\delta\omega_k = \left| \frac{d\omega_k}{dk} \right| \delta k \ll \frac{\omega_H^2}{\omega_k} . \tag{3.108}$$

Hence the frequency separation is obtained not from (3.101) but from (3.108). This at once yields

$$\begin{aligned} &\left(\frac{\Delta\omega_1}{\delta\omega_k}\right)^2 \gtrsim 1 \qquad (\delta_1 \gg \delta_2), \\ &\left(\frac{\Delta\omega_2}{\Delta\omega_k}\right)^2 \gtrsim 1 \qquad (\delta_2 \gg \delta_1), \end{aligned} \tag{3.109}$$

where $\Delta\omega_1$ and $\Delta\omega_2$ are given by (3.100) and (3.105), respectively.

The effect of a wave packet is most pronounced for sufficiently strong magnetic fields, when $k\rho < 1$, or at small values of the wave number k. In this case the resonances can occur even at small numbers of the harmonics, l, but there can exist many of them due to the modes composing the wave packet. This case, however, will not be considered here.

3.10. A KINETIC DESCRIPTION OF TRANSVERSE MOTION

With one of the conditions (3.109) fulfilled, the particle motion can be described by a kinetic equation for the distribution function $F = F(v_\perp, t)$. This equation can be directly derived from (3.66), by putting $k_z = 0$, $v_z = 0$ in the latter and by substituting $\bar{\omega}(I)$ for ω_H in the Δ-function. This yields

$$\frac{\partial F}{\partial t} = \frac{\pi}{2}\frac{e^2}{m^2}\sum_k \sum_l |\Phi_k|^2 l^2 \omega_H^2 \frac{\partial}{v_\perp \partial v_\perp} J_l^2\left(\frac{kv_\perp}{\omega_H}\right)\Delta(l\bar{\omega} - \omega_k)\frac{\partial F}{v_\perp \partial v_\perp}. \tag{3.110}$$

With the condition (3.108) fulfilled, the separation between resonances is determined by the separation between modes in a wave packet. Therefore the characteristic time of the correlation decoupling is given by

$$\frac{1}{\tau_c} \sim \delta\omega_k \ln\left|\frac{\Delta\omega_{1,2}}{\delta\omega_k}\right| \tag{3.111}$$

when $\delta_1/\delta_2 \gg 1$ or $\delta_2/\delta_1 \gg 1$, respectively.

If instead of a wave packet we only consider a single wave then formula (3.110) should not contain the sum over k while formula (3.111) should be replaced, according to (3.103) and (3.106), by the following one:

$$\frac{1}{\tau_c} \sim \frac{\omega_H^2}{\omega_k} \ln K_{1,2}. \tag{3.112}$$

Let us estimate the diffusion coefficient in the latter case.

Let us present Eq. (3.110) in the form

$$\frac{\partial F}{\partial t} = \frac{1}{2}\frac{\partial}{\partial v_\perp^2} D \frac{\partial F}{\partial v_\perp^2} \tag{3.113}$$

and only consider the diffusive acceleration of resonant particles. Then

$$\begin{aligned} D &\sim \pi \frac{e^2 |\Phi_k|^2}{m^2} \omega_k^2 J^2_{l_0}\left(\frac{kv_\perp}{\omega_H}\right)\tau_c \\ &\sim 2\frac{e^2}{m^2} |\Phi_k|^2 \frac{\omega_k^3}{\omega_H k v_\perp} \frac{\sin^2\Psi}{\ln K_{1,2}} \quad (l_0 = \omega_k/\omega_H), \end{aligned} \tag{3.114}$$

where the phase $\Psi = kv_\perp/\omega_H - \pi l_0/2 - \pi/4$ controls high-frequency modulation of the diffusion coefficient. With this modulation neglected, let us evaluate, by Eqs. (3.113) and (3.114), an increase in particle energy

$$\mathscr{E} = \frac{1}{2} m \int v_\perp^2 F(v_\perp^2, t)\, dv_\perp^2. \tag{3.115}$$

Substituting (3.115) into (3.113) yields

$$\begin{aligned}\frac{d\mathscr{E}}{dt} &\sim \frac{1}{2}\frac{e^2}{m} k^2 |\Phi_k|^2 \left(\frac{\omega_k}{kv_\perp}\right)^3 \frac{1}{\omega_H \ln K_{1,2}} \\ &= \frac{e^2k^2}{2m\omega_H} \frac{|\Phi_k|^2}{\ln K_{1,2}} \left(\frac{\omega_k}{k}\right)^3 \left(\frac{2\mathscr{E}}{m}\right)^{-3/2}.\end{aligned} \tag{3.116}$$

Whence as $t \to \infty$

$$\mathscr{E}(t) \sim (Ct)^{2/5}, \tag{3.117}$$

where

$$C = \frac{5}{8}\left(\frac{m}{2}\right)^{1/2} \frac{e^2 |\Phi_k|^2 \omega_k^3}{k\omega_H \ln K_{1,2}}.$$

The last expression indicates that, by the inequality $kv \gg \omega_h$, there occurs the "heating" of particles whose velocities are at the "tail" of the distribution function. Formula (3.106) shows that, as the magnetic field decreases, particles with an ever decreasing ratio kv/ω_k become involved in the stochastic heating. However, the correlation decoupling time simultaneously increases roughly as $1/\omega_H^2$ (see (3.112)).

Strictly speaking, formula (3.117) does not completely describe the energy increase for all particles. The fact is that the stochastization of motion can occur within a wide velocity range, the region of $\omega_k \sim kv$ [3.16] included. However, in different regions the diffusion coefficient has a different form which can be easily derived in each specific case from the general formula (3.110). Expression (3.117) holds when the distribution function provides a majority of particles in the velocity range satisfying the inequality (3.106) at $\omega_k/kv \ll 1$. Then the general postulates of quasi-linear theory enable wave damping to be found by the law of energy conservation as follows:

$$\frac{1}{8\pi}\frac{d|E_k|^2}{dt} = \frac{1}{8\pi}\frac{d}{dt}|k\Phi_k|^2 = -\frac{d\mathscr{E}}{dt} = -\frac{1}{8\pi} C_e |k\Phi_k|^2 \mathscr{E}^{-3/2}, \tag{3.118}$$

where

$$C_e = \frac{2^{1/2}e^2m^{1/2}}{\pi}\frac{\omega_k^3}{k^3}\frac{1}{\omega_H \ln K_{1,2}}.$$

Asymptotically, as $t \to \infty$ the law (3.117) can be used for $\mathscr{E}(t)$. Then (3.118) implies

$$\frac{1}{\mathscr{E}_k}\frac{d\mathscr{E}_k}{dt} = -C_e(Ct)^{-3/5}, \quad \mathscr{E}_k \equiv |E_k|^2 = |k\Phi_k|^2$$

or

$$\mathscr{E}_k = \text{const} \times \exp[-C_e/(Ct)^{3/5}]. \tag{3.119}$$

The last expression describes the formation of an asymptotic energy level of fluctuating fields. This finite level is due to the termination of the increase in particle energy (see (3.116)) at sufficiently high energies.

3.11. QUASI-RESONANCE PARTICLES

Assume again that a wave propagates perpendicular to a magnetic field B_0 and the particle motion is described by Eq. (3.4) or (3.74).

Until now we have considered the resonances of particles with a sufficiently high velocity, $v_x = v \gg \omega/k$. Such particles weakly interact with a wave having a phase velocity ω/k. In fact, all the particles with $v > \omega/k$ have, within a certain time interval, a velocity $v_x \sim \omega/k$. Within this interval there occurs an intense interaction between the oscillations associated with particle trapping by a wave and a gyration in the magnetic field (Fig. 3.1). Let us denote the relevant moments of time, when two successive particle-wave "collisions" take place, as t_i and t_{i+1} (see Fig. 3.1).

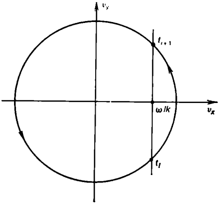

Fig. 3.1

The particle-wave "collision" can actually last for a fairly long time and hence it should be classified as a strong collision. The theory of the relevant process as $\omega_H \to 0$ has been constructed in [3.17, 3.24]. Let us present here its main findings.

Ensuing simple estimates will clarify the qualitative picture of the particle-wave interaction in the limiting case $B_0 \to 0$ ($\omega_H \to 0$).

All particles with $v > \omega/k$ can intensely interact with a wave. Results obtained in [3.8] suggest that the velocity change due to such an interaction

$$\Delta v_x \sim ek\Phi_k/[m\,(\omega_k\omega_H)^{1/2}] \tag{3.120}$$

(accurate to a certain phase factor). On the other hand, according to the equations of motion (3.74),

$$\Delta P_x = m\,\Delta v_x \sim ek\Phi_k\tau_s, \tag{3.121}$$

where τ_s is the duration of the collision with a wave. Comparing (3.120) with (3.121) shows that

$$\tau_s = 1/(\omega_k\omega_H)^{1/2}. \tag{3.122}$$

Hence the particle-wave collisions are instantaneous when $\tau_s \ll \tau_0 = 2\pi/\Omega_0$ or, by taking into account (3.122),

$$\eta \equiv \frac{\Omega_0^2}{\omega_k\omega_H} \ll 1, \quad \Omega_0^2 = \frac{ek^2}{m}\Phi_k. \tag{3.123}$$

It is this condition (3.123) that has been used in [3.8]. However, it does not allow us to pass to the limit $\omega_H \to 0$, therefore in this case one should consider large values of the parameter η, i.e.

$$\eta \gg 1 \tag{3.124}$$

which, as will be seen later, means a longer particle-wave interaction time.

Let the state of a particle be specified by its velocity v_x and the wave phase ϑ at the moment of the collision. Let us introduce the notation $\overline{t}_l = t_l - 0$, where t_l is the collision moment. Then the particle trajectory can be represented by the Poincaré mapping $\hat{T}$ as follows:

$$(\mathscr{E}_{l+2},\ \vartheta_{l+2}) = \hat{T}(\mathscr{E}_l,\ \vartheta_l), \tag{3.125}$$

where

$$\mathscr{E} = mv_x^2/2, \quad v_l = v_x(\bar{t}_l), \quad \vartheta_l = \vartheta(\bar{t}_l).$$

Let us denote by $\tau_{s,l}$ the duration of a particle "trapping" within a resonance region t_l. Then the time T_l needed for one mapping step is

$$T_l \approx \frac{2\pi}{\omega_H} + \tau_{s,\,l} + \tau_{s,\,l+1}$$

By these expressions the mapping (3.125) takes the form

$$\begin{aligned} \mathscr{E}_{l+2} &= \mathscr{E}_l + \Delta\mathscr{E}(\mathscr{E}_l, \vartheta_l), \\ \vartheta_{l+2} &= \vartheta_l + 2\pi/\omega_H + \omega_k(\tau_{s,\,l+1} + \tau_{s,\,l}) \quad (\mathrm{mod}\ 2\pi), \end{aligned} \tag{3.126}$$

where the quantities $\Delta\mathscr{E}$ and τ_s are to be found. They are derived under the condition (3.124) in [3.17, 3.24] by matching solutions for the external (relative to the wave) and internal regions:

$$\begin{aligned} \Delta\mathscr{E} &\sim m\left(\frac{\omega_k}{k}\right)^2 \frac{\omega_H}{\Omega_0} (\ln\eta) f(\vartheta_l), \\ \tau_s &\sim \frac{2\pi}{\Omega_0}\eta\ln\eta, \end{aligned} \tag{3.127}$$

where $f(\vartheta)$ is a periodic phase function satisfying the condition $|f(\vartheta)| \leqslant 1$.

The quantity τ_s is simply the oscillation period of a particle, trapped by a wave, on an energy level

$$\mathscr{E} = \mathscr{E}^{(0)}\left(1 + \frac{1}{\eta}\right), \quad \mathscr{E}^{(0)} = e\Phi_k$$

multiplied by the number of such oscillations, $N = \eta \gg 1$. This very fact represents the effect of the strong interaction with a wave,

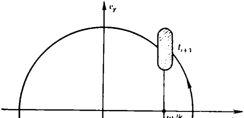

Fig. 3.2

when, over a long period of time, a particle moves along the x-axis at a velocity close to the wave phase velocity ω_k/k [3.1] (see Fig. 3.2, where the resonant interaction regions are hatched).

By formulas (3.127) let us calculate the phase change $\Delta\vartheta$ in the mapping (3.126). We have

$$\begin{aligned}\Delta\vartheta_l &= \omega_k\tau_s(\mathscr{E}_{l+1}, \vartheta_l) + \omega_k\tau_s(\mathscr{E}_{l+2}, \vartheta_l)\\ &= 2\omega_k\tau_s(\mathscr{E}_l) + \omega_k\frac{d\tau_s(\mathscr{E}_l)}{d\mathscr{E}_l}[(\mathscr{E}_{l+1} - \mathscr{E}_l) + (\mathscr{E}_{l+2} - \mathscr{E}_{l+1})]\\ &= 2\omega\tau_s(\mathscr{E}_l) + \omega_k\frac{d\tau_s(\mathscr{E}_l)}{d\mathscr{E}_l}\Delta\mathscr{E}(\mathscr{E}_l, \vartheta_l),\end{aligned} \tag{3.128}$$

$\tau_{s,l} \equiv \tau_s(\mathscr{E}_l)$.

Using Eqs. (3.127) and (3.128) we find

$$K = \left|\frac{d\Delta\vartheta_l}{d\vartheta_l}\right| \sim \frac{\omega_k}{\omega_H}\ln\eta\,|f'(\vartheta_l)|. \tag{3.129}$$

At $K > 1$ there emerges stochastic particle dynamics. It is not difficult to see that the condition (3.124) automatically leads to the inequality

$$K \gg 1. \tag{3.130}$$

Thus, when strongly interacting with a wave, all the particles with the velocities $v > \omega/k$ have stochastic dynamics and they are stochastically heated. Let us use the fact that, according to [3.24],

$$\langle\langle f(\vartheta)\rangle\rangle \approx 0, \quad \langle\langle f^2(\vartheta)\rangle\rangle \sim 1,$$

where the brackets $\langle\langle\ldots\rangle\rangle$ denote averages over the phase ϑ.

Then the energy growth rate can be found from the expression

$$\frac{d\mathscr{E}}{dt} \approx \frac{1}{2}m\frac{\langle\langle(\Delta v_x)^2\rangle\rangle}{T_l} \sim \frac{\omega_H^3}{\Omega_0^2}\mathscr{E}\ln^2\eta, \tag{3.131}$$

which uses the relation $\Delta v_x = \Delta\mathscr{E}/mv_x \approx k\Delta\mathscr{E}/m\omega_k$. Hence the increment is

$$\gamma_{\mathscr{E}} = \frac{1}{\mathscr{E}}\frac{d\mathscr{E}}{dt} \sim \frac{\omega_H^3}{\Omega_0^2}\ln^2\eta. \tag{3.132}$$

Correspondingly, in a self-consistent case an increase in the particle energy results in wave damping. The damping rate can be obtained from the conservation of total energy of both the wave and the particles having velocities $v > \omega/k$. This yields

$$\gamma = \gamma_{\mathscr{E}}\frac{n}{W} \sim \frac{\omega_H^3}{\Omega_0^2}\frac{n}{W}\ln^2\eta, \tag{3.133}$$

where n is the particle density at $v > \omega/k$ and W is the wave energy density.

Equation (3.133) shows that as $B_0 \to 0$ the wave damping rate tends to zero as

$$\gamma \propto B_0^3\ln^2(1/B_0). \tag{3.134}$$

The subsequent development seems to be rather apparent. As $B_0 \to 0$ Eq. (3.134) indicates a rather rapid tendency of γ to zero. Therefore, starting from certain, rather small values of B_0, the escape time of initially trapped particles from the wave potential well becomes sufficiently long and exceeds the value of $1/\gamma$. Then the particle-wave interaction results in the usual nonlinear Landau damping, that is accompanied, however, by dissipative mechanism due to the above collisions. This also means that the usual Landau damping for a transverse wave in the magnetic field is replaced by an irreversible damping, in which, however, the irreversibility (phase mixing) is characterized by the time $\tau_{\text{mix}} \sim 1/(\omega_H \ln K)$ that increases with diminishing value of the magnetic field B_0.

References

3.1. R. Z. Sagdeev and V. D. Shapiro, *Pis'ma Zh. Eksp. Teor. Fiziki*, 17, 389 (1973).
3.2. R. Z. Sagdeev, *Problems in Plasma Theory*, Vol. 4, Atomizdat, Moscow, 1964, p. 20 (in Russian).
3.3. A. A. Galeev and R. Z. Sagdeev, *Problems in Plasma Theory*, Vol. 7, Atomizdat, Moscow, 1973, p. 3 (in Russian).
3.4. A. J. Lichtenberg and M. A. Liberman, *Regular and Stochastic Motion*, Springer-Verlag, 1983.
3.5. A. V. Timofeev, *Nucl. Fusion*, 14, 165 (1974).
3.6. G. R. Smith and A. N. Kaufman, *Phys. Rev. Lett.*, 34, 1613 (1975).
3.7. C. F. F. Karney, *Phys. Fluids*, 21, 1584 (1978).
3.8. C. F. F. Karney, *Phys. Fluids*, 22, 2188 (1979).
3.9. B. I. Meerson and P. V. Sasorov, in: *Studies in Geomagnetism, Aeronomy and Solar Physics*, Vol. 48, Nauka, Moscow, 1979, p. 145 (in Russian).
3.10. B. I. Meerson and P. V. Sasorov, *Planet. Space Sci.*, 27, 503 (1979).
3.11. B. I. Meerson, P. V. Sasorov, and D. R. Schklyar, *Fizika Plazmy*, 5, 1107 (1979).
3.12. E. M. Lifshitz and L. P. Pitayevskii, *Statistical Physics*, Part 2, Nauka, Moscow, 1978 (in Russian).
3.13. M. Robnik, *J. Phys. A*, 14, 3195 (1981).
3.14. G. M. Zaslavskii and B. V. Chirikov, *Uspekhi Fiz. Nauk*, 105, 3 (1971).
3.15. B. V. Chirikov, *Phys. Reports*, 52, 264 (1979).
3.16. G. M. Zaslavskii, *Stochasticity in Dynamic Systems*, Nauka, Moscow, 1984 (in Russian).
3.17. M. A. Malkov and G. M. Zaslavsky, *Phys. Lett.*, 106A, 9, 257 (1984).
3.18. L. A. Artsimovich and R. Z. Sagdeev, *Plasma Physics for Physicists*. Atomizdat, Moscow, 1979 (in Russian).
3.19. G. M. Zaslavskii, S. S. Moiseev, R. Z. Sagdeev, A. V. Tur, G. A. Khomenko, and V. V. Yanovskii, *Fizika Plazmy*, 9, 62 (1983).
3.20. G. M. Zaslavskii and R. Z. Sagdeev, *Zh. Eksp. Teor. Fiziki*, 52, 1083 (1967).
3.21. F. G. Bass, Ya. B. Fainberg, and V. D. Shapiro, *Zh. Eksp. Teor. Fiziki*, 49, 329 (1965).
3.22. G. M. Zaslavskii, *Statistical Irreversibility in Nonlinear Systems*, Nauka, Moscow, 1970 (in Russian).
3.23. A. Fukuyama, H. Momota, R. Itatani, and T. Takizuka, *Phys. Rev. Lett.*, 38, 701 (1977).
3.24. M. A. Malkov, R. Z. Sagdeev, V. D. Shapiro, and G. M. Zaslavskii, Submitted to *Fizika Plazmy* (1985).

4

The Renormalization Group Method and Kolmogorov-Arnold-Moser Theory

K. M. Khanin, Cand. Sc. (Phys.-Math.) and
Ya. G. Sinai, D. Sc. (Phys.-Math.)

4.1. INTRODUCTION

The class of two-dimensional conservative twist maps and, within this class, the standard or Chirikov map serve as main examples where the Kolmogorov-Arnold-Moser theory is applied [4.1]. Recall that the standard map is a cylinder's map $M = S^1 \times R^1$ having in terms of the natural variables (φ, z) (where φ is the phase and z is the amplitude) the form $T(\varphi, z) = (\varphi', z')$, where

$$\begin{aligned} z' &= z + \frac{k}{2\pi} \sin 2\pi\varphi, \\ \varphi' &= \varphi + z' \pmod 1. \end{aligned} \tag{4.1}$$

Let us choose a rotation number ω satisfying some incommensurability conditions [4.2-4.4]. The KAM theory states that if $|k| \leqslant k_{cr}(\omega)$ then there exists an analytical periodic function $a_\omega(\varphi)$ such that a curve $\Gamma_\omega = \{(\varphi, a_\omega(\varphi)), 0 \leqslant \varphi < 1\}$ is invariant with respect to T and on Γ_ω one can choose a new cyclic parameter Ψ such that $T|_{\Gamma_\omega}$ reduces, in terms of the variable Ψ, to a rotation through the angle ω: $\Psi \to \Psi + \omega$. Given sufficiently small k's the set of the invariant curves Γ_ω has a positive measure. According to results of many numerical experiments beginning from a well-known work by Greene [4.5], as k increases, the area occupied by the invariant curves decreases and at $k > k_{cr} = \max\limits_{\omega} k_{cr}(\omega)$ such invariant curves are absent at all. By order of magnitude k_{cr} is the same as the number entering into the Chirikov resonance overlapping criterion [4.1] and at $k > k_{cr}$ it is assumed that the standard map T possesses stochasticity properties, although rigorous mathematical results concerning this problem are not as yet available.

Numerical experiments show that $k_{cr} \approx 0.972$ and is close or even coincides with $k_{cr}(\omega_0)$, where ω_0 is the "golden-mean", i.e. $\omega_0 = \frac{1}{2}(\sqrt{5} - 1) = [1, 1, \ldots, 1, \ldots]$, where $[r_1, r_2, \ldots]$ is the generally accepted notation for the continued fraction $1/(r_1 + 1/(r_2 + \ldots))$ [4.6]. The upper bound of k_{cr} is also theoretically estimated [4.7-4.9]. Most strictly it was estimated by MacKay and Percival [4.9] to be $k_{cr} \leqslant 0.984$. However, the latter estimate belongs to computer-assisted results, while the results of [4.7-4.8] are purely theoretical. The lower bound of k_{cr} can be only obtained by refining the estimates that are provided by proofs of the KAM theory. Here the situation turns out to be much worse. The best result known to us belongs to Herman (see [4.9]) and it is $k_{cr} \geqslant 1/34 \approx 0.03$, i.e. much less than the true k_{cr} value. In multidimensional problems the discrepancy between k_{cr} and theoretical estimates might be even more substantial.

Proofs in the KAM theory are constructed by appropriate changes of variables in ever narrowing domains, which reduce in the limit to a transformation in a required form. In the case of Hamiltonian systems or simplectic transformations the changes of variables are canonical.

New approaches to constructing the invariant curves for twist maps were proposed by Percival [4.10], Mather [4.11], and Aubry [4.8]. These approaches differ but little and we will present here the approach used by Aubry [4.8] in more detail.

Aubry considers the problem of "commensurability-incommensurability" phase transitions within a chain of the Frenkel-Kontorova type [4.12]. A sequence of point masses on a straight line is considered; the masses interact by elastic forces between neighbours and are under the action of a periodic external field. In the simplest case the potential energy of such a system of particles has the form

$$U(\{x_n\}) = \frac{1}{2} \sum_n \left[(x_n - x_{n-1} - \gamma)^2 + \frac{k}{(2\pi)^2} (1 - \cos 2\pi x_n) \right],$$

where γ and k are parameters.

Aubry introduces the following.

Definition 1. A sequence $\{\bar{x}_n\}$ is called a ground state, if for any sequence $\{x_n\}$, obtained from $\{\bar{x}_n\}$ by shifting a finite number of particles, we have $U(\{x_n\}) - U(\{\bar{x}_n\}) \geqslant 0$.

This relation implies that the sequence $\{\bar{x}_n\}$ must satisfy the difference equation of the form

$$\left.\frac{\partial U}{\partial x_n}\right|_{x=\bar{x}} = -\bar{x}_{n+1} + 2\bar{x}_n - \bar{x}_{n-1} + \frac{k}{2\pi} \sin 2\pi \bar{x}_n = 0. \quad (4.2)$$

Let us put $z_n = \bar{x}_n - \bar{x}_{n-1}$, $\varphi_n = \bar{x}_n \pmod 1$, then (4.2) yields

$$\begin{aligned} z_{n+1} &= z_n + \frac{k}{2\pi} \sin 2\pi\varphi_n, \\ \varphi_{n+1} &= \varphi_n + z_{n+1} \pmod 1. \end{aligned} \quad (4.3)$$

and we obtain the standard map (4.1). The relations (4.3) imply that $T(\varphi_n, z_n) = (\varphi_{n+1}, z_{n+1})$, i.e. the sequence (φ_n, z_n) forms the trajectory of the standard map. In other words, the ground states in the Aubry sense correspond to some specific trajectories of the standard map.

It is worthwhile noting that the notion of the ground state according to Aubry is close to other similar notions. As early as in the 1920-30s Morse [4.13] and Hedlund [4.14] studied the general properties of geodesics on two-dimensional Riemannian surfaces. Of main importance was the notion of the class A geodesic. Each geodesic γ that minimizes the length functional among all the curves obtained from γ by a variation over a finite segment is called a geodesic of the class A. It is clear that structurally the notion of the class A geodesic is the same as that of the Aubry ground state. And in general there is much in common between the Aubry and Morse-Hedlund theories. In a more general way, suppose that on the phase space of a Lagrangian system having a Lagrange function $L(\dot{x}, x)$ a system is specified whose trajectories are extremals of the variational principle

$$\delta \int_{t_0}^{t_1} L(\dot{x}, x)\, dt = 0.$$

Let us call a class A extremal any trajectory for which the functional $\int L(\dot{x}, x)\, dt$ is minimal among all the curves obtained from this extremal by a variation on a finite segment. Thus we obtain the definition of the same type as Definition 1.

On the other hand, the general theory of phase transitions in the statistical mechanics of lattice systems also introduces a general definition of the ground state. In [4.15] a configuration $\bar{\varphi} = \{\bar{\varphi}(z),\ z \in \mathbb{Z}^d\}$ is called a ground state, if for any finite $V \in \mathbb{Z}^d$ and any configuration φ coinciding with $\bar{\varphi}$ outside V, an inequality $H(\varphi) - H(\bar{\varphi}) \geqslant 0$ holds, where H is the Hamiltonian of the system. Certainly, this definition is also similar to the Aubry definition. To be more exact, it can be considered as a generalization of the Aubry definition to the case of multidimensional time.

In [4.16] Aubry and Le Daeron proved a number of important properties of ground states. It turned out that for each ground state there exists a rotation number $\omega = \lim\limits_{n\to\infty} \frac{x_n}{n}$. An analogous statement for class A geodesics was proved by Hedlund [4.14] and Morse [4.13]. Moreover, ground states that have irrational rotation numbers and satisfy some other, less important conditions always have the following form: for a certain periodic function $F_\omega(\varphi)$, any ground state can be represented as $x_n = n\omega + \varphi_0 + F_\omega(n\omega + \varphi_0)$. If the function F_ω is continuous, then a relevant trajectory of the standard map lies on a continuous curve encompassing a cylinder M. Yet if F_ω is discontinuous then the relevant invariant set is uniquely projected onto the φ-axis in the form of a closed, nowhere dense set of the Cantor type. Percival [4.17] calls these invariant sets cantori. As follows from the paper by Lazutkin and Terman [4.18] continuous curves in the Aubry theory contain invariant curves that can be constructed in the KAM theory, although in the KAM theory the trajectory as a ground state does not appear in any way. It would be interesting also to investigate analogous problems in the multidimensional case.

The above said partly clarifies the evolution of invariant curves in the KAM theory: when the parameter k increases these curves are not bent and not complicated but they simply transform into cantori. Thus an absolutely novel type of bifurcations emerges here that has not been studied in mathematics before.

In physical publications such bifurcations are studied by the renormalization group method, which has been instrumental in the problems of statistical mechanics and quantum field theory. Let us describe the essence of this method. The mathematical basis of the renormalization group method is extremely simple. First of all, this method belongs to the "hyperbolic" theory. In the simplest cases there emerge fixed points of nonlinear transformations, that are called the renormalization group transformations, for which the spectrum of a differential at a fixed point is examined. It is required that this spectrum is inside a unit circle. Often it is also necessary that the only eigenvalue of the linearization operator lies outside the unit circle. Generically, it is clear that if there is a one-parameter curve C^1 adjacent to the unstable manifold of the fixed point, then this curve will intersect the stable manifold of the fixed point at a certain point. As a rule, phenomena that pertain to this intersection point are of interest to us. The resulting mathematical difficulties are due to the fixed point lying in a complicated functional space so that the studies of the spectrum of the differential and, moreover, the construction of stable and unstable manifolds as well as the analysis of intersections become nontrivial. Sometimes these difficulties are of a physical nature.

The renormalization group method was for the first time applied in the theory of dynamic systems by Feigenbaum [4.19, 4.20] in his studies on the universality of the sequencies of period-doubling bifurcations (see also [4.21]). Subsequently this method was discussed in [4.22–4.24] as applied to the studies of the bifurcations of invariant KAM curves.

In the present publication the renormalization group method is applied to two problems: to that of the rectification of a nonlinear circle transformation and to that of the construction of invariant curves of the type of invariant KAM curves for the standard map and typical rotation numbers. Estimates obtained by the method seem to be much better than those obtained by the KAM theory, so that one can derive realistic boundaries of the existence domain of invariant curves.

Of great importance for us was the Ph.D. thesis by MacKay [4.25] dedicated to related problems. Essentially, our results can be considered as the fulfilment of the MacKay desire to develop the renormalization group method for typical rotation numbers (in a subcritical domain).

4.2. RECTIFICATION OF THE NONLINEAR ROTATION OF A CIRCLE

Let us consider a family of circle maps, $T_\Omega \colon \varphi \to \varphi + \Omega + \frac{k}{2\pi} \sin 2\pi\varphi \pmod 1$. For small k's this family was studied by the KAM theory method in an earlier paper by Arnol'd [4.26]. At $|k| < 1$ the transformation T_Ω is a circle diffeomorphism with a corresponding rotation number $\omega = \omega(\Omega, k)$. Recently Herman [4.27, 4.28] has shown that for typical ω's a coordinate transformation reducing T_Ω to the pure rotation is analytical. Besides, the form of T_Ω implies that, for each k, ω is a monotonic function of Ω. In addition, this function is of the Cantor type and its flat parts correspond to rational rotation numbers and form an open, everywhere dense set. The KAM theory shows that for small k's the set of Ω values corresponding to sufficiently incommensurable irrational numbers forms a Cantor set of a positive measure. Recently Jensen, Bak and Bohr [4.29, 4.30] studied the case of $k = 1$. It is believed that at $k = 1$ in this problem phenomena take place that are close to the destruction of invariant KAM curves and to the bifurcation of the latter into cantori. The numerical results of [4.29, 4.30] show that at $k = 1$ the Hausdorff dimension of the set of the numbers Ω corresponding to irrational rotation numbers is close to 0.9.

Now let us describe in detail how the renormalization group method is applied to our problem. We will take an irrational rotation number ω and its expansion into a continued fraction $\omega = [r_1, r_2, \ldots]$. According to the classical results of Poincaré and Denjoy [4.31, 4.32], the Ω value at which the rotation number ω is realized is unambiguously determined by the fact that for any point $\varphi_0 \in S^1$ and for any m the order of the points $\varphi_0, \varphi_1, \ldots, \varphi_m$, $\varphi_i = T_\Omega^i \varphi_0$, $0 \leqslant i \leqslant m$, on the circle is the same as that of the points φ_0, $\varphi_0 + \omega, \ldots, \varphi_0 + m\omega \pmod 1$. This statement can be expressed in a more compact form. Let us consider successive approximations $p_n/q_n = [r_1, \ldots, r_n]$ for a rotation number ω and points $\varphi_{q_n} = T_\Omega^{q_n}\varphi_0$, $n = 1, 2, \ldots$. Then T_Ω has the rotation number ω if and only if $\varphi_{q_{2n+1}}$'s form a monotonically increasing sequence while $\varphi_{q_{2n}}$'s form a monotonically decreasing sequence, as $n \to \infty$ both sequences converge to φ_0.

Let us fix an arbitrary point φ_0. Here the essence of the renormalization group method consists in that for each n we choose a renormalized coordinate system $\bar{\varphi}$ and $\bar{\Omega}$ in a neighbourhood of $(\varphi_0, \Omega(\omega))$ and write in it representation for a pair $T_\Omega^{q_n}, T_\Omega^{q_{n-1}}$. The transition $n \to n+1$ is our renormalization group transformation, while the parameter n, according to the Chirikov terminology [4.33], is called the renormalization time.

Let us pass to more rigorous statements.

I. The condition of incommensurability of ω: $r_i \leqslant Rq^i$, $i = 1, 2, \ldots$, where $1 < q < q_0 = 1.001$, $1 \leqslant R < \infty$.

II. Inductive assumptions concerning $T_\Omega^{q_n}$, $T_\Omega^{q_{n-1}}$.

$1^{(n)}$. At the nth step there exist unique numbers Ω_{n-1}, Ω_n such that $T_{\Omega_n}^{q_n}\varphi_0 = T_{\Omega_{n-1}}^{q_{n-1}}\varphi_0 = \varphi_0$ and the trajectory of the point φ_0 makes p_n (p_{n-1}) revolutions along the circle in q_n (q_{n-1}) steps.

Thus for the nth step we consider the values of the parameter Ω lying between Ω_{n-1} and Ω_n. Let us introduce a renormalization of the parameter Ω according to the formula: $\Omega = \Omega_n + \bar{\Omega}(\Omega_{n-1} - \Omega_n)$. In terms of the new variables $\bar{\Omega}$ the segment $[0, 1]$ corresponds to the segment over which the initial parameter varies. Note that the sign of $(\Omega_{n-1} - \Omega_n)$ is determined by the evenness of n, i.e. $\operatorname{sign}(\Omega_{n-1} - \Omega_n) = (-1)^n$.

$2^{(n)}$. At the nth step a new variable $\bar{\varphi}$ is chosen according to the formula $\varphi = \varphi_0 + \gamma_n\bar{\varphi}$, where γ_n can be found from the condition $T_{\Omega_n}^{q_{n-1}}\varphi_0 = \varphi_0 - \gamma_n$. Note that $\operatorname{sign}\gamma_n = (-1)^n$. More detailed information on the sequence γ_n will be given below.

$3^{(n)}$. Let us define a sequence of numbers $\rho_0^{(n)} = [r_n, r_{n-1}, \ldots, r_1]$, where the right-hand side means a finite continued fraction constructed with the help of the numbers r_i, $1 \leqslant i \leqslant n$, taken in reverse order. At the nth step closed domains $V_n = \left\{\bar{\varphi} \in \mathbb{C}^1 : |\bar{\varphi}| \leqslant 4 - \frac{13}{8}\rho_0^{(n)}\right\}$, $U = \left\{\bar{\Omega} \in \mathbb{C}^1 : |\bar{\Omega} - \frac{1}{2}| \leqslant \frac{3}{4}\right\}$ are considered.

In the domain $(\bar{\varphi}, \bar{\Omega}) \in V_n \times U$ the transformations $T_\Omega^{q_n}$, $T_\Omega^{q_{n-1}}$ are given by the functions $f_n(\bar{\varphi}, \bar{\Omega})$, $q_n(\bar{\varphi}, \bar{\Omega})$ of the following form:

(a$_1$) f_n, g_n are analytical in the domain $V_n \times U$.

(a$_2$) $$f_n(\bar{\varphi}, \bar{\Omega}) = (\rho^{(n)})^{-1}\bar{\Omega} + \bar{\varphi} + a_0^{(n)}(\bar{\Omega}) + a_1^{(n)}(\bar{\Omega})\bar{\varphi} + a_2^{(n)}(\bar{\Omega})\bar{\varphi}^2 + a_3^{(n)}(\bar{\varphi}, \bar{\Omega}),$$
$$g_n(\bar{\varphi}, \bar{\Omega}) = \bar{\Omega} - 1 + \bar{\varphi} + b_0^{(n)}(\bar{\Omega}) + b_1^{(n)}(\bar{\Omega})\bar{\varphi} + b_2^{(n)}(\bar{\Omega})\bar{\varphi}^2 + b_3^{(n)}(\bar{\varphi}, \bar{\Omega}).$$

(b$_1$) $|\rho^{(n)} - \rho_0^{(n)}| \leqslant A_\rho(1 + 0.6\rho_0^{(n)})\lambda^n$.

(b$_2$) $a_0^{(n)}(\bar{\Omega}) = a_{0,1}^{(n)}\bar{\Omega} + a_{0,2}^{(n)}(\bar{\Omega})$, where $a_{0,1}^{(n)}$ is a constant, $a_{0,1}^{(n)} = -a_{0,2}^{(n)}(1)$, and $a_{0,2}^{(n)}(0) = da_{0,2}^{(n)}/d\bar{\Omega}(0) = 0$,
$|d^2a_{0,2}^{(n)}/d\bar{\Omega}^2(\bar{\Omega})| \leqslant A_0(1-0.5\rho_0^{(n)})\lambda_0^n$, $\bar{\Omega} \in U$,
$b_0^{(n)}(\bar{\Omega}) = b_{0,1}^{(n)}\bar{\Omega} + b_{0,2}^{(n)}(\bar{\Omega})$, where $b_{0,1}^{(n)}$ is a constant, $b_{0,1}^{(n)} = -b_{0,2}^{(n)}(1)$, and $b_{0,2}^{(n)}(0) = db_{0,2}^{(n)}/d\bar{\Omega}(0) = 0$,
$|d^2b_{0,2}^{(n)}/d\bar{\Omega}^2(\bar{\Omega})| \leqslant B_0(1-0.5\rho_0^{(n)})\lambda_0^n$, $\bar{\Omega} \in U$.

(b$_3$)
$$|a_1^{(n)}(\bar{\Omega})| \leqslant A_1\left|1-\frac{8}{13}\bar{\Omega}\right|(1+0.1427\rho_0^{(n)})\lambda_1^n,\ \bar{\Omega} \in U,$$
$$|b_1^{(n)}(\bar{\Omega})| \leqslant B_1\left|1-\frac{8}{13}\bar{\Omega}\right|(1+0.1427\rho_0^{(n)})\lambda_1^n,\ \bar{\Omega} \in U,$$
$$|a_2^{(n)}(\bar{\Omega})| \leqslant A_2\left|1-\frac{8}{13}\bar{\Omega}\right|(1+0.1427\rho_0^{(n)})(1+0.6\rho_0^{(n)})\lambda_2^n,\ \bar{\Omega} \in U,$$
$$|b_2^{(n)}(\bar{\Omega})| \leqslant B_2\left|1-\frac{8}{13}\bar{\Omega}\right|(1+0.1427\rho_0^{(n)})(1+0.6\rho_0^{(n)})\lambda_2^n,\ \bar{\Omega} \in U.$$

(b$_4$)
$$a_3^{(n)}(0, \bar{\Omega}) = \frac{\partial a_3^{(n)}}{\partial \bar{\varphi}}(0, \bar{\Omega}) = \frac{\partial^2 a_3^{(n)}}{\partial \bar{\varphi}^2}(0, \bar{\Omega}) = 0, \quad \bar{\Omega} \in U,$$
$$\left|\frac{\partial^3 a_3^{(n)}}{\partial \bar{\varphi}^3}(\bar{\varphi}, \bar{\Omega})\right| \leqslant A_3\left(1+\frac{7}{4}\rho_0^{(n)}\right)\lambda_3^n,\ (\bar{\varphi}, \bar{\Omega}) \in V_n \times U,$$
$$b_3^{(n)}(0, \bar{\Omega}) = \frac{\partial b_3^{(n)}}{\partial \bar{\varphi}}(0, \bar{\Omega}) = \frac{\partial^2 b_3^{(n)}}{\partial \bar{\varphi}^2}(0, \bar{\Omega}) = 0, \quad \bar{\Omega} \in U,$$
$$\left|\frac{\partial^3 b_3^{(n)}}{\partial \bar{\varphi}^3}(\bar{\varphi}, \bar{\Omega})\right| \leqslant B_3\left(1+\frac{7}{4}\rho_0^{(n)}\right)\lambda_3^n, \quad (\bar{\varphi}, \bar{\Omega}) \in V_n \times U.$$

The transition $n \to n+1$ is determined by the relation $q_{n+1} = r_{n+1}q_n + q_{n-1}$. Due to this fact the transformations $T_\Omega^{q_{n+1}}$, $T_\Omega^{q_n}$ in terms of the variables $(\bar{\varphi}, \bar{\Omega})$ of the nth step can be written as the superpositions

$$\bar{f}_{n+1} = g_n \circ f_n^{(r_{n+1})} = g_n \circ \underbrace{f_n \circ \ldots \circ f_n}_{r_{n+1}},\ \bar{g}_{n+1} = f_n. \tag{4.4}$$

The inductive assumptions $1^{(n+1)}$, $2^{(n+1)}$ define the renormalization of the variables $(\bar{\varphi}, \bar{\Omega})$. The functions $\bar{f}_{n+1}$, $\bar{g}_{n+1}$ in terms of the renormalized variables yield new f_{n+1}, g_{n+1} and we must check that f_{n+1}, g_{n+1} satisfy the inductive assumptions $3^{(n+1)}$.

If the nonlinear transformation of the space of the pairs of functions that corresponds to r superpositions in (4.4) and the transition to renormalized variables is denoted by S_r, then $(f_{n+1}, g_{n+1}) = S_{r_{n+1}}(f_n, g_n)$. Thus our problem cannot be considered as a standard renormalization group problem since here we do not deal with the iteration of a single transformation.* Nevertheless, the ideology of renormalization group method can be applied here. The family

$$f_\rho(\bar\varphi, \bar\Omega) = \rho^{-1}\bar\Omega + \bar\varphi, \quad g(\bar\varphi, \bar\Omega) = \bar\Omega - 1 + \bar\varphi \tag{4.5}$$

acts here as a "fixed point" of the renormalization group in the sense that it transforms into itself under the action of S_r for any $r = 1, 2, \ldots$.

Theorem 1. Suppose that at a certain n a pair (f_n, g_n) satisfies the inductive assumptions $3^{(n)}$, where $\lambda = 0.999$, $\lambda_0 = 0.995$, $\lambda_1 = 0.99$, $\lambda_3 = 0.975$, $\lambda_2 = \sqrt{\lambda_1\lambda_3}$, $A_\rho = \frac{1}{1000R}$, $A_0 = 0.1A_\rho$, $A_1 = \frac{10^{-3}}{16R^3}A_0$, $A_3 = \frac{10^{-10}}{R^4}A_1$, $A_2 = \sqrt{A_1A_3}$, $B_0 = A_0$, $B_1 = \frac{1}{8}A_1$, $B_2 = \frac{1}{8}A_2$, $B_3 = A_3$. Then the pair (f_{n+1}, g_{n+1}) satisfies the inductive assumptions $3^{(n+1)}$.

Proof. At first, let us explain the idea of the proof. Recall once more what is the transformation $S_{r_{n+1}}$. At first we find $\bar f_{n+1} = g_n(f_n^{(r_{n+1})})$, $\bar g_{n+1} = f_n$, then change the variables $\bar\varphi \to -\rho^{(n+1)}\bar\varphi$, $\bar\Omega \to \Omega_0^{(n+1)}(1-\bar\Omega)$, where $\Omega_0^{(n+1)}$ and $\rho^{(n+1)}$ are defined by the relations $\bar f_{n+1}(0, \Omega_0^{(n+1)}) = 0$, $\rho^{(n+1)} = \bar g_{n+1}(0, \Omega_0^{(n+1)})$. As a result we find $f_{n+1}(\bar\varphi, \bar\Omega) = -(\rho^{(n+1)})^{-1}\bar f_{n+1}(-\rho^{(n+1)}\bar\varphi, \Omega_0^{(n+1)}(1-\bar\Omega))$, $g_{n+1}(\bar\varphi, \bar\Omega) = -(\rho^{(n+1)})^{-1}\bar g_{n+1}(-\rho^{(n+1)}\bar\varphi, \Omega_0^{(n+1)}(1-\bar\Omega))$.

Let

$$f_n(\bar\varphi, \bar\Omega) = a^{(n)}(\bar\Omega) + \bar\varphi + \sum_{i=1}^{3} a_i^{(n)}(\bar\Omega)\bar\varphi^i,$$

$$g_n(\bar\varphi, \bar\Omega) = b^{(n)}(\bar\Omega) + \bar\varphi + \sum_{i=1}^{3} b_i^{(n)}(\bar\Omega)\bar\varphi^i,$$

where

$$a^{(n)}(\bar\Omega) = (\rho_0^{(n)})^{-1}\bar\Omega + a_0^{(n)}(\bar\Omega), \quad b^{(n)}(\bar\Omega) = \bar\Omega - 1 + b_0^{(n)}(\bar\Omega).$$

Suppose that

$$\begin{gathered} |a_i^{(n)}(\Omega)| \leqslant A_i^{(n)}, \quad |b_i^{(n)}(\Omega)| \leqslant B_i^{(n)}, \quad i \geqslant 0, \\ 1 \gg A_0^{(n)} \gg A_1^{(n)} \gg A_2^{(n)} \gg A_3^{(n)} \gg (A_0^{(n)})^2, \\ 1 \gg B_0^{(n)} \gg B_1^{(n)} \gg B_2^{(n)} \gg B_3^{(n)} \gg (B_0^{(n)})^2 \end{gathered} \tag{4.6}$$

---

* This is not so for ω's that can be expanded into a periodic continued fraction, this explaining their special role in the theory.

and for each i the constants $A_i^{(n)}$ and $B_i^{(n)}$ have the same order of magnitude. Then, since in the main order (f_n, g_n) are linearly dependent on $\bar{\varphi}$, $\bar{\Omega}$, we obtain

$$\bar{f}_{n+1}(\bar{\varphi}, \bar{\Omega}) = r_{n+1}(\rho_0^{(n)})^{-1}\bar{\Omega} + \bar{\Omega} - 1 + \bar{\varphi} + \sum_{i=0}^{3} \bar{a}_i^{(n+1)}(\bar{\Omega})\bar{\varphi}^i, \tag{4.7}$$

where, up to the terms of a higher order of smallness,

$$\bar{a}_i^{(n+1)}(\bar{\Omega}) = r_{n+1}a_i^{(n)}(\bar{\Omega}) + b_i^{(n)}(\bar{\Omega}). \tag{4.8}$$

Relation (4.7) implies that in the main order

$$\Omega_0^{(n+1)} = \frac{\rho_0^{(n)}}{r_{n+1} + \rho_0^{(n)}}, \quad \rho^{(n+1)} = \frac{1}{r_{n+1} + \rho_0^{(n)}}. \tag{4.9}$$

Thus

$$f_{n+1}(\bar{\varphi}, \bar{\Omega}) = (\rho_0^{(n+1)})^{-1}\bar{\Omega} + \bar{\varphi} + \sum_{i=0}^{3} a_i^{(n+1)}(\bar{\Omega})\bar{\varphi}^i,$$

$$g_{n+1}(\bar{\varphi}, \bar{\Omega}) = \bar{\Omega} - 1 + \bar{\varphi} + \sum_{i=0}^{3} b_i^{(n+1)}(\bar{\Omega})\bar{\varphi}^i,$$

where

$$a_i^{(n+1)}(\bar{\Omega}) = (-\rho_0^{(n+1)})^{i-1}[r_{n+1}a_i^{(n)}(\Omega_0^{(n+1)}(1-\bar{\Omega})) + b_i^{(n)}(\Omega_0^{(n+1)}(1-\bar{\Omega}))], \tag{4.10}$$

$$b_i^{(n+1)}(\bar{\Omega}) = (-\rho_0^{(n+1)})^{i-1} a_i^{(n)}(\Omega_0^{(n+1)}(1-\bar{\Omega})).$$

One can easily see that at $i = 0$ and $i > 2$ relations (4.10) result in the decreasing of relevant coefficients, i.e. from the viewpoint of the renormalization group ideology they correspond to stable eigenvalues. On the other hand, at $i = 1, 2$ the relations (4.10) are unstable and in eliminating this instability the decisive role is played by the commutativity condition of the (f_n, g_n) pair. Let us discuss relevant arguments in somewhat more detail. Using the hierarchy of the decreasing of the coefficients $a_i^{(n)}$, $b_i^{(n)}$ and the commutativity condition one can easily show that

$$a_i^{(n)}(\bar{\Omega}) = b_i^{(n)}(\bar{\Omega})\frac{a^{(n)}(\bar{\Omega})}{b^{(n)}(\bar{\Omega})} + \Delta_i^{(n)}, \quad i = 1, 2, \tag{4.11}$$

where the errors $\Delta_i^{(n)}$ can be evaluated explicitly. The $\Delta_i^{(n)}$'s have the following orders of smallness: $\Delta_1^{(n)}$ is of the order of $A_2^{(n)}$, $B_2^{(n)}$ and $\Delta_2^{(n)}$ is of the order of $A_3^{(n)}$, $B_3^{(n)}$. It is important to note that the relations (4.10) conserve, in the main order, the commutativity conditions (4.11). This fact is associated with the invariance of the manifold of commuting pairs due to the transformations S_r. Now, using the relations (4.11), instead of the two-dimensional transformation (4.10) we obtain the one-dimensional transformation $b_1^{(n)} \to b_1^{(n+1)}$ whose main order form is

$$b_i^{(n+1)}(\bar{\Omega}) = (-\rho_0^{(n+1)})^{i-1} \frac{(\rho_0^{(n)})^{-1}\Omega_0^{(n+1)}(1-\bar{\Omega})}{\Omega_0^{(n+1)}(1-\bar{\Omega})-1} \times b_i^{(n)}(\Omega_0^{(n+1)}(1-\bar{\Omega})), \quad i=1,\ 2. \tag{4.12}$$

Relations (4.12) yield essentially the stability, since at $0 \leqslant \bar{\Omega} \leqslant 1$ we have

$$\left| \frac{(\rho_0^{(n)})^{-1}\Omega_0^{(n+1)}(1-\bar{\Omega})}{\Omega_0^{(n+1)}(1-\bar{\Omega})-1} \right| \leqslant 1.$$

The logic of reasoning is based here on the assumption that at the nth step estimates like $|a_i^{(n)}|$, $|b_i^{(n)}| \leqslant \text{const}\, \lambda_i^n$ are valid for some $1 > \lambda_0 > \lambda_1 > \lambda_2 > \lambda_3$ and then by the commutativity condition we check that analogous estimates for the $(n+1)$th step are conserved.

Now let us proceed to the formal proof. To simplify notation, we will omit the index n everywhere. The pairs (f_n, g_n) and (f_{n+1}, g_{n+1}) will be denoted as (f, g) and $(\tilde{f}, \tilde{g})$, respectively. Besides, we put $r \equiv r_{n+1}$, $\rho_0 \equiv \rho_0^{(n)}$, $\rho \equiv \rho^{(n)}$ and the renormalized variables $(\bar{\varphi}, \bar{\Omega})$ will be simply denoted as (φ, Ω). Thus

$$f(\varphi, \Omega) = a(\Omega) + \varphi + a_1(\Omega)\varphi + a_2(\Omega)\varphi^2 + a_3(\varphi, \Omega),$$

$$g(\varphi, \Omega) = b(\Omega) + \varphi + b_1(\Omega)\varphi + b_2(\Omega)\varphi^2 + b_3(\varphi, \Omega),$$

where

$$a(\Omega) = \rho^{-1}\Omega + a_0(\Omega),\ b(\Omega) = \Omega - 1 + b_0(\Omega).$$

Let us also introduce the following notation:

$$C_1 = \max_{\Omega \in U} \max_{0 \leqslant \rho \leqslant 1} \left[A_1 \left| 1 - \frac{8}{13}\Omega \right| (1 + 0.1427\rho) \right] = 1.1427 \times \frac{15}{13} A_1,$$

$$C_2 = \max_{\Omega \in U} \max_{0 \leqslant \rho \leqslant 1} \left[A_2 \left| 1 - \frac{8}{13}\Omega \right| (1 + 0.1427\rho)(1 + 0.6\rho) \right] = 1.1427 \times \frac{24}{13} A_2,$$

$$C_3 = \max_{0 \leqslant \rho \leqslant 1} \left[A_3 \left(1 + \frac{7}{4}\rho \right) \right] = \frac{11}{4} A_3.$$

At first we obtain the estimates for $f^{(r)} = \underbrace{f \circ \ldots \circ f}_{r}$. The estimates for f are valid in the domain $(\varphi, \Omega) \in V \times U = \{\varphi \in \mathbb{C}^1 : |\varphi| \leqslant \varphi_0\}, \left\{\Omega \in \mathbb{C}^1 : \left|\Omega - \frac{1}{2}\right| \leqslant \frac{3}{4}\right\}$. Here $\varphi_0 = 4 - \frac{13}{8}\rho_0$. Let us determine the domains $V_i = \left\{\varphi \in \mathbb{C}^1 : |\varphi| \leqslant \varphi_0 - \frac{(i-1)}{r+\rho}\right\}$, $1 \leqslant i \leqslant r$, $U_0 = \left\{\Omega \in \mathbb{C}^1 : \left|\Omega - \frac{\rho}{2(r+\rho)}\right| \leqslant \frac{7\rho}{8(r+\rho)}\right\}$.

Suppose that

$$f^{(i)}(\varphi, \Omega) = \underbrace{f \circ \ldots \circ f}_{i} = a^{(i)}(\Omega) + \varphi + a_1^{(i)}(\Omega)\,\varphi + a_2^{(i)}(\Omega)\,\varphi^2$$
$$+ a_3^{(i)}(\varphi, \Omega), \quad 1 \leqslant i \leqslant Rq^{n+1}.$$

Lemma 1. For all $1 \leqslant i \leqslant Rq^{n+1}$ in the domain $(\varphi, \Omega) \in V_i \times U_0$ the following estimates are valid:

$$a^{(i)} = ia + \Delta a^{(i)}, \qquad |\Delta a^{(i)}| \leqslant \frac{4}{3} i^2 D C_1 \lambda_1^n,$$
$$a_1^{(i)} = ia_1 + \Delta a_1^{(i)}, \qquad |\Delta a_1^{(i)}| \leqslant \frac{8}{3} i^2 D C_2 \lambda_2^n,$$
$$a_2^{(i)} = ia_2 + \Delta a_2^{(i)}, \qquad |\Delta a_2^{(i)}| \leqslant \frac{2}{3} i^2 D D_1^2 C_3 \lambda_3^n,$$
$$\left|\frac{\partial^3}{\partial\varphi^3} a_3^{(i)}(\varphi, \Omega)\right| \leqslant i C_3 \lambda_3^n + \Delta a_3^{(i)}, \qquad \Delta a_3^{(i)} = 28 i^2 C_2^2 \lambda_2^{2n},$$

where

$$D = \max_{\Omega \in U_0} |a(\Omega)|, \quad D_1 = \max_{\Omega \in U_0} |1 + a_1(\Omega)|.$$

Lemma 1 is easily proved by induction in i. The following relations are used for the superposition:

$$a^{(i+1)} = a^{(i)} + a + a_1^{(i)} a + a_2^{(i)} a^2 + a_3^{(i)}(a, \Omega),$$
$$a_1^{(i+1)} = a_1^{(i)} + a_1 + a_1^{(i)} a_1 + a_2^{(i)}(2a + 2a_1 a) + \frac{\partial a_3^{(i)}}{\partial\varphi}(a, \Omega)(1 + a_1),$$
$$a_2^{(i+1)} = a_2^{(i)} + a_2 + a_1^{(i)} a_2 + a_2^{(i)}(a_1^2 + 2a_1 + 2a_2 a)$$
$$+ \frac{1}{2}\frac{\partial^2 a_3^{(i)}}{\partial\varphi^2}(a, \Omega)(1 + a_1)^2 + \frac{\partial a_3^{(i)}}{\partial\varphi}(a, \Omega)\, a_2.$$
$$a_3^{(i+1)} = a_3^{(i)}(f, \Omega) + a_3(\varphi, \Omega) - \frac{\partial a_3^{(i)}}{\partial\varphi}(a, \Omega)(1 + a_1)\,\varphi$$
$$- \left(\frac{1}{2}\frac{\partial^2 a_3^{(i)}}{\partial\varphi^2}(a, \Omega)(1 + a_1)^2 + \frac{\partial a_3^{(i)}}{\partial\varphi}(a, \Omega)\, a_2\right)\varphi^2 + a_1^{(i)} a_3(\varphi, \Omega)$$
$$+ a_2^{(i)}(2a_1 a_2 \varphi^3 + 2a_2 \varphi^3 + a_2^2 \varphi^4 + 2a a_3(\varphi, \Omega)$$
$$+ 2(1 + a_1)\, a_3(\varphi, \Omega)\,\varphi + 2a_2 a_3(\varphi, \Omega)\,\varphi^2 + a_3^2(\varphi, \Omega)).$$

Thus we have the estimates for $f^{(r)}$.

Now consider the superposition

$$\bar{f} \equiv g(f^{(r)}) = \bar{a}(\Omega) + \varphi + \bar{a}_1(\Omega)\varphi + \bar{a}_2(\Omega)\varphi^2 + \bar{a}_3(\varphi, \Omega).$$

It can easily be shown that in the domain $|\varphi| \leqslant \varphi_0 - \frac{3}{2}\frac{r}{r+\rho}$, $\Omega \in U_0$, we have

$$|a^{(r)}| \leqslant \varphi_0, \quad |f^{(r)}| \leqslant \varphi_0.$$

Consequently, when calculating the superposition we can use the estimates made for g. As a result we obtain

$$\bar{a} = ra + b + \Delta\bar{a}, \quad \bar{a}_1 = ra_1 + b_1 + \Delta\bar{a}_1, \quad \bar{a}_2 = ra_2 + b_2 + \Delta\bar{a}_2,$$

$$\left|\frac{\partial^3}{\partial\varphi^3}\bar{a}_3(\varphi, \Omega)\right| \leqslant (rA_3 + B_3)\left(1 + \frac{7}{4}\rho_0\right)\lambda_3^n + \Delta\bar{a}_3,$$

where

$$|\Delta\bar{a}| \leqslant \left(\frac{1}{4} + \frac{4}{3}r^2D\right)C_1\lambda_1^n,$$

$$|\Delta\bar{a}_1| \leqslant C_2\lambda_2^n\left(1 + \frac{8}{3}r^2D\right),$$

$$|\Delta\bar{a}_2| \leqslant C_3\lambda_3^n\left(\frac{2}{3}r^2D_1^2D + 2\right),$$

$$\Delta\bar{a}_3 = C_2^2\lambda_2^{2n}(16(r+1) + 28r^2).$$

Now let us use the commutativity conditions.

Since $f(g(0, \Omega), \Omega) = g(f(0, \Omega), \Omega)$, we have

$$a + b + a_1b + a_2b^2 + a_3(b, \Omega) = a + b + b_1a + b_2a^2 + b_3(a, \Omega)$$

or

$$a_1 = b_1\left(\frac{a}{b}\right) + \frac{b_2a^2 + b_3(a, \Omega) - a_2b^2 - a_3(b, \Omega)}{b}. \tag{4.13}$$

The second commutativity condition

$$\frac{\partial}{\partial\varphi}f(g(\varphi, \Omega), \Omega)|_{\varphi=0} = \frac{\partial}{\partial\varphi}g(f(\varphi, \Omega), \Omega)|_{\varphi=0}$$

yields

$$a_2 = b_2\left(\frac{a}{b}\right) + \frac{b_2aa_1 - a_2bb_1}{b} + \frac{\frac{\partial}{\partial\varphi}b_3(a, \Omega)(1 + a_1) - \frac{\partial}{\partial\varphi}a_3(b, \Omega)(1 + b_1)}{2b}. \tag{4.14}$$

In the domain $\Omega \in U_0$ the following inequalities are valid:

$$\frac{1}{4} \leqslant b(\Omega) \leqslant 2 < \varphi_0.$$

Thus the denominators in (4.13) and (4.14) are nonzero and we can estimate

$$\begin{aligned} |\Delta_1| &= \left|a_1 - b_1\left(\frac{a}{b}\right)\right| \leqslant 19C_2\lambda_2^n, \\ |\Delta_2| &= \left|a_2 - b_2\left(\frac{a_0}{b_0}\right)\right| \leqslant 6C_3\lambda_2^n. \end{aligned} \tag{4.15}$$

Now let us proceed to the change of variables. We should find Ω_0 such that $\bar{a}(\Omega_0) = 0$. It can easily be shown that $\Omega_0 = \frac{\rho}{r+\rho}\xi$, where $|\xi - 1| \leqslant \gamma\lambda_0^n$, and $\gamma = 0.15A_\rho$. Therefore $a(\Omega_0) = \frac{1}{r+\rho}\xi'$, $|\xi' - 1| \leqslant 2\gamma\lambda_0^n$.

Now let us make the following changes of variables:

$$\Omega \to \Omega_0(1 - \Omega), \ \varphi \to -\tilde{\rho}\varphi,$$

where $\tilde{\rho} = a(\Omega_0)$.

As a result we obtain

$$\begin{aligned} \tilde{f} &= -\tilde{\rho}^{-1}\bar{f}(-\tilde{\rho}\varphi, \ \Omega_0(1-\Omega)), \\ \tilde{g} &= -\tilde{\rho}^{-1}f(-\tilde{\rho}\varphi, \ \Omega_0(1-\Omega)), \\ \tilde{f} &= \tilde{a}(\Omega) + \varphi + \tilde{a}_1(\Omega)\varphi + \tilde{a}_2(\Omega)\varphi_2 + \tilde{a}_3(\varphi, \ \Omega), \\ \tilde{g} &= \tilde{b}(\Omega) + \varphi + \tilde{b}_1(\Omega)\varphi + \tilde{b}_2(\Omega)\varphi^2 + \tilde{b}_3(\varphi, \ \Omega), \end{aligned}$$

where

$$\begin{cases} \tilde{a}(\Omega) = (\tilde{\rho})^{-1}\Omega + \tilde{a}_{0,1}\Omega + \tilde{a}_{0,2}(\Omega), \\ \tilde{b}(\Omega) = \Omega - 1 + \tilde{b}_{0,1}\Omega + \tilde{b}_{0,2}(\Omega). \end{cases}$$

$$\tilde{a}_{0,1} = -\tilde{a}_{0,2}(1), \quad \tilde{b}_{0,1} = -\tilde{b}_{0,2}(1).$$

$$\begin{cases} \tilde{a}_{0,2}(\Omega) = -(\tilde{\rho})^{-1}[ra_{0,2}(\Omega_0(1-\Omega)) + b_{0,2}(\Omega_0(1-\Omega)) \\ \qquad\qquad + \Delta\bar{a}(\Omega_0(1-\Omega))] + \text{linear terms}, \\ \tilde{b}_{0,2}(\Omega) = -(\tilde{\rho})^{-1}a_{0,2}(\Omega_0(1-\Omega)) + \text{linear terms}. \end{cases}$$

$$\begin{cases} \tilde{a}_1(\Omega) = ra_1(\Omega_0(1-\Omega)) + b_1(\Omega_0(1-\Omega)) + \Delta\bar{a}_1(\Omega_0(1-\Omega)), \\ \tilde{b}_1(\Omega) = a_1(\Omega_0(1-\Omega)). \end{cases}$$

$$\begin{cases} \tilde{a}_2(\Omega) = -\tilde{\rho}\,[ra_2(\Omega_0(1-\Omega)) + b_2(\Omega_0(1-\Omega)) + \Delta\bar{a}_2(\Omega_0(1-\Omega))] \\ \tilde{b}_2(\Omega) = -\tilde{\rho}a_2(\Omega_0(1-\Omega)). \end{cases}$$

$$\begin{cases} \left|\frac{\partial^3}{\partial\varphi^3}\tilde{a}_3(\varphi,\ \Omega)\right| \leqslant (rA_3+B_3)\left(1+\frac{7}{4}\rho_0\right)\lambda_3^n(\tilde{\rho})^2 + \Delta\bar{a}_3(\tilde{\rho})^2, \\ \left|\frac{\partial^3}{\partial\varphi^3}\tilde{b}_3(\varphi,\ \Omega)\right| \leqslant A_3(\tilde{\rho})^2\lambda_3^n\left(1+\frac{7}{4}\rho_0\right). \end{cases}$$

Now let us evaluate the errors in the above relations. Since $\tilde{\rho} = \frac{1}{r+\rho}\xi'$, $|\xi'-1| \leqslant 2\gamma\lambda_0^n$, we have

$$|\tilde{\rho} - [r,\ r_n,\ \ldots,\ r_1]| \leqslant \frac{A_\rho(1+0.6\rho_0)\lambda^n}{r(r+\rho_0)} + \frac{2\gamma\lambda_0^n}{r+\rho}. \qquad (4.16)$$

The relations for $\tilde{a}_{0,2}(\Omega)$, $\tilde{b}_{0,2}(\Omega)$ must be differentiated twice with respect to Ω. The contribution of $\overline{\Delta a}\,(\Omega_0(1-\Omega))$ will be estimated with the help of the Cauchy theorem. To do this, note that the estimate $\overline{\Delta a}\,(\Omega_0(1-\Omega))$ is proved in the domain $\left|\Omega_0(1-\Omega) - \frac{\rho}{2(r+\rho)}\right| \leqslant \frac{7}{8}\frac{\rho}{r+\rho}$, while at $\left|\Omega - \frac{1}{2}\right| \leqslant \frac{3}{4}$ the estimate $\left|\Omega_0(1-\Omega) - \frac{\rho}{2(r+\rho)}\right| \leqslant \frac{\rho}{r+\rho}\left(\frac{3}{4}+\frac{7}{4}\gamma\right) < \frac{7\rho}{8(r+\rho)}$ is valid. Therefore

$$\frac{d^2}{d\Omega^2}\Delta\bar{a}(\Omega_0(1-\Omega))\Big| \leqslant 220\,C_1\lambda_1^n\left(\frac{1}{4}+\frac{4}{3}r^2D\right).$$

Thus

$$\begin{cases} \left|\frac{d^2}{d\Omega^2}\tilde{a}_{0,2}(\Omega)\right| \leqslant \frac{\Omega_0^2}{\tilde{\rho}}(rA_0+B_0)(1-0.5\rho_0)\lambda_0^n + \Delta\tilde{a}_{0,2}, \\ \left|\frac{d^2}{d\Omega^2}\tilde{b}_{0,2}(\Omega)\right| \leqslant \frac{\Omega_0^2}{\tilde{\rho}}A_0(1-0.5\rho_0)\lambda_0^n,\ |\Omega-1/2| \leqslant 3/4, \end{cases} \qquad (4.17)$$

where $|\Delta\tilde{a}_{0,2}| \leqslant 230(r+\rho)\left(\frac{1}{4}+\frac{4}{3}r^2D\right)C_1\lambda_1^n$.

Using the estimates resulting from the commutativity relations we obtain

$$\begin{cases} \tilde{a}_1(\Omega) = \left(r\frac{a(\Omega_0(1-\Omega))}{b(\Omega_0(1-\Omega))}+1\right)b_1(\Omega_0(1-\Omega)) + \Delta\tilde{a}_1, \\ \tilde{b}_1(\Omega) = \frac{a(\Omega_0(1-\Omega))}{b(\Omega_0(1-\Omega))}b_1(\Omega_0(1-\Omega))\lambda_1^n + \Delta_1(\Omega_0(1-\Omega)), \end{cases} \qquad (4.18)$$

where $|\Delta\tilde{a}_1| \leqslant |\Delta\bar{a}_1| + r|\Delta_1|$. Analogously we obtain for $\tilde{a}_2(\Omega)$, $\tilde{b}_2(\Omega)$:

$$\begin{cases} \tilde{a}_2(\Omega) = \tilde{\rho}\left(r\dfrac{a(\Omega_0(1-\Omega))}{b(\Omega_0(1-\Omega))} + 1\right) b_2 + \Delta\tilde{a}_2, \\ \tilde{b}_2(\Omega) = \tilde{\rho}\dfrac{a(\Omega_0(1-\Omega))}{b(\Omega_0(1-\Omega))} b_2 + \tilde{\rho}\Delta_2(\Omega_0(1-\Omega)), \end{cases}$$

where $|\Delta\tilde{a}_2| \leqslant (|\Delta\bar{a}_2| + r|\Delta_2|)\tilde{\rho}$.

Let us take together all the estimates and demonstrate that the inductive assumptions $3^{(n+1)}$ hold for $(\tilde{f}, \tilde{g})$. First of all, let us check that the range of the variable φ contains the domain V_{n+1}. Indeed, $|\varphi| \leqslant \dfrac{1}{\tilde{\rho}}\left(\varphi_0 - \dfrac{3}{2}\dfrac{r}{r+\rho}\right)$, where $\varphi_0 = 4 - \dfrac{13}{8}\rho_0$. Using the estimate for $\tilde{\rho}$ one can easily verify that for any $r \geqslant 1$, $\dfrac{1}{\tilde{\rho}}\left(\varphi_0 - \dfrac{3}{2}\dfrac{r}{r+\rho}\right) \geqslant 4 - \dfrac{13}{8}\tilde{\rho}_0$. Thus all the estimates proved above are valid in the domain $\Omega \in U$, $\varphi \in V_{n+1}$.

Consider now the inductive assumptions for $\tilde{\rho}$. We can use the estimate (4.16) and take into account the fact that for any $r \geqslant 1$, $0 \leqslant \rho_0 \leqslant 1$, we have

$$\frac{(1+0.6\rho_0)\lambda^n}{r(r+\rho)} \leqslant \frac{5}{8}(1+0.6\tilde{\rho}_0)\lambda^n.$$

Since the error in the estimate (4.16) does not exceed $(\lambda - 5/8) \times (1 + 0.6\tilde{\rho}_0)\lambda^n$ we obtain the inequality required. The inductive assumptions for $\tilde{a}_{0,2}$, $\tilde{b}_{0,2}$ and $\tilde{a}_3$, $\tilde{b}_3$ can be proved in a similar way.

It now remains only to check the validity of the inductive assumptions $3^{(n+1)}$ for the coefficients $\tilde{a}_1$, $\tilde{b}_1$ and $\tilde{a}_2$, $\tilde{b}_2$. To be specific, let us treat the case of $\tilde{a}_1$, $\tilde{b}_1$ and use relations (4.18). At first, let us estimate

$$M = \max_{|\Omega - 1/2| \leqslant 3/4} \max_{\substack{0 \leqslant \rho_0 \leqslant 1 \\ r \geqslant 1}} \left| \frac{(\Omega-1)\left(1 - \frac{8}{13}\frac{\rho_0}{r+\rho_0}(1-\Omega)\right)(1+0.1427\rho_0)}{(\rho_0\Omega + r)\left(1 - \frac{8}{13}\Omega\right)\left(1 + 0.1427\frac{1}{r+\rho_0}\right)} \right|.$$

Since the modulus maximum is reached at the boundary of the domain $|\Omega - 1/2| \leqslant 3/4$, we can assume that $|\Omega - 1/2| = 3/4$.

Note that $\left|\dfrac{(\Omega-1)}{\left(1 - \frac{8}{13}\Omega\right)}\right| = \dfrac{13}{12}$ for all Ω's lying on the circle $|\Omega - 1/2| = 3/4$. Thus

$$M = \frac{13}{12} \max_{|\Omega - 1/2| = 3/4} \max_{\substack{0 \leqslant \rho_0 \leqslant 1 \\ r \geqslant 1}} \left| \frac{\left(1 - \frac{8}{13} \frac{\rho_0}{r+\rho_0} (1-\Omega)\right)(1+0.1427\rho_0)}{(\rho_0\Omega + r)\left(1 + 0.1427 \frac{1}{r+\rho_0}\right)} \right|.$$

It can be easily verified that the modulus maximum is reached on the real axis, i.e. at $\Omega = 5/4$ or $\Omega = -1/4$. Hence

$$M = \frac{13}{12} \max_{\substack{0 \leqslant \rho_0 \leqslant 1 \\ r \geqslant 1}} \left\{ \frac{4(13r + 15\rho_0)(1 + 0.1427\rho_0)}{13(4r + 5\rho_0)(1 + \rho_0 + 0.1427)}, \frac{4(13r + 3\rho_0)(1 + 0.1427\rho_0)}{13(4r - \rho_0)(r + \rho_0 + 0.1427)} \right\}.$$

One can show that the latter expression reaches its maximum at $r = 1$, $\rho_0 = 1$ and this maximum is equal to

$$M = \frac{16\,(1.1427)}{9\,(2.1427)} < 0.949 < \lambda_1.$$

Since the error in relations (4.18) does not exceed $(\lambda_1 - M)\lambda_1^n B_1 \times \left| 1 - \frac{8}{13}\Omega \right| (1 + 0.1427\tilde{\rho}_0)$ we obtain the estimate for $\tilde{b}_1$. Of course, the decisive role in the proof is played by the inequality $M < 1$. The estimate for $\tilde{a}_1$ can be proved in a fairly simple manner. In fact, it is only necessary to obtain the upper bound

$$\left| \frac{(r + \rho_0)\Omega}{(\rho_0\Omega + r)} \frac{\left(1 - \frac{8}{13}\frac{\rho_0}{r+\rho_0}(1-\Omega)\right)}{\left(1 - \frac{8}{13}\Omega\right)} \frac{(1 + 0.1427\rho_0)}{\left(1 + 0.1427\frac{1}{r+\rho_0}\right)} \right| \leqslant 7.$$

Theorem 1 is proved.

Let us discuss some corollaries of Theorem 1.

(1) As a matter of fact, Theorem 1 has proved the stability of the fixed point of the renormalization group (4.5) and indicated an attracting neighbourhood for this point. To use the results proven one has to be sure that at a certain n_0 the maps (f_{n_0}, g_{n_0}) will belong to this neighbourhood. Apparently, the family T_Ω converges to the fixed family (4.5) for all $0 \leqslant k < 1$, yet it is not easy to see that this is so, since, due to the local character of our arguments, we can prove the convergence to the fixed family only for a small neighbourhood. Therefore, for k's close to 1, the number $n_0(k)$, for which the pair (f_{n_0}, g_{n_0}) falls within a guaranteed neighbourhood of the convergence, becomes too large and tends to ∞ as $k \to 1$. This is due to the fact that the value $k = 1$ is critical and the family T_Ω in this case is not attracted to the fixed family constructed above.

The critical case of $k = 1$ is much more difficult to resolve [4.34-4.36] and it requires other fixed points of the renormalization group to be constructed. We will not discuss this case in the present paper. In the subcritical domain $0 \leqslant k < 1$ the fulfilment of the inductive assumptions at the initial step of the induction process can be checked with the help of a computer. To do this one should construct numerically the pair (f_{n_*}, g_{n_*}) and make sure that deviation from the fixed family is sufficiently small. Note that at sufficiently small k's the convergence to the fixed family is evident.

(2) According to the classical results obtained by Poincaré, a map T of a circle into itself with an irrational rotation number ω is conjugated with the pure rotation transformation through an angle ω, i.e. there exists a monotonic homeomorphism of the circle S such that

$$S^{-1}TS\,(\varphi) = \varphi + \omega \pmod 1.$$

The conjugation S is uniquely determined up to the rotation and constructed in the following may. Let us fix a certain value $\bar{\varphi}_0$ and put $S\,(\bar{\varphi}_0) = \bar{\varphi}_0$. Let us denote $\bar{\varphi}_n = \bar{\varphi}_0 + n\omega \pmod 1$, then $S\,(\bar{\varphi}_n) := T^n\,(\bar{\varphi}_0)$ and in the remaining points the conjugation $S\,(\varphi)$ is determined by continuity.

Suppose that a rotation number $\omega = [r_1, r_2, \ldots]$ satisfies the incommensurability conditions I and, in addition, for a certain n_0 and for all points $0 \leqslant \varphi_0 < 1$ the pairs $(f_{n_0,\varphi_0}, g_{n_0,\varphi_0})$ corresponding to ω belong to the convergence domain, i.e. they satisfy the inductive assumptions $3^{(n_*)}$. (Recall that in constructing the pair (f_n, g_n) we fixed a certain point on the circle, $\varphi = \varphi_0$.) Then, due to Theorem 1, a sequence $\rho^{(n)}(\varphi_0)$ is determined (now we explicitly indicate the φ_0-dependence) and a limit $R\,(\varphi_0) = \lim\limits_{n\to\infty} \prod\limits_{k=1}^{n} \left(\frac{\rho^{(n)}(\varphi_0)}{\rho_0^{(n)}}\right)$ exists ($R\,(\varphi_0)$ is a continuous function of φ_0). It can be easily verified that in this case the conjugation $S\,(\varphi) \in C^1\,([0, 1))$ and

$$\frac{dS}{d\varphi} = R\,(S\,(\varphi)). \tag{4.19}$$

Relation (4.19) simply follows from the fact that $\prod\limits_{k=1}^{n} \rho^{(n)}(\varphi_0)$ controls the change in the scale in the variable φ in a neighbourhood of the point φ_0 for n steps of the renormalization group procedure, while $\prod\limits_{k=1}^{n} \rho_0^{(n)}$ controls the appropriate change in the scale for the pure rotation through the angle ω: $\varphi \to \varphi + \omega \pmod 1$.

Evidently, the above techniques make it possible to investigate the smoothness of the conjugation $S\,(\varphi)$ in more detail. However, we will not consider this question since this follows from the results obtained by Horman on the analyticity of the conjugation S [4.28].

(3) Finally, note that the analyticity condition for the pair (f_n, g_n) has been introduced into the inductive assumptions $3^{(n)}$ for convenience. In fact, it is sufficient to require that all the functions involved in the expansion for (f_n, g_n) would be triply differentiable with respect to $\bar{\varphi}$ and twice differentiable with respect to $\bar{\Omega}$. However, in this case the inductive assumptions $3^{(n)}$ must be supplemented by the estimates for the first- and second-order derivatives with respect to $\bar{\Omega}$.

4.3. CONSTRUCTION OF INVARIANT KAM CURVES BY THE RENORMALIZATION GROUP METHOD

In this section we will consider the construction of invariant curves for cylinder twist maps. As a basic example we will consider the standard map (4.1) yet ensuing results are related to a more general class of maps. Relevant rigorous assumptions will be formulated below.

Recall (see, e.g. [4.3]) that the KAM theory is based on the construction of successive changes of variables within ever contracting domains which gradually reduce the initial transformation to the form required. The renormalization group method is based on different considerations. We fix a vertical $B_{\varphi_0} = \{(\varphi, z) \in M: \varphi = \varphi_0\}$ and search for an intersection point of an invariant curve sought for with this vertical. The construction is carried out for all φ_0's and its dependence on φ_0 is also successfully traced. As a result we obtain the invariant curve sought for.

Let us fix, in addition to φ_0, a rotation number $\omega = [r_1, r_2, \ldots]$ satisfying the same incommensurability condition as that in Sec. 4.2: $r_i \leqslant Rq^i$, $i = 1, 2, \ldots$, $1 < R < \infty$. We denote by $p_n/q_n = [r_1, \ldots, r_n]$ the appropriate fractions. The construction of the point of the intersection of B_{φ_0} with an invariant curve on which the map has a rotation number ω is based on the following statement that can be naturally considered as an analogue of the Poincaré theorem for circle homeomorphism. For each n we will consider a transformation T^{q_n} and single out on the vertical B_{φ_0} a point (φ_0, z_n) possessing the property that in q_n steps it makes p_n revolutions around the cylinder and returns onto the initial vertical. Note that such points appear in the proof of the well-known Birkhoff theorem on the existence of periodic trajectories in a neighbourhood of an elliptic fixed point of general kind [4.37]. In the generic case the segment $\Delta_n = \{(\varphi_0, z): z_{2n} \leqslant z \leqslant z_{2n-1}\}$ possesses the property that $T^{q_{2n}}\Delta_n$ consists of points lying to the right of B_{φ_0}, while $T^{q_{2n-1}}\Delta_n$ consists of points lying to the left of B_{φ_0}. The segments Δ_n, when contracting, yield in the limit the point sought for, $(\varphi_0, z(\varphi_0))$; $\{z_{2n}\}$ monotonically increases and $\{z_{2n-1}\}$ monotonically decreases.

The sequence of the segments Δ_n is constructed inductively. For each n we choose a renormalized coordinate system in which a representation for T^{q_n}, $T^{q_{n-1}}$ is written and the transition $n \rightarrow n + 1$ is essentially a renormalization group transformation.

Let us formulate the inductive assumptions that determine the choice of the coordinate system at the nth step.

$1^{(n)}$. At the nth step the values z_{n-1}, z_n are given, which can be found from the following conditions:

$$T^{q_{n-1}}(\varphi_0, z_{n-1}) = (\varphi_0, z'_{n-1}), \quad T^{q_n}(\varphi_0, z_n) = (\varphi_0, z'_n).$$

The interval (z_n, z_{n-1}) at even n's (or (z_{n-1}, z_n) at odd n's) prescribes a natural scale for the variable z. According to this fact we pass to a new variable $\tilde{z}$ by the formula $z = z_n + \tilde{z}(z_{n-1} - z_n)$. The renormalized variable $\tilde{\varphi}$ can be chosen by the formula $\varphi = \varphi_0 + \chi_n\tilde{\varphi}$, where χ_n is found from the condition: $T^{q_{n-1}}(\varphi_0, z_n) = (\varphi_0 - \chi_n, \tilde{z}_n)$. The maps T^{q_n}, $T^{q_{n-1}}$ written in terms of the new coordinates $(\tilde{\varphi}, \tilde{z})$ will be denoted by $\tilde{f}_n$, $\tilde{q}_n$ or, more accurately, $\tilde{f}_n = (\tilde{f}_{n,1}, \tilde{f}_{n,2})$, $\tilde{g}_n = (\tilde{g}_{n,1}, \tilde{g}_{n,2})$. It follows from the above conditions of choosing the scaling constants that

$$\tilde{f}_{n,1}(0, 0) = 0, \quad \tilde{g}_{n,1}(0, 1) = 0, \quad \tilde{g}_{n,1}(0, 0) = -1.$$

Here and hereafter the subscript "1" stands for the projection onto the φ-axis, while the subscript "2", for the projection onto the z-axis.

Subsequent changes of variables and inductive assumptions depend on conditions imposed on the initial map T. Here we will consider two different cases. The first one concerns reversible maps that satisfy a certain symmetry condition, the second one deals with area-preserving maps having a zero Calabi invariant. Rigorous definitions will be given below. Let us treat the first case in more detail.

I. Reversible symmetric maps

Let the map T be reversible.

Definition (see [4.37]). The map T is called symmetric if there exists an involution A such that $T^{-1} = A^{-1}TA$.

Since by a change of variables the involution A can be reduced to the normal form

$$A(\varphi, z) = (-\varphi, z), \tag{4.20}$$

then we, from the very beginning, will consider reversible maps that satisfy the symmetry condition $T^{-1} = A^{-1}TA$ with respect to the involution (4.20). Let us demonstrate that the standard map belongs to this case. Indeed, it is easily seen that the standard map satisfies the symmetry condition with respect to the involution $B(\varphi, z) = (z - \varphi, z)$. Changing the variables $\varphi' = \varphi + \frac{1}{2}z$, $z' = z$ we will obtain the map in terms of the new coordinates

$$T\begin{pmatrix} \varphi' \\ z' \end{pmatrix} = \begin{pmatrix} \varphi' + z' + \frac{k}{4\pi}\sin 2\pi\left(\varphi' + \frac{z'}{2}\right) \\ z' + \frac{k}{2\pi}\sin 2\pi\left(\varphi' + \frac{z'}{2}\right) \end{pmatrix}$$

that is symmetric with respect to (4.20).

$2^{(n)}$, I. The coordinates $(\tilde{\varphi}, \tilde{z})$ and maps $\tilde{f}_n$, $\tilde{g}_n$ have been defined above. Now we will make another change of variables $\bar{\varphi} = \tilde{\varphi}$, $\bar{z} = \tilde{z} + \varepsilon_n \tilde{\varphi}^2$ and denote the maps $\tilde{f}_n$, $\tilde{g}_n$ in terms of the new coordinates as f_n, g_n. The constant ε_n will be chosen from the following condition:

$$\frac{\partial^2}{\partial\bar{\varphi}^2} f_{n,1}\Big|_{(\bar{\varphi}, \bar{z})=(0,0)} = 0, \text{ i.e.}$$

$$\varepsilon_n = \frac{\dfrac{\partial^2}{\partial\tilde{\varphi}^2}\tilde{f}_{n,1}\Big|_{(\tilde{\varphi},\tilde{z})=(0,0)}}{2\,\dfrac{\partial\tilde{f}_{n,1}}{\partial\tilde{z}}\Big|_{(\tilde{\varphi},\tilde{z})=(0,0)}} = \frac{\chi_n^2}{2(z_{n-1} - z_n)} \frac{\dfrac{\partial^2}{\partial\varphi^2} T_1^{q_n}(\varphi_0, z_n)}{\dfrac{\partial}{\partial z} T_1^{q_n}(\varphi_0, z_n)}.$$

Now let us formulate inductive assumptions related to the maps f_n, g_n.

$3^{(n)}$, I. Let us write $f_n = (f_{n,1}, f_{n,2})$, $g_n = (g_{n,1}, g_{n,2})$ as

$$\begin{cases} f_{n,1} = (\rho^{(n)})^{-1}\bar{z} + \bar{\varphi} + \sum\limits_{\substack{i+j\leqslant 3 \\ i\geqslant 0,\, j\geqslant 0}} a_{ij}^{(n)}\bar{\varphi}^i\bar{z}^j + \alpha^{(n)}(\bar{\varphi}, \bar{z}), \\ f_{n,2} = \bar{z} + \sum\limits_{\substack{i+j\leqslant 3 \\ i\geqslant 0,\, j\geqslant 0}} b_{ij}^{(n)}\bar{\varphi}^i\bar{z}^j + \beta^{(n)}(\bar{\varphi}, \bar{z}) \\ g_{n,1} = \bar{z} + \bar{\varphi} - 1 + \sum\limits_{\substack{i+j\leqslant 3 \\ i\geqslant 0,\, j\geqslant 0}} c_{ij}^{(n)}\bar{\varphi}^i\bar{z}^j + \gamma^{(n)}(\bar{\varphi}, \bar{z}), \\ g_{n,2} = \bar{z} + \sum\limits_{\substack{i+j\leqslant 3 \\ i\geqslant 0,\, j\geqslant 0}} d_{ij}^{(n)}\bar{\varphi}^i\bar{z}^j + \delta^{(n)}(\bar{\varphi}, \bar{z}). \end{cases} \tag{4.21}$$

where $\alpha^{(n)}$, $\beta^{(n)}$, $\gamma^{(n)}$, $\delta^{(n)}$ contain only the monomials of the higher powers in terms of $\bar{\varphi}$, $\bar{z}$, while $\rho^{(n)}$ is obtained from the condition $(\rho^{(n)})^{-1} = f_{n,1}(0, 1)$. Let us also define $\rho_0^{(n)} = [r_n, r_{n-1}, \ldots, r_1]$, where r_i's are the coefficients of the expansion of the rotation number ω into the continued fraction.

(a$_1$) $a_{00}^{(n)} = c_{00}^{(n)} = 0, \quad a_{01}^{(n)} = -a_{02}^{(n)} - a_{03}^{(n)} - \alpha^{(n)}(0, 1),$
$c_{01}^{(n)} = -c_{02}^{(n)} - c_{03}^{(n)} - \gamma^{(n)}(0, 1), \quad a_{20}^{(n)} = 0.$

(a$_2$) $b_{00}^{(n)} = 0, \quad d_{00}^{(n)} = -d_{01}^{(n)} - d_{02}^{(n)} - d_{03}^{(n)} - \delta^{(n)}(0, 1).$

(a$_3$) $|\rho^{(n)} - \rho_0^{(n)}| \leqslant A_\rho (1 + 0.6\rho_0^{(n)}) \lambda^n.$

(b$_1$) $|a_{ij}^{(n)}|, \quad |c_{ij}^{(n)}| \leqslant A_{ij} \lambda_{ij}^n, \ (i, j) = (1, 0), (1, 1), (3, 0),$
$|c_{20}^{(n)}| \leqslant A_{20} \lambda_{20}^n.$
$|b_{ij}^{(n)}|, \quad |d_{ij}^{(n)}| \leqslant B_{ij} \bar{\lambda}_{ij}^{(n)}, \ (i, j) = (0, 1), (1, 0), (1, 1), (2, 0), (3, 0).$

(b$_2$) $|a_{02}^{(n)}|, \quad |c_{02}^{(n)}| \leqslant A_{02} (1 - 0.5\rho_0^{(n)}) \lambda_{02}^n,$
$|b_{02}^{(n)}|, \quad |d_{02}^{(n)}| \leqslant B_{02} (1 - 0.5\rho_0^{(n)}) \bar{\lambda}_{02}^n,$
$|a_{ij}^{(n)}|, \quad |c_{ij}^{(n)}| \leqslant A_{ij} (1 + 2\rho_0^{(n)}) \lambda_{ij}^n, \ (i, j) = (0, 3), (1, 2), (2, 1),$
$|b_{ij}^{(n)}|, \quad |d_{ij}^{(n)}| \leqslant B_{ij} (1 + 2\rho_0^{(n)}) \bar{\lambda}_{ij}^n, \ (i, j) = (0, 3), (1, 2), (2, 1).$

(b$_3$) The functions $\alpha^{(n)}(\bar{\varphi}, \bar{z})$, $\beta^{(n)}(\bar{\varphi}, \bar{z})$, $\gamma^{(n)}(\bar{\varphi}, \bar{z})$, $\delta^{(n)}(\bar{\varphi}, \bar{z})$ are four times differentiable in the domain $U_n = \{(\bar{\varphi}, \bar{z}): -0.1 \leqslant \bar{z} \leqslant 1.1,$ $|\bar{\varphi}| \leqslant 4 - 1.5\rho_0^{(n)}\}$,

$$\alpha^{(n)}(0, 0) = \beta^{(n)}(0, 0) = \gamma^{(n)}(0, 0) = \delta^{(n)}(0, 0) = 0,$$

$$\left.\frac{\partial^{i+j}}{\partial \bar{\varphi}^i \, \partial \bar{z}^j} \alpha^{(n)}, \ \beta^{(n)}, \ \gamma^{(n)}, \ \delta^{(n)} \right|_{(\bar{\varphi}, \bar{z}) = (0, 0)} = 0, \quad 1 \leqslant i + j \leqslant 3,$$

$$\left| \frac{\partial^{i+j}}{\partial \bar{\varphi}^i \, \partial \bar{z}^j} \alpha^{(n)}, \ \gamma^{(n)}(\bar{\varphi}, \bar{z}) \right| \leqslant A_{ij} (1 + 2\rho_0^{(n)}) \lambda_{ij}^n,$$

$$(i, j) = (1, 3), (2, 2), (3, 1), (4, 0), (0, 4), \ (\bar{\varphi}, \bar{z}) \in U_n,$$

$$\left| \frac{\partial^{i+j}}{\partial \bar{\varphi}^i \, \partial \bar{z}^j} \beta^{(n)}, \ \delta^{(n)}(\bar{\varphi}, \bar{z}) \right| \leqslant B_{ij} (1 + 2\rho_0^{(n)}) \bar{\lambda}_{ij}^n,$$

$$(i, j) = (1, 3), (2. 2), (3,1), (0, 4), (\bar{\varphi}, \bar{z}) \in U_n,$$

$$\left| \frac{\partial^4}{\partial \bar{\varphi}^4} \beta^{(n)}, \ \delta^{(n)}(\bar{\varphi}, \bar{z}) \right| \leqslant B_{40} \rho_0^{(n)} (1 + 2\rho_0^{(n)}) \bar{\lambda}_{40}^n, \quad (\bar{\varphi}, \bar{z}) \in U_n.$$

Now let us consider the second case.

II. Area-preserving maps

We will consider area-preserving maps that satisfy the twist condition. Besides, the condition of the zero Calabi invariant is imposed [4.25]. Let us clarify the latter in more detail.

Let γ be a closed curve going around a cylinder and $T\gamma$ be the image of the curve γ under the action of T. Let us denote by F_1 and F_2 the subsets of cylinder's points lying under the curves γ and $T\gamma$, respectively. Note that $F_2 = TF_1$. Consider the difference mes $(F_1 - F_2)$ — mes $(F_2 - F_1)$, where mes $(\cdot)$ is the Lebesgue measure on the cylinder. The value of this difference is independent of the curve γ and is called the Calabi invariant. If there exists a closed invariant curve going around a cylinder then the Calabi invariant is evidently zero. Thus the condition of the zero Calabi invariant is necessary for invariant curves to exist. It can be easily verified that the standard map satisfies this condition.

$2^{(n)}$, II. Let us construct the maps f_n, g_n. To this end we will change the variables $\bar\varphi = \tilde\varphi$, $\bar z = \tilde z + \xi_n\tilde\varphi + \eta_n\tilde\varphi^2$. The maps $\tilde f_n$, $\tilde g_n$ in new coordinates will be denoted as f_n, g_n. The constants ξ_n, η_n are obtained from the conditions $\frac{\partial}{\partial\bar\varphi} f_{n,1}(0,\ 0) = 1$, $\frac{\partial^2}{\partial\bar\varphi^2} f_{n,1}(0,0) = 0$. One can easily verify that

$$\xi_n = \left(\frac{\partial\tilde f_{n,1}}{\partial\tilde\varphi}(0,\ 0) - 1\right)\Big/\frac{\partial\tilde f_{n,1}}{\partial\tilde z}(0,\ 0),$$

$$\eta_n = \frac{1}{2\,\dfrac{\partial\tilde f_{n,1}}{\partial\tilde\varphi}(0,\ 0)}\left[\frac{\partial^2\tilde f_{n,1}}{\partial\tilde\varphi^2}(0,0) - 2\xi_n\frac{\partial^2\tilde f_{n,1}}{\partial\tilde\varphi\,\partial\tilde z}(0,\ 0) + \xi_n^2\frac{\partial^2\tilde f_{n,1}}{\partial\tilde z^2}(0,0)\right].$$

Now let us formulate the inductive conditions corresponding to case II.

$3^{(n)}$, II. Let us represent $f_n = (f_{n,1}, f_{n,2})$, $g_n = (g_{n,1}, g_{n,2})$ in the form of (4.21):

(a_1) $a_{00}^{(n)} = c_{00}^{(n)} = 0$, $\quad a_{01}^{(n)} = -a_{02}^{(n)} - a_{03}^{(n)} - \alpha^{(n)}(0,\ 1)$,
$c_{01}^{(n)} = -c_{02}^{(n)} - c_{03}^{(n)} - \gamma^{(n)}(0,\ 1)$, $\quad a_{10}^{(n)} = a_{20}^{(n)} = 0$.

(a_2) $|b_{00}^{(n)}|$, $\quad |d_{00}^{(n)}| \leqslant B_{00}\bar\lambda_{00}^n$.

(a_3) $|\rho^{(n)} - \rho_0^{(n)}| \leqslant A_\rho(1 + 0.6\rho_0^{(n)})\,\lambda^n$.

(b_1) $|c_{10}^{(n)}| \leqslant A_{10}\lambda_{10}^n$,
$|c_{20}^{(n)}| \leqslant A_{20}\lambda_{20}^n$,
$|b_{ij}^{(n)}|$, $|d_{ij}^{(n)}| \leqslant B_{ij}\bar\lambda_{ij}^n$,
$(i,\ j) = (0,\ 1),\ (1,\ 0),\ (1, 1),\ (2,\ 0),\ (3,\ 0)$.

(b_2) $|a_{ij}^{(n)}|$, $|c_{ij}^{(n)}| \leqslant A_{ij}(1 - 0.5\rho_0^{(n)})\,\lambda_{ij}^n$, $\quad (i,\ j) = (0,\ 2),\ (1,\ 1)$,
$|b_{02}^{(n)}|$, $|d_{02}^{(n)}| \leqslant B_{02}(1 - 0.5\rho_0^{(n)})\,\bar\lambda_{02}^n$,
$|a_{ij}^{(n)}|$, $|c_{ij}^{(n)}| \leqslant A_{ij}(1 + 2\rho_0^{(n)})\,\lambda_{ij}^n$,
$(i,\ j) = (0,\ 3),\ (1,\ 2),\ (2,\ 1),\ (3,\ 0)$,
$|b_{ij}^{(n)}|$, $|d_{ij}^{(n)}| \leqslant B_{ij}(1 + 2\rho_0^{(n)})\,\bar\lambda_{ij}^n$, $(i,\ j) = (0,\ 3), (1,\ 2),\ (2,\ 1)$.

(b_3) This inductive assumption concerning the functions $\alpha^{(n)}$, $\beta^{(n)}$, $\gamma^{(n)}$, $\delta^{(n)}$ is transferred unchanged from the inductive assumptions $3^{(n)}$, I formulated above.

The scheme of the subsequent reasoning is the same as in the preceding section. We will show that if f_n, g_n satisfy the inductive assumptions $3^{(n)}$, I or $3^{(n)}$, II, then f_{n+1}, g_{n+1} also satisfy the corresponding inductive assumptions. The maps f_{n+1}, g_{n+1} are controlled by the action of the renormalization group transformation $S_{r_{n+1}}$ on the maps f_n, g_n. One begins with finding $\bar{f}_{n+1} = g_n(f_n^{(r_{n+1})})$, $\bar{g}_{n+1} = f_n$ and then changes the variables according to the conditions $1^{(n+1)}$, $2^{(n+1)}$. The inductive assumptions $3^{(n)}$ essentially state the convergence of (f_n, g_n) to a one-parameter family of pairs of maps (f_ρ, g)

$$f_\rho(\bar{\varphi}, \bar{z}) = (\rho^{-1}\bar{z} + \bar{\varphi}, \bar{z}), \quad g(\bar{\varphi}, \bar{z}) = (\bar{z} + \bar{\varphi} - 1, \bar{z}). \tag{4.22}$$

This family should be treated as a fixed point of the renormalization group.

Prior to formulating the main theorem, note a substantial difference between cases I and II. In case I it is necessary that the symmetry property should be conserved under the renormalization group transformations S_r. The latter condition is fulfilled only if we construct the transformations of the renormalization group corresponding to the vertical B_{φ_0}, $\varphi_0 = 0$. Thus, in case I this vertical, that is a fixed straight line for the involution (4.20), plays a special role. But in case II one can consider an arbitrary vertical B_{φ_0}.

Let us formulate the main theorem. Let $\omega = [r_1, r_2, \ldots]$ satisfy the incommensurability condition $r_i \leqslant Rq^i$, where $q < q_0 = 1.0001$. Let us choose the following values of the constants λ, λ_{ij}, $\bar{\lambda}_{ij}$ that are controlled by the inductive assumptions $3^{(n)}$: $\lambda = 0.9$; $\lambda_{ij} = 0.89 - \varepsilon\,(2.5i + 2j)$, $\varepsilon = 0.005$, $\bar{\lambda}_{ij} = \lambda_{ij} - \frac{1}{800}$.

Theorem 2. For any $R > 0$ constants $A_\rho(R)$, $A_{ij}(R)$, $B_{ij}(R)$ can be found such that if for a pair (f_n, g_n) constructed by means of the map T, corresponding to case I (II), the assumptions $3^{(n)}$, I ($3^{(n)}$. II) are fulfilled then for the pair (f_{n+1}, g_{n+1}) the assumptions $3^{(n+1)}$, I ($3^{(n+1)}$, II) are also fulfilled.

Proof. We will not present a formal proof but will only give the idea of it. To be specific, consider case I, i.e. let us assume that f_n, g_n satisfy the symmetry condition $f_n^{-1} = A^{-1}f_nA$, $g_n^{-1} = A^{-1}g_nA$, where $A\,(\bar{\varphi}, \bar{z}) = (-\bar{\varphi}, \bar{z})$. To simplify notation, we will omit the superscript n for the coefficients $a_{ij}^{(n)}$, $b_{ij}^{(n)}$, $c_{ij}^{(n)}$, $d_{ij}^{(n)}$, $\rho^{(n)}$, $\rho_0^{(n)}$ as well as for the functions $\alpha^{(n)}$, $\beta^{(n)}$, $\gamma^{(n)}$, $\delta^{(n)}$. The relevant coefficients and functions for the pair (f_{n+1}, g_{n+1}) will be denoted as $\tilde{a}_{ij}$, $\tilde{b}_{ij}$, $\tilde{c}_{ij}$, $\tilde{d}_{ij}$, $\tilde{\rho}$, $\tilde{\rho}_0$, $\tilde{\alpha}$, $\tilde{\beta}$, $\tilde{\gamma}$, $\tilde{\delta}$. Besides, we will denote the variables as (φ, z) instead of $(\bar{\varphi}, \bar{z})$.

Suppose that the constants $A_\rho(R)$, $A_{ij}(R)$, $B_{ij}(R)$ are chosen so that $(A_{ij}, B_{ij}) \gg (A_{i_1 j_1}, B_{i_1 j_1})$ at $i + j < i_1 + j_1$ or $i + j = i_1 + j_1$, $i < i_1$ and, besides, $1 \gg A_\rho \gg A_{ij} \gg B_{ij} \gg A_\rho^2$. Since corrections due to a_{ij}, b_{ij}, c_{ij}, d_{ij} are small, one can consider the action of the renormalization group transformation in a linear approximation. As can be easily shown, the hierarchy of coefficients is chosen so that in the main order each pair of the coefficients (a_{ij}, c_{ij}), (b_{ij}, d_{ij}) is transformed independently of the remaining pairs. Let us write the main-order transformation

$$
\begin{gathered}
\begin{pmatrix} \tilde{a}_{ij} \\ \tilde{c}_{ij} \end{pmatrix} = \frac{1}{(r+\rho_0)^{i+j-1}} \rho_0^j \begin{pmatrix} r & 1 \\ 1 & 0 \end{pmatrix} \begin{pmatrix} a_{ij} \\ c_{ij} \end{pmatrix}, \quad (i, j) \neq (2, 0), (0, 0)\ (0, 1), \\
\tilde{a}_{00} = \tilde{c}_{00} = 0, \\
\tilde{a}_{01} = -\sum_{j \geqslant 2} \tilde{a}_{0j}, \ \tilde{c}_{01} = -\sum_{j \geqslant 2} \tilde{c}_{0j}, \\
\tilde{a}_{20} = 0, \quad \tilde{c}_{20} = -c_{20} \frac{1}{(r+\rho_0)^2}, \\
\begin{pmatrix} \tilde{b}_{ij} \\ \tilde{d}_{ij} \end{pmatrix} = \frac{1}{(r+\rho_0)^{i+j-1}} \rho_0^{j-1} \begin{pmatrix} r & 1 \\ 1 & 0 \end{pmatrix} \begin{pmatrix} b_{ij} \\ d_{ij} \end{pmatrix}.
\end{gathered}
\tag{4.23}
$$

Here r denotes the integer r_{n+1}. The specific feature of the formula for $\tilde{a}_{20}$, $\tilde{c}_{20}$ is the substitution $z \to z + \varepsilon\varphi^2$. Note that exact relationships differ from the above by values of a higher order of smallness as compared with $A_{ij}(R)\lambda_{ij}^n$, $B_{ij}(R)\bar{\lambda}_{ij}^n$.

Generally, relations (4.23) are stable. Let us show, e.g. that the relations for $(\tilde{b}_{02}, \tilde{d}_{02})$ are stable. Indeed, due to the inductive assumptions $3^{(n)}$, I, we have $|b_{02}|$, $|d_{02}| \leqslant B_{02}(1-0.5\rho_0)\bar{\lambda}_{02}^n$. Since $\tilde{\rho}_0 = \frac{1}{r+\rho_0}$ we obtain

$$
\begin{aligned}
&\frac{1}{B_{02}(1-0.5\tilde{\rho}_0)\bar{\lambda}_{02}^n} (|\tilde{b}_{02}|, |\tilde{d}_{02}|) \leqslant \frac{(r+1)\rho_0(1-0.5\rho_0)}{(r+\rho_0)\left(1-\frac{0.5}{r+\rho_0}\right)} \\
&= \frac{(r+1)\rho_0(1-0.5\rho_0)}{r+\rho_0-0.5} \leqslant \frac{2\rho_0(1-0.5\rho_0)}{1+\rho_0-0.5} < 0.77 < \bar{\lambda}_{02}
\end{aligned}
$$

and hence the inductive assumptions $3^{(n+1)}$, I are valid for $(\tilde{b}_{02}, \tilde{d}_{02})$.

It can be easily shown that unstable are only relations for $(\tilde{a}_{10}, \tilde{c}_{10})$, $(\tilde{b}_{00}, \tilde{d}_{00})$, $(\tilde{b}_{01}, \tilde{d}_{01})$, $(\tilde{b}_{10}, \tilde{d}_{10})$, $(\tilde{b}_{11}, \tilde{d}_{11})$, $(\tilde{b}_{20}, \tilde{d}_{20})$, $(\tilde{b}_{30}, \tilde{d}_{30})$. Note that the relations for $(\tilde{a}_{00}, \tilde{c}_{00})$, $(\tilde{a}_{01}, \tilde{c}_{01})$, $(\tilde{a}_{20}, \tilde{c}_{20})$ become stable due to the changes of variables. The instabilities in the above relations can be eliminated by means of the symmetry, $f_{n+1}^{-1} = A^{-1}f_{n+1}A$, $g_{n+1}^{-1} = A^{-1}g_nA$, and commutativity, $f_{n+1} \circ g_{n+1} = g_{n+1} \circ f_{n+1}$, conditions. Indeed, writing out these conditions up to the terms of the order of $B_{30}(R)\,\bar{\lambda}_{30}^{n}$, we obtain the equalities

$$\begin{aligned}\tilde{a}_{10} &= \tilde{c}_{10} = \tilde{b}_{00} = \tilde{d}_{00} = \tilde{b}_{01} = \tilde{d}_{01} = \tilde{b}_{10} = \tilde{d}_{10} = \tilde{b}_{11} = \tilde{d}_{11} = \tilde{b}_{20}\\ &= \tilde{d}_{20} = \tilde{b}_{30} = \tilde{d}_{30} = 0.\end{aligned} \tag{4.24}$$

These equalities are valid accurate to the terms of the higher order of smallness as compared with $B_{30}\bar{\lambda}_{30}^{n}$. Let us derive, e.g. the last two equalities, $\tilde{b}_{30} = \tilde{d}_{30} = 0$.

Let us verify the identities $f_{n+1}^{-1} \circ f_{n+1} = I$, $g_{n+1}^{-1} \circ g_{n+1} = I$ by taking into account the symmetry conditions $f_{n+1}^{-1} = A^{-1}f_nA$, $g_{n-1}^{-1} = A^{-1}g_nA$. At the same time we will only trace the coefficient at the monomial φ^3. As a result we arrive at

$$2\tilde{a}_{30} - \tilde{\rho}^{-1}\tilde{b}_{30} = 0, \quad 2\tilde{c}_{30} - \tilde{d}_{30} = 0.$$

Let us write the commutativity condition $f_{n+1} \circ g_{n+1} = g_{n+1} \circ f_{n+1}$ and also trace the coefficient at φ^3

$$\tilde{\rho}^{-1}\tilde{d}_{30} + \tilde{c}_{30} + \tilde{a}_{30} = -\tilde{b}_{30} + \tilde{a}_{30} + \tilde{c}_{30}, \text{ i.e. } \tilde{\rho}^{-1}\tilde{d}_{30} = -\tilde{b}_{30}.$$

$$\text{Thus, } \tilde{d}_{30} = -\tilde{\rho}\tilde{b}_{30},\ \tilde{a}_{30} = \frac{\tilde{\rho}^{-1}}{2}\,\tilde{b}_{30},\ \tilde{c}_{30} = -\frac{\tilde{\rho}}{2}\,\tilde{b}_{30}.$$

Now let us show that $\tilde{b}_{30} = 0$. To do this, we write out the commutativity condition while tracing the coefficients at φ^2. Then

$$\tilde{d}_{20} + \tilde{b}_{20} + 3\tilde{b}_{30} = \tilde{b}_{20} + \tilde{d}_{20}, \quad \text{i.e.} \quad \tilde{b}_{30} = 0.$$

In an analogous way, other relationships (4.24) can be proved. Thus all the instabilities can be eliminated, this proving Theorem 2. With area-preserving maps (case II), the theorem can be proved according to the same scheme. Changes of variables, conservation and commutativity conditions eliminate all instabilities except that in the relation for $(\tilde{b}_{00}, \tilde{d}_{00})$. This instability can be eliminated by the zero Calabi invariant. Here the equality $\tilde{b}_{00} = 0$ holds accurate to terms of the higher smallness order while for maps that satisfy the symmetry condition the equality $\tilde{b}_{00} = 0$ is rigorously fulfilled.

In conclusion, let us discuss the construction of an invariant curve. Consider a vertical B_φ and determine, by the renormalization group procedure, a sequence of pairs of maps $(f_{n,\varphi}, g_{n,\varphi})$. Suppose that there exists a number n_0 such that for all $0 \leqslant \varphi < 1$ a pair of maps $(f_{n_0,\varphi}, g_{n_0,\varphi})$ lies within the attraction domain of the fixed family (4.22), i.e. it satisfies the inductive assumptions $3^{(n_0)}$. Then for each $0 \leqslant \varphi < 1$ there will be defined an embedded sequence of segments $[z_{2n}(\varphi), z_{2n-1}(\varphi)]$. Let us put $z(\varphi) = \bigcap_n [z_{2n}(\varphi), z_{2n-1}(\varphi)]$. Due to the continuous dependence of the renormalization group procedure on the parameter φ, $z(\varphi)$ is a continuous function on the circle $0 \leqslant \varphi < 1$. Consider a closed curve $\gamma = \{(\varphi, z(\varphi)), 0 \leqslant \varphi < 1\}$. Each point of the curve γ is unambiguously specified by the following property: $T^{(q_{2n})}(\varphi, z(\varphi))$ lies to the right of the vertical B_φ, while $T^{(q_{2n-1})}(\varphi, z(\varphi))$ lies to the left of B_φ, for any $n \geqslant 1$. Whence it easily follows that γ is an invariant curve with a rotation number ω with respect to the map T.

References

4.1. B. V. Chirikov, *Phys. Reports*, 52, 5, 263 (1979).
4.2. A. N. Kolmogorov, *Dokl. Acad. Nauk SSSR*, 98, 4, 527 (1954).
4.3. V. I. Arnol'd, *Uspekhi Mat. Nauk*, 18, 6, 91 (1963).
4.4. J. Moser, *Lectures on Hamiltonian Systems*. Mem. AMS, Vol. 81, 1968.
4.5. J. M. Greene, *J. Math. Phys.*, 20, 1183 (1979).
4.6. A. Ya. Khinchin, *Continued Fractions*, Nauka, Moscow, 1978.
4.7. J. N. Mather, *Erg. Theory and Dyn. Systems*. 4. 301 (1984).
4.8. S. Aubry, *Physica* 7D, 240 (1983).
4.9. R. S. MacKay and I. C. Percival. *Comm. Math. Phys.*, 98, 469 (1985).
4.10. I. C. Percival, *J. Phys. A*, 12, 57 (1979).
4.11. J. N. Mather, *Topology*, 21, 457 (1982).
4.12. Ya. I. Frenkel and T. A. Kontorova, *Zh. Eksp. Teor. Fizikl*, 8, 364 (1938).
4.13. H. M. Morse, *Am. Math. Soc. Pub.*, 18 (1934).
4.14. G. A. Hedlund, *Ann. Math.*, 33, 719 (1932).
4.15. Ya. G. Sinai, *Phase Transitions. Rigorous Results*. Nauka, Moscow, 1980 (in Russian).
4.16. S. Aubry and P. V. Le Daeron, *Physica* 8D, 381 (1983).
4.17. I. C. Percival, *Symp. on Nonlinear Dyn. and Beam-Beam Interactions, Amer. Inst. Phys. Conf. Proc.*, No. 57, 310, 1980.
4.18. V. F. Lazutkin and D. Ya. Terman, *Comm. Math. Phys.*, 94, 511 (1984).
4.19. M. J. Feigenbaum, *J. Stat. Phys.*, 19, 25 (1978).
4.20. M. J. Feigenbaum, *J. Stat. Phys.*, 21, 669 (1979).
4.21. E. B. Vul, Ya. G. Sinai, and K. M. Khanin, *Uspekhi Mat. Nauk*, 39, 3, 3 (1984).
4.22. L. P. Kadanoff, *Phys. Rev. Lett.*, 47, 1641 (1981).
4.23. S. J. Shenker and L. P. Kadanoff. *J. Stat. Phys.*, 27, 631 (1982).
4.24. R. S. Mackay, *Physica* 7D, 283 (1983).
4.25. R. S. Mackay, Ph. D. Thesis, Princeton University, Princeton, 1982.
4.26. V. I. Arnol'd, *Izv. Akad. Nauk SSSR, Ser. Mat.*, 25, 21 (1961).
4.27. M. R. Herman, *Publ. Math. IHES*, 49, 5 (1979).
4.28. M. R. Herman, Preprint No. 050-84-4, Berkeley, California, 1984.
4.29. M. H. Jensen, P. Bnk, and T. Bohr, *Phys. Rev. Lett.*, 50, 1637 (1983).
4.30. M. H. Jensen, P. Bak, and T. Bohr, *Phys. Rev. A*, 30, 1960 (1984).
4.31. E. A. Coddington and L. Levinson. *Theory of Ordinary Differential Equations*, McGraw-Hill, New York, 1955.
4.32. I. P. Kornfeld, Ya. G. Sinai, and S. V. Fomin, *Ergodic Theory*, Nauka, Moscow. 1980 (in Russian).
4.33. B. V. Chirikov, Preprint IYaF SO AN SSSR, No. 84-147, 1984.
4.34. M. J. Feigenbaum, L. P. Kadanoff, and S. J. Shenker, *Physica* 5D, 370 (1982).
4.35. S. Ostlund, D. Rand, J. Sethna, and E. D. Siggia, *Physica* 8D, 303 (1983).
4.36. J. D. Farmer and I. I. Satija, *Phys. Rev. A*, 31, 3520 (1985).
4.37. G. D. Birkhoff, *Dynamical Systems*, Providence, R. I., 1927.

5 Nonlinear Problems of Turbulent Dynamo

Ya. B. Zel'dovich, Mem. USSR Acad. Sc. and
A. A. Ruzmaikin, D. Sc. (Phys.-Math.)

5.1. INTRODUCTION

That hydrodynamic motions in plasma can amplify and maintain a magnetic field, i.e. act as a self-excited dynamo yet without wires and coils, was first pointed out by Larmor in his impressive brief report [5.1]. In the 1930s the problem was stated mathematically as that of an asymptotic temporal behaviour of an initial, decreasing at infinity not slower than r^{-3}, magnetic field in a given plasma flow (kinematic dynamo). Cowling [5.2], proved that it is impossible to maintain an axially symmetric magnetic field by an axially symmetric flow. He believed that plasma motions proper, i.e. in the absence of dissipation, cannot produce new magnetic loops and thereby cannot amplify the magnetic flux. It has been shown [5.3] that an arbitrary field, properly decreasing at infinity, decays in a two-dimensional flow. This provoked a sceptical attitude towards the dynamo problem reinforced by the fact that in cosmic conditions the dissipation of a magnetic field is weak as compared with convective transfer by motions. In other words, the magnetic Reynolds number $R_m = lv/\nu_m$ is very large (here v is the velocity, ν_m is the magnetic diffusivity, and l is the characteristic scale, typically very large).

A positive solution was first clearly demonstrated by Alfvén in his paper [5.4] which has been hardly known until now even to experts in the field. Alfvén has demonstrated that a small-scale magnetic diffusion at the points of loop connection is sufficient for effective reproduction of magnetic loops. In the Alfvén mechanism the characteristic rate of the field growth (the inverse time of loops doubling) nevertheless dramatically depends on magnetic diffusivity and, in particular, it vanishes as $R_m \to \infty$, i.e. the field grows slowly at large magnetic Reynolds numbers. The same property is exhibited by mathematical examples of nondecaying solutions for magnetic fields in laminar flows (see, e.g. [5.5]) including the well-known dynamo of Braginskii. The class of slow dynamos also includes flows with stationary velocities concentrated on surfaces [5.6, 5.7].

As was shown by one of the authors (see [5.8]), the reproduction of magnetic lines can proceed at a growth rate independent of magnetic diffusion in the limit $R_m \to \infty$. To do this, a magnetic loop should be made into a figure "eight" and then the rings of the latter should be superimposed. The description of this topological procedure and its comparison to the Alfvén mechanism are given in the monograph [5.7] and review [5.9]. Let us only stress that magnetic diffusion to some extent shapes the solution yet in the limit $R_m \to \infty$ the field growth rate is independent of it. Dynamos of this type are called fast. The classification was clarified in [5.6], where the notions of fast and slow dynamos were rigorously formulated.

Figure "eight" dynamo is a physical notion rather than mathematical example. However, there is a class of plasma flows capable to act as a fast dynamo. These include practically important, three-dimensional turbulent flows and, in general, random three-dimensional flows with adequate ergodic properties [5.9]. First of all, we can mention dynamos of mean magnetic fields in mirror-nonsymmetric, or helical, turbulence [5.5, 5.7, 5.10]. The combined action of helicity and non-uniform rotation (the $\alpha\omega$-dynamo) acts in the Sun [5.11-5.13] and other astrophysical objects [5.5, 5.7, 5.13]. The helicity alone can also act as a dynamo (the α^2-dynamo). However, to maintain the helicity needs a large-scale flow, say, a rotation.

In the last few years progress has been made in solving the problem of the generation of magnetic fields with a zero mean value in a mirror-symmetric turbulence. This problem has been formulated in the well-known work by Batchelor [5.14] who advanced a correct hypothesis on the possibility of field generation, and estimated the growth rate and the stationary field strength. Vainstein [5.8. 5.15] drew attention to a model by Kazantsev [5.16]. Subsequently it was studied in [5.17] that shows that this model is a fast dynamo.

Equations for a random (α being zero on average) reproduction, $\partial n/\partial t = \alpha(r, t)\, n + D\,\Delta n$, are known to have solutions growing proportionally to $\exp \gamma t$, with $\gamma \sim \langle\alpha^2\rangle$. But in a mirror-symmetric turbulence the field generation mechanism is of another nature—here at work are the "Hubble" stretchings [5.18].

A special class is presented by flows with stationary velocities but ergodic trajectories. The possibility of a dynamo in such flows was shown in [5.19, 5.20] (see also the earlier paper [5.21]). A typical feature of the solutions found is the emergence of magnetic structures that are strongly concentrated in the limit of large magnetic Reynolds numbers. An analogous phenomenon for the class of fast dynamos, viz. field concentrations in the form of sparse peaks in space and time (intermittence), was demonstrated in [5.22]. Here, the Hubble idealization of the local flow is also essential.

Thus, in solving the problem of kinematic dynamo both conceptual clarity and concrete results have been achieved. This problem is linear in a magnetic field, since the induction equation is solved for a given velocity field. The dynamo leads to an exponential growth of the magnetic field and thereby to due regard for the back action of the field on the flow, i.e. to a nonlinear problem. Generally, the growth rate is complex, i.e. an exponential growth is accompanied by oscillations. Near the critical value of the magnetic Reynolds number the real part of the growth rate is usually small, therefore the nonlinearity damps Re γ and leaves the oscillations unaffected. At a small difference $R_m - (R_m)_{cr}$ the oscillations are nearly harmonic, therefore sharply nonharmonic oscillations, e.g. reversals of the geomagnetic field or the solar cycle indicate a strong nonlinearity.

The development of the theory of nonlinear dynamo is at the very beginning. First results were obtained by nonrigorous methods, some of them will hardly survive. It is quite natural that at this level only principal qualitative results can be discussed. We concentrate on two of them.

The first concerns the magnetic field effect on mean characteristics of a turbulent flow. First of all, according to [5.8], one can expect that the most sensitive element of the dynamo, the mean helicity, is influenced. Based on this, a semi-phenomenological self-consistent system of equations for the mean magnetic field and mean flow parameters can be constructed. Such a system serves as the model to explain such phenomena as reversals of the geomagnetic field or solar activity minima.

The second topic concerns the structure of MHD turbulence, where the velocity and magnetic field are equally important and self-consistent. Even the consideration of the two-dimensional case is instrumental here. Dynamo is absent in this case [5.3] yet there are field structures that are pertinent to the three-dimensional case [5.23]. From the conceptual point of view it becomes clear that the chaotic phase approximation cannot be applied. A simple example of a flow with a linear (Hubble) velocity field [5.18] and the dynamo theorem for a randomly renovated flow [5.22] give an idea about the field distribution in the three-dimensional situation.

5.2. NONLINEAR MEAN FIELD DYNAMO

Basic achievements of the dynamo theory, especially as applied to cosmic physics, are connected with studies of the mean magnetic field, $\langle \mathbf{H} \rangle = \mathbf{B}$. Its transfer and amplification are due mainly to the turbulent diffusion β, the mean helicity α, and the large-scale flow $\mathbf{V}$ [5.5, 5.7, 5.10, 5.13]:

$$\begin{aligned} \frac{\partial \mathbf{B}}{\partial t} &= -\operatorname{curl} \langle \mathbf{E} \rangle, \\ -\langle \mathbf{E} \rangle &= \mathbf{V} \times \mathbf{B} + \alpha \mathbf{B} - \beta \operatorname{curl} \mathbf{B}, \end{aligned} \tag{5.1}$$

where

$$\alpha = -\frac{\tau}{3} \langle \mathbf{v} \operatorname{curl} \mathbf{v} \rangle, \quad \beta = \frac{\tau}{3} \langle \mathbf{v}^2 \rangle + \nu_m.$$

For simplicity, here α and β are assumed to be isotropic, in general case they are tensors.

The magnetic field influences the motion due to the Ampère force in the Navier-Stokes equation

$$\frac{\partial \mathbf{v}}{\partial t} + (\mathbf{v}\nabla)\,\mathbf{v} - \nu\Delta\mathbf{v} = \mathbf{f} + \frac{1}{4\pi\rho}\,\mathrm{curl}\,\mathbf{H} \times \mathbf{H}, \tag{5.2}$$

where $\mathbf{f}$ includes both the pressure gradient and forces driving the motion. It can be readily seen from (5.2) that the mean velocity and the mean statistical parameters α, β are affected not only by the mean field $\mathbf{B}$ but also by the fluctuation field $\mathbf{h} = \mathbf{H} - \mathbf{B}$ (see the term $\langle \mathrm{curl}\,\mathbf{h} \times \mathbf{h} \rangle$ in (5.2), the terms like $\langle \mathrm{curl}\,\mathbf{h} \times \mathbf{B} \rangle$ vanish, since $\langle \mathbf{h} \rangle = 0$). The nonlinearity acts as if at once to deprive the mean field magnetohydrodynamics of its main attractive feature, i.e. possibility to obtain a closed equation for the mean field of the type (5.1). The case of $|\mathbf{h}| \ll |\mathbf{B}|$ is of little practical interest since at large magnetic Reynolds numbers fluctuation fields are strong.

The role of the fluctuating magnetic fields is especially evident in the following example. For the constant α and β, and $\mathbf{V} = 0$, Eq. (5.1) has, in an infinite domain, solutions of the force-free type, i.e. $\mathrm{curl}\,\mathbf{B} \times \mathbf{B} = 0$, and, in particular, a trivial solution $\mathbf{B} = 0$. However, this does not imply the absence of the back action of the field on the flow, since $\langle \mathrm{curl}\,\mathbf{h} \times \mathbf{h} \rangle \neq 0$.

Nevertheless, the nonlinear statement of the problem also enables us to derive closed systems of equations that interrelated the mean quantities $\mathbf{B}$, α, β, etc. This is achieved when the field $\mathbf{b}$ is expressed in terms of the mean field in a functional or operator manner.

Let us consider schematically how such a system can be derived referring to the case of back action of the field on the mean helicity [5.24-5.26].

5.2.1. Dynamics of the Mean Helicity

The magnetic field effect on helicity was taken into account even in early applications of the dynamo theory, e.g. to the solar cycle where this effect produces the stable oscillations of the mean magnetic field [5.10, 5.12]. This was accomplished phenomenologically by multiplying the hydromagnetic mean helicity α by a decreasing, generally quadratic function of $\mathbf{B}$, say

$$\alpha_N = \alpha\,(1 - \xi\mathbf{B}^2), \tag{5.3}$$

where ξ is a dimensional parameter inversely proportional to the kinetic energy density of a fluid. This yielded a stationary oscillatory solution with a finite magnetic field amplitude for all dynamo numbers exceeding the critical value and with $0 < \alpha_N/\alpha < 1$.

Expressions similar to (5.3) implicitly assume that the helicity instantaneously follows variations of the magnetic field. Indeed, the helicity $\mathbf{v}$ curl $\mathbf{v}$ implies the presence of a screw motion and the mean helicity characterizes the degree of predominance of right-hand screws over left-hand ones (or vice versa). The twisting time of a turbulent cell does not exceed the correlation time τ (i.e. the lifetime of an energy-range turbulent cell), therefore the relaxation time for the mean helicity $\langle \mathbf{v}\,\mathrm{curl}\,\mathbf{v}\rangle$ is small, of the order of τ.

However, the dynamo produces knotted magnetic lines, i.e. the magnetic helicity which, as general arguments like the Le Chatelier principle suggest, should weaken the action of the hydrodynamic helicity [5.24]. The relaxation time of the magnetic helicity is related to the magnetic diffusivity and it is therefore large for highly conducting fluids. At large magnetic Reynolds numbers the magnetic helicity fails to follow the mean magnetic field and its evolution is described by a differential equation.

Let us describe a rough scheme to derive the evolution equation for the magnetic helicity, with the mean velocity omitted for simplicity (details and references can be found in [5.26]).

Let us decompose the magnetic field and the relevant vector potential into mean and fluctuation components,

$$\mathbf{H} = \mathbf{B} + \mathbf{h}, \quad \mathbf{A} = \langle \mathbf{A} \rangle - \mathbf{a}.$$

Multiplying the induction equation

$$\frac{\partial \mathbf{H}}{\partial t} = -\mathrm{curl}\,(-\mathbf{v} \times \mathbf{H} + \nu_m\,\mathrm{curl}\,\mathbf{H}) \tag{5.4}$$

by a and the relevant vector potential equation

$$\frac{\partial \mathbf{A}}{\partial t} = \mathbf{v} \times \mathbf{H} - \nu_m\,\mathrm{curl}\,\mathrm{curl}\,\mathbf{H}$$

by **h**, adding them and averaging over a fluctuation distribution, we obtain

$$\frac{\partial}{\partial t}\langle \mathbf{ah}\rangle = -2\langle \mathbf{v} \times \mathbf{h}\rangle\,\mathbf{B} - 2\nu_m \langle \mathbf{h}\,\mathrm{curl}\,\mathbf{h}\rangle. \tag{5.5}$$

The quantity $\chi \equiv \langle \mathbf{ah}\rangle$ characterizes the knottedness of magnetic lines of fluctuation fields [5.5, 5.7].

Now this quantity remains to be expressed in terms of $\langle \mathbf{h}\,\mathrm{curl}\,\mathbf{h}\rangle$. Roughly speaking, these are related by a coefficient of the dimension of the length squared. To find an exact relation is a more subtle problem. The fact is that under freezing-in conditions the quantity χ is associated with a conservation law, known as the Woltjer invariant (see, e.g. [5.5]). Therefore, when allowing for dissipation, this helicity is transferred along the spectrum from the basic scale, k_0^{-1}, with a maximum χ, to smaller scales. The lower limit of the inertial range for the helicity, as opposed to energy transfer, is determined not by the dissipation scale k_d^{-1} but rather by the part of the magnetic field that is of helical nature (the realizability condition [5.5]):

$$|\chi(k)| \leqslant 2k^{-1}M(k),$$

where $M(k)$ is the spectral density of magnetic energy. The equality is valid when all magnetic lines are linked, i.e. the magnetic helicity is at its maximum. If, as it is generally the case [5.5], the spectra $\chi(k)$ and $M(k)$ are similar, e.g. proportional to k^{-q}, the realizability condition results in the appearance of a specific scale k_1^{-1} that cuts off the inertial interval from below. The calculation of k_1 requires the knowledge of helicity and energy spectra. Estimates [5.25, 5.26] show that, at large magnetic Reynolds numbers, k_1 is close to k_0, while at small ones, $k_1 \sim k_\alpha$. The appearance of the cut-off scale looks fairly uncommon (what happens at $k > k_1$?!). This calls for a serious investigation with the use of the modern methods of the turbulence theory.

Expressing χ in terms of $\langle \mathbf{h} \operatorname{curl} \mathbf{h} \rangle$ we obtain the required equation [5.24-5.26]:

$$\frac{\partial \alpha_{\mathrm{m}}}{\partial t} = \frac{Q}{4\pi\rho} \left(\mathbf{B} \operatorname{curl} \mathbf{B} - \frac{\alpha + \alpha_{\mathrm{m}}}{\beta} B^2 \right) - \frac{\alpha_{\mathrm{m}}}{T}, \tag{5.6}$$

where

$$\alpha_{\mathrm{m}} = \frac{\tau}{3} \frac{\langle \mathbf{h} \operatorname{curl} \mathbf{h} \rangle}{4\pi\rho}.$$

The coefficients Q and T depend on k_1. In the limit $k_1 \to k_0$, we have $Q \simeq 4$ and $T \simeq \tau \mathrm{R_m}$ is large. As $k_1 \to k_\alpha$, we have $Q \sim \mathrm{R_m^{\frac{2}{3} \frac{2-q}{3-q}}} \sim \mathrm{R_m^{1/2}} \left(q = \frac{5}{3} \right)$ and $T \sim \tau$ is small. Thus, the characteristic relaxation time of the quantity α_{m} is strongly dependent on the position of the realizability boundary. However, the very form of Eq. (5.6) seems to be only weakly dependent on this position.

Equation (5.6) shows that α_{m} closely follows the mean magnetic field only at a small $T \sim \tau$, when one can put $\partial/\partial t = 0$ and derive an expression like (5.3).

5.2.2. Generation of Large-Scale Flows

Along with influence on the mean turbulent characteristics α and β the growing magnetic field drives additional large-scale flows.* In [5.27] and [5.28] a large-scale flow was numeriallry explored that arises at fixed α and β, when the dimensionless nucmbe $\mathrm{R}_\alpha = |\alpha_{\max}| L/\beta$ exceeds the critical value for the dynamo action. The stationary level of magnetic energy is controlled by the balance between the magnetic force (due to the mean field only) and the

---

* It is assumed that the basic turbulence (at $\mathbf{H} = 0$) is due to an initial large-scale motion. In this case we evaluate a velocity perturbation. In principle, the situation can be different, e.g. if the turbulence is due to a convection caused by thermal or compositional differences.

Coriolis force: $B^2/4\pi \sim \rho\Omega\beta$. The magnetic energy approaches this level in an oscillatory manner so that in the limit of large R_α's the oscillations are not damped and their frequency is of the order of $(\Omega\beta/L^2)^{1/2}$. Proctor [5.28] identified them with large-scale oscillations around the stationary rigid-body rotation.

The interest in the generation of mean velocities by magnetic fields has grown sharply after the discovery of torsional waves [5.29] and meridional flows associated with them [5.30] on the Sun. A travelling torsional wave is superimposed on the general differential rotation of the Sun. The wave period is 11 years, i.e. it is half the period of the variation of the mean magnetic field (the 22-year cycle). The amplitude of the wave velocity is as high as several meters per second. Note that the rotation velocity at the equator is some 2 km/s and towards the poles Ω decreases by about 20%. Observations reveal four latitudinal zones of slower and faster rotation in each hemisphere. A new zone appears near a pole and reaches the equator in about 22 years. There is a distinct correlation of the torsional wave with the magnetic activity: in the sunspot region, a phase shift between the torsional wave crest and the dynamo wave crest is about 1/8 of the wavelength.

The fact that the period of the torsional wave is proportional to the period of the solar cycle and that it correlates with solar activity suggests that this phenomenon is due to the action of dynamo waves, that are generated in the convection zone, on the differential rotation of the solar surface [5.31-5.34].*

Let us describe this effect following the paper [5.33]. The angular velocity is given in the form

$$\Omega = \Omega_0 (r, \theta) + \Omega' (r, \theta, t),$$

where Ω_0 is the angular velocity in the absence of the field.

The acceleration caused by the magnetic force, $(4\pi\rho)^{-1}$ curl $\mathbf{H} \times \mathbf{H}$, increases towards the surface due to a substantial decrease in density. The differential rotation, as has been noted above, is more pronounced near the bottom of the convective zone due to a large radial gradient. Therefore the convection effects near the surface mainly manifest themselves in the form of turbulent viscous stresses. Over the time span comparable with the magnetic activity period, a quasi-stationary state is established in which the perturbation due to the magnetic force is balanced out by the turbulent viscous force. As a result of the integration of the azimuthal component of the Navier-Stokes equation (5.2), we obtain near the surface [5.33]

$$\Omega' \simeq -\frac{1}{4\pi\rho\nu_T} B_r B_\varphi, \qquad (5.7)$$

where ρ is the density and ν_T is the turbulent viscosity.

---

* In the basic theory of the solar cycle it is assumed that the inner core rotates nearly twice as fast as the surface.

If we assume that Ω' is small as compared with Ω_0, we can use the solutions of the dynamo equations with $\Omega = \Omega_0$ for the magnetic field

$$\begin{aligned} B_\varphi &= b_\varphi(r, \theta)\cos(\omega_c t - k\theta), \\ B_r &= b_r(r, \theta)\cos(\omega_c t - k\theta - \psi), \end{aligned} \tag{5.8}$$

where $\omega_c = 2\pi/(22 \text{ years})$ is the solar cycle frequency, ψ is the phase shift between the components of a dynamo wave propagating from the pole to the equator. Substituting (5.8) into (5.7) we obtain two kinds of terms. One of them is time-independent and affects the distribution $\Omega_0(r, \theta)$. The second is proportional to $-\cos(2\omega_c t - 2k\theta - \psi)$, i.e. it has the form of a wave that propagates in the same direction and with the same phase velocity as the dynamo wave, yet with a period twice as small (11 years). In the simplest model of the solar dynamo, $\psi \simeq 3\pi/4$, therefore the phase of the torsional wave is larger by $\pi/4$ than that of the magnetic one.

Note that the magnetic force, along with rotational perturbations, also drives meridional flows. Both these effects are considered in a numerical model constructed in [5.34].

5.2.3. Chaotic Evolution of Mean Fields

If the back action of the magnetic field on mean characteristics (helicity, differential rotation) is taken into account, a self-consistent system of equations emerges that can have not only stationary or oscillatory solutions but can also describe chaotic behaviour.

A widely cited and discussed example is the two-disk dynamo of Rikitake [5.35], which is described by the following system of equations:

$$\dot I_1 = -I_1 + \Omega_1 I_2, \quad \dot I_2 = -I_2 + \Omega_2 I_1, \quad \dot\Omega_1 = \dot\Omega_2 = 1 - I_1 I_2. \tag{5.9}$$

Here Ω_1 and Ω_2 are the angular velocities of the disks, and I_1 (I_2) is the current in the wire that connects the rim and the axis of the first (second) disk and winds round the second (first) disk. The example is of interest in connection with the problem of the irregular reversals of the Earth's dipole magnetic field (it is considered in detail in [5.36]).

It is less known that a system with a chaotic behaviour and, more than that, having a real strange attractor (in contrast to (5.9)) can be also obtained on the basis of one homopolar disk. As has been shown by Malkus and studied in detail by Robbins [5.37], the system

$$\dot J = \sigma(I - J), \quad \dot I = -I + \Omega J, \quad \dot\Omega = K - IJ - \nu\Omega \tag{5.10}$$

describes the behaviour of currents in the disk and coil and the angular velocity in the homopolar dynamo supplemented by a shunt (Fig. 5.1). Here I is the current in the disk, J is the current in the coil wound round the disk, Ω is the angular velocity, K is the constant torque which drives the disk, ν is the friction coefficient, and σ is controlled by the ratio of the shunt and coil resistances as well

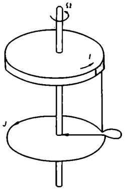

Fig. 5.1

as by that of the coil and brush inductances (with the shunt inductance neglected). A simple substitution reduces this system to the well-known Lorentz system.

Another example of a nonlinear dynamo of the mean field that is reducible to the Lorentz system was independently constructed by the authors [5.38] in attempt to explain irregular long-term declines of the solar activity like the Maunder minimum. In the axial symmetry approximation the following system of dynamo equations has been considered:

$$\begin{aligned} \frac{\partial A}{\partial t} &= (\alpha + \alpha_{\mathrm{m}}) B + \beta \Delta A, \\ \frac{\partial B}{\partial t} &= \hat{\Omega} A + \beta \Delta B, \\ \frac{\partial \alpha_{\mathrm{m}}}{\partial t} &= -\frac{\alpha_{\mathrm{m}}}{T} + F(\alpha, \beta, \alpha_{\mathrm{m}}, B, A), \end{aligned} \tag{5.11}$$

where $A_\varphi \equiv A$ is the azimuthal component of the vector potential that describes the B_r and B_θ components, $B_\varphi \equiv B$ is the azimuthal magnetic field, α_{m} is the magnetic helicity, $\hat{\Omega}$ is the operator that describes the action of the differential rotation on the poloidal field, the function F can be taken e.g. from Eq. (5.6). The equation in terms of partial derivatives (5.11) is reduced to the Lorentz system by means of rough substitution of Ω for the operator $\hat{\Omega}$ and $-L^2A$, $-L^2B$ for the Laplacians ΔA, ΔB, this procedure is equivalent to the consideration of one spatial mode for A and B. As a result, we obtain the system in terms of dimensionless variables

$$\dot{A} = -A + DB - CB, \quad \dot{B} = -\sigma B + \sigma A,$$
$$\dot{C} = -\frac{C}{T} + AB, \tag{5.12}$$

where C corresponds to α_m, and D is the dynamo number, a main parameter that controls bifurcations in this system, $D = \alpha\Omega R^3/\beta^2$.

In contrast to the usual situation, in which the Lorentz system is studied ($T^{-1} = 8/3$, $o = 10$, $D \gtrsim 24$), here of interest is the parameter range where $\sigma \to 1$, $T^{-1} \ll 1$ and the critical dynamo number for the existence of nondecaying solutions, $D_{cr} = 4/(\sigma - 1)$, is very large.

Of main importance in explaining the global activity minima is a singular point that represents the trivial solution $(A, B, C) = (0, 0, 0)$, i.e. the nonmagnetic Sun. For large T the time of residence in a neighbourhood of this point, $\tau_M \sim T\,(D - D_{cr})^{-1/2}$, is fairly large. As is generally known, the probability of entering the neighbourhood of the zero point is very small. Thus the behaviour is qualitatively consistent with observations.

The weakest point in simplifying Eqs. (5.11) is where the first-order differential operator $\hat{\Omega}$ is changed for Ω. This allows us to obtain three real Eqs. (5.12), but as can be easily verified, the resulting linearized system does not have oscillatory solutions that correspond to dynamo waves when the spatial dependence is taken into account. A more realistic approach, that preserves the dynamo waves, results in a system of three complex equations.

Such an approach has been developed in [5.39], where the third equation describes the back action of magnetic field on differential rotation rather than on helicity. As a result, a complex analogue of the Lorentz system was derived

$$\dot{A} = -A + DB, \quad \dot{B} = -B + iA - \frac{i}{2}\omega A^*, \quad \dot{\omega} = -\nu\omega - iAB, \tag{5.13}$$

where $A\ (t)$ and $B\ (t)$ as well as the disturbances of the angular velocity $\omega\ (t)$ are complex while ν and D are real positive parameters.

For $\nu < 1$, with an increasing dynamo number a sequence of bifurcations occurs that finally leads to a chaotic behaviour with episodic declines in magnetic activity.

As long as $D < 2$, the trivial solution $(0, 0, 0)$ is stable. The first bifurcation occurs at $D_1 = 2$, when an oscillatory solution emerges that corresponds to the dynamo wave. This periodic solution exists for all $D \geqslant 2$:

$$B = |B|\, e^{ipt}, \quad A = |A|\, e^{(ipt+\varphi)}, \quad \omega = |\omega|\, e^{2ipt},$$

where, for large dynamo numbers, we have $p \sim 4D/(2+\nu)$, $|A| \sim 8D/(2+\nu)$, $|B| \sim |\omega| \sim 16D/(2+\nu)^2$. This periodic solution corresponds to a limit cycle in the six-dimensional phase space A, B, ω, while in the plane (Re A, Re B) this cycle has an elliptic form. Let us describe in brief the bifurcations for a concrete value $\nu = 0.5$ used in the cited paper.

The limit cycle becomes unstable at $D_2 \simeq 4.14$, and there appears a double-periodic solution or a two-dimensional torus in the phase

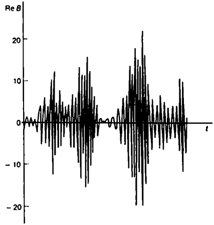

Fig. 5.2

space. This solution, in turn, becomes unstable at $D_3 \simeq 6.94$ and transforms into a three-dimensional torus. After $D_4 \simeq 7.612$ there occurs the Feigenbaum cascade of period-doublings that converges to $D_5 \simeq 7.68$. At larger dynamo numbers the solution is chaotic, with noticeable periods of weakened magnetic activity. Figure 5.2 shows a part of the temporal dependence of the field at $D = 32$ taken from [5.39].

From the viewpoint of applications it is important to stress that, first, the parameter ν in (5.13) is determined by the inverse time of turbulent viscous dissipation and thus it is far from being small in the solar convective zone, in contrast to the parameter T^{-1} in the system (5.12). Second, the magnetic field effect on the mean helicity is undoubtedly stronger than that on differential rotation. Hence it is desirable to study a complex system analogous to (5.13) yet with the third equation for α_m.

5.3. MHD TURBULENCE

It is well known that the behaviour of a passive magnetic field in a turbulent flow is governed by two concurrent processes, viz. the field intensification due to the stretching of magnetic lines by the deformation of a fluid element and by its dissipation which is enhanced by a decrease in the characteristic scale of the field. The proper account of the magnetic field effect on motion complicates the picture but enables one to find the stationary field amplitude. Note that in cosmic applications we deal, as a rule, with stationary regimes.

5.3.1. Two-Dimensional Turbulence

Now the situation seems to be clear for the case of the two-dimensional turbulence. The evolution of a passive magnetic field in a plane flow $v_z = 0$, $v_x\,(x,\ y)$, $v_y\,(x,\ y)$ was first considered in [5.3]. In the absence of external fields the initial field undergoes a temporal growth up to the value of the order of $\mathrm{R}_{\mathrm{m}}^{1/2} H_0$ and then it decays. This growth is a specific property of the field component lying in the $(x,\ y)$-plane while the z-component decays monotonically. Besides, a fluid acts as a diamagnetic, it expells the mean field from regions with intense motions to less intense or rest regions.

This situation is typical of an unbounded domain. Also of interest is the case of a bounded region with a field specified at infinity. In [5.38], as an example a zone of a turbulent fluid, $x_1 < x < x_2$, is considered where the fluid is at rest to the right and to the left of the zone. If the magnetic field is orthogonal to the zone, $H_x = H_0$, $H_y = 0$, a turbulent tangling in the zone causes the growth of the mean square of the field according to the law $\langle H_x^2 + H_y^2 \rangle = \mathrm{R}_{\mathrm{m}} H_0^2$. When the field is directed along the zone, $H_y = H_0$, $H_x = 0$, the mean field within the turbulent region proves to be weaker than the average value $B_y = \langle H_y \rangle = \mathrm{R}_{\mathrm{m}}^{-1} H_0$, i.e. the turbulence acts like a diamagnetic with $\mu = \mathrm{R}_{\mathrm{m}}^{-1}$. As can be seen, in the two-dimensional turbulence the effect of the field expulsion appears to be $\mathrm{R}_{\mathrm{m}}^{1/2}$ times stronger than the effect of tangling.

It is interesting that the specification of the field at infinity determines the field within the given region. This property is common for the kinematic problem with an external field and for the nonlinear problem in a bounded region, where a certain field value should be also established.

The generalization of the analysis [5.3] to the case when a plane flow also depends on the third coordinate, z, is considered in [5.6] which demonstrates how the situation changes when a plane flow is replaced by a motion along arbitrary two-dimensional surfaces.

The evolution of the magnetic field in a flat convective layer is numerically studied in the elegant paper by Weiss [5.40].

The two-dimensional hydrodynamic turbulence has specific features which distinguish it from the three-dimensional one (see, e.g. the review [5.41]). These features are due to an inviscid flow having an additional integral of motion, the enstrophy $\int \mathrm{curl}^2\, \mathbf{v}\, dx\, dy$. With viscosity taken into account, the enstrophy is transported from larger scales to smaller ones and dissipates. Yet energy is transported in the opposite direction (the inverse cascade). Recall that in the case of a three-dimensional turbulence, over a time span of the order of one revolution of the largest vortex, energy is transferred to smaller scales, where gradients grow in such a manner as to keep the energy dissipation rate finite even in the limit of vanishing viscosity.

The two-dimensional MHD turbulence is much more dynamically versatile than its hydrodynamic counterpart, albeit it does not resemble the three-dimensional turbulence [5.42, 5.23].

Equations that describe a plane flow of an incompressible conductive fluid, with a magnetic field present, have the following simple form:

$$\begin{aligned}
&\frac{\partial \omega}{\partial t} + (\mathbf{v}\nabla)\,\omega = H\nabla j + \nu\Delta\omega,\\
&\frac{\partial A}{\partial t} + (\mathbf{v}\nabla)\,A = \nu_m \Delta A,
\end{aligned} \tag{5.14}$$

where $\omega i_z = \mathrm{curl}\, \mathbf{v}$ is the vorticity, $j i_z = \frac{c}{4\pi}\, \mathrm{curl}\, \mathbf{H}$ is the current density and A is the vector potential having also only the z-component.

In the inviscid case, when $\nu = 0$, and $\nu_m = 0$, the system has three quadratic integrals of motion

$$\frac{1}{2}\int\left(\rho v^2 + \frac{H^2}{8\pi}\right) dx\, dy, \quad \int A^2\, dx\, dy, \quad \int \mathbf{v}\mathbf{H}\, dx\, dy. \tag{5.15}$$

The first is the total energy, the third is known as cross-helicity, while the second does not have a particular name and is typical only of a two-dimensional field. Note that, due to the presence of the magnetic field in the first of Eqs. (5.14), enstrophy is *not* conserved. It determines, together with Joule losses, the energy dissipation rate at ν, $\nu_m \neq 0$

$$\frac{d\mathscr{E}}{dt} = -\nu \int \omega^2\, dx\, dy - \nu_m \int j^2\, dx\, dy.$$

The problem (5.14) was explored by various techniques in [5.42, 5.23] under regular and random initial conditions.

When only kinetic energy is injected, then, according to [5.3], the magnetic energy temporally grows and then decays (for the magnetic field vanishing at infinity). Of interest is the fact that the decay time at small v_m's is very large. When the magnetic energy is also injected, the direct energy cascade and inverse cascade of $\int A^2\,dx\,dy$ occur.

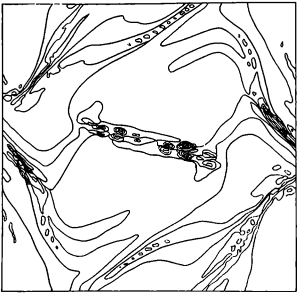

Fig. 5.3

As a result of these studies, essentially non-uniform spatial distribution of vorticity, current density, and magnetic field have been obtained for a rather smooth velocity distribution. Note that in a two-dimensional hydrodynamic turbulence such an intermittency in the vorticity distribution was absent. Figure 5.3 shows a fragment of a numerical simulation of the vorticity distribution [5.23] with the initial conditions $v_0 = (-\sin y, \sin x)$, $A_0 = \cos y + \frac{1}{2}\cos 2x$,

$\nu = \nu_m = 0.005$ taken after several revolution periods of the initial vortex.

Of interest is the question concerning the singularities of the two-dimensional turbulence in the limit $\nu \to 0$, $\nu_m \to 0$ [5.42, 5.23]. In nonmagnetic turbulence enstrophy is conserved for $\nu = 0$ in a two-dimensional flow and explodes in a three-dimensional one over finite time. In this respect the two-dimensional MHD turbulence resembles the three-dimensional one: as ν, $\nu_m \to 0$, enstrophy also explodes in a finite time [5.42].

5.3.2. Three-Dimensional Case

At first glance the case of three-dimensional MHD turbulence seems hopeless. A sceptic would advise first to settle the issue of the three-dimensional hydrodynamic turbulence. Nevertheless, studies are conducted and there is a number of interesting results concerning the three-dimensional MHD situation.

First of all, recall a known result by Kraichnan [5.43] (see also the earlier paper [5.44]) who assumed that turbulence has the form of random MHD waves that propagate in various directions with Alfvén velocities determined by the value of the magnetic field of the greatest scale. In other words, this implies the equality of kinematic and magnetic spectral densities within the inertial range, $E(k) = M(k)$, where $\int E\,dk = \langle v^2\rangle/2$ and $\int M\,dk = \langle h^2\rangle/8\pi$. Time-scale at which the energy cascades along the spectrum is determined by nonlinear wave interaction. For a weak MHD turbulence, when three-wave interactions prevail, we have, according to Sagdeev and Galeev [5.45]:

$$\tau(k) = \frac{1}{kV_A}\,\frac{U}{kM(k)},$$

where U is the homogeneous function of dimension cm^3 s^{-2}. Putting $U = V_A^2$ and presuming the conservation of the energy flux in the inertial range,

$$\frac{\int M\,dk}{\tau(k)} \sim \frac{k^3M^2(k)}{V_A} = \text{const},$$

we obtain the spectrum

$$E(k) \approx M(k) \sim k^{-3/2}. \tag{5.16}$$

This spectrum is discussed in astrophysical applications [5.46, 5.47]. The lower wavelength boundary of the spectrum can be found by equating $\tau(k)$ to the time of ohmic (or any other kind of) dissipation, $\tau_d = (\nu_m k^2)^{-1}$,

$$k_d \simeq k_0 R_m^{2/3}\left(\frac{v}{V_A}\right)^{1/3},$$

where k_0^{-1} is the dominant turbulent scale and v is the velocity within this scale.

One of essential assumptions in these arguments is the random phase approximation. As has been shown in the preceding section, the magnetic field introduces intermittency, structures arise, i.e. disturbances appear in phase with each other, which is absolutely inconsistent with the assumption of chaotic phases of different modes.

But may be the phase locking of modes is typical only of the two-dimensional case? Negative answer to this question follows from the studies of kinematic dynamo in random flows. These studies show a structural and intermittent distribution of the magnetic field.

The paper by Zel'dovich *et al.* [5.18] analyzes the behaviour of the magnetic field in a given linear (Hubble) flow, $\mathbf{v} = \mathcal{C}(t)\,\mathbf{r}$, where $\mathcal{C}$ is the deterministic or random matrix with vanishing trace. The presence of an arbitrary finite magnetic diffusivity $\nu_m \neq 0$ results in an exponential decay of the field at a rate independent of ν_m. However, the magnetic energy grows exponentially with time owing to an increase in a volume occupied by an initially localized field. The magnetic field spectrum is highly anisotropic and the random phase approximation is out of question here. The spatial distribution of the field has the form of thin (at small ν_m's) ropes or layers depending on the number of positive eigenvalues of the matrix $\mathcal{C}$, one or two, respectively. It is clear, e.g., that for one positive eigenvalue an expansion occurs along the relevant direction and a contraction, along the other two directions thus forming a rope.

The problem of kinematic dynamo has been solved for a random three-dimensional smooth flow of a general type which is renovated in an arbitrary finite time [5.22, 5.9]. The magnetic field grows exponentially in time at a rate independent of the magnetic field diffusivity in the limit $\nu_m \to 0$ (the fast dynamo). The distribution of the generated field is essentially inhomogeneous and anisotropic, there are sparse high peaks against a general growing background. The existence of such a non-Gaussian distribution is proved by the fact that the exponential growth rate of the successive statistical moments $\langle HH\rangle$, $\langle HHHH\rangle^{1/2}$, . . . increases with the order of the moment. Although the number of the peaks of a given height is exponentially small and it decreases exponentially with time, it is these peaks that would feature the most prominent effect of the nonlinear field on the motion. One can hope that the nonlinearity consecutively freezes-in the peaks starting from stronger ones so that the MHD distribution would be intermittent despite the fact that in the kinematic picture the intermittency is an intermediate asymptotic [5.49].

Finally note a direct numerical simulation of a consistent set of the induction and Navier-Stokes equations for an incompressible flow with a random δ-correlated force [5.48]. Although a spatial resolution corresponding to Reynolds numbers as low as 100 has been obtained (even using the CRAY computer), the results of this study are of significant interest for the theory of MHD turbulence.

First, the calculations support the possibility of dynamo in helical and nonhelical random flows. Second, the magnetic energy generated in the mirror-symmetric case amounts to about 10% of the kinetic energy while the peak field amplitude is comparable with the peak velocity amplitude. Thus the numerical simulations also demonstrate intermittency.

References

5.1. J. Larmor, *Reports Brit. Assoc. Adv. Sci.*, 159 (1919).
5.2. T. G. Cowling, *Mon. Not. RAS*, 94, 39 (1934).
5.3. Ya. B. Zel'dovich, *Zh. Eksp. Teor. Fiziki*, 31, 154 (1956).
5.4. H. Alfvén, *Tellus*, 2, 74 (1950).
5.5. H. K. Moffatt, *Magnetic Field Generation in Electrically Conducting Fluids*, Cambridge University Press, Cambridge, 1978.
5.6. Ya. B. Zel'dovich and A. A. Ruzmaikin, *Zh. Eksp. Teor. Fiziki*, 78, 980 (1980).
5.7. Ya. B. Zel'dovich, A. A. Ruzmaikin, and D. D. Sokoloff, *Magnetic Fields in Astrophysics*, Gordon and Breach, 1983.
5.8. S. I. Vainstein and Ya. B. Zel'dovich, *Uspekhi Fiz. Nauk*, 106, 431 (1972).
5.9. S. A. Molchanov, A. A. Ruzmaikin, and D. D. Sokolov, *Uspekhi Fiz. Nauk*, 145, 593 (1985).
5.10. F. Krause and K.-H. Rädler, *Mean Field Electrodynamics and Dynamo Theory*, Pergamon Press, Oxford, 1980.
5.11. M. Stix, in: *Basic Mechanisms of Solar Activity, IAU Symp.*, 1976, p. 71.
5.12. T. S. Ivanova and A. A. Ruzmaikin, *Astron. Zhurn.*, 54, 846 (1977).
5.13. E. N. Parker, *Cosmical Magnetic Fields*, Oxford University Press, Oxford, 1979.
5.14. G. K. Batchelor, *Proc. Roy. Soc. London*, A201, 405 (1950).
5.15. S. I. Vainstein, *Zh. Eksp. Teor. Fiziki*, 79, 2175 (1980).
5.16. A. P. Kazantsev, *Zh. Eksp. Teor. Fiziki*, 53, 1806 (1967).
5.17. V. G. Novikov, A. A. Ruzmaikin, and D. D. Sokolov, *Zh. Eksp. Teor. Fiziki*, 85, 909 (1983).
5.18. Ya. B. Zeldovich, A. A. Ruzmaikin, S. A. Molchanov, and D. D. Sokoloff, *J. Fluid Mech.*, 144, 1 (1984).
5.19. V. I. Arnol'd and E. I. Korkina, *Vestnik MGU, Ser. Mat. i Mech.*, 3, 43 (1983).
5.20. D. Galloway and U. Frisch, *Geophys. Astrophys. Fluid Dyn.*, 29, 13 (1984).
5.21. V. I. Arnol'd, Ya. B. Zel'dovich, A. A. Ruzmaikin, and D. D. Sokolov, *Zh. Eksp. Teor. Fiziki*, 81, 2052 (1981).
5.22. S. A. Molchanov, A. A. Ruzmaikin, and D. D. Sokoloff, *Geophys. Astrophys. Fluid Dyn.*, 30, 242 (1984).
5.23. S. A. Orszag and Cha-mei Tang, *J. Fluid Mech.*, 90, 129 (1979).
5.24. S. I. Vainstein, Ya. B. Zel'dovich, and A. A. Ruzmaikin, *Turbulent Dynamo in Astrophysics*, Nauka, Moscow, 1980 (in Russian).
5.25. S. I. Vainstein, *Magnit. Gidrodin.*, 2, 3 (1980).
5.26. N. I. Kleeorin and A. A. Ruzmaikin, *Magnit. Gidrodin.*, 2, 17 (1982).
5.27. W. V. R. Malkus and M. R. E. Proctor, *J. Fluid Mech.*, 67, 417 (1975).
5.28. M. R. E. Proctor, *J. Fluid Mech.*, 80, 769 (1977).
5.29. R. F. Howard and B. J. LaBonte, *Astrophys. J.*, 239, L33 (1980).
5.30. J. Tuominen, I. Tuominen, and J. Kyröläinen, *Mon. Not. RAS*, 205, 691 (1983).
5.31. H. Yoshimura, *Astrophys. J.*, 247, 1102 (1981).
5.32. M. Schüssler, *Astron. and Astrophys.*, 94, L17 (1981).
5.33. N. I. Kleeorin and A. A. Ruzmaikin, *Pis'ma Astron. Zhurn.*, 10, 925 (1984).

5.34. J. Tuominen, H. Virtanen, F. Krause, and G. Rüdiger, in: *Proc. Fourth European Meet. Solar Phys.*, ESA, 1984, p. 225.
5.35. T. Rikitake, *Proc. Camb. Phil. Soc.*, 54, 89 (1958).
5.36. A. E. Cook and P. H. Roberts, *Proc. Camb. Phil. Soc.*, 68, 547 (1970).
5.37. K. A. Robbins, *Math. Proc. Camb. Phil. Soc.*, 82, 309 (1977).
5.38. Ya. B. Zeldovich and A. A. Ruzmaikin, *Astrophys. and Space Phys. Reviews*, Vol. 2, Gordon and Breach, 1983, p. 333.
5.39. C. A. Jones, N. O. Weiss, and F. Cattaneo, *Physica* D14, 161 (1985).
5.40. N. O. Weiss, *Proc. Roy. Soc. London*, A293, 310 (1966).
5.41. A. P. Mirabello and A. S. Monin, *Adv. Mech.*, 2, 47 (1979).
5.42. A. Pouquet, *J. Fluid Mech.*, 88, 1 (1978).
5.43. R. H. Kraichnan, *Phys. Fluids*, 8, 1385 (1965).
5.44. R. S. Iroshnikov, *Astron. Zhurn.*, 40, 742 (1963).
5.45. R. Z. Sagdeev and A. A. Galeev, *Nonlinear Plasma Theory*, Benjamin Press, New York-Amsterdam, 1969.
5.46. A. A. Ruzmaikin and A. M. Shukurov, *Astrophys. Space Sci.*, 82, 397 (1982).
5.47. J. H. Simonetti, J. M. Cordes, and S. R. Spangler, *Astrophys. J.*, 284, 126 (1984).
5.48. M. Meneguzzi, U. Frisch, and A. Pouquet, *Phys. Rev. Lett.*, 47, 1060 (1981).
5.49. Ya. B. Zel'dovich, S. A. Molchanov, A. A. Ruzmaikin, and D. D. Sokolov, *Zh. Eksp. Teor. Fiziki*, 89, 2061 (1985).

6

~~Problems of the Theory of Strong Turbulence and Topological Solitons~~

R.Z. Sagdeev, Mem. USSR Acad. Sc.,
S.S. Moiseev, D. Sc. (Phys.-Math.),
A.V. Tur, Cand. Sc. (Phys.-Math.), and
V.V. Yanovskii, Cand. Sc. (Phys.-Math.)

6.1. INTRODUCTION

The present review considers some problems of the theory of strong turbulence and nonlinear phenomena in nondispersive media. The subsequent exposition does not pretend to be complete, it only reflects certain interests of the authors.

It is well known that the modern theory of strong turbulence is far from being complete. Even though the main result of the theory of developed hydrodynamic turbulence, i.e. Kolmogorov's spectrum, was obtained more than forty years ago [6.1] and was corroborated experimentally (see, e.g. [6.2]), its "microscopic" theory has not been constructed as yet. This is due to an extremely strong nonlinearity in the Navier-Stokes equations at very large Reynolds numbers Re ($\mathrm{Re} \gg 1$). Since Re is an effective coupling constant, at $\mathrm{Re} \gg 1$ no methods will be instrumental in truncating the hierarchy of moment equations for the velocity field. This calls for use of either the functional formulation of the turbulence theory [6.3] or some version of diagram techniques [6.4, 6.5]. Besides, some essential results have been obtained by the renormalization group method [6.6-6.8] which has been successfully applied in the field theory [6.9] and in the theory of phase transitions [6.10]. The use of the functional turbulence formulation has not made considerable advances due to inadequate progress in continuum integration techniques. However, in some cases, e.g. for the turbulence of compressible fluid at considerable Mach numbers, the use of the functional formulation, together with the scale transformation group, gives effective information on turbulence and, in particular, on the energy spectrum [6.11-6.14].

The functional turbulence formulation and results obtained with the help of the scale transformation group are considered in Sec. 6.2. At present, the most promising seems to be the Wyld diagram technique [6.4] or its versions. This technique describes turbulence by two diagram series, one for Green's function and the other for the spectral density. In the case of strong turbulence these diagram series cannot be truncated, as opposed to the case of weak turbulence, where such a truncation results in a kinetic wave equation [6.5]. Nevertheless, it is the theory of weak turbulence which yields exactly solvable examples supporting Kolmogorov's ideology [6.15].

It appears that kinetic wave equations have exact solutions in an inertial range. These solutions correspond e.g. to a constant energy flux along the spectrum [6.16-6.17]. It has become clear [6.16] that Kolmogorov's solutions are feasible only when integrals converge in the regions of the turbulence source and sink. This fact (turbulence locality) implies that perturbations within the inertial range are not affected by processes at its boundaries and hence, according to Kolmogorov's ideology, the spectrum in this k-space region is self-similar.

Now let us return to the case of strong hydrodynamic turbulence. A search for the solutions of general diagram series in the self-similar Kolmogorov form is hampered by infrared and ultraviolet divergencies. Moreover, one can easily see that in the absence of these divergencies Kolmogorov's spectrum would become an exact solution of diagram equations. Attempts to modify this spectrum near the source and sink have failed. Indeed, if the divergencies on Kolmogorov's spectrum have not been eliminated, then integrals describing the interaction of vortices from the inertial range with all remaining ones would be dominated by the source and sink regions. This disrupts the local nature of the interaction and the self-similarity of the spectrum over the inertial range. Obviously, the last fact contradicts experimental data. All this clearly shows that the general nature of Kolmogorov's spectrum is naturally related to the convergence of the diagram series. The studies of diagram divergencies have a long history. Even the early papers [6.18-6.20] indicated that infrared divergencies emerge due to the convection of smaller vortices by the large-scale inhomogeneities of the velocity field. Since then emphasis has been placed on the exclusion of this convection and the elimination of infrared divergencies in general. Ultraviolet divergencies are presumed to be less important. Recently this point of view has been supported by the renormalization group studies [6.6-6.8].

In this review we shall also restrict ourselves to the consideration of infrared divergencies. To exclude the large-scale convection, it was proposed in [6.21] to use an interaction representation while in [6.22] it was demonstrated how the convection could be excluded within Kraichnan's direct interaction approximation.

The main step in the convection exclusion has been made in [6.23], where the most divergent diagram sequence has been summed. Nevertheless, this has not resulted in the total elimination of infrared divergencies. In the present review we analyze the nature of this effect following [6.24, 6.25]. We shall show that the theory of turbulence should include generalized solutions of the type of Van Kampen-Case modes [6.26, 6.27]. These solutions, called by us "null-modes", are concentrated at $k = 0$ and describe free moving groups of Lagrangian particles. The inclusion of the "null-modes" enables us to cancel out dangerous contributions in diagrams at $k = 0$ made by interaction between harmonics with adjacent wave vectors. This provides the cancellation of infrared divergencies in diagram equations.

Section 6.3 is devoted to the development of diagram techniques, introduction of "null-modes", and cancellation of infrared divergencies. It demonstrates that the "null-modes" can be introduced by an appropriate modification of diagrams. It should be noted that strong turbulence properties are fairly diversified, this being quite natural for strongly interacting systems. For example, in a system of hydrodynamic type, the emergence of additional relations like integrals, Lagrangian or topological invariants leads to a substantial change in statistical characteristics. To illustrate, one can refer to two-dimensional turbulence [6.28], helical turbulence [6.29, 6.30], etc. As a result, this calls for more profound studies of the links between Lagrangian invariants, frozen-in fields, and topological properties of motions of nondispersive media. In this context, in Sec. 6.4 some general invariant properties are analyzed that are typical of many hydrodynamic models. It is shown how, based on Lagrangian invariants, one can construct the "frozen-in" fields and, vice versa, how, based on the "frozen-in" quantities, one can obtain Lagrangian invariants [6.31]. The application of this method results in a number of new invariants and integrals of "frozenness", e.g. in the two-fluid plasma hydrodynamics [6.31] which may be useful in various problems of the plasma theory. Given the Lagrangian invariants, one can derive a number of conservation laws for homogeneous turbulence that describe the non-evolutionary behaviour of a large-scale turbulent component. These results are exposed in Sec. 6.4.1. On the other hand, the invariant properties of "frozen-in" vector fields, i.e. those transported by fluid particles, can be explored by the topological approach. Appropriate mathematical apparatus is geometrically illustrative and especially convenient for the analysis of the continuous deformations of vector fields, motions of a continuous medium in particular.

Of utmost interest are here the topologically nontrivial configurations of vector fields described by nonvanishing topological invariants. Here we quite naturally encounter localized nonlinear formations, known as topological solitons. Such a term is due to the field theory. It stems from the fact that the field configuration in such a soliton is topologically non-equivalent to the ground state.

It is well known that the conventional soliton exists due, in a sense, to a balance between nonlinearity and dispersion [6.32]. In hydrodynamic systems, dispersion is absent while nonlinearity is strong, therefore the conventional mechanism of soliton formation is absent. In the topological soliton the action of nonlinearity is limited by topological exclusion principles, e.g. by the linkage of stream lines. Such solutions can play the role of stable quasi-particles in nondispersive media. Besides, such solutions can be produced by a turbulence with topologically nontrivial properties. As examples we can cite large-scale magnetic field generation by helical turbulence [6.33] or a model equation [6.34] describing large-scale atmospheric vortices. Using topological approach, one can produce a fairly general classification of topological solitons [6.35] that is exposed in Sec. 6.4.3. Next, we construct a number of exact solutions describing topological solitons in two-fluid plasma hydrodynamics and in magnetohydrodynamics (MHD). It is interesting that there exists a topological soliton realizable within a wide class of hydrodynamic models. It is not improbable that the concept of the topological soliton is essentially the multidimensional generalization of the concept of the conventional soliton.

6.2. THE SCALING GROUP AND FUNCTIONAL METHOD

6.2.1. The Scaling Theorem, Locality Hypothesis and Kolmogorov's Spectrum

The most specific feature of strong turbulence is that the hierarchy of correlation equations is not closed that results from the large value of the coupling constant [6.2] (in hydrodynamics, the Reynolds number $\mathrm{Re} \gg 1$). As a consequence, we should treat the whole correlation chain as a single object. One of the feasible versions of the exact statistical treatment of a wave field is accomplished by introducing a characteristic functional φ [6.3].

For example, for a compressible fluid we have

$$\varphi[y, y_\rho] = \left\langle \exp i \int \{V_i(x, t)\, y_i(x) + \rho(x, t)\, y_\rho(x)\}\, dx^3 \right\rangle , \qquad (6.1)$$

where $\langle \ldots \rangle$ is the average over an ensemble, V is the velocity, ρ is the density, and $y_i(x)$, $y_\rho(x)$ are the functional arguments (arbitrary vector fields vanishing at infinity). Differentiating (6.1) with respect to time and using hydrodynamic equations one can easily derive a closed equation for φ [6.3, 6.11] (the MHD case is discussed in [6.36])

$$\frac{i\partial\varphi}{\partial t} = \hat{L}\varphi + \hat{I}\varphi, \qquad (6.2)$$

where $\hat{L}$ is the linear integro-differential operator containing the common and variational derivatives $(\delta/\delta y_i, \delta/\delta y_\rho)$, while the linear operator $\hat{I}$ is involved in (6.2) due to a turbulence source, and the random external force is assumed for simplicity Gaussian (the explicit forms of $\hat{L}$ and $\hat{I}$ see below). The advantage of such a functional method is a compact formulation that reduces the description of the random wave field evolution to the analysis of a single linear equation. Its disadvantage is also evident. It is the presence of the variational derivatives that renders it difficult to obtain an explicit solution. It is this disadvantage that stimulated the development of another approach [6.11] that is discussed in this section based on the transformational properties of the characteristic functional equation with respect to a scale transformation group. This approach analyzes average and spectral properties of strong turbulence. Taking into account the physically obvious fact that the energy spectrum falls off within the viscous domain, one succeeds in deriving, with a high accuracy, a relation between various global turbulent properties (such as total energy and the average rate of energy dissipation). As to the spectral features of turbulence, the hypothesis of the spectrum locality in the inertial subrange enables us to obtain its explicit analytical expression in a number of interesting situations.

In this section we deal with this second problem following [6.11] and [6.13]. First of all, consider a statistical description of the random velocity field $\mathbf{V}(x, t)$ of an incompressible fluid with the use of the characteristic functional (6.2). As is well known (see, e.g. [6.2] and references therein), the evaluation of the variational derivatives of φ with respect to y makes it possible to obtain all moments of the statistical field V. The characteristic functional satisfies the equation of the type (6.2) that acquires, for an incompressible fluid, the following form [6.2]:

$$\frac{\partial\varphi}{\partial t} = i \int \mathbf{y} \frac{\partial}{\partial x_i} \mathbf{D} D_i \varphi \, dx^3 + \nu \int \mathbf{y} \Delta \mathbf{D} \varphi \, dx^3 - \frac{i}{2} \int \varphi y_i(x_1) \, y_j(x_2) \, B_{ij} \, dx_1^3 \, dx_2^3, \tag{6.3}$$

where ν is the viscosity.

Recall that the averaging in (6.1) is performed over the distribution of an external force switched on at $t = 0$ and $D_i = \delta/\delta y_i(x) \, dx^3$ is the variational derivative. In deriving (6.3) the force has been assumed to be Gaussian, statistically stationary, delta-correlated in time, and spatially homogeneous with the correlation tensor

$$\langle f_i(x_1 t_1) \, f_j(x_2 t_2) \rangle = B_{ij}(x_1 - x_2) \, \delta(t_1 - t_2). \tag{6.4}$$

The steady-state condition for turbulence energy corresponding to the balance between a source and a sink,

$$\langle V_i f_i \rangle = \frac{\nu}{2} \left\langle \left(\frac{\partial V_i}{\partial x_h} + \frac{\partial V_h}{\partial x_i} \right)^2 \right\rangle \equiv \bar{\varepsilon}, \tag{6.5}$$

where $\bar{\varepsilon}$ is the average energy dissipation, results, as can be easily shown, in the restriction on the spatial part of (6.4)

$$\frac{1}{2} B_{ii}(0) = \bar{\varepsilon}.$$

The tensor B_{ij} that has, under the single assumption of a homogeneous random force, six independent components with the characteristic scales L_m (L_1, L_2, . . ., L_6) can then be written as

$$B_{ij} = 2\bar{\varepsilon} b_{ij},$$

where b_{ij} is the dimensionless tensor and $b_{ii}(0) = 1$.

Since the field f can be considered solenoidal, without loss of generality, the number of independent spatial scales in b_{ij} reduces to three. Further detalization of the tensor structure is not essential for our purpose.

Let us complement Eq. (6.3) with the initial condition corresponding to a fluid being at rest at $t = 0$. This condition determines the unique solution to Eq. (6.3)

$$\varphi\{[\mathbf{y}],\ t\}|_{t=0} = 1. \tag{6.6}$$

Equation (6.3) and the initial condition (6.6) are invariant with respect to the group

$$\begin{aligned} &\alpha x = x', \qquad \alpha^{1-\beta} t = t', \qquad \alpha^{-(\beta+3)} y(x) = y'(x'), \\ &\alpha^{1+\beta}\nu = \nu', \qquad \alpha^{3\beta-1}\bar{\varepsilon} = \bar{\varepsilon}', \qquad \alpha L_i = L_i' \quad (i = 1,\ 2,\ 3), \end{aligned} \tag{6.7}$$

where α and β are arbitrary parameters. This invariance implies the scaling relation

$$\varphi\{\mathbf{y}(x),\ \nu,\ \bar{\varepsilon},\ L,\ t\} = \varphi\{\mathbf{y}'(x'),\ \nu',\ \bar{\varepsilon}',\ L',\ t'\}. \tag{6.8}$$

Let us stress that, as opposed to the scaling hypothesis (see, e.g. [6.37]), (6.8) is an exact relation. The relations (6.7) and (6.8) enable us to find the spectral characteristics of turbulence within the inertial range. Consider the turbulence spectrum of an incompressible fluid

$$E_{ij}(k) = -\frac{1}{(2\pi)^3} \int e^{-ik\mathbf{k}_0\mathbf{r}} \{D_i D_j' \varphi\}|_{y=0}\, dr^3, \tag{6.9}$$

where $\mathbf{k}_0 = \mathbf{k}/|\mathbf{k}|$. By making use of (6.8) we can transform (6.9) into a functional dependent on primed variables. Assuming $\alpha \equiv k$, integrating (6.9) with respect to kr, and allowing for the infinity of integration limits, we obtain

$$E_{ij}(k,\ t) = k^{-(2\beta+3)} f(k^{1-\beta} t,\ k^{1+\beta}\nu,\ k^{3\beta-1}\bar{\varepsilon},\ kL)\, \Psi_{ij}(k_0).^{*} \tag{6.10}$$

In the stationary case $\frac{\partial}{\partial t} E_{ij} = 0$. The arbitrariness of β implies $\frac{\partial}{\partial \beta} E_{ij} = 0$, whence we arrive at the equation

$$\xi_1 \frac{\partial f}{\partial \xi_1} + 3\xi_2 \frac{\partial f}{\partial \xi_2} = 2f,$$

---

* Here L is the minimal value of the L_i's.

with

$$\xi_1 = k^{1+\beta}\nu; \quad \xi_2 = k^{3\beta-1}\bar{\varepsilon},$$

whose solution can be written as

$$f = \xi_2^{2/3} f_1 (\xi_1/\xi_2^{1/3}),$$

where f_1 is a dimensionless function. Thus, the spectral density proves to be as follows:

$$E_{ij}(k) = \bar{\varepsilon}^{2/3} k^{-11/3} f_1 (k\lambda,\ kL)\, \Psi_{ij}(k_0), \tag{6.11}$$

where $\lambda = \nu^{3/4}\bar{\varepsilon}^{-1/4}$ is the viscous scale.

On integrating with respect to angles in the k-space we obtain the expression for the spectral energy $E(k)$ with a given modulus of k

$$E(k) = \bar{\varepsilon}^{2/3} k^{-5/3} f(k\lambda,\ kL). \tag{6.12}$$

Let us emphasize that (6.12) has been derived without any hypotheses adopted. However, the further advance to obtain the explicit form of the spectrum requires some additional assumptions to be made. Suppose that the asymptotic expansion of $f(kL,\ k\lambda)$ exists at $k\lambda \ll 1$; $(kL)^{-1} \ll 1$, this being equivalent to the locality hypothesis, i.e. to the negligible effect of interval boundaries on the spectrum development within its inner (inertial) subrange. Then in the first approximation, we get

$$E(k) = \text{const} \times \bar{\varepsilon}^{2/3} k^{-5/3}, \tag{6.13}$$

i.e. the Kolmogorov-Obukhov law. Higher moments can be evaluated in an analogous manner.

Thus, the description of the turbulence of an incompressible fluid within the framework of the model of random forces by the characteristic functional leads to the results that are consistent with Kolmogorov's theory [6.1].

Now let us find the turbulence spectrum of a compressible fluid. Since we are interested here in spectral characteristics within the k-space interval, where dissipative coefficients can be neglected, we do not allow for the temporal variations in the spectrum and take the equation of state in the form $P = C_0^2\rho_0 (\rho/\rho_0)^\gamma$, where γ is the adiabatic exponent and P is the pressure. At the point with $\rho = \rho_0$ the sound velocity is γC_0^2. Equations of motion for velocity and density have well-known forms and will not be given here. The assumptions concerning the turbulence source will remain the same as for an incompressible fluid. The equation for the characteristic functional φ has the structure of (6.2) and its finer structure is of no importance here. Note, however, two principal points. The first concerns the initial condition for φ. As before, we assume that the medium is at rest prior to switching on the external force at $t = 0$. But now, as follows from (6.1), the initial value of the characteristic functional is $\varphi_0 = \langle \exp i \int \rho_0 y_\rho \, dx^3 \rangle$ (in the above case, $\varphi_0 = 1$) and the question arises on how relevant spectral characteristics depend on φ_0.

But such a dependence, generally speaking, would imply the dependence of the energy spectrum $E(k)$ on initial conditions. From the formal viewpoint, it becomes clear when in the Navier-Stokes equations and, accordingly, in (6.2) we change to the variables $\mathcal{P}_l = \rho V_l$, $\mathcal{E} = \rho V^2$ (momentum and energy, respectively). Then the initial condition for φ becomes simpler ($\varphi_0 = 1$) and independent of the group transformation of variables. This yields the above statement. Taking this into account and neglecting the dependence of $E(k)$ on φ_0 we, nevertheless, will use the former variables ρ, V_l to simplify calculations. The second point is more essential, since both the Navier-Stokes equations and the equation for φ explicitly contain the constant $A_0 = C_0^2 \rho_0^{1-\gamma}$ and it would seem that we have too many parameters, which precludes the existence of self-similar spectral domains. Yet in fact this is, generally speaking, not the case since increasing the number of parameters leads to the generalization of the invariant group of Eq. (6.2), i.e. this two-parametric group transforms into the three-parametric one in accordance with possible changes in the length, time and mass scales. The group of the scale transformations has now the following form:

$$\begin{aligned}
&\delta^{-1}\alpha^{-(2\beta+3)} y_\rho(x) = y'_\rho(x'), \quad \delta^{-1}\alpha^{-(\beta+3)} y_l(x) = y'_l(x'),\\
&\delta\alpha^{\beta+1}\eta = \eta', \quad \delta\alpha^{\beta+1}\xi = \xi', \quad \alpha L = L',\\
&\delta\alpha^{3\beta-1}\bar{\varepsilon} = \bar{\varepsilon}', \quad \alpha^{2\beta}\delta^{1-\gamma}C = C', \quad (C = \gamma\rho_0^{1-\gamma}C_0^2).
\end{aligned} \tag{6.14}$$

where η, ξ are the dynamic viscosity coefficients, L is the scale of the external force correlation scale, and α, β, δ are arbitrary finite positive constants.

The scaling theorem is formulated as an invariance property with respect to the transformation (6.4). Let us require that $\alpha^{2\beta}\delta^{1-\gamma} = 1$ (i.e. $C = 1$). This enables us to eliminate the sound velocity from the nonlinear terms in the Navier-Stokes equation while renormalizing appropriately the source and sink. This yields

$$\begin{aligned}
&\bar{\varepsilon}^* = C_0^{\frac{2}{\gamma-1}}\bar{\varepsilon}, \quad \tilde{\eta} = C_0^{\frac{2}{\gamma-1}}\eta, \quad \tilde{\xi} = C_0^{\frac{2}{\gamma-1}}\xi,\\
&\delta = \rho_0^{-1} C_0^{\frac{2}{\gamma-1}} \alpha^{\frac{2\beta}{\gamma-1}} \gamma^{\frac{1}{\gamma-1}}.
\end{aligned} \tag{6.15}$$

After the renormalization the scale transformation group takes the form

$$\alpha^{-(\beta+3)}\mathrm{y}(x)=\mathrm{y}'(x'),\ \alpha^{-\left(\frac{2\beta}{\gamma-1}+3\right)}y_\rho(x)=y'_\rho(x'),$$
$$\alpha x=x' \quad \alpha^{1-\beta}t=t', \quad \alpha L=L', \tag{6.16}$$
$$\alpha^{3\beta-1+\frac{2\beta}{\gamma-1}}\bar{\varepsilon}^{*\prime}=\bar{\varepsilon}^{*\prime}, \quad \alpha^{1+\beta+\frac{2\beta}{\gamma-1}}\eta=\eta'.$$

As in the case of an incompressible fluid, one can evaluate, by means of φ, any statistical field moment including the following one

$$\langle\rho(x_1t)V_l(x_1t)V_l(x_2t)\rangle=\frac{1}{i^3}\left.\frac{\delta^3\varphi}{\delta y_\rho(x_1)\,\delta y_l(x_1)\,\delta y_l(x_2)}\right|_{y=0}, \tag{6.17}$$

whence for the energy spectrum of vortices we have

$$E(k,t)=\frac{t}{(2\pi)^3}\int\int_{|\mathbf{k}|=k}e^{-ikk_0r}\left\{\left.\frac{\delta^3\varphi}{\delta y_\rho(x_1)\,\delta y_l(x_1)\,\delta y_l(x_2)}\right|_{y=0}\right\}dr\,dS(k), \tag{6.18}$$

where $r=|\mathbf{x}_2-\mathbf{x}_1|$, $\mathbf{k}_0=\frac{\mathbf{k}}{|\mathbf{k}|}$, $dS(k)$ is the area element of a sphere, $|\mathbf{k}|=k$. It is seen from (6.17) that

$$\left\langle\frac{\rho V^2}{2}\right\rangle=\frac{1}{2}\rho_0C_0^{-\frac{2}{\gamma-1}}\int_0^\infty E(k,t)\,dk$$

To evaluate $E(k,t)$, we use the scaling theorem in the form

$$\varphi\{[\mathrm{y}(x)],\ [y_\rho(x)],\ \tilde{\eta},\ \tilde{\xi},\ \bar{\varepsilon}^*,\ L,\ t\}$$
$$=\varphi\{[\mathrm{y}'(x')],\ [y'_\rho(x')],\ \tilde{\eta}',\ \tilde{\xi}',\ \bar{\varepsilon}^{*\prime},\ L',\ t'\}. \tag{6.19}$$

Using (6.16) and (6.19) we shall obtain, in perfect analogy to an incompressible fluid,

$$E(k,t)=k^{-\left(1+\frac{2\beta\gamma}{\gamma-1}\right)}f_1\left(k^{1-\beta}t,\ k^{1+\beta+\frac{2\beta}{\gamma-1}}\tilde{\eta},\quad k^{3\beta-1+\frac{2\beta}{\gamma-1}}\bar{\varepsilon}^*;\ kL\right) \tag{6.20}$$

To derive the explicit expression for $E(k)$, we resort to the locality hypothesis, this yielding

$$E(k)=k^{-\left(1+\frac{2\beta\gamma}{\gamma-1}\right)}f_2\left(k^{3\beta-1+\frac{2\beta}{\gamma-1}}\bar{\varepsilon}^*\right).$$

Since $\frac{\partial E}{\partial\beta}=0$, the final result is

$$E(k)=\mathrm{const}\times\rho_0C_0^{\frac{2}{1-3\gamma}}\bar{\varepsilon}^{\frac{2\gamma}{3\gamma-1}}k^{-\frac{5\gamma-1}{3\gamma-1}}. \tag{6.21}$$

Note that as $\gamma \to \infty$ the expression for $E(k)$ reduces to the Kolmogorov-Obukhov law. Let us stress also that deriving the spectra (6.13) and (6.21) needs no assumptions on the nature of the energy transfer along the spectrum.

Let us briefly dwell on turbulence in a stratified medium following [6.38]. Stratification naturally affects the turbulence dynamics. At sufficiently large scales, buoyancy forces specified by the parameter $g\beta$ (g is the free fall acceleration and $\beta = -\frac{1}{\rho}\frac{\partial\rho}{\partial T}$ is the thermal expansion coefficient) play an important role. According to the scaling theory advanced by Boldgiano [6.39] and Obukhov [6.40], the scale of the lowest inhomogeneity, where the Archimedean force becomes essential, is given by the expression

$$L_* = \bar{\varepsilon}^{5/4}\,\bar{\varepsilon}_T^{-3/4}\,(g\beta)^{-3/2}, \tag{6.22}$$

where $\bar{\varepsilon}_T$ is the average "dissipation" rate of temperature inhomogeneities. At scales below L_* the kinetic energy spectrum is isotropic and is fairly well described by the Kolmogorov-Obukhov law. The asymptotic form of the spectrum within the interval $kL_* \ll 1$ can be explored by means of a physical hypothesis advanced by Boldgiano [6.39] which states that, given a strong stable stratification, the energy supplied into this interval is mainly spent on the work against the buoyancy forces and therefore the parameter $\bar{\varepsilon}$ could not noticeably affect the spectrum. From dimensional considerations it follows then that [6.40]

$$E(k) \sim \varepsilon_T^{2/5}\,(g\beta)^{4/5}k^{-11/5}. \tag{6.23}$$

(For simplicity, here and below we only discuss the kinetic energy spectrum.) These results can be also obtained by the functional method [6.38]. Let us describe the properties of hydrodynamic velocity and temperature fields by the characteristic functional

$$\Phi = \left\langle \exp i \int \{y_i(x)\,V_i(x,\ t) + z(x)\,T(x,\ t)\}\,dx^3 \right\rangle, \tag{6.24}$$

where y_i, z are the functional variables and $T(x,\ t)$ is the temperature field. The equation for Φ can be obtained from the Navier-Stokes equations and equation of thermal balance in the form of (6.2). It proves to be invariant with respect to the following transformation group:

$$\begin{aligned}
&\alpha x = x', \quad \alpha^{1-\beta} t = t', \quad \alpha^{2\beta-\delta-1}(g\beta) = (g\beta)',\\
&\alpha^{-(\beta+3)}\,y(x) = y'(x'), \quad \alpha^{-(\delta+3)}\,z(x) = z'(x'),\\
&\alpha^{3\beta-1}\bar{\varepsilon} = \bar{\varepsilon}', \quad \alpha^{2\delta+\beta-1}\bar{\varepsilon}_T = \bar{\varepsilon}_T',
\end{aligned} \tag{6.25}$$

where α, β, δ are arbitrary parameters.

The scale L_* is assumed to be small as compared with the source scales and to be large as compared with the dissipation scales and hence it is neglected. Then the scaling theorem takes the form

$$\Phi\{y(x),\ z(x),\ t,\ \bar{\varepsilon},\ \bar{e}_T,\ (g\beta)\} = \Phi\{y'(x'),\ z'(x'),\ t',\ \bar{\varepsilon}',\ \bar{\varepsilon}'_T,\ (g\beta)'\}. \tag{6.26}$$

In complete analogy to the preceding examples we have for $E(k)$ [6.38]

$$E(k) = f(k^{3\beta-1}\bar{\varepsilon},\ k^{2\delta+\beta-1}\bar{\varepsilon}_T,\ k^{2\beta-\delta-1}(g\beta),\ k^{1-\beta}t)\, k^{-(2\beta+1)}. \tag{6.27}$$

In the stationary case, using the arbitrariness of δ and β, we reduce $E(k)$ to the form

$$E(k) = \text{const} \times \bar{\varepsilon}^{2/3}k^{-5/3}\Psi(kL_*), \tag{6.28}$$

where Ψ is an arbitrary function. In the absence of the gravitational force that induces stratification (i.e. as $g\beta \to 0$, $L_* \to \infty$) expression (6.28) should transform into the conventional formula for a locally isotropic turbulence in a nonstratified fluid. Hence $\Psi(\infty) \to 1$ and thus the assumption that buoyancy forces are negligible at $kL_* \gg 1$ is justified. For $kL_* \ll 1$, with $\bar{\varepsilon}$ neglected, we shall obtain the spectrum (6.23) from (6.27). A more general transformation group with different scales in longitudinal and transverse direction is considered in [6.38]. This makes it possible to study anisotropic spectra. However, here we shall not consider this problem. Note that the application of the scale transformation group is feasible in problems involving both the magnetic field and the Coriolis force [6.36, 6.41], given a proper choice of relevant parameters.

6.2.2. The Universal Equation of State in the Theory of Strong Turbulence

In the last few years a considerable interest has been aroused to the statistical theories of nonlinear non-equilibrium ensembles. This entails the relevant problems of thermodynamic relations and the possibility of constructing a nonlinear non-equilibrium thermodynamics. Hydrodynamic turbulence is a system of this type. Indeed, the strong turbulence can be treated as an ensemble with an infinite number of strongly interacting degrees of freedom that is far from equilibrium. In contrast to the preceding section, where we discuss the universal power distributions of energy over the spectrum within the inertial subrange, here we will show that the turbulent parameters averaged over all scales obey a universal relation [6.14] as well. Our result points to the fact that the nonlinear non-equilibrium thermodynamics can be constructed within the framework of unified concepts describing a strongly non-equilibrium steady state that arises due to an interaction between a subsystem and a "thermostat".

The evaluation of the total turbulence energy is mainly hampered by the fact that the main energy-range in the k-space is due to the source. Therefore it is impossible to evaluate the energy by universal turbulence spectra in the inertial range. Other statistical considerations cannot be applied here because of an inadequate advances in the statistical theories of such systems. However, we exploit the fact that exact spectral relations have been obtained in [6.11] and [6.36] on the basis of functional approach and scaling group application (see the preceding section). Thus, for an incompressible fluid we have

$$E(k) = \bar{\varepsilon}^{2/3} k^{-5/3} f(kL \quad k\lambda) \tag{6.29}$$

Let us recall that in deriving (6.29) we have only assumed that the turbulence energy spectrum is stationary. To calculate the total energy, we integrate (6.29) with respect to k

$$E = \int\limits_0^\infty \bar{\varepsilon}^{2/3} k^{-5/3} f(kL, k\lambda)\, dk. \tag{6.30}$$

Changing to an integration variable $kL = z$ and taking into account integration limits we arrive at

$$E = (\bar{\varepsilon} L)^{2/3} f(\lambda/L).$$

where

$$f(\lambda/L) = \int\limits_0^\infty f\left(\frac{\lambda}{L} z,\ z\right) dz$$

In the case of strong turbulence the source and sink are known to be widely separated in the k-space according to $\mathrm{Re} \gg 1$ so that $\lambda/L \ll 1$. Some authors have proved the possibility of an asymptotic expansion in terms of λ/L (see, e.g. [6.42]). Following these results we obtain

$$E = f(0)(\bar{\varepsilon} L)^{2/3} \tag{6.31}$$

where $f(0)$ is independent of $\bar{\varepsilon}$ and L. The possibility of expressing E in terms of $f(0)$ can be also justified by simple and obvious considerations. The expansion in terms of λ/L implies that the spectrum at $k > \lambda^{-1}$ is of the Kolmogorov type as before, i.e. we neglect the faster spectrum decay in the viscous domain. Hence we have calculated the total energy value with an error that does not exceed an energy within the interval $[\lambda^{-1}, \infty)$ (without allowance for an even faster decay due to viscosity).

Calculating this correction by the Kolmogorov spectrum we estimate the error

$$E_1 < \text{const} \times \varepsilon^{2/3}\lambda^{2/3}.$$

Finally,

$$\frac{E_1}{E} \leqslant \left(\frac{\lambda}{L}\right)^{2/3}. \tag{6.32}$$

Physically, this means that the energy within the viscous domain is small as compared with the energy in the remainder of the k-space and expression (6.31) for E is very accurate. This expression describes the relation between the total turbulence energy and the "thermostat" parameters, L and $\bar{\varepsilon}$ (here effects of external factors, i.e. of the processes of turbulence energy pumping and energy dissipation loss are referred to as "thermostat"). This relation known as "the first law" of turbulence is reliably corroborated by experimental results [6.43]. However, it has not been derived rigorously yet. Other global properties of turbulence can be calculated in a similar manner. To illustrate, we present here the variance of the pressure P for the homogeneous turbulence of an incompressible fluid

$$\langle P^2\rangle - \langle P\rangle^2 = \tilde{f}(0)\,\bar{\varepsilon}^{4/3}L^{1/3}. \tag{6.33}$$

Equations (6.31) and (6.33) yield

$$E = \text{const} \times \{L\,(\langle P^2\rangle - \langle P\rangle^2)\}^{1/2}. \tag{6.34}$$

It is noteworthy that the equation of state (6.34) is of universal nature, preserving its form also in the case of homogeneous turbulence of a compressible fluid [6.14]. Indeed, using the scaling theorem and the spectrum form in the compressible case we, quite similarly to the preceding distributions, obtain

$$E = \text{const} \times (\bar{\varepsilon}L)^{\frac{2\gamma}{3\gamma-1}}. \tag{6.35}$$

Expressing $\bar{\varepsilon}$ in terms of the pressure variance for a compressible fluid (dependent also on γ) we shall again obtain the equation of state (6.34).

To conclude the present section, let us point out that Eq. (6.34) establishes the relation between E (acting as temperature), a pressure-dependent parameter, and L (replacing the system's volume V: $L \sim V^{1/3}$), this relation is thus a turbulent analogue of the equation of state.

6.2.3. On Possible Departures from Self-Similarity in the Theory of Strong Turbulence

The ideas of Kolmogorov and Obukhov, which have resulted in the spectrum $k^{-5/3}$ in an incompressible fluid, were based on the assumptions of the conservation of the energy flux P_k along the spectrum, on the energy cascade from larger vortices to smaller ones, and on the independence of the inertial-range spectrum on the positions of the energy source and sink. The existence of the conserved quantity P_k in the inertial range of the wave number space makes it possible to express the stationary energy distribution $E(k)$ in terms of this "integral of motion". Note that, as indicated above, the use of the scaling theorem yields the Kolmogorov-type spectra without any assumptions on the nature of the energy transfer along the spectrum. However, for an incompressible nonstratified fluid the hypothesis of the conservation of P_k along the spectrum seems to be quite reasonable. In a sense, the turbulence of sawtooth waves is another limiting case. In this case, the energy flux is noticeably damped due to dissipation at discontinuities in all spectral ranges.

However, as shown in [6.44], here one can also use the concept of energy flux if the flux nonconservation is included into the continuity equation for the spectral energy density $E(k)$, i.e. if one writes

$$\frac{\partial E}{\partial t}+\frac{\partial P_k}{\partial k}=-D\frac{P_k}{k}, \tag{6.36}$$

where D is the absorption coefficient. According to [6.44], $D = 1$ when discontinuities are present. The simple phenomenological equation (6.36) has an obvious physical meaning, hence it is natural to use it in other situations as well, when the flux losses are small. From this viewpoint, consider the effect of compressibility on the vortical turbulent component by starting from small Mach numbers [6.13, 6.44]:

$$V/C = M \ll 1,$$

where $V = \sqrt{\langle V^2\rangle}$ is the characteristic velocity of turbulent pulsations. Here the energy flux in a vortical component is weakly damped due to the transfer of a part of vortical energy into the potential turbulent component. It is well known (see, e.g. [6.2]) that

$$V_s/V_\omega \sim M^2, \tag{6.37}$$

where V_s and V_ω denote the potential and solenoidal velocity components, respectively. Taking into account (6.37) it is easily verified that the sink term in the equation for the spectral density of vortical energy is related to the fifth-power nonlinearity while the flux component, to a cubic nonlinearity in V_ω. After the scaling of the spectral equation by the characteristic velocity V and scale L, a small factor $V^2/C^2 = M^2$ appears at the sink term, i.e. the ratio of the sink to flux terms is proportional to M^2. This fact is evidently independent of the model form of the nonlinearity and indicates that the Mach number enters also into the exact continuity equation.

Taking into account the above considerations we obtain

$$D = \alpha M^2, \quad \alpha \sim 1. \tag{6.38}$$

Here the inverse transfer of the potential motion energy into a vortical component can be neglected.

Using (6.36) and (6.38), in the stationary case we arrive at

$$P_k = P_0 (kL)^{-\alpha M^2}. \tag{6.39}$$

Applying now Kolmogorov's arguments (the spectrum should depend on k and the flux only) we find the expression for $E(k)$ as follows:

$$E(k) = P_0^{2/3} L^{5/3} (kL))^{-5/3-(2/3)\alpha M^2}. \tag{6.40}$$

Thus, when weak compressibility is taken into account, the spectrum loses its self-similarity due to the Mach number inclusion. In physical terms, the loss of self-similarity can be explained in the following way. The constant of the interaction between potential and vortical components is M^2 and the main interaction proceeds via large vortices. The energy flux along the spectrum "remembers" the situation in the large vortices since it flows from the region of small k's into that of large k's. Since, in turn, the flux controls the spectrum, this leads to the loss of the self-similarity of the spectrum. It can be said that the vortices, when interacting with a potential field that is dependent on the energy of the corresponding source (this energy $V^2 \sim (\bar{\varepsilon}L)^{2/3}$), are additionally affected by the large vortices via the above field. This effect is preserved even after the exclusion of kinematic transfer.

We used the simple phenomenological Eq. (6.36) to clarify qualitatively the spectrum dependence on the Mach number. To find an explicit expression for the spectrum we shall proceed in a different way. Let us resort to Eq. (6.21) for the vortical energy spectrum that is derived under the assumption of a perfect self-similarity of the spectrum. This hypothesis requires, however, some refinements. As follows from the above considerations, the spectrum should depend on the Mach number squared, M^2, and, via M^2, on L:

$$M^2 = \frac{1}{\gamma}\left(\frac{\bar{\varepsilon}L}{C_0^3}\right)^{2/3}. \tag{6.41}$$

Because of this, the violation of Kolmogorov's self-similarity is due to the dependence of $E(k)$ on the Mach number. Let us recall that, for the adiabatic equation of state, the sound velocity squared is $C^2 = \gamma C_0^2$. The spectrum ceases to be L-dependent, as follows from

(6.41), at $\bar{\varepsilon}L = C_0^3$. Here $M^2 = \gamma^{-1}$, i.e. Eq. (6.21) contains the Mach number in the form of a γ-dependence of the spectrum. This implies the formal point that Eq. (6.21) transforms into the Kolmogorov-Obukhov law as $\gamma \to \infty$. Suppose now that, according to the above exposition, the loss of self-similarity in a distribution along the spectrum within the inertial range is only due to the Mach number. It can be then easily seen that to derive an exact formula needs the substitution

$$\gamma^{-1} \to M^2. \tag{6.42}$$

Next, taking into account the dependence of $E(k)$ on $\bar{\varepsilon}$ which stems from (6.21) after the substitution $C_0 \to (\bar{\varepsilon}L)^{2/3}$ and using (6.42) we arrive at the vortical energy spectrum in a compressible fluid at $M^2 < 1$

$$E(k) \sim f_0 \bar{\varepsilon}^{2/3} k^{-5/3} (kL)^{\frac{2M^2}{3(3-M^2)}}. \tag{6.43}$$

The formula (6.21) is a special case of (6.43) at $L\bar{\varepsilon} \sim C_0^3$.

It follows from (6.43) [6.12] that at $M^2 \ll 1$

$$E(k) \sim k^{\left(-\frac{5}{3}-\frac{2}{9}M^2\right)}.$$

Thus, at $0 \leqslant M \leqslant 1$ the spectra are within the interval $(k^{-5/3}\text{-}k^{-2})$.

As to the effect of the vortices on the potential component, an interaction between sound and vortices, as shown in [6.45, 6.46], can result in establishing the $k^{-3/2}$ spectra [6.47].

6.3. "NULL-MODES"
AND THE SELF-SIMILAR SPECTRUM

6.3.1. The Nature of Infrared Divergencies and Ballistic Modes

As has been stated above, even though Kolmogorov's spectrum stems from the most general concepts and is reliably verified by experimental data [6.2], its consistent theory till now has not been constructed. Such a theory should be developed using a mathematical framework within which a nonlinear wave field can be explored for an arbitrary level of nonlinearity. One such approach, a functional one, has been used in Sec. 6.2. Here we use another effective tool, the diagram techniques. At a low level of nonlinearity this technique makes it possible to ignore all but first terms and to derive a kinetic equation that describes weakly turbulent states. The theory of strong turbulence needs all diagram equations. Nevertheless it is the theory of weak turbulence that provides us with an example of applying Kolmogorov's ideas [6.15]. This suggests that Kolmogorov's spectra must be searched for as the exact solutions to the kinetic equations corresponding, within the inertial range, to the flux conservation along the spectrum [6.16]. The main point of this approach is the independence of the self-similar spectrum of the inertial range boundaries, where a real spectrum is distorted by the source and sink. From the formal viewpoint, integrals that describe the interaction of waves belonging to the inertial range with all other waves must be convergent. If spectral integrals within the inertial range are divergent (on the source or sink), then any correction of this spectrum at the inertial range boundaries will be of no help since the spectrum loses its self-similarity.

Returning now to the strong hydrodynamic turbulence, the role of the divergencies in diagram techniques becomes more clear. Moreover, in the theory of hydrodynamic turbulence the divergencies are a sole obstacle to obtain Kolmogorov's spectrum as an exact solution of diagram equations. Now it is generally assumed that the most troublesome ones are infrared divergencies. Therefore below we are going to restrict ourselves only to these divergencies.

Even the early papers [6.18-6.20] argued that the infrared divergencies could arise due to the convection of small vortices by large-scale flows. In [6.21] it is proposed to eliminate this convection by the interaction representation while [6.22] demonstrates how this convection can be eliminated within the framework of the direct interaction approximation of Kraichnan [6.48]. In a sense, the ultimate elimination of the convection (summation of the most divergent diagram) has been performed in [6.23]. Unfortunately, this has not resulted in the complete elimination of infrared divergencies.

What is the reason of this situation? First of all, note that the main source of infrared divergencies is a troublesome contribution near $k = 0$ that arises steadily due to an interaction between the vortices and adjacent wave vectors. To cancel out this contribution, we need to include the generalized solutions of the ballistic-mode type. These solutions are generally not considered in the theory of turbulence.

From the physical viewpoint, the solutions similar to the Van Kampen-Case modes [6.26, 6.27] describe freely moving beams of Lagrangian particles and have a continuous spectrum. The arbitrary spectral parameter for these modes can be chosen so that the troublesome contributions near $k = 0$ will be cancelled out [6.24, 6.25]. Below these generalized solutions will be termed "null-modes". By a proper choice of a group of Lagrangian particles one can construct a velocity field consistent with Kolmogorov's self-similarity.

In a sense, the role of the "null-modes" is analogous to that of the Van Kampen waves in collisionless plasma.

Now let us turn to calculations.

We proceed from the Navier-Stokes equations which, in terms of the Clebsch variables λ, μ, have the following form [6.49]:

$$\frac{\partial\lambda}{\partial t}+(\mathbf{u}\nabla)\lambda=0;\quad \frac{\partial\mu}{\partial t}+(\mathbf{u}\nabla)\mu=0, \tag{6.44}$$

$$\mathbf{u}=\lambda\nabla\mu+\nabla\Phi. \tag{6.45}$$

The potential part $\nabla\Phi$ of the velocity field is determined by the incompressibility condition $\operatorname{div}\mathbf{u}=0$ and has the form

$$\Phi=-\Delta^{-1}(\nabla(\lambda\nabla\mu)). \tag{6.46}$$

In terms of the variables

$$a_k=\frac{1}{\sqrt{2}}(\lambda_k+i\mu_k),$$

where λ_k and μ_k are the Fourier transforms of λ and μ, respectively, we obtain the following expression for the velocity u:

$$\mathbf{u}_k=\int \Phi_{k_1k_2}a_{k_1}a^{*}_{k_2}\delta(\mathbf{k}+\mathbf{k}_2-\mathbf{k}_1)\,d\mathbf{k}_1\,d\mathbf{k}_2, \tag{6.47}$$

where $\Phi_{k_1k_2}$ is the matrix element

$$\Phi_{k_1k_2}=\frac{1}{2(2\pi)^{3/2}}\left[\mathbf{k}_1+\mathbf{k}_2-(\mathbf{k}_1-\mathbf{k}_2)\frac{k_1^2-k_2^2}{|\mathbf{k}_1-\mathbf{k}_2|^3}\right]. \tag{6.48}$$

The quantity $\Phi^{*}_{k_1k_2}$ has the following asymptotic forms:

$$\Phi_{k_1k_2}=\frac{1}{(2\pi)^{3/2}}\left[\mathbf{k}_2-\mathbf{k}_1\left(\frac{k_2}{k_1}\right)\cos\theta\right]\sim k_2\to 0, \tag{6.49}$$

$$k_1\gg k_2,\quad \cos\theta=\frac{(\mathbf{k}_1\mathbf{k}_2)}{|\mathbf{k}_1|\,|\mathbf{k}_2|}$$

If both vectors simultaneously tend to zero, i.e. $k_1\approx k_2\to 0$, then

$$\Phi_{k_1k_2}=\frac{1}{(2\pi)^{3/2}}[\mathbf{k}_1-\boldsymbol{\varepsilon}(\mathbf{k}_1\boldsymbol{\varepsilon})|\boldsymbol{\varepsilon}|^{-2}], \tag{6.50}$$

$$\boldsymbol{\varepsilon}=\mathbf{k}_2-\mathbf{k}_1.$$

Expression (6.50) implies that the vector $\Phi_{k_1k_2}$ is indeterminate. An attempt to define Φ_{kk} as a limit of $\Phi_{k,\,k+\varepsilon}$ as $\varepsilon\to 0$ does not succeed since (6.48) suggests that

$$(\boldsymbol{\varepsilon}\Phi_{k,\,k+\varepsilon})\equiv 0 \tag{6.51}$$

for any $\boldsymbol{\varepsilon}$. Thus, Φ_{kk} proves to be dependent on the direction along which the vector $\boldsymbol{\varepsilon}$ tends to zero.

It is seen from (6.47) that the indeterminate form of Φ_{kk} leads to the indeterminate form of $\mathbf{u}_k$ at $k=0$. What is the nature of this indeterminacy? In connection with this question let us return to the definition of the potential part of the velocity field $\mathbf{\Phi}_k$. The latter can be found from the incompressibility condition

$$\mathbf{k}\mathbf{V}_k = 0. \tag{6.52}$$

Evidently, the general solution of this equation is

$$\mathbf{V}_k = \mathbf{U}_k + \mathbf{C}\delta(\mathbf{k}), \tag{6.53}$$

where $\mathbf{U}_k$ is the smooth part of the velocity field (6.47) and $\mathbf{C}$ is an arbitrary function of time.

The second term in (6.53) is analogous to the modes of a continuous spectrum of the Van Kampen-Case type [6.26, 6.27]. In analogy to ballistic mode terminology, $\mathbf{C}$ can be called a spectral parameter.

Below the term $\mathbf{C}\delta(\mathbf{k})$ will be referred to as a "null-mode". From the physical standpoint, "null-modes" describe either free motion of Lagrangian particles at $\mathbf{C} = \text{const}$ or modulated beams of Lagrangian particles at $\mathbf{C} = \mathbf{C}(t)$. Using the arbitrariness of $\mathbf{C}(t)$ we can put

$$\mathbf{C} = -\int \mathbf{\Phi}_{k_1 k_2} a_{q_1} a^*_{q_2}\, dq_1\, dq_2, \tag{6.54}$$

$$q = (\omega, \mathbf{k}).$$

With the spectral parameter so chosen, the velocity takes the form [6.24, 6.25]

$$\mathbf{V}_q = \int \mathbf{\Phi}_{k_1 k_2} a_{q_1} a^*_{q_2} \{\delta(q + q_2 - q_1) - \delta(q)\}\, dq_1\, dq_2. \tag{6.55}$$

The earlier indeterminacy in $\mathbf{\Phi}_{kk}$ means that the interaction between vortices with $k_1 \approx k_2$ produces the motion with nearly vanishing momentum $k \approx 0$. This fact was illustrated by the asymptotic form (6.50) that led to infrared divergencies within the standard approach [6.5]. As follows from (6.55), the spectral parameter $\mathbf{C}$ chosen in the form of (6.54) cancels out the contribution from the interaction between adjacent vortices at $k = 0$ and results in the cancellation of infrared divergencies.

6.3.2. Diagram Techniques

Diagram techniques for hydrodynamic equations in terms of natural variables have been developed in [6.4]. However, more convenient are the Clebsch variables reducing relevant equations to the Hamiltonian form. The diagram techniques for Hamiltonian systems, in particular, in terms of the Clebsch variables have been developed in the paper by Zakharov and L'vov [6.5]. These authors also stressed that, in the absence of divergencies, Kolmogorov's spectrum became an exact solution to diagram equations and the problem of divergencies as a whole was treated as that of the modification of the diagram equations. Below we show that a proper modification of the diagram equations enables the "null-modes" to be introduced.

In our case the Hamiltonian

$$H=\int |u_{\mathbf{k}}|^2\, d\mathbf{k}$$

would include the terms like $\delta^2(\mathbf{k})$, hence using the standard diagram techniques [6.5] presents some difficulties. Not rejecting the convenient Clebsch variables we are going to construct the diagram techniques by starting directly from Eqs. (6.44). In terms of the variables a_k the latter take the form

$$a_q=G_q^{(0)}\int W_{qq_1q_2q_3}a_{q_1}a_{q_2}a^*_{q_3}\,dq_1\,dq_2\,dq_3, \tag{6.56}$$

where

$$W_{qq_1q_2q_3}=(\mathbf{k}\Phi_{k_1k_2})\,\delta(q_1+q_2-q_3-q)$$

is the interaction matrix element which for convenience will be used in a nonsymmetric form, while $G_q^{(0)}=(\omega+i0)^{-1}$ is Green's function of free field.

The "null-modes" discussed at the beginning of this section can be introduced into (6.56) via identical transformations. Indeed, let us denote

$$\mathbf{V}_0=\int \Phi_{k_1k_1}a_{q_1}a^*_{q_1}\,dq_1\,dq_3. \tag{6.57}$$

Then we obtain

$$a_q=\frac{1}{\omega-\mathbf{k}\mathbf{V}_0+i0}\int T_{qq_1q_2q_3}a_{q_1}a_{q_2}a^*_{q_3}\,dq_1\,dq_2\,dq_3, \tag{6.58}$$

$$T_{qq_1q_2q_3}=(\mathbf{k}\Phi_{k_1k_2})\{\delta(q_1+q_2-q_3-q)-\delta(q_2-q)\}. \tag{6.59}$$

Since $\mathbf{V}_0=\text{const}$, then by changing the variables we arrive at

$$a_{k\tilde{\omega}}=G_q^{(0)}\int T_{qq_1q_2q_3}\,a_{k_1\tilde{\omega}_1}a_{k_2\tilde{\omega}_2}a^*_{k_3\tilde{\omega}_3}\,dq_1\,dq_2\,dq_3, \tag{6.60}$$

$$\tilde{\omega}_i=\omega_i+\mathbf{k}_i\mathbf{V}\quad (i=1,\ 2,\ 3).$$

To construct the diagram techniques, both a random external force and a small dissipation should be included in Eq. (6.55). The random force is assumed Gaussian, statistically homogeneous, isotropic, and stationary.

The introduction of an external force is of auxiliary nature and is necessary only for deriving diagram equations. The correlator of this external force enters into the final equations additively and can be tended to zero along with small dissipation. For the diagram equations to be independent of the properties of this force, it is necessary to supplement the above conditions by another property, viz. the external force must be a Galilean invariant. Below we assume that all these properties exist. Note that the incompressibility condition suggests the property

$$(\mathbf{k}_1-\mathbf{k}_3)\,\Phi_{k_1k_3}=0,$$

thus enabling us to assume that in the matrix element $T_{qq_1q_2q_3}$

$$(\mathbf{k}\Phi_{k_1k_3})=(\mathbf{k}_2\Phi_{k_1k_3}). \tag{6.61}$$

In the construction of the diagram techniques we start from the equation

$$a_{\tilde{q}}=G_q^{(0)}\left[\int T_{qq_1q_2q_3}a_{\tilde{q}_1}a_{\tilde{q}_2}a^*_{\tilde{q}_3}\,dq_1\,dq_2\,dq_3+f_q\right], \tag{6.62}$$

$$\tilde{q}_i=(k_i,\ \omega_i+\mathbf{k}_i\mathbf{V}_0)\quad(i=1,\ 2,\ 3),$$

where $G_q^{(0)}=(\omega+i\nu)^{-1}$ and ν is the damping that was introduced phenomenologically simultaneously with f_q, the random external force, whose correlator is

$$\langle f_qf^*_{q'}\rangle=\langle f_q^2\rangle\,\delta(q-q'). \tag{6.63}$$

Let us draw the vertex $T_{qq_1q_2q_3}$ graphically (Fig. 6.1). Besides, let us denote $G_q^{(0)}=$ ————, $f_q=$ - - - - -. Then the first terms

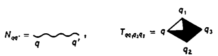

Fig. 6.1

of the formal perturbation theory in external force will have the form shown in Fig. 6.2. Conventional Green's function is

$$\left\langle\frac{\delta a_q}{\delta f_{q'}}\right\rangle=g_q\delta(q-q'). \tag{6.64}$$

Let us also introduce Green's function of a Doppler-shifted argument

$$\left\langle\frac{\delta a_{k,\ \omega+\mathbf{k}\mathbf{V}_0}}{\delta f_{k',\ \omega'}}\right\rangle=G_{qq'}. \tag{6.65}$$

Here the averaging is assumed to be performed over the external force. In addition, let us introduce the spectral densities

$$\langle a_qa^*_{q'}\rangle=n_q\delta(q-q'), \tag{6.66}$$

$$\langle a_{k,\ \omega+\mathbf{k}\mathbf{V}_0}a^*_{k',\ \omega'+\mathbf{k}'\mathbf{V}_0}\rangle=N_{qq'}. \tag{6.67}$$

Let us denote

$$G_{qq'} = \underset{q \qquad\quad q'}{\overline{\qquad\qquad}}, \quad N_{qq'} = \underset{q \qquad\quad q'}{\overline{\qquad\qquad}}. \tag{6.68}$$

Performing a standard averaging over the external force we shall obtain, from the series shown in Fig. 6.1, new diagram series which

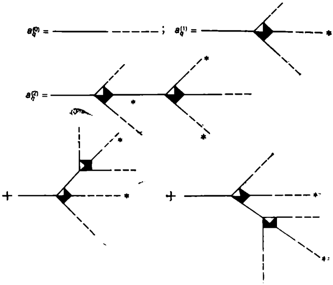

Fig. 6.2

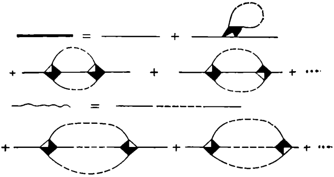

Fig. 6.3

include the functions $G_{qq'}$ and $N_{qq'}$ in the left-hand sides (see Fig. 6.3). Note that the form of the vertex $T_{qq_1q_2q}$ suggests that the pairing shown in Fig. 6.4 yields an identical zero. Taking into account

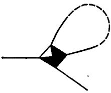

Fig. 6.4

that the average velocity is zero and passing, by means of a partial summation, to irreducible diagrams we arrive at the diagram equations for the functions $G_{qq'}$ and $N_{qq'}$ (see Fig. 6.5). The topological

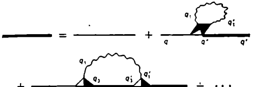

Fig. 6.5

pattern of the diagrams obtained is the same as that for n_q and g_q. They differ only in that, in the diagram equations of Fig. 6.5, on each line connecting two vertices the integration is performed with respect to two momenta $q_i^{(1)}$ and $q_i^{(2)}$, one of which is positioned at the beginning of the line and another, at its end. Since the external force correlator enters into the equations of Fig. 6.5 additively we can tend it to zero along with the dissipation ν. Consequently, $G_q^0 \rightarrow (\omega + i0)^{-1}$. Thus, for the subsequent exposition, the basic equations will be those of Fig. 6.5 without the external force correlator.

6.3.3. Reduction of Diagram Equations and Cancellation of Infrared Divergencies

The matrix element $T_{qq_1q_2q_3}$ contains the difference of two δ-functions which is transformed as

$$\delta(q_1+q_2-q_3-q)-\delta(q_2-q)$$
$$=\left\{1-\exp(\mathbf{k}_1-\mathbf{k}_3)\frac{\partial}{\partial\mathbf{k}}\exp(\omega_1-\omega_3)\frac{\partial}{\partial\omega}\right\}\delta(q_1+q_2-q_3-q). \quad (6.69)$$

In (6.69) we have used the shift operator. Expanding (6.69) into a series yields

$$T_{qq_1q_2q_3}=(\mathbf{k}\Phi_{k_1k_3})\left\{-(\mathbf{k}_1-\mathbf{k}_3)\frac{\partial}{\partial\mathbf{k}}-(\omega_1-\omega_3)\frac{\partial}{\partial\omega}-\dots\right\}$$
$$\times\delta(q_1+q_2-q_3-q). \quad (6.70)$$

The interaction matrix element $T_{qq_1q_2q_3}$ will be used below in the form of (6.70).

As has been stated before, from the standpoint of Kolmogorov's theory, the statistical properties of turbulence must be independent of the inertial range boundaries. This means that the functions $G_{qq'}$, $N_{qq'}$ have a purely self-similar form, i.e. they have no parameters of the dimensions of length and time. Hence we can write

$$N_{qq'}=\frac{1}{k^5\omega}f\left(\frac{\omega}{k^{2/3}};\ \frac{k'}{k};\ \frac{\omega'}{\omega}\right),$$
$$G_{qq'}=\frac{1}{k^{11/3}\omega}\Psi\left(\frac{\omega}{k^{2/3}};\ \frac{k'}{k};\ \frac{\omega'}{\omega}\right). \quad (6.71)$$

The dimensionless functions f, Ψ determine the constants in the expression for Kolmogorov's spectrum. Substituting the expressions (6.71) into the diagrams of Fig. 6.5 enables us to trace how the infrared divergencies are cancelled out.

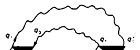

Fig. 6.6

Since higher-order diagrams are cumbersome we consider, as an example, the second-order diagram. The first-order diagram is of no interest since it converges without any cancellations. Were it not for the cancellations of divergencies, then among the second-order diagrams there would be a diverging diagram shown in Fig. 6.6 denoted by I_2:

$$I_2 = \int T_{qq_1q_2q_3} T_{q_2'q_3'q''q_1'} N_{q_1q_1'} N_{q_3q_3'} G_{q_2q_2'} G_{q''q'}$$
$$\times dq''\, dq_1\, dq_1'\, dq_2\, dq_2'\, dq_3\, dq_3'. \tag{6.72}$$

At the vertices T we retain, in the infrared limit, the terms that tend to zero most slowly

$$T_{qq_1q_2q_3} = (\mathbf{k}\Phi_{k_1k_3})\,\delta(\mathbf{k}_1 + \mathbf{k}_2 - \mathbf{k}_3 - \mathbf{k})$$
$$\times \left[(\omega_3 - \omega_1)\frac{\partial}{\partial\omega}\,\delta(\omega_1 + \omega_2 - \omega_3 - \omega)\right] + \dots \,. \tag{6.73}$$

Substituting (6.73) and (6.71) into (6.72) and introducing the following variables:

$$\frac{\mathbf{k}_1'}{k_1} = \eta_1, \quad \frac{\omega_1'}{\omega_1} = \zeta_1, \quad \frac{\omega_1}{k_1^{2/3}} = \xi_1,$$
$$\frac{\mathbf{k}_2'}{k_2} = \eta_2, \quad \frac{\omega_2'}{\omega_2} = \zeta_2, \quad \frac{\omega_2}{k_2^{2/3}} = \xi_2,$$
$$\frac{\mathbf{k}_3'}{k_3} = \eta_3, \quad \frac{\omega_3'}{\omega_3} = \zeta_3, \quad \frac{\omega_3}{k_3^{2/3}} = \xi_3,$$
$$\mathbf{k}''/k' = \boldsymbol{\eta}', \quad \omega''/\omega' = \zeta',$$

we obtain the expression

$$I_2 = \int (\mathbf{k}\Phi_{k_1k_3})(\eta_2\Phi_{k_3\eta_3;\,k_1\eta_1})\,k_2^{1/3}\,\delta(\mathbf{k}_1 + \mathbf{k}_2 - \mathbf{k}_3 - \mathbf{k})$$
$$\times \delta(k_2\eta_2 + k_3\eta_3 - k'\boldsymbol{\eta}' - k_1\eta_1)$$
$$\times \left[(k_3^{2/3}\xi_3 - k_1^{2/3}\xi_1)\frac{\partial}{\partial\omega}\,\delta(k_1^{2/3}\xi_1 + k_2^{2/3}\xi_2 - k_3^{2/3}\xi_3 - \omega)\right]$$
$$\times \left[(k_1^{2/3}\xi_1\zeta_1 - k_3^{2/3}\xi_3\zeta_3)\frac{\partial}{\partial\zeta_2}\,\delta(k_2^{2/3}\xi_2\zeta_2 + k_3^{2/3}\xi_3\zeta_3 - \omega'\zeta' - k_1^{2/3}\xi_1\zeta_1)\right]$$
$$\times \frac{1}{k_1^{13/3}k_3^{13/3}}\,\frac{1}{(k')^{2/3}}\,\Psi\left(\frac{\omega'}{(k')^{2/3}},\ \boldsymbol{\eta}',\ \zeta'\right)$$
$$\times \xi_2^{-1}\Psi(\xi_2,\ \eta_2,\ \zeta_2)\,f(\xi_1,\ \eta_1,\ \zeta_1)\,f(\xi_3,\ \eta_3,\ \zeta_3)$$
$$\times (d\zeta'\,d\boldsymbol{\eta}')(d\xi_1\,d\eta_1\,d\zeta_1)(d\xi_2\,d\eta_2\,d\zeta_2)(d\xi_3\,d\eta_3\,d\zeta_3)\,d\mathbf{k}_1\,d\mathbf{k}_2\,d\mathbf{k}_3. \tag{6.74}$$

The question of the convergence of the integral (6.74) reduces to that of the following integral in momenta:

$$I = \int (\mathbf{k}\Phi_{k_1k_3})(\eta_2\Phi_{k_3\eta_3,\,k_1\eta_1})\,k_1^{-13/3}k_3^{-13/3}$$
$$\times [(k_3^{2/3}\xi_3 - k_1^{2/3}\xi_1)(k_1^{2/3}\xi_1\zeta_1 - k_3^{2/3}\xi_3\zeta_3)]\,d\mathbf{k}_1\,d\mathbf{k}_3. \tag{6.75}$$

Such an integral did not contain the bracketed multiplier and was thus divergent for k_1 and k_3 tending simultaneously to zero.

In our case this integral is convergent. To see that it is so, let us change the variables

$$\rho=(k_1^2+k_3^2)^{1/2}, \quad k_1=\rho\cos\chi, \quad k_3=\rho\sin\chi, \quad \rho\geqslant 0, \quad 0\leqslant\chi\leqslant\pi/2.$$

As a result,

$$I=\int d\Omega\int\frac{d\rho}{\rho^{1/3}}\int_0^{\pi/2}d\chi\,(\mathbf{k}\Phi_{\cos\chi,\,\sin\chi})(\eta_2\Phi_{\eta_3\sin\chi,\,\eta_1\cos\chi})\cos^{-7/3}\chi\sin^{-7/3}\chi$$
$$\times(\xi_3\sin^{2/3}\chi-\xi_1\cos^{2/3}\chi)(\xi_1\zeta_1\cos^{2/3}\chi-\xi_3\zeta_3\sin^{2/3}\chi), \tag{6.76}$$

where $d\Omega$ means integration with respect to nonsingular angular variables. The integral with respect to ρ in (6.76) converges as $\rho^{2/3}$ while the integral with respect to the angle χ converges as $\chi^{2/3}$ at the singular points $\chi=0$ and $\pi/2$. Thus, the convergence of the diagrams of the second order is proved. This analysis of the second-order diagrams for Green's function $G_{qq'}$ demonstrates the general mechanism of cancelling out the divergencies.

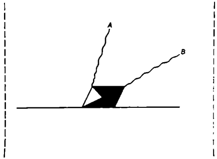

Fig. 6.7

Let us consider the higher-order diagrams in a somewhat simplified manner. The diagrams for $N_{qq'}$ have the same topological structure as those for $G_{qq'}$ and it is only necessary to replace one of the wavy lines in the main section of the $N_{qq'}$ diagram by the line →, therefore we are going to restrict ourselves only to the $G_{qq'}$ diagrams. (A set of wavy lines after whose disruption one can split a diagram into two disconnected parts is called the main section in the diagram.)

The higher-order diagram, with Q vertices, contains Q wavy lines. A vertex has two troublesome momenta in which it converges only slowly. In Fig. 6.7 they are denoted by A and B. In the novel techniques, with the "null-modes" excluded, each pair of the momenta enters with the multiplier $(\alpha k_A^{2/3}-\beta k_B^{2/3})$. In terms of the variable

$\rho^2 = k_1^2 + k_2^2 + \ldots + k_Q^2$, as with the second-order diagrams, the Qth-order diagram becomes proportional to the integral

$$I_Q \sim \int \frac{\rho^n \rho^{2n/3} \rho^{3n-1}\, d\rho}{\rho^{13n/3}} \sim \int \rho^{(n-3)/3}\, d\rho. \tag{6.77}$$

The first multiplier in (6.77) arises due to the vertices Φ, the second one, due to the "null-modes" cancellation, and the third one, due to a volume element in the momentum space. Evidently, the integral I_Q is convergent. In a version of the diagram techniques without the "null-modes" cancelled out we have, instead of (6.77), the divergent integral

$$I \sim \int \frac{\rho^n \rho^{3n-1}\, d\rho}{\rho^{13n/3}} \sim \int \rho^{-(n+3)/3}\, d\rho. \tag{6.78}$$

Thus, the procedure of diagram modification and of "null-modes" isolation from an interaction matrix element results in cancelling out the infrared divergencies.

6.4. INVARIANT PROPERTIES OF HYDRODYNAMIC MODELS AND TOPOLOGICAL SOLITONS

Studies of the turbulence in strongly interacting systems come across a number of generally known difficulties. Therefore it is important to find ways to overcome some of these difficulties. The analysis of the invariant properties of hydrodynamic models may, on the one hand, assist in advancing in this direction and, on the other hand, indicate some finer properties of turbulent motion.

6.4.1. Freezing-in Integrals, Topological and Lagrangian Invariants

Let us consider the principal invariants of hydrodynamic models and obtain general relations between them. Lagrangian invariants are the quantities that satisfy, in terms of the Eulerian variables, the equation

$$\frac{\partial I}{\partial t} + (\mathbf{V}\nabla) I = 0, \tag{6.79}$$

that describes the conservation of I when it is convected by fluid elements. Another typo of invariant quantities is represented by the freezing-in integrals described by the equation

$$\frac{\partial \mathbf{J}}{\partial t} + (\mathbf{V}\nabla)\, \mathbf{J} = (\mathbf{J}\nabla)\, \mathbf{V}. \tag{6.80}$$

This equation describes the freezing of the lines of force of the field **J** into a fluid.

Let us consider some relations that are independent of the specific form of the equations describing the velocity field. These were derived using only the continuity equation for the density ρ (or some other quantity). Hence the relations derived below are valid for any dissipationless hydrodynamic model. Suppose that, in addition to the Lagrangian invariants x_0 (the initial coordinates of Lagrangian particles), we have a number of other Lagrangian invariants I_1, I_2, I_3. Choosing these as the basis of a new Lagrangian coordinate system we change from x_1^0, x_2^0, x_3^0 to I_1, I_2, I_3 ($x^0 \rightarrow x \rightarrow I$). Clearly, because the volume elements in terms of both the old and the new coordinates are Lagrangian invariants, the transition Jacobian is also a Lagrangian invariant. Thus we obtain the Lagrangian invariant

$$I_4 = \frac{1}{\rho} \frac{\partial (I_1, I_2, I_3)}{\partial (x_1, x_2, x_3)}. \tag{6.81}$$

The derived relationship can be used in constructing the Lagrangian conservation laws in terms of three or more known Lagrangian invariants by means of repeated consecutive use of (6.81).

As another relationship to construct the Lagrangian invariants in terms of the known freezing-in integrals we can use the following [6.31]:

$$I' = \mathbf{J} \nabla I. \tag{6.82}$$

Indeed, direct calculation of dI'/dt, with (6.79) and (6.80) taken into account, shows that I' is a Lagrangian invariant. This can be also easily verified by simple physical arguments. To do this, let us consider a surface $I = \text{const}$ and choose an elementary contour lying on this surface. It is evident that for any motions the contour will remain on this surface due to the conservation of the Lagrangian invariant I. The orientation of the area element $d\mathbf{S}$ of the elementary contour coincides with the orientation of ∇I. Moreover, noting that the equation for ∇I coincides with that for $\rho\, d\mathbf{S}$, one can select the constant so that $\nabla I = \text{const} \times \rho\, d\mathbf{S}$. Relation (6.82) may be then interpreted as the conservation of the flux of a frozen-in quantity, thus proving that the quantity I' is a Lagrangian invariant. Relation (6.82) admits a certain generalization because in the above arguments of importance is only the fact that the quantity ∇I is a vector field satisfying an equation whose form coincides with that of the equation for $\rho\, d\mathbf{S}$. Then introducing the fields which satisfy the equation

$$\frac{\partial S_i}{\partial t} + (\mathbf{V} \nabla) S_i = - S_j \frac{\partial V_j}{\partial x_i} \tag{6.83}$$

results in generalization of (6.82)

$$I' = \mathbf{J}\mathbf{S}. \tag{6.84}$$

For an incompressible fluid this relation is given in [6.50]. The introduction of the field S is substantiated by physical applications. In particular, it emerges as the momentum of a small annular vortex [6.51].

Now let us construct the frozen-in quantities from Lagrangian invariants. Consider in a Lagrangian coordinate space the surfaces $I_1(x_0) = I_1^0$ and $I_2(x_0) = I_2^0$ where two Lagrangian invariants have fixed values. In the general case these surfaces intersect along a certain curve. Let us choose an element $d\mathbf{l}$ along the intersection line of these surfaces, this being the element of length of a fluid line specified by the invariants I_1 and I_2. It is clear that the vector $[\nabla I_1, \nabla I_2]$ is tangential to $d\mathbf{l}$, i.e. it always coincides with the latter's orientation. This makes it possible, by passing to the Eulerian coordinate system, to derive the expression for the freezing-in integral [6.31]

$$\mathbf{J} = \frac{1}{\rho}[\nabla I_1, \nabla I_2]. \tag{6.85}$$

Thus, the Lagrangian integrals enable us to construct the quantities frozen into a medium and satisfying (6.85). Of course, this can be also verified directly, by differentiating (6.85) with respect to time. The linearity of Eq. (6.80) in $\mathbf{J}$ implies that the sum of frozen-in quantities will be again frozen-in. Besides, multiplying $\mathbf{J}$ by a Lagrangian invariant also does not violate its freezing-in state. Proceeding from this simple reasoning one can easily see that the quantity constructed from the three Lagrangian invariants I_1, I_2, I_3 is frozen into a medium [6.31]

$$J_\alpha = \frac{1}{\rho}\varepsilon_{\alpha\beta\gamma}\varepsilon_{ikl}I_i\frac{\partial I_k}{\partial x_\beta}\frac{\partial I_l}{\partial x_\gamma}, \tag{6.86}$$

where the subscripts take on the values of 1, 2. 3. This quantity has an independent sense as well. e.g. in terms of n-fields [6.52]. It should be noted that the relation (6.85) can be also generalized (by a reasoning similar to the above) by s-fields. Then (6.85) transforms into the following relation [6.50]:

$$\mathbf{J} = \frac{1}{\rho}[\mathbf{S}, \mathbf{S}'].$$

Let us stress one specific feature of (6.85). All known fields frozen into a medium (e.g. $\mathbf{J} = \frac{\mathbf{H}}{\rho}$; curl $\frac{\mathbf{V}}{\rho}$, etc.), as the quantities from (6.85), possess the property of div $\mathbf{J}\rho = 0$. In physical terms, it means that the charges of the field $\mathbf{J}$ are absent. In other words, the lines of force of these fields can be either closed lines going to infinity or everywhere densely fill a manifold of dimension higher than 1. Generically, the constructed fields (6.86) do not have such a property and exemplify the frozen-in quantities of a new type. Moreover, two forms of the differential relations for a frozen-in state, i.e. (6.80) and

$$\frac{\partial \rho \mathbf{J}}{\partial t} = \operatorname{curl} [\rho \mathbf{J}, \mathbf{V}] \tag{6.87}$$

are not equivalent since (6.80) implies the following equation for $\rho\mathbf{J}$:

$$\frac{\partial \rho \mathbf{J}}{\partial t} = \operatorname{curl} [\rho \mathbf{J}, \ \mathbf{V}] - \mathbf{V} \operatorname{div} \rho \mathbf{J},$$

which at $\operatorname{div} \rho\mathbf{J} \neq 0$ does not coincide with (6.87). As a consequence of nonvanishing $\operatorname{div} \rho\mathbf{J}$ we have the nonzero flux of a frozen-in quantity through a closed surface and, thus, the appearance of an analogue of the charges of these fields. If the Lagrangian invariants in (6.86) are interdependent (i.e. there exists a relation $\varphi(I_1, I_2, I_3) = 0$), then $\operatorname{div} \rho\mathbf{J}$ vanishes and we return to conventional frozen-in quantities.

Besides the above difference, Eqs. (6.86) and (6.85) differ also topologically within the same class. However, these differences will be discussed after introducing the topological characteristics of freezing-in integrals. To obtain these integrals we consider a purely vortical field of the quantities $\rho\mathbf{J}$ (i.e. $I_3 = f(I_1, I_2)$). In this case the vector potential $\mathbf{A}$ ($\rho\mathbf{J} = \operatorname{curl} \mathbf{A}$) can be introduced. Consider the quantity [6.31]

$$I^\tau = \int_{\mathcal{V}_0} \rho \mathbf{J} \mathbf{A} \, d\mathcal{V}, \tag{6.88}$$

where the integration is performed over the volume bounded by the surface S_0 whose normal is always orthogonal to $\mathbf{J}$, i.e. $(\mathbf{n}\mathbf{J}) = 0$.

The quantity introduced describes the entanglement of the lines of force of the frozen-in quantities and is conserved. To prove this, we use the equation for the vector potential $\mathbf{A}$ that follows from the specific form of $\mathbf{J}$

$$\frac{\partial \mathbf{A}}{\partial t} = [\mathbf{V}, \ \operatorname{curl} \mathbf{A}] + \nabla \Psi. \tag{6.89}$$

The form of the function Ψ is not essential here. Using (6.89) and (6.80) we obtain

$$\frac{\partial \mathbf{J}\mathbf{A}}{\partial t} = (\mathbf{J}\nabla)(\Psi + \mathbf{A}\mathbf{V}).$$

Taking into account this equation one can easily show that

$$\frac{dI^\tau}{dt} = \int_{S_0} \rho \mathbf{J} (\Psi + \mathbf{A}\mathbf{V}) \, d\mathbf{S} = \int_{S_0} \rho (\mathbf{J}\mathbf{n}) (\Psi + \mathbf{A}\mathbf{V}) \, dS$$

and, since $\mathbf{J}\mathbf{n} = 0$, by definition, I^τ is conserved, i.e. $\frac{dI^\tau}{dt} = 0$.

The physical interpretation of the Lagrangian invariants (6.88) is completely analogous to the interpretation of their particular cases for a compressible fluid and MHD [6.53].

Now let us return to the topological differences between the introduced quantities (6.85) and (6.86). It is evident that the lines of intersection of two surfaces determined by Lagrangian invariants do not admit any linkage. This is why the invariant (6.88) for the quantities (6.85) vanishes (we discuss here the case when the Lagrangian invariants prescribe the one-to-one mapping $R^3 \to R^3$). For the freezing-in integral (6.86) the invariant (6.88) can be non-vanishing. Thus the lines of force of the freezing-in integral (6.85) are a set of unlinked lines while in the case of (6.86) the lines of force can form knots and be linked.

In deriving the topological invariants of the frozen-in fields of another type we use the quantity called a mapping degree (see e.g. [6.54]). Then the quantity

$$I^{\tau} = \frac{1}{4\pi} \int\limits_{S} d\theta \, d\varphi \, \mathbf{j} \left[\frac{\partial \mathbf{j}}{\partial \theta} , \ \frac{\partial \mathbf{j}}{\partial \varphi} \right], \tag{6.90}$$

where $\mathbf{j} = \mathbf{J}/|\mathbf{J}|$, that is equal to the number of times the vector $\mathbf{j}$ goes around the unit sphere, when r passes over S, is conserved. The fact is that the temporal evolution of the field of a frozen-in quantity boils down to its continuous deformation by the flow of a continuous medium this enabling a homotopy between the initial state and the state at the moment t to be established. It is known that under the homotopy the mapping degree is conserved [6.54], and consequently I^{τ} is conserved.

Thus, to construct the freezing-in integrals and Lagrangian invariants reflecting a topological structure, a certain initial set of Lagrangian invariants is sufficient. In the canonical form, such a set can be easily produced by formulating relevant equations in terms of a variational principle. Indeed, in the variational formulation of the equations of motion of dissipationless media, that is based on Lagrangian multipliers [6.55], the trivial Lagrangian invariants $X_{0k}(x, t)$ (the initial positions of Lagrangian particles) serve as coordinates. The Lagrangian invariants λ_k, that in this case have the sense of generalized Hamiltonian momenta, are supplementary to the trivial invariants. Hence, one can naturally use a set arising from the variational principle as the initial set of the Lagrangian invariants. Such an approach to constructing the invariants for an incompressible fluid in the adiabatic case was adopted in [6.31]. As another example, consider invariants arising in the two-fluid plasma hydrodynamics. Let us illustrate another possibility of applying the above relations without use of canonical variables. To derive the initial set, we use the known system of equations of the two-fluid plasma hydrodynamics without dissipation in the adiabatic case. Evaluating the curl of the equations of motion one can easily obtain the freezing-in integral [6.56]

$$\frac{d}{dt}\left\{\frac{\operatorname{curl}\mathbf{V}_\alpha+\frac{e_\alpha\mathbf{H}}{m_\alpha c}+\boldsymbol{\Omega}_\alpha}{n_\alpha}\right\}=\left\{\frac{\operatorname{curl}\mathbf{V}_\alpha+\frac{e_\alpha\mathbf{H}}{m_\alpha c}+\boldsymbol{\Omega}_\alpha}{n_\alpha}\nabla\right\}\mathbf{V}_\alpha, \qquad (6.91)$$

where $\boldsymbol{\Omega}_\alpha$ is the rotation velocity of the α-component as a whole (the remaining notation is conventional).

Thus, we have the freezing-in integral and the Lagrangian invariant S_α (entropy) for each component. By (6.82), we obtain another Lagrangian invariant

$$I_1^\alpha=\nabla S_\alpha\frac{\operatorname{curl}\mathbf{V}_\alpha+\frac{e_\alpha\mathbf{H}}{m_\alpha c}+\boldsymbol{\Omega}_\alpha}{n_\alpha} \qquad (6.92)$$

that is analogous, to some extent, to the Ertel integral for a compressible fluid [6.57]. Using consecutively relations (6.82) and (6.85) one can construct the freezing-in integrals and the Lagrangian invariants of higher order with respect to derivatives, e.g.

$$\mathbf{J}_1^\alpha=\frac{1}{n_\alpha}\left[\nabla S_\alpha,\ \nabla\left(\nabla S_\alpha\,\frac{\operatorname{curl}\mathbf{V}_\alpha+\frac{e_\alpha\mathbf{H}}{m_\alpha c}+\boldsymbol{\Omega}_\alpha}{n_\alpha}\right)\right], \qquad (6.93)$$

etc.

Finally, by using (6.88), we obtain the topological invariants

$$I_\alpha^\tau=\int\limits_{\mathcal{V}_0}\left(\operatorname{curl}\mathbf{V}_\alpha+\frac{e_\alpha\mathbf{H}}{m_\alpha c}+\boldsymbol{\Omega}_\alpha\right)\left(\mathbf{V}_\alpha+\frac{e_\alpha\mathbf{A}}{m_\alpha c}+\frac{1}{2}[\boldsymbol{\Omega}_\alpha,\mathbf{r}]\right)d\mathcal{V}, \qquad (6.94)$$

where the integration is performed over the volume whose surface has a normal vector that is orthogonal to the vector $(\operatorname{curl}\mathbf{V}_\alpha+\frac{e_\alpha\mathbf{H}}{m_\alpha c}+\boldsymbol{\Omega}_\alpha)$.

The invariant (6.94) reflects the entanglement of the lines of force of the curl of the generalized momentum field for each plasma component.

The invariants for the hydrodynamic models considered here play an important part in the studies of dynamic processes in continuous media. They facilitate the use of graphic geometric properties of the hydrodynamic models for a qualitative analysis of specific situations (e.g. the change in the "minimum B" principle for plasmas, with vortical motions present, due to (6.91)). Their use substantially facilitates both the search for exact solutions of dynamic equations [6.31] and the construction of various approximate computational schemes. Moreover, the dynamic invariant features manifest themselves also in turbulent processes, and, in principle, allowance for them must result in a finer classification of turbulence patterns than accepted at present. Let us consider how these properties are related to the invariant properties of strong homogeneous turbulence.

As before, we shall not specify a hydrodynamic model since the resulting relations will be valid in all dissipationless media. (Moreover, in relations described below dissipation is of minor importance.) Consider an arbitrary hydrodynamic model with the Lagrangian invariants $I^{\alpha}(x, t)$ $(\alpha = 1, 2, \ldots)$. Let us introduce the correlator

$$K^{\alpha\beta}(r, t) = \langle I^{\alpha}(x_1 t)\, I^{\beta}(x_2 t)\, \rho(x_1 t)\, \rho(x_2 t)\rangle.$$

By virtue of homogeneity it depends on $\mathbf{r} = \mathbf{x}_1 - \mathbf{x}_2$. For the sake of simplicity, we assume that $\langle I^{\alpha}\rho\rangle = 0$ (this is not essential since otherwise one can consider $K^{\alpha\beta} - \langle I^{\alpha}\rho\rangle\langle I^{\alpha}\rho\rangle$. The equation describing the temporal evolution of the correlator can be easily derived using the continuity equation and Eq. (6.79)

$$\frac{\partial K^{\alpha\beta}}{\partial t} + \operatorname{div} \mathbf{P}^{\alpha\beta} = 0;$$

$$\mathbf{P}^{\alpha\beta} = \langle I^{\alpha}(x_1 t)\, I^{\beta}(x_2 t)\, \rho(x_1 t)\, \rho(x_2 t)\, \mathbf{V}(x_1)\rangle - \langle I^{\alpha}(x_1 t)\, I^{\beta}(x_2 t)\, \rho(x_1 t)\, \rho(x_2 t)\, \mathbf{V}(x_2)\rangle.$$

This equation implies that, taking into account $\mathbf{P}^{\alpha\beta}|_{r \to \infty} \to 0$, the quantity

$$I_{\tau}^{\alpha\beta} = \int_{-\infty}^{+\infty} K^{\alpha\beta}(r, t)\, d^3 r \tag{6.95}$$

is conserved, i.e.

$$\frac{\partial I_{\tau}^{\alpha\beta}}{\partial t} = 0.$$

Thus, in the case of homogeneous turbulence, the presence of Lagrangian invariants gives rise to the conservation laws that characterize its large-scale properties. It can be easily understood that using the relations (6.82) brings about other invariants of the homogeneous turbulence that contain the freezing-in integrals

$$I_{\tau}^{\alpha\beta} = \int \langle \nabla I^{\alpha}(x_1 t)\, \mathbf{J}(x_1 t)\, \nabla I^{\beta}(x_2 t)\, \mathbf{J}(x_2 t)\, \rho(x_1 t)\, \rho(x_2 t)\rangle\, dr^3. \tag{6.96}$$

The relations (6.95) and (6.96) enable us to construct statistical invariants in specific hydrodynamic models. This, quite naturally, leads to different kinds of homogeneous turbulence which are characterized by nonvanishing statistical invariants. Such a classification of turbulent modes may be justified since the presence of the invariants affects the basic turbulence properties (such as spectral parameters, transfer coefficients, etc.). To see that this is so, note that the invariants if they exist enter into the set of arguments of the characteristic functional. This, in turn, modifies the scaling theorem (see Sec. 6.2) and results in emergence of spectral regions of a non-Kolmogorov form. The effect of the additional invariants on spectral characteristics can be illustrated by helical or two-dimensional turbulence [6.28, 6.29].

6.4.2. Topological Solitons and Their Classification

In what follows, we consider vortical motions in hydrodynamic media that possess a nontrivial topology and that are main candidates for stable localized formations. Such vortices are usually referred to as topological solitons. Such a term has emerged under the influence of works on quantum and classical field theories. It is based on the fact that the action of a nonlinearity is restricted by topological exclusion rules for a transition from one localized state to another (of course, concurrent with energy principles). In this sense topology contains another general mechanism bringing about localized quasi-particle solutions. An example of another mechanism is well known, it is the formation of a dynamic soliton, when the action of a nonlinearity is compensated by dispersion. Prior to describing topological solitons, let us consider in more detail, from a somewhat less formal standpoint, the basic physical properties of the above hydrodynamic models.

(1) All hydrodynamic models of dissipationless media involve freezing-in integrals.

(2) Usually, the fields **J** frozen in a medium are described by solenoidal fields (i.e. div. $\rho \mathbf{J} = 0$, where ρ is the medium density).

(3) The fields **J** possess topological invariants associated with the conservation of the linkage number for the force lines of the frozen-in fields.

Let us discuss the properties (1)-(3) in more detail. In hydrodynamic models, the freezing-in integrals can be derived from the Lagrangian invariants whose existence in dissipationless media is obvious. There are well-known examples of frozen-in fields, such as (curl **V**)/ρ in a compressible ideal fluid, **H**/ρ in MHD, $\frac{1}{\rho_\alpha}\left(\text{curl } \mathbf{V}_\alpha + \frac{e_\alpha}{m_\alpha c}\mathbf{H}\right)$ in the two-fluid plasma model, etc. It is easily seen that property (2) is fulfilled for all the above examples. The main property of the frozen-in fields, viz. the temporal evolution of the lines of force of such fields, reduces to their convection by motion, i.e. the lines of force are permanently attached to the medium. This phenomenon justifies the term "frozen-in" for these fields. As shown above, property (3) results from property (1) and is only introduced for convenience.

Indeed, in physical terms, property (3) means that an attempt to uncouple linked lines of force by medium motions would inevitably end in their intersection. Then at some spatial point there could be defined two vectors tangential to both lines of force, this resulting in the violation of uniqueness of the field of a frozen-in quantity. This violation, naturally, contradicts basic properties of continuous media. However, it seems that such an unlinkage could be performed by another method, viz. by considering not only the closed lines of force but also those tending to infinity. The simplest example of such a situation is the field $\mathbf{H} = tH_0 [\mathbf{l}_z, \mathbf{r}] + H_0\mathbf{l}_z (t - 1)$ having at $t = 1$ closed lines of force and at $t = 0$, straight lines tending to infinity. Nevertheless, physically such a situation is meaningless. Indeed, the process of unlinkage should be accomplished due to the motion of medium [6.1] yet, since velocities are finite, it requires an infinite time. It is quite evident that such situations are not to be studied since allowance for dissipative processes invalidates the adopted model. A more rigorous justification of property (3) is associated with differential topology and may be formulated in terms of topological invariants [6.54], where the infinite transition time is not forbidden due to compactifying R^3 (thereby the transitions from the closed lines of force to the unclosed ones via infinity are forbidden).

Now let us return to property (2) that provides abundant information on freezing-in integrals. Physically, this property implies the absence of the J-field charges. In other words, the lines of force of these fields can be either closed lines going to infinity or they can cover everywhere densely a manifold of dimension higher than 1. The latter type of lines of force is most probable since it is related to the general case. Unclosed lines of force within a finite volume that are wound round a torus with an irrational ratio of rotation-frequencies is an example of this type. In this situation the line of force forms a dense set on T^2. A more sophisticated behaviour has not been detected analytically, even though numerical results [6.58] indicate the existence of lines filling in the whole domains of the space R^3. Information on the types of lines of force and their evolution in time makes it possible to use the advanced apparatus of the manifold foliation theory [6.59], this being the most conforming to the natural physical language of the problems under consideration. The partition of a manifold M^n (of dimension n) into submanifolds (folia) of the same dimension $k < n$, that are locally diffeomorphic to the partition of an n-dimensional cube into parallel k-dimensional planes, is referred to as a foliation of dimension k. Foliations are exemplified by the lines of force of frozen-in fields (a one-dimensional foliation). Now let us clarify on which manifolds foliations will be of interest for physical applications. Boundary conditions play a prime role in the determination of a manifold. Since we are interested in localized solutions, this means that starting from a certain sphere (can be of an infinite radius) the field $\mathbf{J}$ takes on a constant value $\mathbf{J}_\infty$. Upon identifying domain boundary points or supplementing R^3 with an infinitely removed point we obtain the three-dimensional sphere S^3 while the field **J** transforms into a vector field **Y** tangential on S^3 [6.60]. Let us stress the fact that the infinity point is no longer distinguished and so it is impossible to unlink the lines of force via infinity. As a result, a nontrivial topology emerges that is conserved over arbitrary time spans. Thus, below we consider one-dimensional foliations on S^3 corresponding to the lines of force of the frozen-in fields of the localized solutions of hydrodynamic models. Such foliations are determined by a nonvanishing vector field (or by a direction field). The vector field **Y** defining a foliation on S^3 simultaneously defines a mapping $R^3 \cup \infty \equiv S^3 \rightarrow S^2$, $(\mathbf{J}/|\mathbf{J}\,|)^2 = 1$. Therefore the classification of vector fields reduces to the classification of mappings. If we consider mappings as topologically nonequivalent if they cannot be reduced one into another by continuous deformation, we arrive at the notion of the homotopic classification of mappings [6.54]. Such a classification of the mapping $S^3 \rightarrow S^2$ is well known and is defined by the homotopic group $\pi_3(S^2) = \mathbb{Z}$ [6.54] ($\mathbb{Z}$ is the additive group of integers). This means that there exists a countable number of irreducible foliations. Whether a mapping belongs in one or another homotopic class is determined by the value of the Hopf invariant [6.54]. This invariant is defined as an integer H of the linkages of the pre-images of two points belonging to S^2:

$$H = \{f^{-1}(x),\ f^{-1}(y)\}, \quad x,\ y \in S^2; \quad f\colon\ S^3 \rightarrow S^2,$$

where $\{\ldots\}$ denotes the linkage coefficient that coincides, in the simplest case, with the number of times one contour goes around another and that, in the Euclidean space R^3, can be calculated for two curves γ_1 and γ_2 as

$$\{\gamma_1,\ \gamma_2\} = \frac{1}{4\pi} \oint\limits_{\gamma_1} \oint\limits_{\gamma_2} \frac{[d\mathbf{r}_1,\ d\mathbf{r}_2]\,(\mathbf{r}_2 - \mathbf{r}_1)}{|\mathbf{r}_2 - \mathbf{r}_1|^3}\,. \tag{6.97}$$

Thus, a countable number of the vector fields exists on S^3 which are mutually irreducible in a continuous manner. The above considerations are fairly general and hold even for a velocity field and not only for frozen-in fields. However, a question arises whether these fields satisfy the main properties of frozen-in fields (i.e. whether they are solenoidal). It is intuitively clear that the absence of zeros of these fields implies that their lines of force behave in the same manner as those of frozen-in fields. And this means an affirmative answer to the question. This can be proved by choosing a more convenient mapping $S^3 \rightarrow S^2$ that is analogous to the mapping used earlier for an incompressible fluid [6.61]. As demonstrated above [6.31], the frozen-in quantities can be represented as

$$J_\alpha = \frac{1}{\rho}\, \varepsilon_{ikl} e_{\alpha\beta\gamma} I_i\, \frac{\partial I_k}{\partial x_\beta}\, \frac{\partial I_l}{\partial x_\gamma}\,, \tag{6.98}$$

where the quantities I_l are the Lagrangian invariants. **J** satisfies the freezing-in equation and, with the coupling $f(I_1\ I_2\ I_3) = 0$ between the Lagrangian invariants I_1, I_2, I_3 the **J**-field is solenoidal ($\operatorname{div} \rho \mathbf{J} = 0$). The relation $f(I_1\ I_2\ I_3) = 0$ determines a two-dimensional manifold M^2 whose temporal evolution reduces to a continuous deformation by a motion. It can be easily understood if we take into account that I_l are the Lagrangian invariants. Such deformations preserve the topological structure of the manifold. Since M^2 can be a surface with edge or a closed surface of kind m [6.54], the kind of the manifold M^2 is the topological invariant. Now consider how the **J**- and **I**-fields are related. It can be easily shown that the level lines of the field **I** (i.e. x: $\mathbf{I}(x) = \mathbf{I}_0$) coincide with the lines of force of the **J**-field. Indeed, suppose that the field $\mathbf{I}(x)$ takes on a constant value $(\mathbf{I}(x(S)) = \mathbf{I}_0$ along the line $\mathbf{x} = \mathbf{x}(S)$. Let us calculate the vector product of **J** and of the tangential vector of this line, $d\mathrm{x} = \frac{\partial \mathbf{x}}{\partial S} dS$, i.e.

$$[\mathbf{J},\ d\mathbf{x}]_\beta = 2\varepsilon_{ikl}\, dx_\gamma \frac{\partial I_l}{\partial x_\gamma} I_l \frac{\partial I_k}{\partial x_\beta}.$$

The directional derivative $d\mathbf{x}$ of the **I**-field vanishes, by the definition $\mathbf{x} = \mathbf{x}(S)$, and, hence,

$$[\mathbf{J},\ d\mathbf{x}] = 0.$$

On the other hand, this relation coincides with the equation for the lines of force of the **J**-field. Hence, the line of force of the frozen-in **J**-field does coincide with the level line of the **I**-field. Thus we obtain the mapping $S^3 \to M^2$ that puts a point on the manifold M^2 (I_{0l}) into a correspondence with the line of force of **J**. Returning to the homotopic invariant of the mappings $S^3 \to S^2$ (for $M^2 = S^2$) one can easily see its physical sense. The Hopf invariant coincides with the linkage coefficient of the lines of force of the frozen-in fields.

It should be noted that the above classification of topological solitons is not complete. Indeed, two linked circles and a three-fold knot have the same Hopf invariant. For frozen-in fields, it is evident that a transition, in a continuous way, of one configuration of lines of force into another is impossible. Thus, within a single class of topological solitons having the same Hopf invariant, the topologically different configurations exist which cannot be transformed one into another. Physically, such an ambiguity implies that the notion of the homotopy of mappings does not adequately reflects the conservation of the structure of the lines of force of frozen-in fields. Such lines are deformed by a medium motion in a continuous way, without discontinuities and matchings, this meaning that more adequate is the following equivalence relation. Foliations are equivalent (i.e. they are mutually reducible due to a medium motion), if there exists a homeomorphism h: $S^3 \to S^3$ such that h transforms the folia of one foliation into those of another. Yet now this equivalence relation distinguishes between different types of knots, linked circles not being pairwise linked, etc. Thus, the classification of topological solitons must also include the classification of the types of closed trajectories. In addition, the different types of lines of force are realizable in a single soliton. Therefore the type of a topological soliton is determined by the Hopf invariant, by the number of topologically independent classes of lines of force and, finally, by the type of lines of force belonging to each class.

The most complicated classification concerns the types of lines of force, particularly, the types of knots and it is far from being complete. As is well known, now only toric knots are classified [6.62]. Different types of topological solitons will be considered below.

6.4.3. Examples of Topological Solitons

Now we turn to the construction of topological solitons of different types. To do this, we construct one-dimensional foliations on S^3 whose folia are the lines of force of the solitons under study. Since we are interested in topologically nontrivial foliations, it is necessary to find foliations with linkages (which is possible, if the folia are closed). Let us begin with a somewhat more general situation. Consider a sphere S^3 embedded into R^4 with the coordinates $(q_1, q_2, q_3, q_4) \equiv q$. Introducing for convenience the complex numbers $Z_1 = q_1 + iq_2$, $Z_2 = q_3 + iq_4$ we describe the sphere by

$$|Z_1|^2 + |Z_2|^2 = 1.$$

The folia of a one-dimensional foliation on S^3 will be defined via the following equivalence relation: $(Z_1, Z_2) \sim (Z_1', Z_2')$, if $Z_1' = Z_1 e^{i\omega_1 t}$, $Z_2' = Z_2 e^{i\omega_2 t}$ ($t \in R$ and ω_1, ω_2 are real numbers). Each equivalence class defines a one-dimensional folium on S^3. It can be easily understood that, under commensurable ω_1 and ω_2, the foliation so introduced contains only closed folia, while under incommensurable ω_1 and ω_2 almost all the folia are unclosed, except of the two, $(Z_1, 0)$ and $(0, Z_2)$. Consequently, for any ω_1 and ω_2 the foliation contains the folia with the same properties as those of the lines of force of frozen-in fields. This means that a vector field with such lines can be chosen as frozen-in quantity. It should be noted that the field thus reconstructed can be multiplied by an arbitrary nonvanishing function, because such a procedure does not change the topological structure of lines of force. An integral curve in a neighbourhood of an arbitrary point (Z_1, Z_2) is described by the relation

$$l(t) = (Z_1 \exp(i\omega_1 t),\ Z_2 \exp(i\omega_2 t)),$$

which gives the relevant vector field

$$\mathbf{Y}(\omega_1, \omega_2) = (-\omega_1 q_1,\ \omega_1 q_2,\ -\omega_2 q_4,\ \omega_2 q_3). \qquad (6.99)$$

The field $\mathbf{Y}(\omega_1, \omega_2)$ admits a graphic physical interpretation. Indeed, it coincides with the field of two uncoupled oscillators ($\dot{Z}_1 = i\omega_1 Z_1$, $\dot{Z}_2 = i\omega_2 Z_2$) having the oscillation frequencies ω_1 and ω_2, respectively. Evidently, such a field is nonsingular and tangential to S^3, i.e. $\mathbf{Y}\mathbf{q} = 0$. This circumstance is not a pure coincidence.

Let us consider Hamiltonian flows in R^4. As is well known, the phase volume is conserved for such flows, i.e. they are solenoidal in R^4. By virtue of the tangentiality of the Hamiltonian field to S^3, local coordinates have no radial field component and the divergence in R^4 reduces to that in the independent S^3 coordinates. Thus, the Hamiltonian flows, tangential to S^3, conserve the volume in S^3 and hence their lines of force possess all the properties of those of frozen-in fields. This circumstance makes it possible to construct various examples of localized configurations of such fields (to be more exact, of the initial conditions for them). Returning to the above example, let us study the properties of the vector field $\mathbf{Y}(\omega_1, \omega_2)$. As a graphic example, we consider these properties not on S^3 but in a real physical space R^3 having the coordinates (x_1, x_2, x_3). By mapping R^3 into S^3 via the stereographic projection we get

$$q_i = \frac{2x_i}{1+x^2}, \quad q_4 = \frac{1-x^2}{1+x^2} \quad (i = 1, 2, 3).$$

Next, we induce the mapping of the linear form $\omega_Y = Y_\alpha dq_\alpha$ ($\alpha = 1, 2, 3, 4$) defined on S^3 into the linear form $\omega_J = J_i dx_i$ on R^3. Taking into account the fact that the linear forms are invariant under the mapping [6.58, 6.63], i.e.

$$J_i dx_i = Y_\alpha dq_\alpha,$$

and the tangentiality of $\mathbf{Y}$ to S^3, we obtain for $\mathbf{J}$ in R^3 the following expression:

$$\mathbf{J} = \frac{2}{(1+x^2)^2}\{-2(\omega_1 x_2 + \omega_2 x_1 x_3),\ 2(\omega x_1 - x_2 x_3 \omega_2),$$
$$-\omega_2(1 - x_1^2 - x_2^2 + x_3^2)\}.$$

The vector field $\mathbf{J}$ possesses, by construction, the same lines of force as those of frozen-in fields. Therefore, multiplying by a nonvanishing function (see the remark above) we obtain a purely vortical field

$$\mathbf{J}_{\omega_1\omega_2} = \frac{2}{(1+x^2)^2}\{-2(\omega_1 x_2 + \omega_2 x_1 x_3),\ 2(\omega_1 x_1 - \omega_2 x_2 x_3),$$
$$-\omega_2(1 - x_1^2 - x_2^2 + x_3^2)\}. \tag{6.100}$$

Since the line of force that passes through the point (Z_1^0, Z_2^0) is described in R^4 by the equation $(Z_1, Z_2) = (Z_1^0 e^{i\omega_1 t}, Z_2^0 e^{i\omega_2 t})$, then passing to R^3 by means of the stereographic projection we obtain the following expression for the force line:

$$
\begin{aligned}
x_1(t) &= \frac{2(x_1^0 \cos\omega_1 t - x_2^0 \sin\omega_1 t)}{1 + x_0^2 + (1 - x_0^2)\cos\omega_2 t + 2x_3^0 \sin\omega_2 t}, \\
x_2(t) &= \frac{2(x_2^0 \cos\omega_1 t + x_1^0 \sin\omega_1 t)}{1 + x_0^2 + (1 - x_0^2)\cos\omega_2 t + 2x_3^0 \sin\omega_2 t}, \\
x_3(t) &= \frac{2x_3^0 \cos\omega_2 t - (1 - x_0^2)\sin\omega_2 t}{1 + x_0^2 + (1 - x_0^2)\cos\omega_2 t + 2x_3^0 \sin\omega_2 t},
\end{aligned}
\tag{6.101}
$$

where x_i^0 are the R^3-coordinates of the point (Z_1^0, Z_2^0). Eliminating time from (6.101) and using trigonometric identities one can easily show that these curves lie on stratified tori

$$
\begin{aligned}
&x_1^2 + \left(\sqrt{x_1^2 + x_2^2} - a\right)^2 = a^2 - 1, \\
&a = \frac{1}{2}(1 + x_0^2)(x_{01}^2 + x_{02}^2)^{-1/2}
\end{aligned}
$$

that are produced by the rotation of the circle $x_3^2 + (x_1 - a)^2 = a^2 - 1$ around the x_3-axis. The central torus degenerates into a circle with the coordinates $x_3 = 0$, $x_1^2 + x_2^2 = 1$. The lines of force wind round the tori with the rotation frequencies ω_1 and ω_2. This can be verified by passing to the angular coordinates defined on a torus. Thus, under incommensurable ω_1 and ω_2 the field $\mathbf{J}_{\omega_1\omega_2}$ has the unique closed trajectory $x_1^2 + x_2^2 = 1$ and all other trajectories everywhere densely cover the tori while being unclosed. For the commensurable ω_1 and ω_2 (e.g. $\omega_1 = m$, $\omega_2 = n$ are relatively prime numbers), the lines of force will be linked into (m, n) knots which at different (m, n) are topologically nonequivalent and form the known class of toric nodes [6.62].

Next, we are going to determine the linkage number of the lines of force using relation (6.97) and determining the topological soliton charge by the invariant

$$
I^\tau = \int_{\mathcal{V}_0} JA\, d\mathcal{V}_0.
$$

However, here the linkage number can be easily obtained from simple geometric considerations. Indeed, the central line of force is coupled with any trajectory on a torus ($\omega_1 = m$, $\omega_2 = n$) mn times, i.e. the topological charge is equal to mn. Therefore, the analyzed field $\mathbf{J}_{\omega_1\omega_2}$ chosen as an initial condition exemplifies the topological solitons with any topological charge $H = \pm 1, \pm 2, \pm 3, \ldots$, whose lines of force form knots of type (mn), and for an irrational ω_1/ω_2 it provides an interesting example of a vortex with one closed line of force.

Let us stress that for $\omega_1 = m$, $\omega_2 = n > 1$ and the topological charge mn the solitons contain three classes of topologically nonequivalent trajectories (a circle, a straight line tending to infinity, and an (mn) type knot) and for $\omega_1 = \omega_2 = 1$, two classes of trajectories (a circle and a straight line). The above examples include solitons with coincident topological charges ($\omega_1 = m$, $\omega_2 = n$, $\omega_1 = 1$, $\omega_2 = mn$) that belong nevertheless to different topological types according to the above classification. For each soliton type one can easily produce an antisoliton with the charge $-mn$, by changing the sign of one of the frequencies to the opposite one. Soliton-antisoliton interaction results in the plane parallel field $\sim(x_2\mathbf{e}_1 + x_1\mathbf{e}_2)$ with a vanishing topological charge ($\mathbf{e}_1$ and $\mathbf{e}_2$ are unit vectors).

The vortices corresponding to $\omega_1 = \omega_2 = 1$ were found by different arguments in [6.61, 6.63] for an incompressible fluid and MHD, respectively. In the general case, vortices with $\omega_1 = n$, $\omega_2 = m$ have been found in [6.35].

Let us consider exact MHD solutions. For the stationary case, the basic system of equations is

$$\begin{gathered}\operatorname{div}\mathbf{V} = \operatorname{div}\mathbf{H} = 0,\\ (\mathbf{V}\nabla)\mathbf{H} = (\mathbf{H}\nabla)\mathbf{V},\\ (\mathbf{V}\nabla)\mathbf{V} - \frac{1}{4\pi\rho}(\mathbf{H}\nabla)\mathbf{H} = -\frac{1}{\rho}\nabla\left(P + \frac{H^2}{8\pi}\right).\end{gathered} \tag{6.102}$$

where H is the magnetic field. The partial solutions of this system corresponding to the motions along the lines of force of the magnetic field $\mathbf{H}$ are known:

$$\mathbf{V} = \pm\frac{\mathbf{H}}{(4\pi\rho)^{1/2}}. \tag{6.103}$$

This relation is the specific MHD version of the one-parameter class of the solutions of the freezing-in equation that exists for all hydrodynamic models:

$$\mathbf{J} = c\mathbf{V}. \tag{6.104}$$

This class of motions contains topologically nontrivial configurations. Moreover, for localized motions this very class is of utmost interest. The point is that under stationary conditions the J- and V-fields commute, and two commuting fields, tangential to S^3, must be linearly dependent [6.64].

The fields $\mathbf{J}_{\omega_1\omega_2}$ constructed above are exact solutions of the system of equations (6.102) and in terms of dimensional variables they take the form

$$\begin{aligned}\mathbf{H} = \frac{2H_0L^4}{(L^2+x^2)^3}\big(&-2(\omega_1Lx_2 + \omega_2x_1x_3),\ 2(\omega_1Lx_1 - \omega_2x_2x_3),\\ &-\omega_2(L^2 - x_1^2 - x_2^2 + x_3^2)\big),\end{aligned} \tag{6.105}$$

where L is the vortex characteristic scale. The qualitative structure of the solutions has been discussed in detail above. All the cited soliton types possess finite macrocharacteristics (total energy E, Moffatt's invariant I^{τ})

$$E_H = \frac{\pi(\omega_1^2 + \omega_2^2)}{16} H_0^2 L^2,$$
$$I^{\tau} = 8\pi \frac{\omega_1 \omega_2 L}{\omega_1^2 + \omega_2^2} E_H. \tag{6.106}$$

These relations show that solitons with the same topological charge mn but with different types of the lines of force, (m, n) and $(1, mn)$, have different energies

$$(E_{mn} \sim (m^2 + n^2), \quad E_{1\,mn} \sim (1 + m^2 n^2)),$$

$E_{1,mn} > E_{m,n}$, i.e. favourable in energy terms is a soliton with lines of force of (m, n) type, as compared with a soliton with lines of force of $(1, mn)$ type. Other examples of exact MHD solutions can be obtained by taking into account the above mentioned relation with Hamiltonian flows.

An example of a topological soliton of a more complex type is presented by the field **H** (6.105), with $\omega_1 = f\,(1 + x^2 - 2\sqrt{x_1^2 + x_2^2})$ (f is an arbitrary function). The choice of this function affects the winding frequency ω_1 when passing from one torus onto another. Here the soliton contains the lines of force of different (m, n) types that occur intermittently with tori having the irrational ratio of winding frequencies. These solitons are also the exact solutions of the MHD equations.

We have considered the solitons that exist in all hydrodynamic models. In particular, the soliton with $\omega_1 = \omega_2$ is the exact solution of systems of equations for a compressible fluid, two-component plasma model, and incompressible fluid.

In conclusion we present the topological solitons as the exact solutions of two-fluid plasma hydrodynamics.

In this case relation (6.104) is replaced by the following system of equations:

$$\operatorname{curl} \mathbf{V}_\alpha + \frac{e_\alpha \mathbf{H}}{m_\alpha c} = C_\alpha n_\alpha \mathbf{V}_\alpha \tag{6.107}$$

Supplementing (6.107) by the Maxwell equation

$$\operatorname{curl} \mathbf{H} = \frac{4\pi}{c} \sum e_\alpha n_\alpha \mathbf{V}_\alpha \tag{6.108}$$

in the incompressible case we obtain a closed system of equations that describes stationary flows and fields with a "generalized helicity".

We shall search for **H** and $\mathbf{V}_\alpha$ in the form

$$\mathbf{H} = \operatorname{curl}\operatorname{curl}(\mathbf{x}\Psi) + \operatorname{curl}(\mathbf{x}\varphi),$$
$$\mathbf{V}_\alpha = \operatorname{curl}\operatorname{curl}(\mathbf{x}F_\alpha) + \operatorname{curl}(\mathbf{x}\Phi_\alpha). \tag{6.109}$$

From the system (6.107) and (6.108) we derive equations that define the potentials Ψ, φ, F_α, Φ_α:

$$\begin{gathered}\Delta F_\alpha + C_\alpha n_\alpha \Phi_\alpha = \frac{e_\alpha}{m_\alpha c}\varphi, \quad \Phi_\alpha = C_\alpha n_\alpha F_\alpha - \frac{e_\alpha \Psi}{m_\alpha c}, \\ \Delta\Psi + \frac{4\pi}{c}\sum e_\alpha n_\alpha \Phi_\alpha = 0, \quad \varphi = \frac{4\pi}{c}\sum e_\alpha n_\alpha F_\alpha. \end{gathered} \tag{6.110}$$

Eliminating φ and Φ_α we obtain

$$\begin{gathered}\Delta F_\alpha + C_\alpha^2 n_\alpha^2 F_\alpha = \frac{e_\alpha}{m_\alpha c}\left(C_\alpha n_\alpha \Psi + \frac{4\pi}{c}\sum e_\beta n_\beta F_\beta\right), \\ \Delta\Psi - \frac{\omega_p^2}{c^2}\Psi + \frac{4\pi}{c}\sum e_\alpha C_\alpha n_\alpha^2 F_\alpha = 0, \\ \frac{\omega_p^2}{c^2} = \frac{4\pi}{c}\sum \frac{e_\alpha^2 n_\alpha}{c m_\alpha}. \end{gathered} \tag{6.111}$$

The simplest specific solutions of (6.111) can be easily found by assuming that $F_\alpha = b_\alpha F$, $\Psi = \varkappa F$ (b_α, $\varkappa$ are some arbitrary constants). The consistency condition for (6.111) yields the system of equations for b_α and $\varkappa$:

$$\begin{gathered} b_\alpha C_\alpha^2 n_\alpha^2 - \varkappa \frac{e_\alpha C_\alpha n_\alpha}{m_\alpha c} - \frac{4\pi}{c}\frac{e_\alpha}{m_\alpha c}\sum e_\beta n_\beta b_\beta = \beta b_\alpha \\ \frac{4\pi}{c}\sum e_\beta C_\beta n_\beta^2 b_\beta = \left(\beta + \frac{\omega_p^2}{c^2}\right)\varkappa, \end{gathered} \tag{6.112}$$

while the system of equations (6.111) reduces to the single equation

$$\Delta F + \beta F = 0.$$

This equation contains β that can be either positive or negative depending on the C_α values (for more detail, see [6.31]). In the spherical domain, at $\beta > 0$, the solution has the form

$$F = F_0 r^{-1/2} J_{3/2}(\beta^{1/2} r)\cos\theta. \tag{6.113}$$

By selecting the boundary conditions

$$J_{3/2}(\beta^{1/2}R) = 0, \quad 3H_0 = -F_0 \varkappa \frac{d}{dR}\left(R^{-1/2} J_{3/2}(\beta^{1/2}R)\right),$$

one can match the resulting solution with that of the external problem (even in the absence of plasma outside a sphere of radius R) having a field constant at infinity. Lines of force and stream lines are wound round a family of embedded tori (Fig. 6.8). On an outer torus nonvanishing are only $V_{0\alpha}$ and H_0 components of the field and velocity.

The overwhelming majority of lines of force of magnetic field and of plasma stream lines, when in a closed volume ($r \leqslant R$), are wound round tori with an irrational ratio of rotation frequencies. The topological invariant (6.94) is nonvanishing, this indicating the topological nontriviality of the relations obtained. The magnetic field configuration in the obtained vortex coincides with that of the well-known MHD vortex [6.65]. Similar vortices can exist in plasma flows, where two cases as dependent on C_α are possible, when V_i and V_e at the boundary have the same or opposite directions. In the latter case such vortices can be observed in counter-current flows of ionic and electronic plasma components.

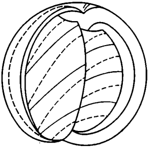

Fig. 6.8

References

6.1. A. N. Kolmogorov, *Dokl. Akad. Nauk SSSR*, 30, 4, 299 (1941); A. M. Obukhov, *Izv. Akad. Nauk SSSR, Ser. Geogr. i Geofiz.*, 5, 4-5, 453 (1941).
6.2. A. S. Monin and A. M. Yaglom, *Statistical Hydromechanics*, Part 2, Nauka, Moscow, 1967 (in Russian).
6.3. E. Hopf, *J. Rat. Mech. Anal.* 1, 1, 87 (1952).
6.4. H. W. Wyld, *Ann. Phys.*, 14, 2, 143 (1961).
6.5. V. E. Zakharov and V. S. L'vov, *Izv. VUZov, Radiofizika*, 28, 10, 1470 (1975).
6.6. D. Foster, D. R. Nelson, and M. J. Stephen, *Phys. Rev.*, A16, 732 (1977).
6.7. C. DeDominicis and D. C. Martin, *Phys. Rev.*, A19, 419 (1979).
6.8. L. Ts. Ajemyan, A. N. Vasil'ev, and Yu. M. Pis'mak, *Teor. Mat. Fiz.*, 57, 2, 268 (1983).
6.9. N. N. Bogolyubov and D. V. Shirkov, *Introduction to the Theory of Quantized Fields*, Nauka, Moscow, 1976 (in Russian).
6.10. K. G. Wilson, *Phys. Rev.*, B4, 3175, 3184 (1971).
6.11. S. S. Moiseev, A. V. Tur, and V. V. Yanovskii, *Zh. Eksp. Teor. Fiziki*, 71, 9, 1062 (1976).
6.12. S. S. Moiseev, A. V. Tur, and V. V. Yanovskii, *Dokl. Akad. Nauk SSSR*, 250, 4, 848 (1980).
6.13. S. S. Moiseev, V. I. Petviaschvili, A. V. Tur, and V. V. Yanovsky, *Physica* 2D, 218 (1981).
6.14. S. S. Moiseev, A. V. Tur, and V. V. Yanovskii, *Dokl. Akad. Nauk SSSR*, 269, 3, 600 (1983).

6.15. V. E. Zakharov, in: *The Fundamentals of Plasma Physics*, Vol. 2, Energoatomizdat, Moscow, 1984 (in Russian).
6.16. V. E. Zakharov, *Prikl. Mekh. Tekhn. Fiz.*, 4, 35 (1965).
6.17. A. V. Kats and V. M. Kantorovich, *Zh. Eksp. Teor. Fiziki*, 64, 1, 151 (1973).
6.18. R. H. Kraichnan, *Phys. Fluids*, 7, 1723 (1964).
6.19. B. B. Kadomtsev, *Problems of Plasma Theory*, Issue 4, Atomizdat, Moscow, 1964 (in Russian).
6.20. R. H. Kraichnan, *J. Fluid Mech.*, 83, 2, 349 (1977).
6.21. G. A. Kuz'min and A. Z. Patashinskii, Preprint IYaF SO AN SSSR, No. 76-20, Novosibirsk, 1976 (in Russian).
6.22. E. A. Kuznetsov and V. S. L'vov, *Phys. Lett.*, 64A, 157 (1977).
6.23. V. S. L'vov, Preprint IAiE SO AN SSSR, No. 53, Novosibirsk, 1977 (in Russian).
6.24. A. V. Tur, V. V. Yanovsky, and S. S. Moiseev, *Nonlinear and Turbulent Processes*, Vol. 3, Gordon and Breach, 1984, p. 1683.
6.25. S. S. Moiseev, A. V. Tur, and V. V. Yanovskii, *Dokl. Akad. Nauk SSSR*, 279, 1, 96 (1984).
6.26. N. G. Van Kampen, *Physica*, 21, 949 (1955).
6.27. K. M. Case, *Phys. Fluids*, 3, 143 (1960).
6.28. A. T. Mirabel' and A. S. Monin, *Uspekhi Mekhaniki*, 2, 3, 47 (1979).
6.29. E. A. Kuznetsov and N. N. Noskov, *Zh. Eksp. Teor. Fiziki*, 75, 4, 1309 (1978).
6.30. R. H. Kraichnan and S. Nagarajan, *Phys. Fluids*, 10, 859 (1967).
6.31. S. S. Moiseev, R. Z. Sagdeev, A. V. Tur, and V. V. Yanovskii, *Zh. Eksp. Teor. Fiziki*, 83, 1 (7), 215 (1982).
6.32. R. Z. Sagdeev, *Problems of Plasma Physics*, Issue 4, Atomizdat, Moscow, 1964 (in Russian).
6.33. M. Steenbeck, F. Krause, and K. H. Rädler, *Z. Naturforsch.*, 21a, 369 (1966).
6.34. S. S. Moiseev, R. Z. Sagdeev, A. V. Tur, G. A. Khomenko, and A. M. Shukurov, *Dokl. Akad. Nauk SSSR*, 273, 3, 549 (1983).
6.35. A. V. Tur and V. V. Yanovsky, in: *Nonlinear and Turbulent Processes*, Vol. 2, Gordon and Breach, 1984, p. 1079.
6.36. S. S. Moiseev, A. V. Tur, and V. V. Yanovskii, *Zh. Eksp. Teor. Fiziki*, 47, 3, 473 (1977).
6.37. G. A. Kuz'min and A. Z. Patashinskii, *Zh. Eksp. Teor. Fiziki*, 62, 1175 (1972).
6.38. A. G. Sazontov, *Izv. Akad. Nauk SSSR, Ser. Fiz. Atm. i Okeana*, 25, 8, 820 (1979).
6.39. R. Boldgiano, *J. Geophys. Res.*, 64, 12, 851 (1959).
6.40. A. M. Obukhov, *Dokl. Akad. Nauk SSSR*, 125, 6, 1246 (1959).
6.41. V. M. Loginov, *Zeitschrift für Phys.*, B37, 363, (1980)
6.42. M. I. Vishik and A. V. Fursikov, *Mathematical Problems of Statistical Hydrodynamics*, Nauka, Moscow, 1980 (in Russian).
6.43. G. Tennekes, in: *Handbook of Turbulence. Fundamentals and Applications*, Vol. 1, ed. W. Frost and T. Moulden, New York, 1977.
6.44. B. B. Kadomtsev and V. I. Petviashvili, *Dokl. Akad. Nauk SSSR*, 208, 4, 794 (1973).
6.45. S. S. Moiseev, R. Z. Sagdeev, A. V. Tur, and V. V. Yanovskii, in: *Nonlinear Waves*, Nauka, Moscow, 1979 (in Russian).
6.46. V. S. L'vov and A. V. Mikhailov, *Zh. Eksp. Teor. Fiziki*, 74, 4, 1445 (1978).
6.47. V. E. Zakharov and R. Z. Sagdeev, *Dokl. Akad. Nauk SSSR*, 192, 2, 297 (1970).
6.48. R. H. Kraichnan, *J. Fluid Mech.*, 5, 497 (1959).
6.49. H. Lamb, *Hydrodynamics*, Dover Publications, New York, 1945.
6.50. G. A. Kuz'min, Preprint IYaF SO AN SSSR, No. 87-83, Novosibirsk, 1983 (in Russian).

6.51. P. H. Roberts, *Matematica*, 19, 169 (1972).
6.52. L. D. Faddeev, *Lett. Math. Phys.*, 1, 289 (1976).
6.53. H. K. Moffatt, *J. Fluid Mech.*, 35, 117 (1969).
6.54. B. A. Dubrovin, S. P. Novikov, and A. T. Fomenko, *Modern Geometry*, Nauka, Moscow, 1979 (in Russian).
6.55. P. Penfeld, *Phys. Fluids*, 9, 1184 (1966).
6.56. S. S. Moiseev, R. Z. Sagdeev, A. V. Tur, and V. V. Yanovskii, *Dokl. Akad. Nauk SSSR*, 258, 318 (1981).
6.57. H. Ertel, *Meteorol. Zeitschr.*, B159, 277 (1942).
6.58. V. I. Arnol'd, *Mathematical Methods of Classical Mechanics*, Nauka, Moscow, 1974 (in Russian).
6.59. I. Tamura, *Topology of Foliations*, Iwanami Shoten, 1976 (in Japan); Mir Publishers, Moscow, 1979 (in Russian).
6.60. D. Finkelstein, *J. Math. Phys.*, 7, 7, 1218 (1966).
6.61. E. A. Kuznetsov and A. V. Mikhailov, *Phys. Lett.*, 77A, 1, 37 (1980).
6.62. R. Crowell and R. Fox, *Introduction to Knot Theory*, New York, 1963.
6.63. A. M. Kamchatnov, *Zh. Eksp. Teor. Fiziki*, 82, 1, 117 (1982).
6.64. E. Lima, *Ann. Math.*, 81, 70 (1965).
6.65. S. Chandrasekhar, *Proc. Nat. Acad. Sci.*, 42, 1 (1956).

7

Self-Oscillations and Auto-Waves in Chemical Systems

A.M. Zhabotinskii, D. Sc. (Phys.-Math.)

7.1. INTRODUCTION

In this section, homogeneous systems with isothermic chemical reactions will be considered. Only some 25 years ago it was a widespread opinion that in such systems the only possible stationary modes were steady states in which variables (concentrations of intermediate compounds) were independent of time and space coordinates. Now it is known that such systems allow transitions from some steady states to others, arbitrary periodic self-oscillations, chaotic self-oscillations, periodic and other non-uniform distributions of concentrations in space, and travelling concentration waves. Usually, two simplest experimental situations are used for theoretical analysis and interpretation of results obtained. The first concerns a well-stirred reactor, where hydrodynamic and diffusion processes are intense enough to provide an averaging over space. Here mathematical models are essentially systems of ordinary differential equations corresponding to the scheme of chemical transformations

$$\sum_{i=1}^{n} \alpha_{ij} A_i \xrightarrow{k_j} \sum_{i=1}^{n} \beta_{ij} A_i, \quad j=1, \ldots, m, \tag{7.1}$$

where A_i's are compounds and α_{ij}'s, β_{ij}'s are stoichiometric coefficients. According to the mass action law, the transformation rates of the compounds A_i correspond to each stage in (7.1) as follows:

$$W_{ji} = k_j (\beta_{ij} - \alpha_{ij}) \prod_{i=1}^{n} C_i^{\alpha_{ij}}, \tag{7.2}$$

where $C_i \equiv [A_i]$. In a closed system the complete scheme (7.1) is described by the system of equations

$$\dot{C}_i = \sum_j W_{ji}, \quad i = 1, \ldots, n. \tag{7.3}$$

In chemical systems, the k_j and C_i values differ by many orders of magnitude. Therefore the model (7.3) has a hierarchy of time scales.

To reveal nontrivial dynamic modes needs to have no less than three scales

$$\begin{aligned}\dot{R} &= \varepsilon f(R,\ n,\ u),\\ \dot{n} &= g(R,\ n,\ u),\\ \varepsilon\dot{u} &= h(R,\ n,\ u).\end{aligned} \tag{7.4}$$

Usually, in place of the model (7.4) we study its asymptotics

$$\begin{aligned}R &= R_0,\\ \dot{n} &= g(R_0,\ n,\ u),\\ 0 &= h(R_0,\ n,\ u).\end{aligned} \tag{7.5}$$

Often a continuous-flow stirred-tank reactor (CSTR) is used. Then the model (7.3) is replaced by

$$\dot{C}_i = \sum_j W_{ji} + d(C_{i0} - C_i), \tag{7.6}$$

where d is the exchange rate and C_{i0} are the transformed concentrations in an external tank (the majority of the C_{i0} values are zeros).

Spatial effects are usually studied in reaction-diffusion systems, where the only transfer process is molecular diffusion. Such systems are modelled by the quasi-linear parabolic equations

$$\frac{\partial C}{\partial t} = f(C,\ \alpha) + D\Delta C, \tag{7.7}$$

where the matrix of the diffusion coefficients D is usually diagonal.

7.2. EXPERIMENTAL STUDIES

Belousov [7.1] has discovered the first of the reactions which have permitted to obtain the majority of spatial and temporal modes. The different versions of this reaction were realized and studied by the author [7.2]. The reactions of this type (BZ reactions) turned out to be extremely suitable for various dynamic experiments.

The BZ reactions proceed in an acid water solution. In the course of these reactions bromate ($HBrO_3$) oxidizes various organic compounds by means of a metal ion redox catalyst. The conventional scheme of chemical transformation in these reactions was proposed by Field, Kōros, and Noyes [FKN] [7.3]. Here we present the modified version of the FKN scheme, with the reducing agent in the form of malonic and/or bromomalonic acids

$$
\begin{aligned}
&\mathrm{H^+ + Br^- + HBrO_3 \rightleftharpoons HOBr + HBrO_2},\\
&\mathrm{H^+ + Br^- + HBrO_2 \rightleftharpoons 2HOBr},\\
&\mathrm{H^+ + Br^- + HOBr \rightleftharpoons Br_2 + H_2O},\\
&\mathrm{HBrO_3 + HBrO_2 \rightleftharpoons 2BrO_2 + H_2O},\\
&\mathrm{BrO_2 + Me^{n+} + H^+ \rightleftharpoons Me^{(n+1)+} + HBrO_2},\\
&\mathrm{2HBrO_2 \rightleftharpoons HBrO_3 + HOBr},\\
&\mathrm{Me^{(n+1)+} + CHBr\,(COOH)_2 \rightleftharpoons CBr\,(COOH)_2^{\bullet} + Me^{n+} + H^+},\\
&\mathrm{CBr\,(COOH)_2^{\bullet} + H_2O \rightarrow COH\,(COOH)_2^{\bullet} + H^+ + Br^-},\\
&\mathrm{Me^{(n+1)+} + COH\,(COOH)_2^{\bullet} \rightarrow CO\,(COOH)_2 + H^+ + Me^{n+}}, \qquad (7.8)\\
&\mathrm{COH\,(COOH)_2^{\bullet} + CHBr\,(COOH)_2 \rightleftharpoons CHOH\,(COOH)_2 + CBr\,(COOH)_2^{\bullet}},\\
&\mathrm{Me^{(n+1)+} + CH_2\,(COOH)_2 \rightleftharpoons CH\,(COOH)_2^{\bullet} + Me^{n+} + H^+},\\
&\mathrm{Me^{(n+1)+} + CH\,(COOH)_2^{\bullet} + H_2O \rightarrow CHOH\,(COOH)_2 + Me^{n+} + H^+},\\
&\mathrm{Me^{(n+1)} + CHOH\,(COOH)_2 \rightleftharpoons COH\,(COOH)_2^{\bullet} + Me^{n+} + H^+},\\
&\mathrm{CO\,(COOH)_2 \rightarrow OCHCOOH + CO_2},\\
&\mathrm{HOBr + CH_2\,(COOH)_2 \rightarrow CHBr\,(COOH)_2 + H_2O},\\
&\mathrm{Br_2 + CH_2\,(COOH)_2 \rightarrow CHBr\,(COOH)_2 + H^+ + Br^-},\\
&\mathrm{HOBr + CHBr\,(COOH)_2 \rightarrow CBr_2\,(COOH)_2 + H_2O},\\
&\mathrm{Br_2 + CHBr\,(COOH)_2 \rightarrow CBr_2\,(COOH)_2 + H^+ + Br^-}.
\end{aligned}
$$

The quasi-stationary concentration method of the reduction of the model (7.8) provides the following model of the (7.5) type for a closed system, with the initial reducing agent being bromomalonic acid:

$$
\begin{aligned}
&\dot{u} = -k_5 Hu\,(C-x) + k_{-5}yx + 2k_4 Ay - 2k_{-4}u^2,\\
&\dot{y} = k_5 Hu\,(C-x) - k_{-5}yx - k_4 Ay + k_{-4}u^2\\
&+ k_1 HAz - k_2 Hyz - 2k_6 y^2, \qquad (7.9)\\
&\dot{x} = k_5 Hu\,(C-x) - k_{-5}yx - k_7 Bx/(k_8 + (C-x)),\\
&\dot{z} = -k_1 HAz - k_2 Hyz + qk_7 Bx/(k_8 + (C-x)) + k_9 B,
\end{aligned}
$$

where

$u = [\mathrm{BrO_2}]$, $y = [\mathrm{HBrO_2}]$, $x = [\mathrm{Me^{(n+1)+}}]$,
$z = [\mathrm{Br^-}]$, $C = [\mathrm{Me^{n+}}] + [\mathrm{Me^{(n+1)+}}]$,
$A = [\mathrm{HBrO_3}]$, $B = [\mathrm{CHBr\,(COOH)_2}]$.

When the catalyst is in the form of complex ions—ferrophenanthrolin, the model (7.9) can be simplified to a third-order system with respect to x, y, z and even to the second-order system [7.4]

$$\begin{gathered}\frac{d\xi}{d\tau}=\eta-\alpha\frac{\xi}{1-\xi}\,,\\ \varepsilon\frac{d\eta}{d\tau}=\eta(1-\eta)+2q\alpha\left(\frac{\xi}{1-\xi}+\beta\right)\frac{\mu-y}{\mu+y}\,,\\ x=C\xi,\quad y=\frac{k_4A}{2k_6}\eta.\end{gathered}\tag{7.10}$$

The model (7.10) has the S-shaped zero-isocline of the fast variable

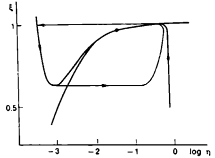

Fig. 7.1. Phase plane of the model (7.10) and limit cycle corresponding to relaxation self-oscillations [7.4].

(Fig. 7.1) and within the self-oscillation domain its solutions are relaxation oscillations that quantitatively fit experimental data.

7.2.1. A Well-Stirred Reactor

When BZ reactions proceed in a closed system, self-oscillations are generally observed in a closed domain of the concentration space of initial reagents (Fig. 7.2) [7.5]. Relaxation self-oscillations usually take place inside this region. The domain boundary has a complicated structure: in one zone the harmonic low-amplitude self-oscillations are observed (supercritical Hopf bifurcation) (Fig. 7.3), in other zones we detect complex self-oscillations (Fig. 7.4) and a finite-amplitude break (subcritical Hopf bifurcation). A closed system is inconvenient for studying the modes susceptible to the small drift of parameters. Therefore stationary modes either induced by a periodic external force or in a vicinity of high-codimension singularities, where bifurcation cascades take place, are studied in CSTR's.

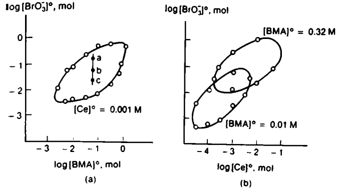

Fig. 7.2. Cross sections of the self-oscillation domain of a BZ reaction in the space of concentrations of initial compounds in a closed system [7.5].

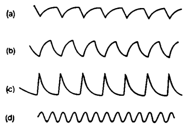

Fig. 7.3. Shape of self-oscillations versus parameters: (*a*), (*b*), (*c*) change in shape when moving along the vertical line in Fig. 7.2*a*; (*d*) quasi-harmonic oscillations at the domain boundary.

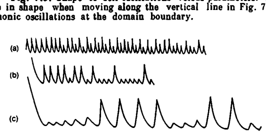

Fig. 7.4. Complex self-oscillations in a BZ reaction.

The cross sections of the parameter space demonstrating the positions of different modes domains are shown in Figs. 7.5 and 7.6 [7.6, 7.7]. The complex oscillation modes including a bursting gener-

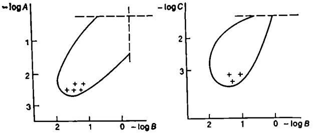

Fig. 7.5. Cross sections of the self-oscillation domain in a BZ reaction in a CSTR [7.6]; $A = [HBrO_3]$, $B = [CH_2(COOH)_2]$, $C = [Ce^{3+}] + [Ce^{4+}]$, "+ "— the domain of complex oscillations.

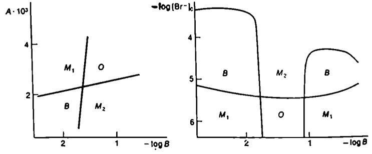

(a) (b)

Fig. 7.6. Cross sections of the BZ reaction parameter space revealing the relative position of the domains of self-oscillations (*O*) and bistability (*B*) [7.7]. M_1 and M_2 are the monostability regions.

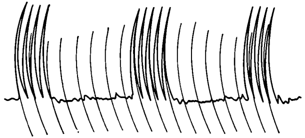

Fig. 7.7. Bursting self-oscillations in a BZ reaction [7.8].

ation (Fig. 7.7) were induced by the ultraviolet irradiation of a reaction solution [7.8]. An intermittent irradiation was used to syn-

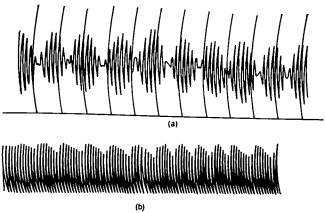

Fig. 7.8. Beats due to a periodic external forcing of chemical self-oscillations [7.9]: (*a*) quasi-harmonic oscillations; (*b*) relaxation oscillations.

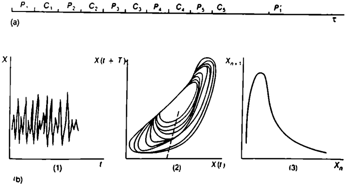

Fig. 7.9. Alternation of periodic and chaotic modes in a BZ reaction under a change in flow rate [7.14]: (*a*) $\tau = V/\mathcal{V}$, where V is the reactor volume and $\mathcal{V}$ is the flow rate. P_i's are the periodic oscillations composed of one large-amplitude cycle and $(i-1)$ small-amplitude cycles, C_i's are the chaotic oscillations, and P'_i's are the periodic small-amplitude oscillations; (*b*) chaotic oscillations in the region C_1: *1*—potential versus time, *2*—two-dimensional cross section of phase space, *3*—the Poincaré mappings along the straight line shown in the preceding figure.

chronize the self-oscillations by a periodic external force [7.9]. Synchronization bands were observed at three first harmonics of the natural frequency, while beats appeared near band boundaries (Fig. 7.8).

Of great interest is the study of chaotic modes [7.10, 7.11]. A change in the flow rate (d in the model (7.6)) results in a sequence of periodic and nonperiodic modes [7.12-7.14] (Fig. 7.9). In this figure, P_1's are the simple relaxation self-oscillations of large amplitude (L^1) while P_1''s are the quasi-sinusoidal oscillations of small amplitude, S^1. P_i's denote the periodic self-oscillations with one relaxation cycle (L) and $(i - 1)$ quasi-sinusoidal cycles (S) per one period ($P_i \Leftrightarrow S^{i-1}L^1$). At the boundaries P_iC_i and $P_{i+1}C_i$ the sequences of doubling bifurcations are observed which result in chaos [7.15]. Within the intervals C_i there are the "gaps" of periodic oscillations with the periods nT_i, where $n = 3, 4, 5, \ldots, 10$. Each gap is bounded from below by a cascade of period doublings and from above, by intermittency. The remaining part is filled by stochastic oscillation modes [7.15, 7.16].

Under certain conditions in this system limit tori are observed [7.17].

7.2.2. A Reaction-Diffusion System

The majority of experiments were performed in two-dimensional systems, viz. in thin solution layers. In addition, quasi-one-dimensional and three-dimensional systems were studied. In some cases, to prevent convection, inert gelformers or porous filters were used.

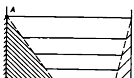

Fig. 7.10. Interaction of travelling waves in a one-dimensional system.

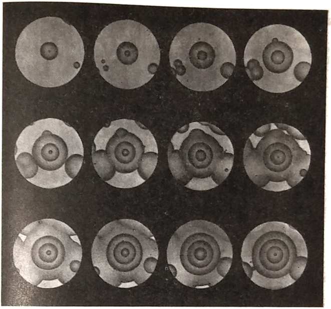

Fig. 7.11. Concentration travelling waves propagating from a leading centre in a BZ reaction.

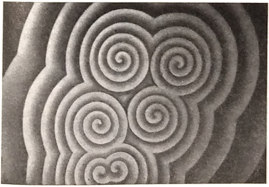

Fig. 7.12. Formation of spiral waves following a break in the front of a travelling wave [7.20].

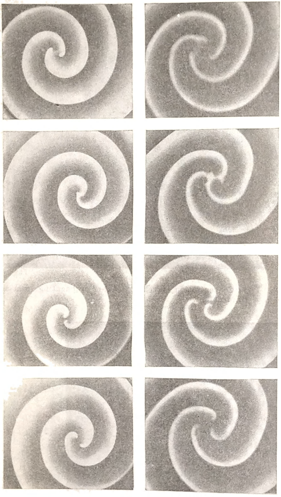

Fig. 7.13. Spiral waves with topological charge 2 and 3 [7.22].

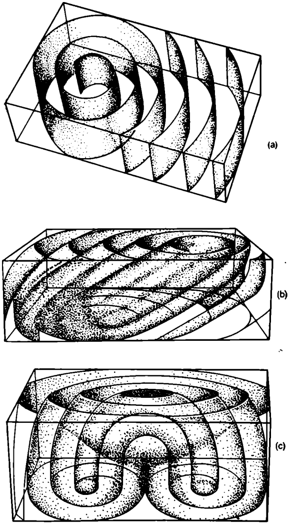

Fig. 7.14. Scroll waves in an active chemical medium [7.23]

All spatial structures observed in BZ systems were composed of travelling waves. Single and periodic travelling waves were observed that propagated from pacemakers. The latter can be external sources or stationary inhomogeneities in a medium [7.18] (Fig. 7.10). It was shown that under certain initial conditions in an initially uniform medium there could arise leading centres, i.e. point excitation sources with an increased frequency which generate periodic travelling waves [7.19] (Fig. 7.11).

A break in the travelling wave front induces spiral waves in a two-dimensional medium (Fig. 7.12) [7.20, 7.21]. A special technique makes it possible to produce multi-arm spiral waves (Fig. 7.13) [7.22]. Twisting the free edge of the two-dimensional wave front that propagates in a three-dimensional medium results in the formation of scroll waves [7.23, 7.24] (Fig. 7.14). The wave velocity in a BZ system is about 0.01 cm/s. Single plane waves have the maximum velocity. The velocity of periodic travelling waves decreases with diminishing period due to refractoriness. There exists a minimum period below which a stationary propagation of periodic waves is impossible. There arise oscillations in the front velocity or periodic loss of pulses. Wave fronts of finite curvature propagate slower than plane ones. There is a maximum front curvature above which the stationary propagation is impossible.

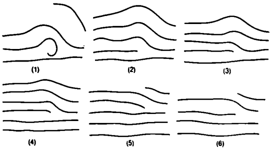

Fig. 7.15. Drift of the front break induced by high-frequency plane waves [7.25].

A wave collision leads to annihilation (Figs. 7.10 and 7.11). The collision point of two periodic wave sequences moves towards a source with a larger period and with the average velocity

$$\mathscr{V} = V \frac{T_2 - T_1}{T_2 + T_1}, \tag{7.11}$$

where V is the wave velocity and $T_2 > T_1$ are the periods of sources. In a two-dimensional medium the collision of periodic plane waves with a spiral one of a larger period results in the gradual disappearance of the spiral wave. However the front break inducing the latter does not vanish and drifts under the action of the periodic waves (Fig. 7.15). If the periodic plane waves vanish before the break reaches the medium boundary, the spiral wave restores [7.25].

Until now in reaction-diffusion systems the stationary Turing structures [7.26] has not been observed.

7.2.3. Other Chemical Systems. Search for and Design of Chemical Oscillators

The above dynamic modes were observed in a great number of chemical systems that are less suitable for experimentation than BZ reactions.

Recently many chemically different oscillatory reactions have been observed [7.27-7.34]. Most interesting are a systematic search for and design of chemical switches and oscillators based on the scheme proposed by Boissonade and De Kepper [7.35, 7.36]. Their approach demonstrated the efficiency of the modern theory of bifurcations in chemical kinetics (see below). It was shown that if in a closed system the reaction proceeded with a self-acceleration, then in an open system a bistability was observed. This generally means that the slow-manifold surface has a cusp. To excite oscillations needs to find the cusp point and pass through the latter along the parameter. If beyond the cusp point the oscillations do not arise, they can be produced by adding an appropriate reagent which provides a slow feedback.

In Epstein's laboratory and elsewhere several families of such chemical oscillators were obtained by this technique [7.37-7.39].

7.3. THEORETICAL STUDIES

7.3.1. A Well-Stirred System

Prior to systematic experimental studies of chemical oscillations the theory of oscillations has been well developed and the qualitative features of main modes have been revealed. The only new dynamic object discovered theoretically recently is the strange attractor.

Therefore theoretical studies in this field were mainly conducted in the following three directions:

(1) The development of mathematical models based on the simplest plausible chemical schemes.

(2) The design of chemical oscillators based on simpler non-oscillatory reactions.

(3) The construction of mathematical models of concrete chemical oscillators.

The third problem is not typical of the theory of oscillations and represents a standard problem of simulating complex systems.

Solving two other problems was hampered by the high complexity of chemical systems, as is illustrated by the simplified scheme (7.8). These systems include dozens of intermediate compounds and elementary stages whose rate constants are often unknown even by order of magnitude.

This is why until recently the theoretical and experimental studies of chemical oscillations were alienated. Oscillatory reactions were detected by chance or produced by trivial modifications of well-known versions.

Theoretical studies have been limited to the analysis of the simplest phenomenological schemes the most known of which are the following:

(1) The Lotka-Volterra oscillator [7.40]:

$$A + x \rightarrow 2x, \quad x + y \rightarrow 2y, \; y \rightarrow, \tag{7.12}$$

$$\begin{aligned} \dot{x} &= k_1 A x - k_2 x y, \\ \dot{y} &= k_2 x y - k_3 y. \end{aligned} \tag{7.13}$$

2. The Prigogine-Lefever Brusselator [7.41]:

$$A \rightarrow x, \; x \rightarrow y, \; 2x + y \rightarrow 3x, \; x \rightarrow. \tag{7.14}$$

$$\begin{aligned} \dot{x} &= k_1 A - (k_2 + k_4)\, x + k_3 x^2 y, \\ \dot{y} &= k_2 x - k_3 x^2 y. \end{aligned} \tag{7.15}$$

These models as well as their modifications with additional chemical stages, flow-through terms, diffusion coupling, etc. were the subject of numerous papers dedicated to the studies of switching, self-oscillations, bifurcation sequences, spatial periodic structures, waves, noise effects, etc.

The models like (7.12) and (7.14) are, in a certain sense, intermediate. These are abstract schemes governed by the mass action law that can be obtained from more general schemes which satisfy all formal requirements to real chemical systems. However, they are neither models of any concrete real system nor normal forms.

7.3.2. Models of Enzyme Reactions

For the first time, realistic models of oscillatory reactions appeared in enzyme kinetics [7.42, 7.43]. Due to some properties enzyme kinetics makes it possible to obtain easily nonlinear mathematical models with a small number of components and parameters from an initial rather complicated scheme.

These properties are as follows:

(1) The enzyme concentration is generally less than the concentrations of substrates and effectors. This at once singles out the small parameter

$$\varepsilon = \frac{e}{S}\,, \tag{7.16}$$

where e is the total enzyme concentration and S is the substrate concentration. The complete system of equations proves to be divided into a subsystem of slow variables, viz. the concentrations of substrates and effectors, and into a subsystem of fast variables, viz. the concentrations of enzyme-ligand complexes including that of a free enzyme.

(2) Usually, enzyme molecules do not interact with each other, therefore the subsystem of fast variables is both linear and stable and the method of quasi-stationary concentrations (singular asymptotic) is applicable directly and without limitations. The fast variables are rational functions of slow variables.

(3) As a rule, an enzyme molecule has many centres of binding small molecules, therefore the formation of multiligand complexes is a much widespread phenomenon in enzyme catalysis. This ensures the appearance of fairly complex expressions in the right-hand sides of relevant equations.

The simplest case of the appearance of an instability in enzyme reactions is due to the substrate inhibition, i.e. due to the formation of an inactive complex of an enzyme with two substrate molecules [7.42]:

$$S_0 \underset{k_{-1}}{\overset{k_1}{\rightleftharpoons}} S, \quad S + E \underset{k_{-2}}{\overset{k_2}{\rightleftharpoons}} SE \overset{k_3}{\rightarrow} E + P, \quad SE + S \underset{k_{-4}}{\overset{k_4}{\rightleftharpoons}} SES. \tag{7.17}$$

This scheme gives the system of four first-order differential equations which can be reduced to the single equation

$$\frac{d\sigma}{d\tau} = \alpha - \beta\sigma - \frac{\sigma}{1+\sigma+\gamma\sigma^2}\,, \tag{7.18}$$

where

$$\sigma = S/K_m, \quad \tau = k_3 et/K_m, \quad e = E + ES + SES,$$
$$\alpha = k_1 S_0/k_3 e, \quad \beta = k_{-1} K_m/k_3 e,$$
$$\gamma = K_m k_4/k_{-4}, \quad K_m = (k_{-2} + k_3)/k_2.$$

Figure 7.16 shows the dependence of σ_0, i.e. of the stationary value of σ, on α. It is seen that there is a domain with three steady states that is enclosed between two bifurcation values of the parameter α. When these values are attained jump transitions take place. It can be easily seen that if one of the parameters is transformed into a slow variable so that in a new system the only steady state would be in the unstable part of zero-isocline $d\sigma/d\tau = 0$, then in the new extended system self-oscillations will arise. In experiment this situation can be realized, e.g. due to the inhibition of an enzyme reaction by its own product. Let us add to the scheme (7.17) the formation of the complexes with a product P as well as the reaction of the product removal:

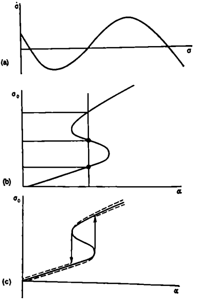

Fig. 7.16. Bistability in an enzyme reaction with substrate inhibition in an open system: (*a*) the time derivative of the substrate concentration versus the concentration; (*b*) the stationary substrate concentration versus its inflow rate α; (*c*) hysteresis under α varied.

$$E+P \underset{k_{-5}}{\overset{k_5}{\rightleftharpoons}} PE, \quad ES+P \underset{k_{-5}}{\overset{k_5}{\rightleftharpoons}} PES, \quad SES+P \underset{k_{-5}}{\overset{k_5}{\rightleftharpoons}} PSES, \quad P\rightarrow. \qquad (7.19)$$

Then we shall obtain from the model (7.18) the new one [7.42]

$$\begin{aligned} \dot\sigma &= \alpha-\beta\sigma-\frac{\sigma}{(1+\sigma+\gamma\sigma^2)(1+\rho)}, \\ \varkappa\dot\rho &= \frac{\sigma}{(1+\sigma+\gamma\sigma^2)(1+\rho)}-\delta\rho, \end{aligned} \qquad (7.20)$$

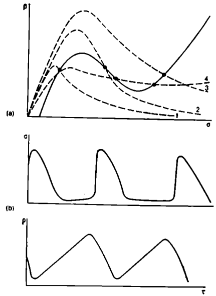

Fig. 7.17. Self-oscillations in an enzyme reaction with the inhibition by substrate and product: (*a*) the zero-isoclines of the model (7.20): *1*, *3*—monostability; *2*—self-oscillations; *4*—bistability; (*b*) the shape of self-oscillations in the model (7.20).

where

$$\rho = Pk_5/k_{-5}, \quad \delta = k_6 K_m/k_3 e, \quad \varkappa = k_{-5}/k_5 K_m.$$

The positions of zero-isoclines in the phase plane of the system (7.20) that correspond to different modes and the shape of self-oscillations at $\varkappa \gg 1$ are shown in Fig. 7.17.

7.3.3. The Behaviour of a Chemical System in a Vicinity of the Critical Point After the First Loss of Stability

Conditions providing one simple asymptotic model within the whole phase space of an initial model in enzyme systems are not, unfortunately, satisfied in the majority of chemical systems. In these systems the subsystems of fast motions are generally nonlinear and they often differ in different regions of the initial phase space. However, in a vicinity of critical points any model can be reduced to a universal (normal) form [7.44]. At an arbitrary point of the parameter space a chemical system is usually in a stable steady state. When the parameters are changed, this state can lose its stability. As a rule, this stability loss occurs via one of two ways:

(1) Saddle bifurcation, when one eigenvalue λ passes through 0.

(2) Oscillatory bifurcation, when the real part of one pair of complex-conjugate λ's passes through 0.

Most often in the stable steady state of a chemical system all λ_i's are real and, as a rule, are quite different in absolute value. As a rule, the absolute value of a maximum negative λ_m is comparatively small so that near a steady state the system behaves as a one-component system. This property is most often conserved during bifurcation, i.e. the latter is of saddle nature.

In a vicinity of a saddle bifurcation dynamics is described by the single equation

$$\begin{aligned} \dot{y} &= \varepsilon_0 + \varepsilon_1 y + a_2 y^2 + a_3 y^3 + \dots, \\ \varepsilon_1 &\equiv \lambda_m, \quad |\varepsilon_0| \approx \varepsilon_1^3. \end{aligned} \tag{7.21}$$

In a real chemical system saddle bifurcation must result in establishing a new finite steady state. Hence, the singularity cannot be a single fold, but should be at least a double one, i.e. a hysteresis must be observed here. Rather often, by a search in the parameter space, it is possible to find a cusp point, where Eq. (7.21) has the following form:

$$\dot{y} = \varepsilon_0 + \varepsilon_1 y - y^3 \tag{7.22}$$

Then, by moving along another parameter in a vicinity of the cusp point, one can find a domain where another component becomes slow and in this case the Hopf bifurcation can appear [7.36]

$$\begin{aligned} \dot{y} &= \varepsilon_0 + \varepsilon_1 y - y^3 - z, \\ \dot{z} &= \varkappa (y - z) \end{aligned} \tag{7.23}$$

Oscillatory bifurcation arises in (7.23) at $\varkappa < \varepsilon_1$ (Fig. 7.18). As indicated above, several families of new chemical oscillators have been designed by this approach.

Figure 7.18 shows that on the right of the point $\varepsilon_1 = 1$ there is a narrow zone, where bistability and oscillations coexist. Hence, by introducing another slow variable it is possible to obtain complex limit cycles, limit tori, and strange attractors.

As a rule, a chemical system possesses a sufficient number of controlled parameters. Therefore after the first loss of stability it is often possible to reach a vicinity of a highly degenerated critical

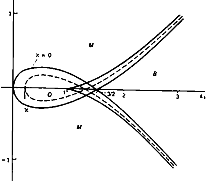

Fig. 7.18. Relative position of the domains of bistability and of self-oscillations in the model with the cubic nonlinearity: *O*—oscillations; *M*—monostability; *B*—bistability.

point where various dynamic modes exist. Naturally, under these conditions the dynamic behaviour of different systems is qualitatively the same. Thus, e.g. the same sequences of complex-periodic and chaotic modes were observed when changing the flow rate in BZ

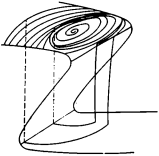

Fig. 7.19. Stochastic self-oscillations in a three-component system with an S-shaped quasi-stationary surface.

reactions (see above) and in the chlorite oxidation reaction of thiosulphate [7.45]. These sequences are described by different versions of the three-component model with an S-shaped quasi-stationary surface (Fig. 7.19) and appropriate quasi-one-dimensional Poincaré mappings (Fig. 7.9) [7.10, 7.14, 7.16, 7.46, 7.47].

In general, two and three-component models with an S-shaped zero-isocline are sufficient for the qualitative description of practically all the phenomena observed in chemical reactions.

7.3.4. Auto-Waves and Bifurcations in Reaction-Diffusion Systems

Unlike the theory of point systems, in the early 1960s the theory of reaction-diffusion systems was practically absent. Only the propagation of a single front in a one-component bistable medium was adequately studied [7.48-7.50]. Also known was the work by Turing on diffusion-induced instability [7.26]. A single pulse propagation was not adequately studied even at the qualitative level. Therefore, to begin with, of interest was the qualitative problem, i.e. what spatio-temporal modes could exist in such media. Such an analysis can be performed in a rather general form in a vicinity of bifurcation points.

7.3.5. Supercritical Bifurcations

Both the type and stability of auto-wave solutions were analytically studied in a vicinity of the soft loss of stability by a uniform steady state. Usually a perturbation has the form

$$C = U \exp(\Omega t + ikx). \tag{7.24}$$

It is seen that an instability can have a saddle (Ω is real) or can be of oscillatory nature ($\Omega = \alpha \pm i\omega$). Besides, instabilities can appear at $k_c = 0$ (long-wave bifurcation) or $k_c \neq 0$ (short-wave bifurcation) (Fig. 7.20). Out of these four cases we shall consider the following three:

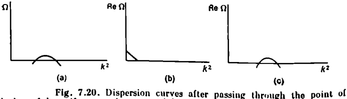

(a) (b) (c)

Fig. 7.20. Dispersion curves after passing through the point of the loss of the uniform steady state stability: (*a*) short-wave aperiodic instability; (*b*) long-wave oscillatory instability; (*c*) short-wave oscillatory instability.

(1) Aperiodic short-wave instability (Turing bifurcation).

Here the system's behaviour can be described by the generalized Ginzburg-Landau equation for the complex amplitude of unstable modes [7.51]:

$$U_t = U + \Delta U - |U|^2 U, \tag{7.25}$$

whose stable solutions are stationary periodic profiles. The amplitude of the first harmonic of the solution is, as usual, proportional to the square root of supercriticality:

$$\begin{aligned} C &= a\sqrt{Q}\exp(ikx) + \dots \\ Q &= \varkappa^2 - (1 - k^2/k_0^2)^2. \end{aligned} \tag{7.26}$$

It should be once more noted that until now Turing structures have not been observed in experiments performed in reaction-diffusion systems.

(2) Long-wave oscillatory bifurcation.

Such a bifurcation is described by the Ginzburg-Landau equation with complex parameters [7.51, 7.52]:

$$U_t = U + (1 + i\beta)\,\Delta U - (1 - i\alpha)\,|U|^2\,U. \tag{7.27}$$

Its basic stable solutions are the travelling waves

$$U = a\sqrt{1 - k^2}\exp[i(\alpha+\beta)k^2t + ikx] + \dots . \tag{7.28}$$

Besides, the model (7.27) provides the local sources of run-away waves (7.28). However, leading centres are unstable [7.53, 7.54]. In the region of leading centres a smooth change in the wave vector takes place (Fig. 7.21).

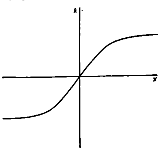

Fig. 7.21. Behaviour of the wave number in a vicinity of a leading centre.

In a two-dimensional medium the solution was studied in the form of a spiral wave that takes the form of the Archimedean spiral as $r \to \infty$ [7.54]

$$U = a\sqrt{1 - k^2}\exp\{i[kr - (\alpha+\beta)k^2t + N\varphi]\} + \cdots , \tag{7.29}$$

where N is the topological charge.

(3) Short-wave oscillatory bifurcation.

This bifurcation can appear in a reaction-diffusion system with no less than three components. The corresponding Ginzburg-Landau equation is [7.55]:

$$U_t = -U - (2 + \lambda^2)\, \Delta U - \Delta^2 U + i\beta\, (U + \Delta U) - |U|^2 U + i\alpha\, |U|^2 U. \qquad (7.30)$$

Here the solutions will be amplitude- and phase-modulated waves

$$U = \exp(i\varphi)\, [a \sin(x + \delta) + ib \cos(x + \delta)] + \ldots, \qquad (7.31)$$

where

$$\varphi = kx + \omega t, \quad \delta = qx + \theta t$$

are the phases slowly varying with respect to the coordinate ($k \ll 1$, $q \ll 1$). The special cases of these solutions are unmodulated and amplitude-modulated travelling waves and standing waves. The latter were detected as pulsations of combustion or detonation fronts [7.56]. Until now modulated and standing waves have not been observed in experiments performed in reaction-diffusion media.

An analysis near bifurcations will exhaust the diversity of the qualitative behaviour of these systems. However, the comparison of theory and experiment often calls for an analysis to be performed far from critical points. First, the region where the theory of bifurcations is effective can be too narrow in the space of real parameters. Second, the auto-wave nature of quasi-harmonic solutions manifests itself only in boundless media while transition processes in such systems are very slow as compared with the characteristic times of the auto-waves themselves.

At the same time, in relaxation systems the parameters of auto-waves cease to be dependent on the dimensions of a medium when the latter become comparable, by order of magnitude, with wave-length and the duration of transition processes becomes shorter than main oscillation periods.

7.3.6. Relaxation Systems

In this case, use is made of the basic model:

$$\begin{aligned} \tau_x \dot{x} &= f(x, y) + \tau_x D_x \Delta x, \\ \tau_y \dot{y} &= g(x, y) + \tau_y D_y \Delta_y \end{aligned} \qquad (7.32)$$

with the S-shaped zero-isocline $f(\cdot) = 0$ (Fig. 7.22). The ratios of the squared characteristic times and lengths,

$$\alpha = \tau_x / \tau_y, \quad \beta = \tau_x D_x / \tau_y D_y, \qquad (7.33)$$

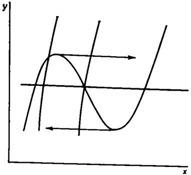

Fig. 7.22. Zero-isoclines of a basic S-system. Shown are the versions of the relative position of the zero-isoclines for monostability, bistability, and self-oscillations.

can be varied over wide limits. Given $\beta \ll 1$, the solutions will be the stationary profiles with the steep fronts of the variable x. These profiles are called contrast dissipative structures [7.57]. There can exist both periodic profiles and single fixed pulses (Fig. 7.23).

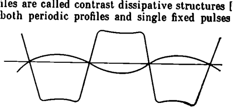

Fig. 7.23. A contrast stationary periodic structure.

The case of $\alpha \ll 1$, $\beta \geqslant 1$ corresponds to the experimentally studied chemical reaction-diffusion systems while the case of $\alpha \ll 1$, $D_y = 0$ corresponds to the propagation of nerve impulses. These cases have been studied in great detail [7.58].

The simplest solution is a stationary travelling pulse. In the phase space of the system with the moving coordinate ($\xi = \eta - Vt$), a closed trajectory that passes through the singular point of saddle type corresponds to this pulse. Usually there exist several such trajectories and, accordingly, several different pulses (Fig. 7.24).

In a system with single pulses, periodic travelling waves can also propagate. They can be represented as limit cycles arising from an asymptotic trajectory of a single pulse when the parameter V changes. As a rule, the velocity of the periodic waves diminishes with decrease in their period. Below a certain period value the stationary propagation of simple periodic waves becomes impossible. Then,

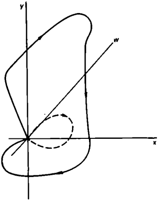

Fig. 7.24. Trajectories corresponding to a travelling pulse in the phase space of a model in a moving coordinate system.

as follows from an analysis, complex-periodic modes appear (Fig. 7.25). All these results as well as the nature of transient processes are in a good agreement with experimental data.

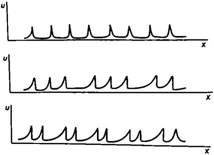

Fig. 7.25. Complex-periodic trains of travelling pulses emerging after the loss of the uniform periodic mode stability.

In principle, the systems of type (7.32) admit the propagation of stochastic waves.

The solutions of the model (7.32) in the form of spiral waves were obtained and studied both analytically and by computer [7.59, 7.60].

Leading centres obtained in a uniform two-component model [7.57] turned out to be unstable. At the same time a spatial parametric non-uniformity easily gives rise to a stable heterogeneous leading centre, i.e. to a pacemaker. The substitution of the parameter by a slow variable that is appropriately related to fast variables provides a stable leading centre in a three-component homogeneous system [7.57].

As a main result of the theoretical research on reaction-diffusion systems during the last decade, the methods have been developed to analyze both weakly nonlinear and very stiff systems which are the generalizations of the relevant methods of the classical theory of oscillations.

In addition to the qualitative reproduction of the modes known experimentally, auto-wave solutions are obtained that until now have not been observed in reaction-diffusion systems. These solutions include stationary concentration profiles, standing, modulated travelling and stochastic waves. The search of these types of auto-waves is the immediate task for experimentors.

7.4. CONCLUSION

At first self-oscillations and auto-waves in chemical systems received attention as the samples of the counter-intuitive self-organization in an initially uniform medium. It took a lot of time to establish the concept of macroscopic ordering whose symmetry elements were absent at the microlevel. Meanwhile, chemists understood the specific features of reaction mechanisms giving rise to the oscillations and now chemical oscillations and auto-waves hold their position among similar phenomena arising in highly non-equilibrium dissipative systems [7.61, 7.62]. It is clear now what combinations of elementary stages lead to the first instability [7.63, 7.64] and how one should move within the parameter space to reach new bifurcations and to produce novel modes.

What will be the role of these studies in future? First, chemically active media are instrumental in verifying theoretical works on auto-waves. Besides, such studies are used to analyze the mechanisms and to develop the methods of treating heart arrhythmia, epilepsy, and a number of other diseases.

Second, these studies are indispensable in ensuring the stability of operation of chemical and biochemical reactors. As follows from the very nature of bifurcations, these are related to the extrema of certain functions and often the appearance of an instability is due to optimizing the reactor operation. The operation of chemical reactors in oscillatory and other nonstationary modes can yield a substantial profit. Similar modes of operation have been used in practice in some individual cases, and, undoubtedly, they will find wide application in future.

References

7.1. B. P. Belousov, *Abstracts of Papers on Radiation Medicine*, ed. A. V. Lebedinskii, Meditsina, Moscow, 1959, p. 145 (in Russian).

7.2. A. M. Zhabotinskii, *Biofizika*, 9, 3, 306 (1964); *idem*, *Dokl. Akad. Nauk SSSR*, 157, 2, 392 (1964); *idem*, *Concentration Self-Oscillations*, Nauka, Moscow, 1974 (in Russian).

7.3. R. J. Field, E. Kōros, and R. M. Noyes, *J. Amer. Chem. Soc.*, 94, 25, 8649 (1972).

7.4. A. M. Zhabotinsky and A. B. Rovinskii, in: *Self-Organization, Autowaves and Structures Far from Equilibrium*, ed. V. I. Krinsky, Springer-Verlag, 1984, p. 140.

7.5. V. A. Vavilin, A. M. Zhabotinskii, and L. S. Yaguzhinskii, *Oscillatory Processes in Biological and Chemical Systems*, Nauka, Moscow, 1967, p. 181, p. 199 (in Russian).

7.6. P. De Kepper, A. Rossi, and A. Pacault, *C. R. Acad. Sci. Paris*, 283C, 10, 371 (1976).

7.7. P. De Kepper and J. Boissonade, *J. Chem. Phys.*, 75, 189 (1981).

7.8. V. A. Vavilin, A. M. Zhabotinskii, and A. N. Zaikin, *Z. Fiz. Khim.*, 42, 12, 3091 (1968)

7.9. A. N. Zaikin and A. M. Zhabotinsky, *Biological and Biochemical Oscillators*, ed. B. Chance *et al.*, Acad. Press, New York, London, 1973, p. 81.

7.10. R. A. Schmitz, K. R. Graziani, and J. L. Hudson, *J. Chem. Phys.*, 67, 3040 (1977)

7.11. O. Rossler and K. Wegmann, *Nature*, 271, 5640, 89 (1978).

7.12. J. L. Hudson, M. Hart, and D. Marinko, *J. Chem. Phys.*, 71, 1601 (1979).

7.13. C. Vidal, J. C. Roux, S. Bachelart, and A. Rossi, *Ann. N.Y. Acad. Sci.*, 357, 377 (1980).

7.14. J. S. Turner, J. C. Roux, W. D. McCormick, and H. L. Swinney, *Phys. Lett.*, 85A, 1, 9 (1981).

7.15. K. Coffman, W. D. McCormick, H. L. Swinney, and J. C. Roux, in *Non-Equilibrium Dynamics in Chemical Systems*, ed. C. Vidal and A. Pacault, Springer-Verlag, 1984, p. 251.

7.16. H. L. Swinney, *ibid.*, p. 124.

7.17. J. C. Roux and A. Rossi, *ibid.*, p. 141.

7.18. A. M. Zhabotinskii, *Oscillatory Processes in Biological and Chemical Systems*, ed. G. M. Frank, Nauka, Moscow, 1967, p. 252 (in Russian).

7.19. A. N. Zaikin and A. M. Zhabotinsky, *Nature*, 225, 535 (1970); A. M. Zhabotinskii and A. N. Zaikin, *Oscillatory Processes in Biological and Chemical systems*, ed. E. E. Sel'kov, Pushchino, 1971, p. 279 (in Russian); A. M. Zhabotinsky and A. N. Zaikin, *J. Theor. Biol.*, 40, 45 (1973).

7.20. A. M. Zhabotinskii and A. N. Zaikin, *Oscillatory Processes in Biological and Chemical Systems*, ed. E. E. Sel'kov, Pushchino, 1971, p. 288 (in Russian).

7.21. A. T. Winfree, *Science*, 175, 634 (1972).

7.22. K. I. Agladze and V. I. Krinsky, *Nature*, 296, 5856, 424 (1982).

7.23. A. T. Winfree, *Science*, 181, 937 (1973).

7.24. A. E. Burgess, *Non-Equilibrium Dynamics in Chemical Systems*, ed. C. Vidal and A. Pacault, Springer-Verlag, 1984, p. 226.

7.25. V. I. Krinsky and K. I. Agladze, *Physica* 4D, 2, 421 (1983).

7.26. A. M. Turing, *Phil. Trans. Roy. Soc. (Lond.)*, B237, 37 (1952).

7.27. J. R. Bischoff and D. M. Mason, *Chem. Eng. Sci.*, 23, 5, 447 1968).

7.28. J. Ogata and T. Morimoto, *J. Chem. Soc.*, 8, 1, 74 (1969).

7.29. R. W. Bigelow, *J. Phys. Chem.*, 81, 88 (1977).

7.30. S. Yesodharan, V. Ramakrishnan, and J. Kuriacose, *Indian J. Chem.*, 21A, 5, 468 (1982).

7.31. J. H. Jensen, *J. Amer. Chem. Soc.*, 105, 2639 (1983); M. G. Roelofs,

E. Wasserman, J. H. Jensen, and A. E. Nader, *J. Amer. Chem. Soc.*, 105, 6329 (1983).

7.32. M. Burger and R. J. Field, *Nature*, 307, 5953, 720 (1984).

7.33. T. S. Zuyeva and E. V. Protopopov, *Teor. Eksp. Khim.*, 19, 104 (1983).

7.34. R. P. Rastogi and I. Das, *Indian J. Chem.*, 23A, 5, 363 (1984).

7.35. J. Boissonade, *J. Chem. Phys.*, 73, 540 (1976).

7.36. J. Boissonade and P. De Kepper, *J. Phys. Chem.*, 84, 5, 501 (1980).

7.37. P. De Kepper, I. R. Epstein, and K. Kustin, *J. Amer. Chem. Soc.*, 103, 8, 2133 (1981); M. Orban, P. De Kepper. I. R. Epstein, and K. Kustin, *Nature*, 292, 5826, 816 (1981); M. Orban, C. Dateo, P. De Kepper, and I. R. Epstein, *J. Amer. Chem. Soc.*, 104, 22, 5911 (1982).

7.38. I. R. Epstein, *Non-Equilibrium Dynamics in Chemical Systems*, ed. C. Vidal and A. Pacault, Springer-Verlag, 1984, p. 24.

7.39. J. Chopin-Dumas and M. N. Papel, *ibid.*, p. 69.

7.40. A. J. Lotka, *J. Amer. Chem. Soc.*, 27, 1595 (1920); V. Volterra, *Leçons sur la Théorie Mathématique de la Lutte pour la Vie*, Paris, 1931.

7.41. I. Prigogine and R. Lefever, *J. Chem. Phys.*, 48, 795 (1968).

7.42. E. E. Sel'kov, *Bionics*, Nauka, Moscow, 1965, p. 173 (in Russian); E. E. Sel'kov, in: *Oscillatory Processes in Biological and Chemical Systems*, ed. G. M. Frank, Nauka, Moscow, 1967, p. 81, 93 (in Russian).

7.43. J. Higgins. *Ind. Eng. Chem.*, 59, 18 (1967).

7.44. V. I. Arnol'd, *Addenda to the Theory of Ordinary Differential Equations*, Nauka, Moscow, 1978 (in Russian).

7.45. M. Orban and I. R. Epstein, *J. Phys. Chem.*, 86, 20, 390 (1982).

7.46. O. E. Rossler, *Z. Naturforsch.*, 31A, 1, 259 (1976).

7.47. A. S. Pikovsky, *Phys. Lett.*, 85A, 13 (1981).

7.48. A. N. Kolmogorov, I. G. Petrovskii, and N. S. Piskunov, *Bull. MGU, Mat. i Mekh.*, 1, 1 (1937).

7.49. Ya. B. Zel'dovich and D. A. Frank-Kamenetskii, *Dokl. Akad. Nauk SSSR*, 19, 693 (1938).

7.50. Ya. I. Kanel, *Mat. Sbornik*, 59, 101, 245 (1962).

7.51. H. Haken, *Z. Phys.*, B21, 105 (1975).

7.52. Y. Kuramoto and T. Tsuzuki, *Prog. Theor. Phys.*, 54, 3, 687 (1975).

7.53. L. N. Howard and N. Kopell, *Stud. Appl. Math.*, 56, 2, 95 (1977).

7.54. P. S. Hagan, *SIAM J. Appl. Math.*, 42, 4, 762 (1982).

7.55. B. A. Malomed, *Zhurn. Tekhn. Fiz.*, 54, 2, 233 (1984); *idem*, *Z. Phys.*, 55B, 241, 249 (1984).

7.56. K. I. Shchelkin and Ya. K. Troshin, *Combustion Gas Dynamics*, Izd. AN SSSR, Moscow, 1963 (in Russian); Yu. M. Maksimov, A. G. Merzhanov, A. T. Pak, and M. N. Kuchkin, *Fiz. Gor. Vzryv.*, 17, 51 (1981).

7.57. V. A. Vasil'ev, Yu. M. Romanovskii, and V. G. Yakhno, *Uspekhi Fiz. Nauk*, 128, 4, 625 (1979); B. S. Kerner and V. V. Osipov, *Mikroelectronika*, 10, 5, 407 (1981).

7.58. A. Scott, *Active and Nonlinear Wave Propagation in Electronics*, Wiley, New York, 1970.

7.59. *Auto-Wave Processes in Diffusive Systems*, ed. M. T. Grekhova, USSR Academy of Sciences, Gorki, 1981 (in Russian).

7.60. V. I. Krinsky and B. A. Malomed, *Physica* 9D, 81 (1983).

7.61. G. Nicolis and I. Prigogine, *Self-Organization in Nonequilibrium Systems*, Wiley, New York, 1977.

7.62. H. Haken, *Synergetics*, Springer-Verlag, 1978.

7.63. B. L. Clarke, *Adv. Chem. Phys.*, 43, 1 (1980).

7.64. A. N. Ivanova, *Kinet. Katal.*, 20, 4, 1019, 1024 (1979).

8 Auto-Waves in Biologically Active Media

V. I. Krinskii, D. Sc. *(Phys.-Math.)*

8.1. INTRODUCTION

Auto-waves [8.1-8.3] are typical of strongly nonlinear active media. Among these are self-sustaining signals which initiate the processes of local release of energy stored in an active medium and spent to drive analogous processes in adjacent regions. The examples are combustion waves, phase transition waves, concentration waves in chemical reactions as well as various auto-wave processes in animate nature (nerve impulse, excitation waves in cardiac muscle, ecological waves of epidemy spread, waves in brain cortex) which attach much importance to the studies of auto-waves.

Since auto-waves propagate at the expense of the energy of an active medium and the wave energy is not conserved, some fundamental differencies exist between auto-waves and well-studied waves that propagate in ordinary (conservative) media (Table 8.1). Propagating auto-waves conserve their amplitude and shape while the amplitude of ordinary waves decays rather fast with distance and their shape is drastically distorted by dispersion. Auto-waves are not reflected from medium boundaries and obstacles. Two colliding auto-waves usually do not propagate through one another, as do waves in conservative media, but annihilate and this effect explains the absence of their interference. As can be seen from Table 8.1, the only common property of both kinds of waves is their capability to diffract.

Table 8.1. Properties of Waves and Auto-Waves

Property	Waves	Auto-waves	Property	Waves	Auto-waves
Energy conservation	+	−	Annihilation	−	+
Conservation of wave amplitude and shape	−	+	Interference	+	−
Reflection	+	−	Diffraction	+	+

In the simplest case, after the propagation of an auto-wave an active medium is in a low energy state. As a result, the wave can run through it only once, as is exemplified by combustion waves. Such media have been studied for a rather long time [8.4, 8.5]. Much more interesting are active media with regeneration, i.e. those with slow processes that bring an active medium from a low energy state (due to the auto-wave propagation) back to a high energy state. In such a medium several auto-waves can propagate one after another. The simplest example of an auto-wave in an active medium with regeneration is a long-term propagation of a combustion wave in steppe (considered over periods of more than one year). Here burnt grass again grows and can be set on fire. Active media with regeneration are widely used by animate nature, as exemplified by nerve fibers, cardiac muscle, neuron ensembles, cells of nonstriated muscles, etc.

8.2. MATHEMATICAL DESCRIPTION

A wave in a medium without regeneration can be described by one equation [8.5]

$$\frac{\partial u}{\partial t} = f(u) + D\Delta u. \tag{8.1}$$

For the above example of a combustion wave, u is the temperature, t is the time. $\dot{u} = f(u)$ is the kinetic equation that describes the process at an isolated point, and the term $D\Delta u$ takes care of the thermal diffusion from adjacent regions. For media with regeneration, the second (as a rule, slow) variable is added that describes the regeneration and a minimal description requires two equations. The system (8.2) describes the behaviour of an isolated point while the system (8.3), a distributed medium:

$$\begin{cases} \dfrac{\partial u}{\partial t} = f(u,\ v), \\ \dfrac{\partial v}{\partial t} = \varphi(u,\ v), \end{cases} \tag{8.2}$$

$$\begin{cases} \dfrac{\partial u}{\partial t} = f(u,\ v) + D_u\Delta u, \\ \dfrac{\partial v}{\partial t} = \varphi(u,\ v) + D_v\Delta v, \end{cases} \tag{8.3}$$

where, for steppe fire, u is the temperature and v describes grass growth. For a nerve impulse, u is the potential on the membrane of a nerve fiber, v is the current of potassium ions that brings the membrane potential back to the initial value. For an active chemical medium (e.g. the oxidation Belousov-Zhabotinskii reaction [8.6]), u

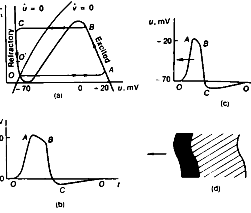

Fig. 8.1. Impulses and waves in the system (8.3): (*a*) phase plane, (*b*) impulse generated by the system (8.2). The trajectories *OA* and *BC* are impulse fronts (fast motions), *AB* and *CO* are the plateaus (slow motions), (*c*) impulses in a one-dimensional medium described by the system (8.3), (*d*) the schematic of a plane wave propagating in a two-dimensional medium. Regions corresponding to the medium states in a vicinity of *AB* are heavily shaded ("excited state"), in a vicinity of *CO'*, half-tone shaded ("refractory state"), and in a vicinity of *OO'* ("rest") are unshaded.

is the concentration of the oxidized form of catalyst and v is that of the inhibitor. For waves in cardiac tissue, the interpretation of the variables in (8.3) is the same as for a nerve impulse yet the Laplacian Δ, unlike the nervous impulse, is now two- or even three-dimensional.

Of crucial importance here is the fact that principles underlying the propagation of auto-waves in active media of physical, chemical and biological nature are the same and thus can be described by a common language. In all instances an active medium is a two-level system. When an auto-wave propagates, a transition from a high energy level to a low energy one takes place and then slow pumping processes bring the medium back to the high energy level. Equations that describe active media of different nature turn out to be of the same type. This is the partial differential Eq. (8.3) of the parabolic type and the relevant lumped-parameter system (8.2) has a self-oscillatory or, in the most interesting cases, excitable kinetics. In these cases u proves to be the fast variable, v is the slow one and the phase plane of the system (8.2) turns out to be of the van der Pol type (Fig. 8.1*a*), an impulse generated by it is shown in Fig. 8.1*b*.

8.3. LOCAL SOURCES OF AUTO-WAVES

The fact that active media can form local sources of auto-waves having extraordinary properties arouses particular interest. These sources can arise during the propagation of auto-waves through a non-uniform active medium [8.7] and this results in certain specific mechanisms of the structurization of the medium as well as in new types of instabilities in them and in the initiation of chaos [8.2, 8.3, 8.8].

Let us consider the mechanism of initiating one of the most interesting auto-wave sources, viz. reverberators. A reverberator is a rotating vortex in which the wave shape resembles the Archimedean spiral [8.9]. Reverberators, naturally, arise in non-uniform media, where propagating waves can break [8.7]. A plane wave in a two-dimensional medium is schematically shown in Fig. 8.1*d* and the wave break in a non-uniform medium, in Fig. 8.2. In moving the broken wave (Wave 2) lags behind the preceding one and the break begins to contact the regions where regeneration processes are over. This enables the excitation wave to propagate also into these regions. Constructing by means of Huygens's principle the successive positions of the wave front one can see that the break begins to roll into a spiral [8.10] (Fig. 8.3).

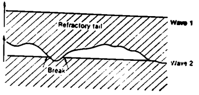

Fig. 8.2. Initiation of the wave break in a non-uniform medium. Two waves propagating upwards are shown. The length of the refractory tail (dashed) of Wave 1 in the centre is somewhat larger than at edges. Wave 2 cannot propagate through the dashed region, this resulting in its break.

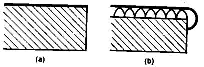

Fig. 8.3. Initiation of a spiral wave from a break: (*a*) the initial position of the wave, (*b*) wave position in a short time interval dt (heavy line). The latter is constructed, according to Huygens's principle, as the envelope of the circles of radius $v\,dt$, where v is the wave velocity.

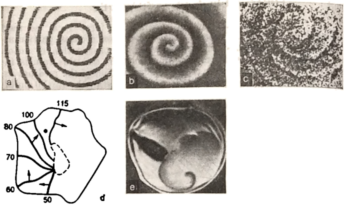

Fig. 8.4. Rotating spiral waves (reverberators) in different active media: (*a*) computer-assisted simulation of an active medium prescribed by the system (8.3) [8.17], (*b*) a chemically active medium [8.11], (*c*) a culture of the social amoebas *Dictyostelium discoideum* [8.12], (*d*) auricle [8.13], (*e*) eye retina [8.14].

Figure 8.4 shows a rotating vortex reverberator in different active media: computer-assisted simulation of a medium specified by Eqs. (8.3), a chemically active medium, a culture of the social amoebas *Dictyostelium discoideum*, in eye retina, and in cardiac tissue.

In addition to rotating vortices, active media admit other types of auto-wave sources, in particular, leading centres of different nature emitting concentric waves. If in an active medium several auto-

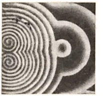

Fig. 8.5

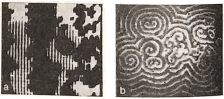

Fig. 8.6

Fig. 8.5. A reverberator destructs the source of a concentric wave in a chemically active medium [8.2].

Fig. 8.6. Wave pictures at the initial stages of developing chaotic modes in active media: (*a*) computer-aided simulation of a non-uniform medium prescribed by the Wiener model [8.3], (*b*) a chemically active medium [8.2].

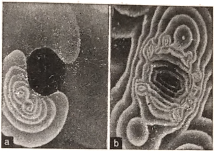

Fig. 8.7. Reverberator breeding on a non-uniformity (a chemically active medium) [8.2].

wave sources exist simultaneously, then emitted waves will annihilate on collisions (see Table 8.1). Due to this effect an auto-wave source of the highest possible frequency suppresses the remaining ones [8.7, 8.8]. The reverberator possesses the highest frequency of all local auto-wave sources, hence it sets the pace of the whole medium and, in particular, suppresses concentric sources (Fig. 8.5).

The most important feature of rotating vortices in active media is their ability to breed. If a reverberator rotates in a non-uniform medium, waves emitted by this reverberator, after break on non-uniformities (Fig. 8.2), can produce new reverberators (Fig. 8.3). As a result of the chain breeding reaction the characteristic scales of the wave picture decrease and the whole medium will be filled in by the fragments of rotating vortices. The resulting chaos outwardly reminds of a small-scale turbulence (Figs. 8.6, 8.7), although here underlying mechanisms are of a substantially different nature.

8.4. CARDIAC DISORDERS

The above properties of vortices in active media, i.e. their ability to arise during a wave propagation in a non-uniform medium, to suppress other wave sources, and to breed, make it possible to understand basic mechanisms underlying some grave disorders of heart work [8.8, 8.18]. If a vortical wave source (reverberator) arises in heart, it inhibits the normal heart pacemaker (SA-node), the heart rate jumps and hemodynamics abruptly deteriorates. This takes place under paroxysmal tachycardia, a severe heart arrhythmia, as was shown in experiments on animals [8.13, 8.16, 8.35-8.38].

The chain reaction of reverberator breeding on non-uniform parts of cardiac tissue results in another grave pathology, the fibrillation of heart ventricles. During the fibrillation the contraction of myocardium cells desynchronizes and heart is no longer a living pump but a chaotically twitching muscular bag that cannot pump blood. This is the heart analogue of the turbulent auto-wave mode of operation.

8.5. MATHEMATICAL SIMULATION OF AUTO-WAVE SOURCES

What we presently know about auto-wave sources and their properties dates back to attempts to comprehend the mechanisms of cardiac muscle action. The first mathematical work in this area was performed in 1946 by the well-known mathematician Wiener and by Rosenblueth, Director of the Cardiology Institute in Mexico [8.9]. Studies of active media were continued in 1964-1966 by participants of a seminar organized by Gel'fand (Moscow). They discovered basic mechanisms of initiating auto-wave sources and investigated their properties in formalized models of active media of the Wiener type. Further, of great importance were computer-assisted studies of active media prescribed by Eqs. (8.3) (see a review in [8.3]). As a result of an interplay between this research branch and studies of the mechanisms of an oscillatory chemical reaction discovered by Belousov in 1951, a chemically active medium was developed (see [8.11]).

8.6. A CHEMICALLY ACTIVE MEDIUM

A chemically active medium is a thin (1mm thick) solution layer, with the Belousov reaction proceeding in it. In this reaction the oxidation of a substrate is initiated and then inhibited by one of oxidation products so that only about one percent of substrate per one run is oxidized. Therefore in the solution the oxidation wave can travel about a hundred times. It is blue against a bright red background. This medium was developed by Zaikin and Zhabotinskii [8.19] and then was modified by Winfree [8.20].

A chemically active medium is the first experimentally studied instance of an active medium with regeneration. It makes it possible to demonstrate all basic properties of auto-waves (Table 8.1) and of auto-wave sources predicted by theory. This medium turned out to be the most convenient experimental object to demonstrate and study auto-waves. Biological specimens of active media, suitable for experimental studies of auto-waves, were constructed later (see Fig. 8.4). The photographs of spiral rotating waves which organize the morphogenesis process for the social amoebas *Dictyostelium discoideum* or the maps of rotating vortices in rabbit auricle under experimentally induced paroxysmal tachycardia are now the famous examples which wander from one book to another. To these can be added the splendid success of the Czechoslovak electrophysiologist Bureš who, together with colleagues from the Institute of Higher Nervous Activity (Moscow), demonstrated the initiation of a reverberator on eye retina in experiments with a propagating depression [8.14]. The fact that a propagating depression wave can develop vortices is very closely related to the mechanisms of developing epilepsy.

8.7. NEW AUTO-WAVE MODES

One of the basic problems in the new, rapidly developing science of auto-waves is a search for new auto-wave modes of operation. For practical applications of fundamental importance is the development of methods to control auto-wave sources (experimental possibilities of preventing spontaneous initiation of auto-wave sources, the inhibition of the rate of the chain reaction of their breeding, the control of their position in an active medium, of their movements across the medium, and of their interactions (see also Fig. 8.5)).

To solve these problems the following techniques are available:

(1) Analytical studies of the solutions of the simplified versions of Eqs. (8.3).

(2) Computer-aided simulation.

(3) Experimental simulation of auto-wave media.

Adequately developed analytical techniques are available to study a relatively simple case—a weakly nonlinear medium, where the solutions turn out to be quasi-harmonic [8.21-8.27]. Yet the main problems and difficulties arise in strongly nonlinear media.

8.8. AUTO-WAVE SOURCES IN THREE-DIMENSIONAL ACTIVE MEDIA

Among the above cited problems of most importance are those of auto-wave sources in three-dimensional active media. Here a vortex rotates not around a point, as in the two-dimensional case, but around an axis (a thread of singularities) which can be intricately arranged in a three-dimensional space. The topological aspects of this problem were explored in [8.28]. The major experimental data on the evolution of vortices in three-dimensional media [8.20] can be explained using a simple hypothesis that in an active medium the thread of a vortex is flexible. Note that the thread flexibility is a well established fact for vortices in conservative media (^{4}He, superconductors, etc.), where it follows from the energy minimum principle. The latter cannot be formulated for active media, where the wave energy is not conserved. However, computer-aided calculations show that in a relaxation system a toroidal vortex contracts ("thread flexibility"), and, in addition, it drifts in the perpendicular direction [8.29]. This effect can be analyzed analytically for weak relaxation systems. In particular, the evolution of the radius R of a toroidal vortex is described by the equation [8.30]

$$dR/dt \sim -D/R$$

(for a nondispersive $\lambda - \omega$ system). It shows that the contraction rate of the vortex thread is proportional to its curvature. The similar problems for relaxation systems remain to be studied.

8.9. THE EFFECT OF MEDIUM PARAMETERS ON AUTO-WAVE SOURCES

An important class of problems is studies of the effect of medium parameters on auto-wave sources. Figure 8.8 demonstrates experimental possibilities for changing the characteristic sizes of reverberators. It is seen that the wavelength and the size of a reverberator core can be increased almost by the order of magnitude when changing parameters corresponding to a decrease in excitability (an increase in threshold) of an active medium.

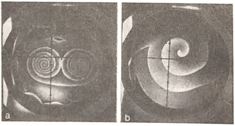

Fig. 8.8. Increase in reverberator wavelength during the excitability inhibition of a chemically active medium: (*a*) $[H_2SO_4] = 0.7$ M, (*b*) $[H_2SO_4] = 0.15$ M [8.15].

Figure 8.9 presents data on the reverberator period obtained with three different objects: numerical simulation within the Fitz-Hugh-Nagumo model, cardiac tissue, and a chemically active medium. It is seen that qualitatively these dependencies are of the same nature, i.e. the reverberator period (as well as the size of the reverberator core not indicated in the figure) increases with the active medium excitability decreased.

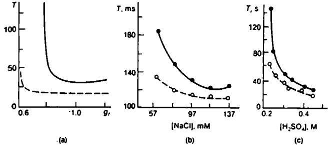

Fig. 8.9. The dependence of the period of waves emitted by a reverberator on the active medium excitability: (*a*) the Fitz-Hugh-Nagumo model [8.17], (*b*) heart [8.16], (*c*) a chemically active medium [8.15].

Note that the studies of the parameters of auto-wave sources (in particular, of more simply measurable parameters, i.e. the period and its change under different pharmacological effects) find wide application in the development of techniques for the differential diagnostics of the mechanisms of heart arrhythmias [8.16].

8.10. AN ANOMALOUS REVERBERATOR

One of the new auto-wave modes discovered in the last years in two-dimensional active media is an anomalous reverberator [8.17]. It is known that in the centre of a normal reverberator there

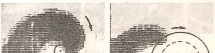

Fig. 8.10. Normal (*a*) and anomalous (*b*) reverberators (computer-aided simulation). Dashed line shows a region where excitation does not penetrate at all [8.17].

is a core, i.e. the region where forced oscillations take place. Their amplitude smoothly decreases from unity (auto-wave amplitude) down to zero and the zero amplitude is detected only at a single point, i.e. in the core centre. An anomalous reverberator (Fig. 8.10*b*) is characterized by the fact that the oscillation amplitude is zero within a whole region that is generally fairly large in size.

In the anomalous reverberator, at the boundary with the central (rest) region, the wave has a critical curvature and thus cannot propagate inside. However, in this region too, the elements of medium conserve normal excitability (unlike the core of a normal reverberator). This can be easily verified if during the rotation of the reverberator one induces an external perturbation: a propagating wave is excited which encloses the entire central region although the reverberator wave could not enter the latter. The anomalous reverberator arises when the most different parameters of active media are changed which leads to a decrease in medium excitability (or to an increase in the medium threshold).

8.11. THEORETICAL STUDIES OF REVERBERATORS

As has been mentioned above, analytical studies of reverberators in strongly nonlinear (relaxation) media present substantial difficulties. Nevertheless, for relaxation media, where the size of the reverberator core exceeds the diffusion length, an approximate theory [8.31] based on the Greenberg transformations [8.32] was constructed to study basic reverberator characteristics (period, core size) as dependent on the medium parameters and a transition from a normal reverberator to an anomalous one.

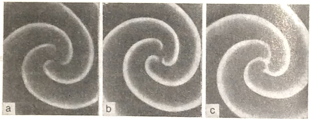

Fig. 8.11. A reverberator with the topological charge $N = 3$ in a chemically active medium [8.33].

Below, some auto-wave modes will be shown which still challenge theorists. Figure 8.11 presents a set of frames of a rotating vortex with topological charge $N = 3$ in a chemically active medium [8.33]. It is interesting that these multi-arm vortices turned out to be stable and were observed for more than half an hour, as opposed to well-known data on multi-arm vortices in conservative media (^{4}He, superconductors, etc.) which are always unstable and decay into simple ones. The stability of multi-arm vortices was analyzed theoretically [8.27] yet only for a very simple and not-true-to-life case, a weakly nonlinear active medium without dispersion (in such media vortices are simply rotating straight lines!). Note also that presently known solutions of reaction-diffusion equations for a vortex with a topological charge N assume that the vortex as a whole rotates as a rigid body

$$u = F(N\theta,\ r), \tag{8.4}$$

where θ and r are the polar coordinates. However, it was shown experimentally (Fig. 8.11) that wave dynamics proves to be much more complicated then the dynamics described by Eq. (8.4), viz. waves in the vortex core are joined together (in Fig. 8.11*a* the first and second waves are joined, in Fig. 8.11*b*, the second and third, in Fig. 8.11*c*, all three).

The experiments with chemically active media discovered an important phenomenon, i.e. the enforced vortex drift [8.34]. It was shown that if a vortex is acted upon by external waves with a frequency (f_0) higher than the vortex rotation frequency (f_c) then the vortex slowly drifts receding from the external wave source. The drift velocity can be described by the empirical formula

$$v_d \simeq v\,(1 - f_c/f_0) \tag{8.5}$$

and it is small as compared with the velocity of wave propagation in a medium (v) and it rises with increase in the external wave frequency (f_0). Using this effect one can both control the vortex position in an active medium and develop new approaches to control heart arrhythmias. Note that a rigorous (based on the solutions of Eqs. (8.3)) theory of this effect is still absent.

8.12. CONCLUSION

In conclusion it should be noted that the auto-wave mechanisms of initiating structures, their interaction and chaos development (see reviews in [8.40-8.46]) form only a small part of studies concerned with non-equilibrium systems, self-organization and synergetics [8.43-8.45, 8.47-8.49]. However, as can be seen from the above examples, these studies compose a rather pithy part of this developing science, with its problems lying at the interface between oscillation theory, the theory of strongly nonlinear waves, and initiation of structures.

References

8.1. *Auto-Wave Processes in Diffusive Systems*, ed. M. T. Grekhova, USSR Academy of Sciences, Gorki, 1981 (in Russian).

8.2. G. R. Ivanitsky, V. I. Krinsky, A. N. Zaikin, and A. M. Zhabotinsky, *Sov. Sci. Rev.*, D2, 280 (1980).

8.3. G. R. Ivanitskii, V. I. Krinskii, and E. E. Sel'kov, *Mathematical Cellular Biophysics*, Nauka, Moscow, 1978 (in Russian).

8.4. A. N. Kolmogorov, I. E. Petrovskii, and N. S. Piskunov, *Vestnik MGU, Ser. Mat. i Mekh.* 1, 1 (1937).

8.5. Ya. B. Zel'dovich, G. I. Barenblatt, V. B. Librovich, and G. M. Makviladze, *The Mathematical Theory of Combustion and Explosion*, Nauka, Moscow, 1980 (in Russian).

8.6. A. M. Zhabotinskii, *Concentration Self-Oscillations*, Nauka, Moscow, 1974 (in Russian).

8.7. V. I. Krinskii, *Biofizika*, 11, 676 (1966).

8.8. V. I. Krinskii, *Problemy Kibernetiki*, 20, 59 (1968).

8.9. N. Wiener and A. Rosenblueth, *Arch. Inst. Cardiologia de Mexico*, 16, 205 (1946).

8.10. N. S. Balakhovskii, *Biofizika*, 10, 1063 (1965).

8.11. A. M. Zhabotinskii and A. N. Zaikin, in: *Oscillatory Processes in Biological and Chemical Systems*, Vol. 2, USSR Academy of Sciences, Pushchino, 1971, p. 279 (in Russian).

8.12. A. J. Durston, *Dev. Biol.*, 37, 221 (1974).

8.13. M. Allessie, F. Bonke, and S. Schopman, *Circ. Res.*, 33, 54 (1973).

8.14. J. Bureš and N. A. Gorelova, *J. Neurobiol.*, 14, 353 (1983).

8.15. K. I. Agladze, Preprint, Pushchino, 1983 (in Russian).

8.16. V. I. Krinskii, *Vestnik AN SSSR*, 1, 6 (1980).

8.17. A. M. Pertsov and A. V. Panfilov, in: *Auto-Wave Processes in Diffusive Systems*, USSR Academy of Sciences, Gorki, 1981 (in Russian).

8.18. V. I. Krinsky, in: *Intern. Encycl. of Pharmacol. and Therapeutics*, Pergamon Press, London, 1981, p. 105.

8.19. A. N. Zaikin and A. M. Zhabotinskii, *Nature*, 225, 535 (1970).

8.20. A. T. Winfree, *Science*, 181, 937 (1973).

8.21. D. C. Cohen, T. C. Neu, and R. R. Rosales, *SIAM J. Appl. Math.*, 35, 536 (1978).

8.22. M. Koppel and L. N. Howard, *Stud. Appl. Math.*, 52, 291 (1973); *idem*, 56, 95 (1977).

8.23. Y. Kuramoto and T. Tsuzuki, *Progr. Theor. Phys.*, 55, 356 (1976).

8.24. T. Erneux and M. Herschkowitz-Kaufman, *J. Chem. Phys.*, 66, 248 (1977).

8.25. A. S. Mikhailov and I. V. Uporov, *Dokl. Akad. Nauk SSSR*, 249, 733 (1979).

8.26. Ya. B. Zel'dovich and B. A. Malomed, *Dokl. Akad. Nauk SSSR*, 254, 93 (1980).

8.27. V. I. Krinsky and B. A. Malomed, *Physica* 9D, 81 (1983).

8.28. A. T. Winfree and S. H. Strogatz, *Physica* 8D, 35 (1983); *idem* 8D, 65 (1983); *idem* 9D, 333 (1983).

8.29. A. V. Panfilov and A. M. Pertsov, *Dokl. Akad. Nauk SSSR*, 6 (1984).

8.30. L. V. Yakushevitz, *Studia biophysica*, 100, 195 (1984).

8.31. A. S. Mikhailov and V. I. Krinsky, *Physica* 9D, 346 (1983).

8.32. J. M. Greenberg, *SIAM J. Appl. Math.*, 30, 199 (1976).

8.33. K. I. Agladze and V. I. Krinsky, *Nature*, 296, 424 (1982); *idem*, 308, 834 (1984).

8.34. V. I. Krinsky and K. I. Agladze, *Physica* 8D, 50 (1983).

8.35. A. M. Pertsov and A. K. Grenadier, in: *Self-Organization. Autowaves and Structures Far from Equilibrium*, ed. V. I. Krinsky, Springer-Verlag, 1984, p. 184.

8.36. M. J. Janse and F. van Capelle, *Circ. Res.*, 50, 527 (1982).
8.37. A. B. Medvinskii and A. M. Pertsov, *Biofizika*, 27, 895 (1982).
8.38. A. B. Medvinsky, A. V. Panfilov, and A. M. Pertsov, in: *Self-Organization. Autowaves and Structures Far from Equilibrium*, ed. V. I. Krinsky, Springer-Verlag, 1984, p. 195.
8.39. V. A. Vasil'ev, Yu. M. Romanovskii, and V. G. Yakhno, *Uspekhi Fiz. Nauk*, 128, 625 (1979).
8.40. I. M. Gel'fand, *Uspekhi Mat. Nauk*, 14, 2 (1959).
8.41. I. M. Gel'fand and M. L. Tsetlin, *Dokl. Akad. Nauk SSSR*, 131, 6 (1960).
8.42. B. Welsh, J. Gomatam, and A. Burgess, *Nature*, 304, 611 (1983).
8.43. L. S. Polak and A. S. Mikhailov, *Self-Organization in Non-Equilibrium Physico-Chemical Systems*, Nauka, Moscow, 1983 (in Russian).
8.44. V. S. Zykov, *Simulation of Wave Processes in Excitable Media*, Nauka, Moscow, 1984 (in Russian).
8.45. *Self-Organization. Autowaves and Structures Far from Equilibrium*, ed. V. I. Krinsky, Springer-Verlag, 1984.
8.46. V. I. Krinskii and A. S. Mikhailov, *Auto-Waves*, Znanie, Ser. Fizika, No. 10, 1984 (in Russian).
8.47. G. Nicolis and I. Prigogine, *Self-Organization in Non-Equilibrium Systems; From Dissipative Structure to Order through Fluctuations*, Wiley, New York, 1977.
8.48. H. Haken, *Synergetics. An Introduction. Nonequilibrium Phase Transitions and Self-Organization in Physics, Chemistry and Biology*, Springer-Verlag, 1983.
8.49. H. Haken, *Advanced Synergetics. Instability Hierarchies of Self-Organizing Systems and Devices*, Springer-Verlag, 1983.

TO THE READER

Mir Publishers would be grateful for your comments on the content, translation and design of this book. We would also be pleased to receive any other suggestions you may wish to make.

Our address is:
Mir Publishers
2 Pervy Rizhsky Pereulok
I-110, GSP, Moscow, 129820
USSR

Printed in the Union of Soviet Socialist Republics

Nonlinear Phenomena in Plasma Physics and Hydrodynamics

Edited by R. Z. Sagdeev, Mem. USSR Acad. Sc.

This collection of articles by leading Soviet scientists reflects the latest investigations dealing with turbulence transitions, the emergence of stochasticity, and the appearance of coherent structures in hydrodynamic-type systems and the theory of strong turbulence. Possible applications of these new approaches to hydrodynamics, plasma physics, astrophysics, the theory of chemical reactions, and biophysics are discussed. Intended for specialists in nonlinear, turbulent and stochastic phenomena in physics.

Mir Publishers
2 Pervy Rizhsky Pereulok
I-110, GSP, Moscow, 129820
USSR